2011 Functional and Structural Nanomaterials: Fabrication, Properties, Applications and Implications: Fabrication of Nanomaterials II

Sponsored by: The Minerals, Metals and Materials Society, TMS Electronic, Magnetic, and Photonic Materials Division, TMS: Nanomaterials Committee

Program Organizers: Jiyoung Kim, Univ of Texas; David Stollberg, Georgia Tech Research Institute; Seong Jin Koh, University of Texas at Arlington; Nitin Chopra, The University of Alabama; Suveen Mathaudhu, U.S. Army Research Office

Thursday AM	Room: 8
March 3, 2011	Location: San Diego Conv. Ctr

Session Chairs: Jud Ready, Georgia Institute of Tech; Vijay Singh, University of Kentucky

8:30 AM Introductory Comments

8:35 AM

Synthesis of Discrete Aluminum Nanoparticles: Christopher Crouse¹; Eunsung Shin²; P. Terry Murray²; Jonathan Spowart¹; ¹Air Force Research Laboratory; ²University of Dayton Research Institute

Conventional, "top-down" methods used to prepare commercial grade aluminum nanoparticles often yield a highly aggregated, polydisperse product. Due to the pyrophoric nature of nano-sized aluminum it is also necessary to passivate these particles, achieved through the formation of a thin amorphous oxide layer at the surface of the particle, to impart stability. In an effort to reduce aggregation and minimize loss of active aluminum, due to oxide formation, we have explored the synthesis of discrete aluminum nanoparticles through the use of conventional laser ablation in the presence of organic solvent and stabilizing ligands. Highly soluble, discrete aluminum nanoparticles, average particle size of 21nm, have been prepared in tetrahydrofuran using oleic acid as a stabilizing ligand. TEM and EDS analysis were used to confirm the metallic nature of the particles. Our investigation concerning chemical effects on particle size and morphology in addition to potential applications will be presented.

8:50 AM

Microstructure of Ball Milled Nanostructured Cu: *Daria Setman*¹; Michael Kerber¹; Hamed Bahmanpour²; Ronald Scattergood²; Carl Koch²; Michael Zehetbauer¹; ¹Research group Physics of Nanostructured Materials, University Vienna, Austria; ²Department of Materials Science and Engineering, North Carolina State University, USA

Copper powder of 99.9% purity and an initial particle size in the micrometer range was subjected to high energy ball milling in a Spex 8000 mixer with ball to powder ratio of 10. Two different surfactants (NaCl solution and stearic acid) of different concentrations were used during milling. The evolution of the microstructure with respect to different processing parameters was determined using differential scanning calorimetry (DSC) and X-ray line profile analysis (XLPA). DSC measurements show a decreasing stored energy of lattice defect annealing with increased ballmilling time. This indicates a surprising decrease of lattice defects concentration of more than one order of magnitude. XLPA measurements allow determining the grain size and the density and arrangement of dislocations. A decrease of grain size with decreasing dislocation density may indicate that in nanometals with grain sizes 30 nm and below dislocation based deformation mechanisms become less important.

9:05 AM

Growth of Bulk, Nano-Composite (RE)-Ba-Cu-O Single Grain Superconductors: *Hari babu Nadendla*¹; YunHua Shi²; Sandeep Pathak²; Anthony Dennis²; David Cardwell²; ¹Brunel University; ²University of Cambridge

Bulk RE-Ba-Cu-O (where RE = Rare earth) superconductors fabricated in the form of large, single grains have the potential to trap magnetic fields than

are significantly greater than those produced by hard, Nd-Fe-B permanent magnets (~ 1 T). Recently, we have introduced successfully nano-scale (RE)2Ba4CuMOy (RE-2411, where M = W, Nb, Ag and Bi) second phase inclusions into the REBa2Cu3O7-d superconducting phase matrix and have shown that these nano-scale inclusions enhance critical current density and trapped magnetic fields in these materials. Achieving a homogeneous distribution of these nano-scale particles in the bulk microstructure is crucial for achieving improved trapped fields. In this paper, we report the pushing/ trapping behavior of various RE-2411 particles by the (RE)Ba2Cu3O7-d growth front during large grain growth and discuss the conditions under which a relatively homogeneous distribution of nano-scale RE-2411 phases within the RE-123 superconducting single grain matrix can be achieved.

9:20 AM

Inkjet Printed Gold Nanoparticulate Pads for Surface Finish in Electronic Package: *Seonhee Jang*¹; Kyoung-Jin Jeong¹; Sungkoo Kang¹; Donghoon Kim¹; ¹Samsung Electro-Mechanics

Gold (Au) pads for surface finish in electronic package were developed by inkjet printing method. The microstructures of inkjet-printed Au film were investigated by various thermal treatment conditions. The film showed the grain growth as well as bonding between nanoparticles (NPs). The film became denser with pore elimination when NPs were sintered under gas flows of N2-bubbled through formic acid (FA/N2) and N2, which resulted in improvement of electrical conductance. The resistivity of film was 4.79 μ O-cm, about twice of bulk value. From organic analyses of FTIR, Raman spectroscopy, and TGA, the amount of organic residue in the film was 0.43 % which meant considerable removal of the solvent or organic capping molecules. The solder ball shear test was adopted for solderability and shear strength value was 820 gf on average. This shear strength is good enough to substitute the inkjet-printed Au nanoparticulate film for electroplating in electronic package.

9:35 AM

Synthesis of Anisotropic Nanoporous Platinum Structures: *Yuan Li*¹; Antonia Antoniou¹; ¹Georgia Institute of Technology

We report on the synthesis of anisotropic porous structures of platinum formed by the preferential dealloying of an amorphous Pt-Si alloy. The nanoporous Pt structures (pores and ligaments 5-30nm in size and grain sizes of 5 nm) are formed in a two-step process involving Pt-Si co-sputtering and subsequent selective electrochemical etching in HF solution. We examine the conditions that can influence the level of anisotropy in the porous structures. The effect of the anisotropy on the mechanical behavior will also be discussed.

9:50 AM

Tailoring the Structure of Iron-Carbon Nanocomposites by Laser Power Variation Throughout the Laser Pyrolysis Process: *Ion Morjan*¹; Florian Dumitrache¹; Rodica Alexandrescu¹; Claudiu Fleaca¹; Ruxandra Birjega¹; Catalin-Romeo Luculescu¹; Iuliana Soare¹; Victor Kuncser¹; Victor Ciupina¹; ¹National Institute for Lasers, Plasma and Radiation Physics

The laser pyrolysis, as a single step synthesis method has been developed to prepare Fe@C nanocomposites with Fe/Fe3C nanoparticles/cores embedded in layered carbon. Fe (CO)5 and pure or Ar-diluted C2H4 were used as the iron and carbon sources, respectively. Ethylene serves also as an energy transfer agent towards the gaseous mixture. The incident laser power, as main experimental parameter was successively varied in order to optimize the chemical structure of the iron-based cores without a deleterious effect on the carbon coverage (which assures the passivation against the ambient). The control of the composition and crystallinity of the nanocomposites was performed by different analytical techniques such as EDAX, XRD, TEM and Moessbauer spectroscopy. In all samples, crystalline phases of alpha-iron and iron carbides (mainly cementite) (with varying relative content) were identified. The decrease of the laser power leads to the decreased carbon content and consequently to the slight superficial powder oxidation.

TMS2011 140th Annual Meeting & Exhibition

10:05 AM Break

10:20 AM

Mechanomutable Nanomaterials: Multiscale Computational and Experimental Studies: *Markus Buehler*¹; Steven Cranford¹; Christine Ortiz¹; ¹Massachusetts Institute of Technology

Mutable materials are found widely in biology, characterized by a material's capacity to change its properties under external cues based on directed structural changes at specific material levels. Here we focus on a class of mechanomutable materials, which change their mechanical properties such as elasticity, deformability, strength and toughness based on external signals. A hierarchical approach, implemented through coarsegrain molecular modeling, is utilized do develop a powerful framework that can successfully collaborate atomistic theory and simulations with material synthesis and physical experimentation, and facilitate the design of mechanomutable structural materials. We review studies of PAA/PAH polymer systems, where a first principles based bottom-up approach is used to predict the structure and mutability of large-scale material properties from the nanoscale up. We demonstrate hierarchical material designs, validated by experimental studies, to realize mechanomutable polymer nanotubes and films. Experimental approaches towards the design of adaptable, mutable and active nanomaterials will be presented.

10:35 AM

Fabrication of Gold-Platinum Nanoalloy by High-Intensity Laser Irradiation of Solution: *Takahiro Nakamura*¹; Yuliati Herbani¹; Shinichi Sato¹; ¹IMRAM, Tohoku University

Gold-platinum nanoalloys were fabricated by high-intensity femtosecond laser irradiation of aqueous solutions of auric and platinum ions with different mixing ratio. The resulting particles were characterized by UVvisible spectroscopy, TEM and XRD. After irradiation, absorption peak arise from surface plasmon resonance of gold nanoparticles were observed in the spectrum of auric solution, and the peak position shifted to shorter wavelength range and the absorption peak in the spectrum decreased with decreasing the composition of auric ion in the solution. The position of XRD peaks of the particles shifted from that of pure gold to platinum, and XRD peaks of the particles prepared in the solutions with a certain mixing ratio of auric and platinum ions were observed between the peak positions of gold and platinum. This finding demonstrates gold-platinum nanoalloy of are successfully fabricated only by high-intensity laser irradiation of aqueous solution of auric and platinum ions.

10:50 AM

Enhancement of CFRP Composites' Lateral Strength by Means of Magnetically Aligned CNTs: Saud Aldajah¹; Yousef Haik¹; ¹United Arab Emirates University

Carbon Reinforced Polymer (CFRP) composites have outstanding mechanical properties in the longitudinal direction due to their light weight and excellent strength. However, they have poor transverse mechanical properties which limit their use in many structural applications. This paper presents a new technique to substantially enhance the transverse mechanical properties of CFRP composites. Multi-wall carbon nanotubes (CNTs) will be added to the CFRP composite aligned in the transverse direction by means of a magnetic field. The CNTs alignment process will be aided by the addition of magnetic nanoparticles which will adhere to the carbon nanotubes by surface adsorption during the curing process. This will result in increasing the transverse stiffness of the CFRP composites. In order to assess the impact of this technique on the mechanical properties, three-point bending tests were carried out. The results showed that the aligned CNTs increased the stiffness and the maximum load carrying capacity.

11:05 AM

Effective Elastic Properties of Solids Containing Imperfectly Bonded Nano-Inhomogeneities Based on Atomistic-Continuum Interphase Model: *Bhasker Paliwal*¹; Mohammed Cherkaoui¹; ¹Unité Mixte Internationale (UMI) Georgia Tech-CNRS & Georgia Institute of Technology

The classical micromechanics is revised to study elastic properties of heterogeneous materials containing nano-inhomogeneities. Contrary to the previous studies, this work introduces the concept of interphase instead of sharp interface to account for the surface/interface excess stress effect at the nano-scale. The interphase's constitutive properties are derived within the continuum framework from atomistics. These properties are then incorporated in micromechanics-based interphase model to compute the effective properties of the nanocomposite. This approach bridges the gap between discreet systems (atomic level interactions) and continuum mechanics. An advantage of this approach is that it combines atomistic with a three-phase micromechanical model that considers inhomogeneity shape. It thereby enables both the shape and the anisotropy of nano-inhomogeneity and nano-interphase to be simultaneously accounted for in computing overall properties.

11:20 AM

Carbon Nanotube and Thin Film RF Antenna: David Stollberg¹; ¹Georgia Tech Research Institute

There is a need a smaller, more efficient, steerable RF antennas. Microstrip antennas (MSAs) have several advantages compared with conventional microwave antenna: lower weight, ease of integration with other microwave integrated circuits, and multiband operations. However, MSAs have several disadvantages compared to other microwave radiators: narrow bandwidth, and lower gain and power handling capability. This work endeavors to overcome these issues with non-conventional materials having superior, tailored electromagnetic properties suitable for applications in RF antennas. The specific design is a carbon nanotube (CNT) or thin metal film patch MSA in a novel design. The prototype MSA is composed of thin film iron or multi-walled carbon nanotubes on a silicon substrate. The two prototype antennas showed excellent response in the X-band, for which it was designed. In addition, an observed left-shift resonance effect points towards significant potential for miniaturization.

11:35 AM

Metallic Nanoparticles in a Polysaccharide Thin Film: *Patricia Farias*¹; Josivandro Silva¹; Igor Cavalcanti²; Beate Santos¹; Adriana Fontes¹; Rosa Dutra²; ¹Federal University of Pernambuco - UFPE; ²RENORBIO

Gold and Silver nanoparticles (NAu and NAg) embedded in thin films of the polysaccharide Chitosan (Ch) were obtained by the heating at 70 Celsius degree of Ch aqueous solution containing NAu and NAg precursors.NAu and NAg were obtained directly into the polymeric matrix. X-Ray Diffractometry and Transmission and Scanning Electronic Microscopies (TEM and SEM), as well as spectroscopic and electrochemical methods (cyclic voltametry and impedimetric measurements) were performed in order to characterize the obtained materials. UV-Vis spectra presented typical plasmons bands which are not observed in the UV-Vis spectra of Ch without NAu and NAg. FT-IR spectroscopy results showed changes in amine groups modes. These features strongly suggest that the NH2 groups effectively actuate on the reduction of the metallic precursors. The films are 25µm thick. MEV images showed that the obtained films are highly homogeneous. The results point to the feasibility of the obtained nanocomposites as potential biosensing substrates.

11:50 AM Concluding Comments

THURSDAY AM

2nd International Symposium on High-Temperature Metallurgical Processing: Sintering and Synthesis

Sponsored by: The Minerals, Metals and Materials Society, TMS Extraction and Processing Division, TMS: Pyrometallurgy Committee, TMS: Energy Committee

Program Organizers: Jiann-Yang Hwang, Michigan Technological University; Jerome Downey, Montana Tech; Jaroslaw Drelich, Michigan Technological University; Tao Jiang, Central South University; Mark Cooksey, CSIRO

Thursday AM	Room: 18
March 3, 2011	Location: San Diego Conv. Ctr

Session Chairs: Xiaohui Fan, Central South University; Xuewei Lv, Chongqing University, China

8:30 AM

Crystallization Behavior of Calcium Ferrite during Iron Ore Sintering: *Xiaohui Fan*¹; Lin Hu¹; Min Gan¹; ¹Central South University

Crystal precipitation behavior of calcium ferrite(CF) during iron ore sintering process along with the effect of cooling rate, SiO2 and Al2O3 on crystalline condensation were studied. The results show that CF, whose ability of precipitation was strong, and barely affected by extenal factors, begans to precipitate when the liquid phase cooling down to about 1200°C. CF could crystallize rapidly at the cooling speed of 150°/ min. Furthermore,slowdowning the cooling rate was obviously favorable for devolopment of crystal. Binder phase transformed from CF system to silicate system when SiO2 content was increased to 5~6%, with a constant basicity(R) 2.0. Increasing Al2O3 content could promote precipitation of CF and development of crystal.

8:50 AM

Numeric Simulation of the Cooling Process of the Iron Ore Sinter: Jiaqing Yin¹; *Xuewei Lv*¹; Chenguang Bai¹; ¹Chongqing University, China

The iron ore sinter is one of the main raw materials for the blast furnace (BF) process. In the production of iron ore sinter, the cooling speed of the sinter determines the quality of the iron ore sinter. In addition, the heat recovery devices are installed in the cooling machine for energy saving. The cooling parameters like gas flow rate and location of the gas blower should be optimized for getting the gas with a higher temperature and a good quality of sinter at the same time. In this study, the commercial simulation software COMSOL was used to establish a model simulating the cooling process of the iron ore sinter. Several factors including gas flow rate, the size of sinter ores and its distribution in the cooling machine were investigated with the model.

9:10 AM

Study on Sintering Properties of A Fine Iron Concentrate Containing Hematite and Limonite: *Tao Jiang*¹; Zheng-wei Yu¹; Yu-feng Guo¹; Yongbin Yang¹; Jian-jun Fan²; ¹Central South University; ²Taiyuan Iron and Steel(Group) Corp.

A fine iron concentrate containing hematite and limonite was used to sinter in sinter pot. It was found that productivity of sinter is only $1.16t/(m2\cdoth)$ when using 100% iron concentrate of this kind. However, productivity is increased to $1.53 t/(m2\cdoth)$ with addition of partial magnetite concentrate, meanwhile, tumble index of sinter is improved from 64.67%to 67.20%. Granulation properties and reactivities at high temperature of the two kinds of iron concentrate were studied. The results indicated that permeability index and liquid fluidity of iron concentrate containing hematite and limonite are much lower than those of magnetite concentrate, which are the key reasons for poor yield and quality of sinter.

9:30 AM Break

9:40 AM

Kinetics Studies of the Zinc Ferrite Synthesis: Mery Gómez¹; José D'Abreu¹; Helio Kohler¹; ¹Puc-rio

This work deals with the kinetics of the zinc ferrite synthesis, occurring through a solid-solid reaction in a selected range of temperatures, using as reactants an equimolar mixture of pure iron oxide- Fe2O3 and zinc oxide - ZnO. This equimolar mixture was thermally characterized using the DTA and TGA techniques. In sequence the zinc ferrite produced were examined using X-Ray Diffraction, Scanning and Transmission Electronic Microscopy. Finally the software Topas 3.0, Difrac Plus, using the Rietveld XRD method was applied to calculate the amount of zinc ferrite generated during the synthesis reaction. The results showed that at the low temperature (873 to 1003 K), the best fitting model was Phase Boundary Reaction, with apparent activation energy of 272 kJ/mol. On the other hand, for the high temperature (1023 to 1273 K), the results showed that Modified Logistic Equation had the best agreement with apparent activation energy of 67 kJ/mol.

10:00 AM

Vitrification of the Thermal State during Iron Ore Sintering: Xuling Chen¹; *Xiaohui Fan*¹; Tao Jiang¹; Xiaoming Mao¹; Hongming Long²; ¹central south university; ²Anhui university of technology

On the basis of deep analysis to characters of iron ore sintering, the threedimensional temperature distribution model was built using temperature of pallet sides and waste gas in windbox. The sintering bed was divided into four parts: wet mix zone, drying and preheating zone, burning zone and sinter zone according to temperature distribution. Some parameters, such as burn though point, rising point of temperature, vertical sintering speed, were soft-sensed. Based on these parameters, the thermal state during iron ore sintering was evaluated comprehensively. The model has been applied successfully in Baoshan Iron and Steel Group Corporation.

10:20 AM

Improving of Compression Strength of Preheated Pellets by High Pressure Roll Grinding: Jianjun Fan¹; Guanzhou Qiu¹; Tao Jiang¹; Yufeng Guo¹; ¹Central South University

The experiments were conducted on pellets roasting properties of one kind of iron concentrate with complicated mineralogical composition. It was found that this pellets required higher preheating temperature and longer time during roasting process, so it is difficult for such preheated pellets to withstand the mechanical collision when roasted in rotary kiln. More research work was carried out on how to improve preheated pellets compression strength by processing this iron concentrate with High Pressure Roll Grinding(HPRG). The researches revealed that not only the compression strength of preheated pellets would improve but that of finished pellets would increase even at lower temperature and shorter time. With the help of HPRG, the preheating and roasting temperature would decrease by 70° and 50°, preheating and roasting time would decrease by 2 and 4 minutes, but compression strength for preheated and roasted pellets would increase by 200 N/P and 220N/P respectively.

10:40 AM Concluding Comments

TMS2011 140th Annual Meeting & Exhibition

Advances in Mechanics of One-Dimensional Micro/Nano Materials: Nanomechanics: In-Situ Techniques

Sponsored by: The Minerals, Metals and Materials Society, TMS Materials Processing and Manufacturing Division, TMS Electronic, Magnetic, and Photonic Materials Division, TMS: Nanomechanical Materials Behavior Committee

Program Organizers: Reza Shahbazian-Yassar, Michigan Technological University; Seung Min Han, Korea Advanced Institute of Science and Technology; Katerina Aifantis, Aristotle University

Thursday AM	Room: 1B
March 3, 2011	Location: San Diego Conv. Ctr

Session Chairs: En Ma, John Hopkins University; Paulo Ferreira, The University of Texas at Austin

8:30 AM Invited

In Situ Mechanical Testing in the TEM as a Window anto Small-Scale Plasticity Phenomena: Andrew Minor¹; ¹UC Berkeley & LBL

Recent progress in both in situ and ex situ small-scale mechanical testing methods has greatly improved our understanding of mechanical size effects in volumes from a few nanometers to a few microns. Besides the important results related to the effect of size on the strength of small structures, the ability to systematically measure the mechanical properties of small volumes through mechanical probing allows us to test samples that cannot easily be processed in bulk form, such as a specific grain boundary or a single crystal. This talk will describe recent technique developments for experimentally probing nanoscale volumes and the resulting insights into dislocation plasticity and small-scale deformation mechanisms. Specifically, the hardening behavior of Cu samples during in situ compression and in situ tension will be compared and the critical stress for basal slip and twinning in Mg will be discussed.

8:55 AM Invited

Application of In-Situ Electron Microscopy in Nanoscience and Energy Research: *Jianyu Huang*¹; Li Zhong²; Chongmin Wang³; Ju Li⁴; Liang Qi⁴; John Sullivan¹; Wu Xu³; Jie Yu⁵; Liqiang Zhang²; Scott Mao²; Nicholas Hudak¹; Xiaohua Liu¹; Arunkumar Subramanian¹; Hongyu Fan¹; Akihiro Kushima⁴; ¹Sandia National Laboratories; ²University of Pittsburgh; ³Pacific Northwest National Laboratory; ⁴University of Pennsylvania; ⁵Harbin Institute of Technology

By integrating an atomically sharp scanning tunneling microscopy (STM) probe into a transmission electron microscope (TEM), the atomic structure and physical properties of individual nanostructures can be directly probed in real time at the atomic length-scale. Such studies have revealed a number of unexpected phenomena that only present themselves at the nano-scale. Cold-welding and surface mediated plasticity were revealed in ultrathin Au nanowires. A nanobattery comprised of an individual nanowire electrode was constructed inside a TEM, and the charge and discharge process was revealed in real time, pushing the forefront of knowledge in the highly technologically relevant area of Li-ion batteries.

9:20 AM Invited

Deformation in Metallic Nanowires under In-Situ TEM: *Scott Mao*¹; He Zheng¹; J. Luo¹; Jianyu Huang²; ¹University of Pittsburgh; ²Sandia National Lab

The mechanical behavior of bulk metals is usually characterized as smooth continuous plastic flow following by yielding. Here we show, by using in-situ TEM and molecular dynamics simulations, that the mechanical deformation behaviors of single-crystalline Ag and Ni nanowires are quite different from their bulk counterparts. Correlation between the obtained stress-strain curves and the visualized defect evolution during deformation processes clearly demonstrates that a sequence of complex dislocation slip processes results in dislocation starvation, involving dislocation nucleation, propagation and finally escaping from the wire system, so that the wires deformed elastically until new dislocation generated. This alternating starvation of dislocations is unique in small-scale structures. Furthermore, the magnitude of yield stress of these nanowires is strongly dependent of the wire size.

9:45 AM Invited

In-Situ Mechanical Testing of Nanowires and Nanodots: *Johann Michler*¹; ¹EMPA, Swiss Federal Laboratories for Materials Science and Technology

We developed recently several instruments for mechanical testing of nanowires in the SEM: an AFM for resonance and bending experiments, a MEMS-tensile tester, a nanoindenter, and a femptogramm mass sensor. The fracture strength of monocrystalline Si and ZnO was found to be close to the theoretical strength. Similarly, the yield stress of monocrystalline Rhenium was found to be close to E/10. Nanocompression tests on gold nanodots were found to be mediated through large strain bursts. The released strain energy can be correlated to the new surface created during the burst in an simple model. Electrodeposited nanocrystalline Cobalt nanowires were loaded in tension and revealed surprisingly low Young's modulus values of around 70GPa. Resonance excitation of the wires in a bending mode allows to assess the ratio of Young's modulus to mass density. Using the Young's modulus from the tensile testing revealed a low mass density of the nanowires.

10:10 AM

In-Situ SEM Micro-Compression Behavior of 1-D Nanostructure Arrays: *Siddhartha Pathak*¹; William Mook¹; Mikhael Bechelany¹; Johann Michler¹; ¹EMPA - Swiss Federal Laboratories for Materials Testing and Research

We study the mechanical response of one-dimensional arrays of highly dense small-diameter (1-3 nm) non-catalytic multiwall (2-4 walls) carbon nanotube (CNT) brushes, measured using SEM in-situ micro-pillar compression testing. These dense CNT pillars, fabricated using focused ion beam (FIB) micromachining, were found to exhibit significantly higher modulus (~150 GPa) and orders of magnitude higher resistance to buckling (~6 GPa) than CNT brushes produced using other methods. Van der Waals' interactions in such dense brushes provide them with the added ability to dissipate energy while withstanding such elevated stresses. In comparison, lower density forests of Si nanowires (SNWs) have also been fabricated by metal induced chemical etching of silicon wafers (to avoid FIB-induced damages). A comparative study of the buckling and failure behavior during compression in these two unique material systems is expected to provide valuable insights into the cluster strengthening characteristics of such 1-D turfs.

10:25 AM Break

10:40 AM Invited

Quantitative In Situ Mechanical Characterization of Carbon Nanotube/ Epoxy Interface and Individual Carbon Nanotube Using Novel Micromechanical Devices: Yogi Ganesan¹; Cheng Peng¹; Yang Lu¹; Phillip Loya¹; Jun Lou¹; ¹Rice University

The knowledge of carbon nanotube (CNT) strength and fundamental mechanisms that govern mechanical behavior at the nanotube-matrix interface are critical for CNT reinforced nanocomposite development. We have recently developed a simple micro-fabricated device that could be used within a scanning electron microscope (SEM) chamber in order to perform in situ tensile tests of individual CNTs treated with different functional groups and nanoscale CNT pullout experiments using different matrices quantitatively. In this work, we report on the usage of such device that works in conjunction with a quantitative inSEM nanoindenter, for the in situ quantitative tensile testing of an individual multi-wall carbon nanotube (MWNT) and for an individual MWNT pullout experiment from an epoxy matrix. The insights gained from this research could potentially help engineer superior CNT reinforced nanocomposites by enabling the development of powerful predictive models.

11:05 AM Invited

Superplastic Shaping of Silica Glass Nanowires and Nanoparticles: Electron-Beam-Assisted Flow Near Room Temperature: Evan Ma¹; ¹Johns Hopkins University

At or near room temperature, oxide glasses (with SiO2 as a prototype) are brittle and fracture upon any mechanical deformation for shape change. As structural and functional members, low-dimensional oxide glasses are widely used in today's electronic devices and microelectromechanical systems, fabricated in the forms of thin films, wires/fibers, pillars, particles and cantilever beams. One may want to plastically deform these glass components to alter their dimensions and configuration, and use the shape change to control properties (e.g., optical performance). In this talk, we demonstrate that with moderate exposure to low-intensity (<1.8×10-2 A/cm2) electron beam, dramatic shape changes can be achieved for amorphous silica at strain rates as high as 10-4/s, not only in compression for nanoparticles but also superplastic elongation larger than 200% in tension for nanowires. We also report the first quantitative comparison with and without the beam, revealing dramatic difference in the flow stress.

11:30 AM Invited

Recent Advances in Characterization with In Situ SPM-TEM Instruments: Oleg Lourie¹; ¹Nanofactory Instruments Inc.

In situ SPM-TEM instruments such as AFM-TEM, STM-TEM and TEMNanoIndenter are used for characterization of the electrical and mechanical properties of various nanomaterials. Piezo actuated and having force or current feedback, the SPM probe in these instruments is also employed for sample surface imaging combined with conventional TEM imaging of the samples. SPM-TEM system is aimed to correlate the electromechanical measurements with on-line HRTEM observations of structural changes in the materials during the experiment. Such combination of SPM and TEM techniques in one instrument becomes especially valuable for in situ studies of variousnanoscale structures like nanotubes, nanoparticles or nanowires. This presentation will outline the recent progress in the instrumentation development aimed to expand the range of available SPM-TEM systems employed to study mechanical properties of nanostructures.

11:55 AM

Quantitative Tensile Testing of Free-Standing Thin Films in a TEM: *Claire Chisholm*¹; Zhiwei Shan²; Jason Oh³; S.A. Syed Asif³; O.L Warren³; Andrew Minor¹; ¹University of California, Berkeley and National Center for Electron Microscopy; ²Xi³an Jiaotong University and Hysitron, Inc.; ³Hysitron, Inc.

In situ transmission-electron-microscopy (TEM) tensile testing is a powerful tool for revealing the underlying physical mechanisms of deformation in materials. Here we report a novel technique for quantitative, in-situ tensile testing of free standing metallic films inside a TEM. Freestanding thin films of Au were loaded onto a microfabricated "push-to-pull" (PTP) device and pulled in tension with a quantitative in-situ nanoindentation/ nanocompression holder. The (PTP) device allows for quantitative load-displacement data in parallel with real time images of the microstructural behavior. Results from the uniaxial tensile testing of Au thin films will be presented including observations of the transition from elastic to plastic loading and the related deformation phenomena. With this technique, it is possible to observe the deformation of thin films with correlated mechanical and microstructural data at high resolution.

12:10 PM Invited

Are Dislocations Possible in Nanoparticles?: C.E. Carlton¹; *Paulo Ferreira*¹; ¹University of Texas at Austin

The deformation behavior of nanoscale metals continues to be an exciting area for materials research. However, in the case of single crystal 0-D nanoscale metals, no deformation experiments, to our knowledge, have been performed at the nanoscale. The one experiment closest to the nanoscale was an in-situ TEM compression of ~200 nm Si nanoparticles. However, the particle tested was too large to extract relevant information at the nanoscale and the mechanical deformation of Si is also expected to be different from that of metals. For nanoparticles it is claimed there is a conspicuous lack

of dislocations, regardless of the materials processing history, even after significant deformation. Therefore, it has been suggested that dislocations cannot exist or/ do not play a role on the deformation of 0-D nanomaterials. To address this issue of the role played by dislocations in the deformation of 0-D nanomaterials, nanoparticles with diameters <20nm were compressed in-situ under phase-contrast in a transmission electron microscope (TEM). Two phase-contrast TEM experiments were done, one in a conventional TEM and the other in an aberration corrected TEM. Evidence for nucleation of dislocations and dislocation motion was observed during in-situ TEM nanoindentation, but upon unloading dislocations were no longer visible. A new model for explaining dislocation instability is introduced. In this model we consider the change in Gibbs free energy of an edge dislocation, as it moves through the nanoparticle, towards the surface. The nanoindentation experiments seem to confirm the model proposed.

Aluminum Reduction Technology: Cells Process Modeling

Sponsored by: The Minerals, Metals and Materials Society, TMS Light Metals Division, TMS: Aluminum Committee, TMS: Aluminum Processing Committee

Program Organizers: Mohd Mahmood, Aluminium Bahrain; Abdulla Ahmed, Aluminium Bahrain (Alba); Charles Mark Read, Bechtel Corporation; Stephen Lindsay, Alcoa, Inc.

Thursday AM	Room: 17B
March 3, 2011	Location: San Diego Conv. Ctr

Session Chair: Marc Dupuis, GéniSim Inc

8:30 AM

Development and Application of an ANSYS Based Thermo-Electro-Mechanical Collector Bar Slot Design Tool: Marc Dupuis¹; ¹GéniSim Inc

After the succesful development and application of an ANSYS based thermo-electro-mechanical anode stub hole design tool, an ANSYS based thermo-electro-mechanical collector bar slot design tool has been developed. Since the average contact resistance at the cast iron/cathode block interface is higher than the contact resistance at the cast iron/anode carbon interface, the potential for mV saving is even greater. A demonstration model has been developed and used to study different collector bar slot configurations, results obtained are presented.

8:50 AM

Impact of Amperage Creep on Potroom Busbars and Electrical Insulation: Thermal-Electrical Aspects: Andre Schneider¹; Daniel Richard¹: Olivier Charette¹; ¹Hatch

Busbars electrical insulation is a critical aspect of aluminium smelters potrooms electrical safety. With amperage creep, busbars are typically running hotter than they were at start-up. The long-term reliability of busbars and the integrity of insulating materials is therefore of concern. To assist smelters evaluate the performance of the busbars systems under realistic operating conditions, a methodology was developed using ANSYS\8482-based numerical simulation, laboratory testing and *in situ* measurements. This approach has been validated on different pot technologies and smelters. A realistic test case based on a demonstration busbar system is presented and the typical impact of line current, ambient temperature and selected operational procedures on thermal-electrical performance and reliability is discussed.

9:10 AM

Modern Design of Potroom Ventilation: Anastasiya Vershenya¹; Umesh Shah¹; Stephan Broek¹; Tom Plikas¹; Jennifer Woloshyn¹; Andre Felipe Schneider¹; ¹Hatch Limited

A typical natural ventilation design of a pot room incorporates incoming ambient air flow dividing into two main streams. The 'under the pot' stream passes through basement infrastructure and sweeps the heat/emissions from 140th Annual Meeting & Exhibition

the pots upward to roof. The 'over the pot' one flows through the Claustra wall and pushes the emissions/heat away from the working zone. This paper describes the use of CFD modeling to accurately predict the ventilation air flow split between these two main streams and improve the ventilation design, thus meeting the defined workplace hygiene standards. The model's success greatly depends on reliable input conditions such as cell emissions and heat release rates. An innovative approach for the calculation of cell emission rates is thus introduced. Furthermore, the ventilation model can be coupled with pot heat balance and busbars thermoelectric analyses in order to obtain proper Joule heat generation and release rates.

9:30 AM

Modeling of Energy Savings by Using Cathode Design and Inserts: René von Kaenel¹; Jacques Antille¹; ¹KAN-NAK SA

The use of modified cathode shape and inserts in the cathode allow drastically redistributing the current density in the aluminium liquid pool. As a result both the cathode voltage drop and the anode to cathode voltage drop can be significantly decreased. Electrical modeling can easily explain the energy savings in the cathode. Magneto-hydrodynamic modeling shows why and how specific energy can be saved in the anode to cathode distance. The energy saving inside the cell depends on the cell initial design but may exceed 1 kWh/kg.

9:50 AM Break

10:00 AM

A Preliminary Finite Element Electrochemical Model for Modelling Ionic Species Transport in the Cathode Block of a Hall-Héroult Cell: *Frédérick Gagnon*¹; Donald Ziegler²; Mario Fafard¹; ¹NSERC/Alcoa Industrial Research Chair MACE3 and Aluminium Research Centre-REGAL, Laval University; ²Alcoa Primary Metals

A first 2D transient isothermal model was developed for the modelling of bath penetration in a Hall-Héroult cell cathode block. The model simulates the 'non convective' ionic species transport. The molten cryolite solution system is defined with an ionic model. The migration and diffusion of the ionic species is followed in the cathode block pores and in an overlying bath layer. The evolution of the potential is simultaneously obtained using charge conservation equations. The model includes a linear kinetic model for the electrochemical formation of metallic aluminum. The porous cathode behaviour is modelled using volume averaging based methods. The aluminofluoride ionic equilibrium is implemented by the penalty method and the electroneutrality criterion as a constraint on the FEM weak form. This is the first application of porous electrode theory, adapted for a molten salt, to Hall-Héroult cell cathodes. The results show the early stage evolution of voltage and ions distribution.

10:20 AM

Anodic Voltage Oscillations in Hall-Héroult Cells: Kristian Etienne Einarsrud¹; Espen Sandnes²; ¹Norwegian University of Science and Technology; ²Hydro Aluminium AS

Experiments on lab- and industrial scale cells have been conducted in order to study the behaviour of anodic gas bubbles under various operating conditions. Traditional voltage measurements have been supplied with high-speed video recordings of the bath surface showing a good correspondence between voltage fluctuations and escaping gas bubbles. On average, 0.5 and 2 bubbles were observed per second in each respective case. Average frequencies obtained by a FFT of the voltage signal however show significantly lower values, approximately half of that observed. It is shown that this discrepancy can be due to large variations in the bubble release times and observed bubble events can be related to FFT frequencies by means of a frequency based on statistically significant periods. For industrial anodes, the possibility of overlapping bubbles is investigated as alternative effect resulting in the mismatch between observed and calculated frequencies.

10:40 AM

CFD Modelling of Alumina Mixing in Aluminium Reduction Cells: Yuqing Feng¹; *Mark Cooksey*²; Phil Schwarz¹; ¹CSIRO Mathematics, Informatics and Statistics; ²Process Science and Engineering

More uniform alumina concentration in an aluminium reduction cell can improves cell performance substantially. Control of alumina dissolution and distribution is more critical for modern cells, given that they are often operated at low anode-cathode distances (ACDs) and increased anode size and current density. This paper presents a numerical study of possible methods to improve alumina feeding system by use of a computational fluid dynamics (CFD) model. Using a typical full-scale industrial cell as a test bed, a simulation was first conducted based on a conventional multipoint alumina feeding method with uniform alumina feeding through each feeder. Following quantification of the alumina concentration over the whole cell and identification of the poor feeding region, a simulation was further conducted with an optimised feeding through each feeder. A better alumina concentration was achieved with the improved feeding strategy, which demonstrates the effectiveness of CFD modelling for improving cell performance.

11:00 AM

Bubble Transport by Electro-Magnetophoretic Foces at Anode Botttom of Aluminium Cells: *Valdis Bojarevics*¹; Alan Roy¹; ¹University of Greenwich

Particles and bubbles experience additional forcing in an electric currentcarrying liquid. The electro-magnetophoretic forces are well known in metallurgical applications, like metal purification in vacuum-arc remelting, electro-slag processes, impurity concentration change in castings. However, this effect appears to be never considered for aluminium cells. We present models to estimate the effect of electric current in the vicinity of the bubbles and the additional pressure distribution resulting from the magnetic forces in liquid electrolyte. According to the estimates, the electro-magnetophoretic force becomes important for the bubbles of size exceeding 2 mm to overcome a typical drag force of electrolyte flow, and potentially can oppose the bubble motion along a mild slope of the nearly horizontal anode bottom. The effect could explain certain features of the anode effect onset. Numerical results are presented, a further implementation in the general MHD code for the aluminium cell design is discussed.

Biological Materials Science: Mechanical Behavior of Biological Materials III

Sponsored by: The Minerals, Metals and Materials Society, TMS Electronic, Magnetic, and Photonic Materials Division, TMS Structural Materials Division, TMS: Biomaterials Committee *Program Organizers:* Jamie Kruzic, Oregon State University; Nima Rahbar, University of Massachusetts, Dartmouth; Po-Yu Chen, University of California, San Diego; Candan Tamerler, University of Washington

Thursday AM	Room: 15A
March 3, 2011	Location: San Diego Conv. Ctr

Session Chairs: Nima Rahbar, University of Massachusetts Dartmouth; Jamie Kruzic, Oregon State University

8:30 AM Invited

Adhesion in Biomaterials: From BioMEMS to Nanoparticles for Cancer Detection and Treatment: Winston Soboyejo¹; ¹Princeton University

This talk explores the role that adhesion can play in the design of interfaces in biomaterials that are relevant to cancer detection and treatment. These include: bio-electro-mechanical systems (BioMEMS) and ligand-conjugated nanoparticles for the early detection and treatment of breast cancer. Dip-coating and atomic force microscopy techniques are used to measure the adhesion between gold/magnetitite nanoparticles and cancer drugs or molecular recognition units that enable them to attach specifically

to breast cancer cells. The adhesion between cancer cells and BioMEMS surfaces is also elucidated via shear assay and atomic force microscopy techniques. The implications of the results are discussed for the design of BioMEMS interfaces and nanoparticle clusters that are being explored for the early detection and treatment of cancer via combinations of localized drug delivery and hyperthermia.

9:00 AM

Micro Tribology of Compression Molded Ultrahigh Molecular Weight Polyethylene Reinforced with Aluminum Oxide, Hydroxyapatite and Carbon Nanotubes: *Ankur Gupta*¹; Debrupa Lahiri²; Sanat Ghosh²; Garima Tripathi¹; Bikramjit Basu¹; Arvind Agarwal²; Kantesh Balani¹; ¹Indian Institute of Technology, Kanpur; ²Florida International University, Miami

Ultrahigh-molecular-weight-polyethylene (UHMWPE) is used as a liner in acetabular cups for total hip and knee replacement. In the present work, compression molding of UHMWPE has been carried out with varying content of nanocrystalline Hydroxyapatite (HAp) (2-5wt%), nanocrystalline Aluminum Oxide (Al2O3) (2-5wt%) and multi-walled-carbon-nanotube (MWNT) (2-4wt%). HAp addition is expected to impart biocompatibility, Al2O3 to improve compressive strength and stiffness, and MWNT to enhance strength and wear resistance. Presence of HAp and Al2O3 create additional interfaces leading to poor interfacial bonding eliciting poor mechanical/tribological properties. Modulus and hardness of 0.66543GPa and 39.08 MPa is observed for UHMWPE-5HAp, increases to 0.97213GPa and 54.17 MPa respectively for UHMWPE-5HAp-2MWNT-2Al2O3. MWNT has shown to significantly reduce the coefficient of friction (from 0.23 for UHMWPE-5HAp to 0.12 for UHMWPE-2HAp-2MWNT-5Al2O3). Pareto charts were developed from quantitative analysis of tribological properties in conjunction with various reinforcements. Cytocompatibility of the UHMWPE-HAp-Al2O3-MWNT biocomposites was confirmed via SAOS-2 cell line.

9:20 AM

Determination of Micro-Mechanical Properties of Bovine Cortical Bone by Uniaxial Compression Testing: *Pravin Ramesh*¹; Katrina Altman¹; Elise Morgan²; Katharine Flores¹; ¹The Ohio State University; ²Boston University

Bone is an anisotropic, hierarchically structured material, and as a result, its mechanical behavior is highly statistical in nature. The application of microscale compression testing to bone will permit modeling of the aggregate material to predict effects of age, disease, or injury on the mechanical properties. The present work analyzes the mechanical behavior of 15-25 µm diameter uniaxial compression pillars prepared by a femtosecond laser micromachining technique. Pillars are selectively machined within regions of interest in the cross-section, for example within osteons near the periosteal and endosteal surfaces. The pillars are then compressed with a modified nanoindenter in wet or dry conditions. Both monotonic and cyclic loading are considered. Modulus, strength, and modes of deformation are compared as functions of specimen size and position. The potential influences of chemical and thermal damage to the bone structure by the femtosecond laser micromachining process are also considered.

9:40 AM

Advanced Mechanical Characterization of Biomaterials by Nanoindentation: *Nicholas Randall*¹; Bo Zhou¹; ¹CSM Instruments

Various conventional methods are currently used to characterize the mechanical behaviour of biomaterials but have major drawbacks. Nanoindentation is particularly appropriate because it allows the characterization of very small material volumes. However, the main drawback of nanoindentation is linked to the low thermal stability of most instruments. The recent development of the Ultra Nanoindentation Tester now permits a precise investigation of the creep behaviour of the sample using very long duration tests. Such results are made possible thanks to a quasi elimination of the thermal drift. A series of long term quasi static tests on several viscoelastic biomaterials will be used to demonstrate the efficiency of this novel instrument design and its ability to almost totally eliminate the thermal drift. This study therefore demonstrates that nanoindentation testing, when performed in good conditions with appropriate apparatus, constitutes a reliable tool to study the time-dependent mechanical properties of biomaterials.

10:00 AM

Broadband Nanoindentation Spectroscopy for Biological Materials: *Joseph Jakes*¹; Daniel Yelle¹; Charles Frihart¹; Donald Stone²; ¹USDA Forest Products Laboratory; ²University of Wisconsin - Madison

Nanoindentation has increasingly been used for probing mechanical properties of biological materials at microscopic length scales. We propose nanoindentation to be used as a tool for mechanical spectroscopy in which detailed information about deformation mechanisms can be gained by characterizing viscoplastic properties across 4-6 decades of strain rate using broadband nanoindentation creep (BNC) and viscoelastic properties across 8 decades in time-scale with broadband nanoindentation viscoelasticity (BNV). In validation studies on poly methyl methacrylate, polycarbonate, and polystyrene the data generated from nanoindentation agree closely with more conventional viscoplastic and viscoelastic measurements. BNC is applied to study wood-adhesive interactions in individual components of the wood cell walls. BNC discriminates among different types of wood-adhesive interaction including formation of covalent bonds with wood polymers, bulking, and formation of interpenetrating networks. Unambiguous chemical information showing formation of covalent bonds between adhesive components and wood polymers is provided by two-dimensional solutionstate nuclear magnetic resonant spectroscopy.

10:20 AM Break

10:30 AM

Fiber Reinforced Tough Hydrogels: Animesh Agrawal¹; Dapeng Li¹; Nima Rahbar¹; *Paul Calvert*¹; ¹University of Massachusetts

A 3D rapid prototyping technique is used to form crossed "logpiles" of elastic fibers that are then impregnated with an epoxy-based hydrogel in order to form a fiber-reinforced gel structure resembling natural cartilage. The presence of the fibers increases the gel modulus and toughness and constrains the swelling. The fracture properties of the gel are expressed in terms of a critical strain energy release rate and compared with theories of gel strength.

10:50 AM

Microstructural and Mechanical Investigation of Macadamia Nutshells on Different Hierarchical Levels: *Claudia Fleck*¹; Ruth Loprang¹; Paul Schüler¹; Paul Zaslansky²; Dietmar Meinel³; ¹Technische Universitaet Berlin; ²Max-Planck-Institute of Colloids and Interfaces; ³Bundesanstalt für Materialforschung und -prüfung BAM

Macadamia nutshells exhibit surprisingly high strength and toughness making them interesting model materials for impact resistant engineering structures. The properties of the nutshell are assumed to be due to the hierarchically organised microstructure. Up to now, the degree of anisotropy of the microstructure and the relationship between microstructure and mechanical properties has not been clear. In the present work, by means of light and scanning electron microscopy and micro-tomography, the anisotropic, hierarchical microstructure of the nutshells was clearly shown. The layered composite structure with local variations in the degree of orientation gives the shell a high resistance against compressive as well as tensile stresses. This was demonstrated on different hierarchical levels in compression tests on whole and half nutshells, C-rings and cylindrical specimens. First results of crack growth tests on notched specimens allow to assume that this structure also lends a rather high resistance against crack growth to the nutshell.

11:10 AM

Characterization of Brazil Nut Shell Fiber: *Nelida Lucia del Mastro*¹; Patricia Inamura¹; Felipe Kraide¹; Maria Aguirre¹; Marcos Scapin¹; Esperidiana Moura¹; ¹IPEN-CNEN/SP

The fruit from Brazil nut (Bertholletia excelsa) is characteristically a spherical capsule, with a thick and hard surface dark brown in color. When mature, the capsule releases seeds through the lower portion. Each capsule contains between 14 and 24 seeds. The Brazil nut seeds are angular nuts with



a very hard hull. Although the Brazil nuts market growths, the nut shell fiber residues have no further application. In this work, an attempt has been made to characterize the Brazil nut shell fiber by various instrumental techniques like thermogravimetric analysis (TGA) and scanning electron microscopy (SEM). The organic composition was established and elemental composition was determined by the methods of Instrumental Neutron Activation Analysis (INAA) and Energy Dispersive X-ray Fluorescence Spectrometry (EDXRF). Some perspectives for these fibers are also presented, as novel markets for lignocellulosics have been identified in recent years, representing an exceptional opportunity of sustainable technological development.

11:30 AM

Armadillo Armor: Mechanical Testing and Micro-Structural Evaluation: *Irene Chen*¹; James Kiang¹; Joshua Yee²; Maria Lopez¹; Po-Yu Chen¹; Joanna McKittrick¹; Marc Meyers¹; ¹University of California at San Diego; ²University of California at Irvine

The armadillo has a unique protective bony armor, called the osteoderm, which confers to its shell-like skin with distinctive mechanical properties. The top layer of the shell is made out of a dark-brownish keratin layer, arranging in a bimodal random pattern. Beneath the keratin layer, the osteoderm consists of hexagonal and triangular tiles with both tiles having a composition that is the same as bone (mainly collagen type I fibers and hydroxyapatite minerals). The tiles are connected by non-mineralized collagen fibers, called Sharpey fibers. The hierarchical structure of armadillo osteoderm is characterized using optical microscopy, SEM, and AFM. Various mechanical tests (tensile, shear, impact, and flexural) are performed and fracture surface is examined under SEM. Toughening mechanisms will be discussed and compared with other mineralized tissues. This research is supported by NSF Grant (Ceramics and Biomaterials Program) 1006931.

11:50 AM

Feathers in Flexure: Why Buckling Up is for the Birds: Sara Bodde¹; James Kiang¹; Joanna McKittrick¹; Marc Meyers¹; ¹UCSD

Having studied microstructure and mechanical properties of feather in a piecewise fashion, we will now present investigations of the mechanical behaviour of the intact system in flexure. We will present data on sandwichstructured feather segments subjected to four-point bending until the buckling with an emphasis on gradient in loading limit from the proximal to the distal end. We will correlate this with geometric characterization of the medulloid pith at the core of the feather. In this study, we will compare the flexural strength of primary flight feathers from two North American Owl species of the same taxonomic family: one a large Horned Owl (~1.4 kg in mass) and the other a small Screech Owl (~200 g in mass). By this intra-familial and inter-specific comparison, we attempt to intimate scaling effects of microstructure on flexural strength. Research support: N.S.F. Biomaterials Program (Grant DMR 0510138).

12:10 PM

Quasi-Static and Dynamic Characterization of Agar: *Vinod Nayar*¹; James Weiland¹; Andrea Hodge¹; ¹University of Southern California

Nanoindentation is used to quasi-statically and dynamically characterize agar. Using a Hysitron Triboscope nanoindenter, the reduced, storage, and loss moduli of agar are presented. Quasi-static tests are performed on agar samples ranging from 0.5 to 5% concentrations using both open and closed-loop methodologies as the effects of proper loading conditions and adhesion are discussed. Dynamic properties, storage and loss modulus, are measured on the softer agar samples to observe the viscoelastic properties of a low modulus biologically-based polymer. Agar concentration, quasi-static load, and dynamic oscillation frequency were controlled to determine the linearity of the viscoelastic response, which was determined to be primarily affected by the frequency of oscillation. Agar is a principally an elastic polymer, with a smaller frequency-dependent viscoelastic response.

Bulk Metallic Glasses VIII: Mechanical and Other Properties I

Sponsored by: The Minerals, Metals and Materials Society, TMS Structural Materials Division, TMS/ASM: Mechanical Behavior of Materials Committee

Program Organizers: Gongyao Wang, University of Tennessee; Peter Liaw, Univ of Tennessee; Hahn Choo, Univ of Tennessee; Yanfei Gao, Univ of Tennessee

Thursday AM	Room: 6D
March 3, 2011	Location: San Diego Conv. Ctr

Session Chairs: Ralph Napolitano, Iowa State Univ; Jianzhong Jiang, International Center for New-Structured Materials (ICNSM)

8:30 AM Invited

Devitrification Kinetics and Phase Selection Mechanisms in Cu-Zr: I. Kalay¹; Y. Kalay²; M. Kramer²; *Ralph Napolitano*¹; ¹Iowa State University; ²Ames Laboratory

Devitrification dynamics and phase selection mechanisms in melt-spun amorphous Cu50Zr50, Cu56Zr44, and Cu45.5Zr54.5 alloys are investigated using in-situ high-energy synchrotron X-ray diffraction (HEXRD), conventional/high resolution transmission electron microscopy (TEM/ HRTEM), and differential scanning calorimetry (DSC). Crystallization sequences and nanoscale structures are analyzed and discussed in terms of binary system thermodynamics, nucleation and growth kinetics, crystalorientation relationships, solute partitioning, and chemical diffusion. This research is supported by U.S. DOE-OS, Ames Laboratory contract No.DE-AC02-07CH11358.

8:50 AM

Crystallization Behavior and Magnetic Properties of FeCoSiBNb BMG with Cu Additions: *Mihai Stoica*¹; Ran Li²; Stefan Roth¹; Gavin Vaughan³; Jürgen Eckert¹; ¹IFW Dresden; ²BUAA University; ³ESRF Grenoble

Fe-Co-B-Si-Nb bulk metallic glasses (BMGs) exhibit high glass-forming ability (GFA) as well as good mechanical and soft magnetic properties. The soft magnetic properties can be enhanced by nanocrystallization. To force the nanocrystallization, small content of Cu was added to the starting composition. Cu has positive heat of mixing with both main constituents, Fe and Co. In this way, the desired fine-tuned nanostructures may be obtained even directly upon casting. In this paper, {[(Fe_{0.5}Co_{0.5})_{0.75}Si_{0.05}B_{0.20}]_{0.96} Nb_{0.04}}_{100.x}Cu_x glassy alloys (x = 1, 2 and 3) were chosen for investigation. The effects of crystallization during heat-treatment processes on the phase evolution, the kinetic parameters and the magnetic properties, including M_x , H_c and T_c , in these alloys were investigated. The phase analyses were done with the help of the X-ray diffraction patterns recorded in-situ by using the synchrotron radiation in transmission configuration.

9:00 AM

Viscosity Measurement and Fragility Calculation in Fe-Based Amorphous Alloys: Jong Hyun Na¹; Marios D. Demetriou¹; Won Tae Kim²; Do Hyang Kim³; William L. Johnson¹; ¹California Institute of Technology; ²Cheongju University; ³Yonsei University

Since bulk metallic glasses(BMGs) have discovered in several multicomponent alloys, viscosity studies of BMGs have been conducted in the past two decades. However, though large-scale Fe-based amorphous alloys have successfully developed by enormous efforts for last six years to apply structural components, there is a limited rheological data due to the experimental difficulties such as their very brittle manner. In the present study, the rheological measurements of Fe-based amorphous alloys are performed in isothermal three-point beam-bending experiments. The experiments lead to the determination of the equilibrium viscosity, which can evaluate the fragility by means of one parameter law proposed by Johnson et al. Finally, the correlation between fragility and glass forming ability in Fe-based amorphous alloys has been investigated.

THURSDAY AM

9:10 AM Invited

Structural Relaxation, Glass-Transition, Viscous Formability and Crystallization of Bulk Metallic Glasses on Heating Including Microwave Treatment: *Dmitri Louzguine*¹; Akihisa Inoue¹; ¹WPI-AIMR, Advanced Institute for Materials Research, Tohoku University

Here we summarize our recent findings on relaxation, glass transition, viscous flow and crystallization of various metallic glasses on heating. We also present structure changes upon microwave treatment of powders. At least two processes related to the diffusivities of different alloying elements take place in the glass-transition region of a Zr-Cu-Al-Ni glassy alloy. Also we report an unusual solidification behavior of the bulk glassy alloy produced using low-purity Zr in which both primary and eutectic-type structural constituents were formed simultaneously during solidification of the melt. As the mechanical properties are not deteriorated these glassy-crystal composites can be used instead of the monolithic glassy alloys. In addition viscous flow of the Cu-Zr-Al-Ag glassy alloy is examined in both the glass-transition and supercooled liquid regions and this alloy is found to exhibit phase separation prior to crystallization. This process opens up possibilities for innovative processing which causes an increase in room-temperature plasticity.

9:30 AM

Effect of Tantalum Substitution on the Crystallization Kinetics and Hydrogen Permeability of Ni-Nb-Zr Amorphous Alloys: Sang-Mun Kim¹; Narendra Pal¹; Wen-Ming Chien¹; Joshua Lamb¹; Anjali Talekar¹; Dhanesh Chandra¹; Michael Dolan²; Stephen Paglieri³; Ted Flanagan⁴; ¹University of Nevada, Reno; ²Commonwealth Scientific and Industrial Research Organisation; ³TDA Research; ⁴The University of Vermont

Amorphous ternary Ni-Nb-Zr and quaternary Ni-Nb-Zr-Ta alloys are promising hydrogen permeable membranes. Amorphous alloy membranes were prepared by melt-spinning technique. The crystallization temperature and kinetics of amorphous membranes were examined by using differential scanning calorimetry (DSC) under various heating rates. It was observed that crystallization of amorphous (Ni_{0.6}Nb_{0.4})₇₀Zr₃₀ and (Ni_{0.6}Nb_{0.4}Ta_{0.1})₇₀Zr₃₀ alloys proceed through two exothermic reactions. Ta substitution resulted in slight decrease in the primary crystallization temperature (T_{x1}) but increase in secondary crystallization temperature (T_{xy}) . The activation energies, E_a, of amorphous alloys have been calculated using Kissinger and Ozawa equations based on DSC data. The activation energies for crystallization of amorphous $(Ni_{0.6}Nb_{0.4})_{70}Zr_{30}$ alloy are determined as 548 kJ/mol and 534 kJ/mol, respectively. The (Ni_{0.6}Nb_{0.4}Ta_{0.1})₇₀Zr₃₀ membrane shows slightly higher values of E₆ (579 kJ/mol and 563 kJ/mol). Ta substitution on the crystallization kinetics and hydrogen permeability of amorphous alloys will be discussed in detail.

9:40 AM Invited

Plastic Deformation Behaviors of Metallic Glasses under Multiaxial Loadings: *Zhefeng Zhang*¹; F. F. Wu¹; J. X. Zhao¹; R. T. Qu¹; ¹Institute of Metal Research

The plastic deformation behaviors and evolution of shear bands in a Zr52.5Ni14.6Al10Cu17.9Ti5 metallic glass were systematically investigated under multiaxial loadings, including tension, compression and small punch tests. First, we find that the Zr-based metallic glass can be controlled to create regularly arrayed fine multiple shear bands under small punch test. Second, we report on the macroscopically tensile plasticity up to ~25% in the Zr-based metallic glass sample with dimension of ~100 nanometers at room temperature. Third, the tensile ductility or brittleness of metallic glasses is found to strongly depend on the critical shear offset. Finally, following the dislocation theory in crystalline materials, we find that the plasticity of Zr-based metallic glass could be improved to a high value of ~10% under compression tests through installing two symmetrical semi-circular notches due to the steady shear deformation by the large-scale stress gradient around the two symmetrical notches.

10:00 AM Break

10:10 AM

Interface Properties of Crystalline-Amorphous Metallic Multilayers: *Christian Brandl*¹; Timothy Germann¹; Amit Misra¹; ¹Los Alamos National Laboratory

The combination of amorphous layers with crystalline layers showed extraordinary high toughness, i.e. ultra-high strength in conjunction with high elongation-to-failure. The plastic deformation, moreover, is confined by the crystalline-amorphous interface, which additionally has to maintain deformation compatibility to mediate homogeneous plastic flow. In nanocrystalline metals molecular dynamics (MD) simulation showed huge varieties of ordered fine structures in the interface, which can be related to the observed dislocation mediated deformation mechanism in the vicinity of the interface structure. Contrary to crystalline-crystalline interfaces, where crystalline phases exhibit long range order, the amorphous structure is characterized by a lack of long-range order. Using MD methods the compensation mechanism of the lacking long-range order at the interface is studied for metallic systems. The observed structural features are discussed in terms of dislocation-based deformation mechanisms such as dislocation transmission, nucleation, and absorption.

10:20 AM Invited

Effect of Minor Additives on Nucleation and Grain Growth Behaviors in Zr-Al-Ni-Cu-Based Metallic Glass: *Junji Saida*¹; Albertus Setyawan¹; Mitsuhide Matsushita²; Akihisa Inoue¹; ¹Tohoku University; ²JEOL Co., Ltd.

Recently, formation of various nanocrystalline phases as primary precipitation phases has been found by addition of minor elements, which deviate from the best composition for glass-forming ability (GFA) in metallic glasses. Especially, nano icosahedral quasicrystalline (QC) phase formation is important for the investigation of mechanism of high GFA as well as the improvement of mechanical properties in Zr-based metallic glasses. The authors have reported that the nano QC phase is easily precipitated by addition of a small amount of elements such as noble metals, Nb, V, Ta, Mo etc.. In this study, we report the transformation kinetics of nucleation and grain growth behaviors of the primary QC phase in Zr-Al-Ni-Cu metallic glasses by addition of Pd and Nb. The results bring us the useful information on nucleation and grain growth controlling for nanostructure formation with minor additives for the improvement of mechanical properties of bulk metallic glasses (BMGs).

10:40 AM

Electrochemical and Wear Properties of Zr₅₅Cu₃₀Ni₅Al₁₀ Bulk Metallic Glass with Respect to Use as a Medical Implant Material: *Steven Savage*¹; Maysam Nezafati²; Magnus Skjellerudsveen³; Dan Persson²; Ragnhild Aune³; ¹FOI; ²Swerea KIMAB AB; ³NTNU

Bulk Metallic Glasses (BMG) are known to have excellent corrosion resistance in aqueous media. However, when a material is used as a medical implant other properties including abrasive wear, tribocorrosion and leaching of metallic ions are also important. Relevant properties of the BMG $Zr_{55}Cu_{30}Ni_5AI_{10}$ have been compared with those of surgical grade Co-Cr-Mo (F75) and stainless steel 316 LVM. All measurements have been made under conditions which approximate those experienced by implants, using a phosphate buffer solution at pH 7.4, with and without the addition of protein (albumin), at 37°C. Abrasive wear measurements using the ball-on-disc method have been made and show that the wear resistance of the BMG is inferior to F75. However, the corrosion resistance measured by potentiodynamic tests was improved, and the amount of metallic ions leached into solution was much reduced. In particular it is noteworthy that nickel-ion release was greatly reduced.



10:50 AM

In-Vitro Biocompatibility of Ni-Free Zr-Al-Cu-Nb-Pd Bulk Metallic Glasses: *Lu Huang*¹; Wei He²; Yoshihiko Yokoyama³; Shujie Pang¹; Peter Liaw²; Akihisa Inoue³; Tao Zhang¹; ¹Beihang University; ²University of Tennessee; ³Tohoku University

Zr-based bulk metallic glasses (BMGs) possess attractive properties for their prospective biomedical applications. The present work investigated the in-vitro biocompatibility of Ni-free Zr-Al-Cu-Nb-Pd BMGs by studying biocorrosion behaviors and cellular responses. Ti-6Al-4V alloy was used as a reference material. Surface composition and wettability were characterized. Electrochemical tests were performed in a physiologically relevant environment using cyclic anodic polarization technique. Cellular behaviors including cell attachment and proliferation activity were investigated with three different types of cells (RAW 246.7 macrophages, NIH3T3 fibroblasts, and MC3T3-E1 pre-osteoblasts). It was found that the Zr-based BMGs exhibited low corrosion penetration rates (CPRs) representing good corrosion resistance. The general biosafety of the Zr-based BMGs were revealed by normal cell responses. This study concluded that the Ni-free Zr-based BMGs demonstrated favorable electrochemical properties and biocompatibility, which made them a potential alternative as a biomedical material. This work was supported by NSFC, NSF, and IMI program.

11:00 AM Invited

Microstructure Evolution and Mechanical Properties of Zr-Cu-Ni-Al Bulk Metallic Glasses by the Bridgman Solidification: Jialin Cheng¹; *Guang Chen*¹; Hongwei Xu¹; ¹Nanjing University of Science and Technology

Microstructure evolution was experimentally studied at growth velocity between 0.1 and 6 mm/s by a Bridgman technique in Zr51.7Cu30Ni8.3A110. Our results show that the critical growth velocity of the glassy sample was 4 mm/s for Zr51.7Cu30Ni8.3A110, the critical growth velocities of the full crystalline sample were 1 mm/s for the alloy. When the growth velocities are between 1 mm/s and 4 mm/s, the in-situ formed eutectic phase/ bulk metallic glass matrix composites could be acquired. Moreover, compressive tests were performed on these samples. The results show that as the growth velocity decreases and the precipitation of eutectic phase, plastic strain decreases, indicating that the precipitated eutectic phase can not block the fast propagation of the localized shear bands and the macroscopically brittle failure.

11:20 AM

Shear Band Patterns in Metallic Glasses under Vickers Indentation: *Zhinan An*¹; Yanfei Gao¹; Fengxiao Liu¹; Peter Liaw¹; ¹University of Tennessee

Vickers indentation was conducted on Zr-based bulk metallic glasses and metallic glass thin films. Both semi-sphere shear bands and radial shear bands were discovered in free-bond metallic glasses, yet only radial shear bands could be seen in non-free-bond metallic glasses. The radial shear bands were generated due to in-plane shear stresses and were in agreement with the maximum shear stress direction according to our finite element analysis. While the semi-sphere shear bands were caused by out-of-plane shear stresses. Shear bands were blocked by the film/substrate. Instead of penetrating into the substrate, the radial shear bands were reflected back into the metallic glass thin film. This phenomenon was both discovered experimentally and predicted in our modeling.

11:30 AM

Effects of Laser-surface Melting Treatment on the Mechanical Behaviors of Zr-Based Bulk Metallic Glasses: *Haoling Jia*¹; Gongyao Wang¹; Junwei Qiao¹; Bingqing Chen²; Tao Zhang²; Peter Liaw¹; ¹University of Tennessee; ²Beihang University

Laser-surface melting (LSM) is a precision manufacturing technique capable of producing materials with highly nonequilibrium microstructures. Due to the localized heat input and high cooling rate inherent to the process, this technology is attractive for the production of metallic glasses. In the present work, an effort has been made to study the effects of LSM on the mechanical behaviors of a Zr55Cu30A110Ni5 bulk metallic glass. The results of high-energy synchrotron diffraction, differential scanning calorimeter, and

scanning electron microscopy indicated that the solidification microstructure in the laser-melted zone was still a single-phase amorphous structure. After the laser-surface remelting, Zr-based alloys exhibited an enhancement in both the compressive strength and plasticity, compared with the as-cast samples. The improvement in mechanical behavior of the LSM-treated metallic glasses may result from complex residual stress distributions and different amorphous structure in the surface layer induced by the LSM treatment.

11:40 AM

Viscosity Measurement of Fe-Based Metallic Glass by Single Particle Compressive Test: *Rui Yamada*¹; Noriharu Yodoshi¹; Akira Kawasaki¹; ¹Tohoku University

Fe-based metallic glasses have attracted much attention due to their excellent properties and are expected to be utilized as micro-components. However, Fe-based metallic glasses have insufficient resistance against crystallization and are difficult to fabricate into the required shape within the incubation time before crystallization. Therefore, we need to investigate the optimal processing conditions and material properties of Fe-based metallic glasses. The viscosity is an important parameter in determining the stresses during processing and the shape of the final products. Conventional viscosity measurement methods, however, cannot be applied to most Fe-based metallic glasses because of their size limitation. To overcome this, we propose a new method in which viscosities are derived from the viscous flow behavior on the micrometer scale of a single metallic glassy particle during the compressive test. Our studies have shown that temperature dependence of the viscosities of [(Fe0.5C00.5)0.75Si0.05B0.2]96Nb4 metallic glass in the supercooled-liquid region can be measured.

Carbon Dioxide and Other Greenhouse Gas Reduction Metallurgy - 2011: Electrochemical Reduction Methods - CO2 Use and Other Metal Production

Sponsored by: The Minerals, Metals and Materials Society, TMS Extraction and Processing Division, TMS Light Metals Division, TMS: Energy Committee

Program Organizers: Neale Neelameggham, US Magnesium LLC; Ramana Reddy, The University of Alabama; Maria Salazar-Villalpando, National Energy Technology Laboratory; James Yurko, 22Ti LLC; Malti Goel, INSA

Thursday AMRoom: 15BMarch 3, 2011Location: San Diego Conv. Ctr

Session Chairs: Aldo Steinfeld, Solar Technology Lab; Mahesh Jha, Department of Energy

8:30 AM Introductory Comments

8:35 AM

Concentrated Solar Power for Producing Liquid Fuels from CO2 and H2O: *Peter Loutzenhiser*¹; Anastasia Stamatiou¹; Daniel Gstoehl²; Anton Meier²; Aldo Steinfeld¹; ¹ETH Zurich; ²Paul Scherrer Institute

A two-step solar thermochemical cycle for producing synthesis gas from H2O and CO2 with Zn/ZnO redox reactions is considered. The first, endothermic step is the thermolysis of the ZnO to Zn and O2 using concentrated solar energy as the source of process heat. The second, nonsolar, exothermic step is the reaction of Zn with mixtures of H2O and CO2 yielding synthesis gas and ZnO; the latter is recycled to the first solar resulting in the net reaction of CO2 + H2O= CO + H2 + O2. Syngas is further processed to liquid fuels via Fischer-Tropsch or other catalytic reforming processes. Second law analysis is used to determine the solar-to-chemical efficiencies attainable for molar ratios of CO to H2 of 0.2-5 and a summary of the experimentation on both steps, including the solar reactor technology and kinetic analyses, is provided.

8:55 AM

CO₂ Electrochemical Reduction by Specifically Adsorbed Anions: Korato Ogura¹; Jack Ferrell²; *Maria Salazar-Villalpando*³; ¹Research and Engineering Services; ²ORISE; ³National Energy Technology Laboratory

Due to concerns of global climate change and depleting fossil fuel resources, there have been many attempts to efficiently electrochemically reduce CO2. However, the net current densities for CO2 reduction described in the literature are very small; this has limited practical applications. Here, we describe a CO2 reduction electrochemical set up which yields a high current density on a Cu-mesh electrode. The CO2 reduction occurs in an acidic solution containing a high concentration of a halide ion. Weakly solvated ions, such as a halide anion, can strip part of their solvation shell and form a direct chemical bond with the metal electrode. This effect has been shown to play an important role in electrochemical CO2 reduction is caused by the specifically adsorbed anion, bonded with a covalent character on the Cu electrode. This anion effectively captures CO2 and accelerates the electro-reduction.

9:15 AM

Photo-Electro-Catalytic Conversion of CO2 to Synthetic Fuels on Surface Modified Nanowires: Jung-Kun Lee¹; Mengjin Yang¹; Maria Salazar-Villalpando²; ¹University of Pittsburgh; ²National Energy Technology Laboratory

The photo-electro-catalytic conversion of CO2 to synthetic fuels is one of the very environment-friendly ways to reduce CO2 concentrations in the air. This is also an energy storage process that converts solar into chemical energy. Here, we report the recent results on the reuse of CO2 by the surface modified TiO2 and ZnO nanowires. The surface of the nanowires is coated with a very thin layer of highly active materials by using an atomic layer deposition (ALD) technique to decrease kinetic reaction barriers. Electron hole recombination is the main challenge to overcome in the photo-electro-catalytic reduction of CO2. Compared with the nanoparticle counterpart, the arrays of 1-dimensional nanomaterials have higher carrier mobility due to the decrease in the concentration of the trapping sites, which allows for the efficient use of the photo-generated carriers. We will show the correlation between carrier transport and CO2-photo-electro-catalytic conversion in the nanowire arrays.

9:35 AM

Solar Thermo-Chemical Splitting of Carbon Dioxide by Metal Oxide Redox Pairs: Martin Roeb¹; Sebastian Stenger¹; *Martina Neises*¹; Christian Sattler¹; ¹DLR

A two-step thermo-chemical cycle process has been developed and investigated. It is based on metal oxide redox pair systems, which can split carbon dioxide as well as water molecules by abstracting oxygen atoms and reversibly incorporating them into their lattice. If concentrated solar radiation is used as the heat source one has a promising method in hand to produce synthesis gas from water and CO_2 . An easy way of operation is gained by the combination of a ceramic substrate as absorber structure, which can be heated to high temperatures with concentrated solar radiation, and of a metal oxide coating which is capable to carry out the reactions. Different redox materials as powders and coated on ceramic substrates were investigated in a laboratory set-up. CO_2 could be reduced to CO with significant yields. In addition several side reactions were observed like the formation of carbon and like the Boudouard reaction.

9:55 AM

Recent Progress in Molten Oxide Electrolysis for Iron Production: *Antoine Allanore*¹; Felipe Carillo¹; Luis Ortiz¹; Donald Sadoway¹; ¹MIT

The steelmaking industry has drastically reduced its energy consumption in the last fifty years, and today's technologies are considered to operate at their optimal efficiency with respect to energy needs. To cope with new constraints related to green-house gases emissions, a change of paradigm is necessary. One of the future technologies which could be deployed to reach CO_2 mitigation targets relies on the intensive use of electricity: molten oxide electrolysis. One possible electrolyte contains molten iron oxide, to directly produce liquid iron. This talk will present the recent progress obtained in the development of molten oxide electrolysis of iron and will discuss the potential energy and CO, impact of the process.

10:15 AM

Perflourocarbon Generation during Electrolysis in Molten Fluorides: Xiangsheng Wang¹; Zuoju Huang¹; Guihua Wang¹; *Hongmin Zhu*¹; ¹University of Science & Technolgoy Beijing

During the electrolysis in oxide-fluoride melts with carbon anode, the main anode products are carbon oxides (CO2, CO), under normal potential. However, when the anode potential exceeds a certain value, the generation of perflourocarbons(PFC) CF4 and C2F6 happens accompanying with the anode effect. The current behavior of the carbon electrode under high potentials largely depends on the composition of the fluoride melts, and temperature.

10:35 AM Break

10:45 AM

Climate Change and Metal and Mining Sector: An Overview of Trends, Project Potential and Its Abatement: Puliyur Krishnaswamy Narasimha Raghavan¹; ¹Bharat Aluminium Co. Ltd.

This paper identifies potential technologies for Carbon dioxide abatement from the mining and metal industry with special reference to the Aluminium industry. Mine reclamation could contribute to this effort to successfully reach the greenhouse gas (GHG) emissions reduction commitments for a nation. An overview of GHG production by the mining and metal industry together with a review of principles used to set the context in which specific options for GHG reduction are described. Options for GHG reduction in the mining and metal industry include reforestation, Addition of soil amendments or neutralizing agents, CO2 capture and storage, initiatives towards energy reduction, waste heat recovery and alternative energy use. An analysis and quantification of the potential GHG reduction of potential carbon sinks and sequestration options for the mining and metal industry are provided. Cost estimates for different options are provided. The paper also identifies sources that could fund research regarding GHG reduction options. The paper concludes with recommendations.

11:05 AM

Fundamental Thermodynamics of Aqueous Carbon Dioxide Systems: *Dave Tahija*¹; H.H. Huang²; ¹Gehenna Corp; ²Montana Tech

Many investigations are being performed with the goal of removing carbon dioxide from the atmosphere and permanently storing it in geologically stable settings. At the same time, carbon dioxide in the form of dissolved carbonate is steadily accumulating in the world's oceans. Both carbon dioxide sequestration and oceanic accumulation are constrained by the aqueous thermodynamics of the carbonate system. These constraints are illustrated using the STABCAL computer model to generate potential-pH and aqueous distribution diagrams of seawater in contact with various pressures of carbon dioxide gas. STABCAL diagrams and titration simulations are also used to model some potentially useful cation-carbonate sequestration systems.

11:25 AM

Electrodeposition of PbTe Thermoelectric Materials in NaOH Solutions: *Zhongning Shi*¹; Ramana Reddy²; ¹School of Materials and Metallurgy, Northeastern University; ²The University of Alabama

The thermoelectric materials such as PbTe are becoming useful material for alternative energy production which helps reduce CO2 emissions. The electrodeposition of lead telluride (PbTe) is reported. Electrochemical behavior on Ag electrode in electrolyte 0.2M NaOH+0.01MPb(NO3)2, 0.2M NaOH +0.01M TeO2 and 0.2M NaOH +0.01MTeO2 +0.01M Pb(NO3)2 solution were carried out at 298K by cyclic voltammetry. The results showed that two different underlying processes are occurring depending on deposition potential. One process involves the reduction of TeO2 to TeO and a subsequent interaction between reduced TeO and Pb2+ to form PbTe at -0.92V. A second process at more negative reduction potentials involves reduction of TeO2 to H2Te at -1.29V followed by the chemical interaction with Pb2+. Both processes result in the production of crystalline PbTe in

140th Annual Meeting & Exhibition

the potential range $-1.38V \le E \le -0.9V$ (vs.Hg/HgO) on Ag substrates. The electrodeposition in 0.2M NaOH +0.01TeO2 +0.01M Pb(NO3)2 is described by the reaction TeO2 + Pb2+ + e-+ H- > PbTe + H2O.

11:45 AM

Study of Bamboo Charcoal Load Ce-Doped Nano-TiO2 Photochemical Catalysis Oxidation Degradation of Formaldehyde Device: *Daowu Yang*¹; Zhuo Ren¹; Hui Liu¹; Yu Su¹; ¹ChangSha University of Science & Technology

The Nano - TiO2 / bamboo charcoal adsorption of formaldehyde, as well as the influences of a certain amount of formaldehyde after adsorption on its photochemical catalysis effect were discussed in this paper. The sol preparation process of Ce-doped Nano-TiO2 was described. Results indicated that: the surface of bamboo Charcoal still has a strong formaldehyde adsorption capacity after Supported by Nano TiO2. After adsorbing formaldehyde, the photochemical catalysis degradation efficiency of formaldehyde of the catalyst at a steady state is basically the same with new prepared catalysts'. When the thickness of the catalyst layer of the multi-ladder-type structure photoreactor is 2mm, the interval is 20mm, the absorption efficiency of formaldehyde of Nano-TiO2 / bamboo charcoal is the best . Nano-TiO2 undoped Ce responded with no degradation of formaldehyde after 2 hours, the formaldehyde decontamination of the equipment reached 94%.

Challenges in Mechanical Performances of Materials in Next Generation Nuclear Power Plants: Session I

Sponsored by: The Minerals, Metals and Materials Society, American Nuclear Society, ASM International, Japan Institute of Metals, National Science Foundation, TMS Materials Processing and Manufacturing Division, TMS Structural Materials Division, ASM Materials Science Critical Technology Sector, TMS: Advanced Characterization, Testing, and Simulation Committee, TMS/ASM: Composite Materials Committee, TMS: Energy Committee, TMS: High Temperature Alloys Committee, TMS/ASM: Nuclear Materials Behavior of Materials Committee, TMS/ASM: Nuclear Materials Committee

Program Organizer: Faramarz Zarandi, CANMET-Materials Technology Laboratory

Thursday AM	Room: 5A
March 3, 2011	Location: San Diego Conv. Ctr

Session Chairs: Amit Misra, Los Alamos National Laboratory; Milo Kral, University of Canterbury

8:30 AM Invited

Materials Selection and Qualification for Advanced Nuclear Reactors: *R. N. Wright*¹; ¹Idaho National Laboratory

The Next Generation Nuclear Plant (NGNP) is a helium cooled high temperature reactor that is being developed in the United States to deliver process heat to industrial processes or for hydrogen generation. The goal of the project is to design and demonstrate a plant that can be licensed for commercial operation for 60 years. In addition to components like fuel cladding that will see nuclear service, selection and qualification of metallic materials focused on the intermediate heat exchanger or steam generator, reactor pressure vessel, and control rod assemblies is critical. The goals for the NGNP of long term operation at high temperature under a commercial license are fairly typical for new reactor systems under development and can be used as a framework for discussing new material development. It is highly desirable for example to design the reactor system using materials that are approved for nuclear service in the ASME Boiler and Pressure Vessel Code, have a well developed experience base, and exhibit stable properties with respect to aging and environmental effects. The ability to fabricate appropriate size and shape components, and joining and inspection are additional significant considerations. The approach to material selection and qualification that is being carried out by the NGNP program will be discussed and key properties of the materials under consideration will be reviewed. The important role of international collaboration on technology development and university programs in the US will be discussed. In addition, elevated temperature design rules that are incorporated in the ASME Code will be discussed and suggestions for extension or modification of the design rules will be presented.

9:10 AM

Creep Behavior of High Temperature Alloys for Generation IV Nuclear Power Plant Applications: *Xingshuo Wen*¹; Laura Carroll²; Richard Wright²; T.-L. (Sam) Sham³; Vijay Vasudevan¹; ¹University of Cincinnati; ²Idaho National Laboratory; ³Oak Ridge National Laboratory

Alloy 617 and 800H were selected as candidate materials for Intermediate Heat Exchangers in the Next Generation Nuclear Plant project with operating temperature in the range of 800 to 950°C and service life of 60 years. In this work, thermomechanically processed plates of alloys 617 and 800H were produced and their creep behavior over the temperature range of 750 to 1050°C and stresses ranging from 5 to 100 MPa was studied. The creep data was analyzed to decipher the various stages, and the stress exponents and activation energies were determined and diffusional versus dislocation creep mechanisms were discriminated. Microstructural changes, deformation structures and damage processes following creep were characterized using electron microscopy techniques, with particular attention given to the evolution of grain size, grain boundaries, second phase precipitates, dislocation structures and void formation. The results relating the creep behavior to microstructural changes in these alloys will be presented and discussed.

9:30 AM

The Influence of a VHTR Environment on the Creep-Fatigue Behavior of Alloy 617: Laura Carroll¹; Celine Cabet²; Rachael Madland³; Richard Wright¹; ¹Idaho National Laboratory; ²CEA, DEN, DPC, SCCME; ³Colorado School of Mines

Alloy 617 is the leading candidate material for an intermediate heat exchanger (IHX) application of the Very High Temperature Nuclear Reactor (VHTR), which may have an outlet temperature as high as 950°C. Previous work on corrosion of nickel base alloys in impure helium has shown that this environment is far from inert with respect to Alloy 617. A series of experiments have been conducted to elucidate the effect of environment, both laboratory air and VHTR impure helium, on the creep–fatigue behavior and the associated deformation mechanisms. The creep–fatigue behavior was investigated at a 0.3% total strain range and tensile hold times of up to 30 minutes at 950°C. Similarly, experiments with the corresponding time, temperature, and environment "no load" condition were conducted for comparison. The microstructural evolution, corrosion layer, and depleted surface region of the controlled chemistry exposures in both the "no load" and creep–fatigue conditions have been analyzed.

9:50 AM

The Effect of Grain Size and Annealing Twin Density on the Creep Properties of Alloy 800H: *Ben Gardiner*¹; Milo Kral¹; ¹University of Canterbury

The overall purpose of the present work is to identify an optimal grain size for an austenitic alloy (INCOLOY Alloy 800H) in a creep susceptible application. In order to accomplish this, an algorithm for measuring grain size in austenite must be developed in conjunction with an understanding of the influence of annealing twins. While the use of Electron Backscatter Diffraction (EBSD) to measure grain size would seem to be an obvious method due to advantages such as automatic identification of Σ 3 boundaries, there are many subtle but significant technical issues with using EBSD for this purpose. This presentation will describe how these issues have been addressed as well as progress towards the relationships between grain size and annealing twin density on the creep properties of INCOLOY Alloy 800H.

10:10 AM Break

10:20 AM Invited

On the Scientific and Engineering Challenges Facing the Development Irradiation Tolerant Nanostructured Ferritic Alloys: *G. Robert Odette*¹; ¹University of California Santa Barbara

Nanostructured ferritic alloys (NFAs) have the potential to make transformational contributions to developing advanced sources of fission and fusion energy. NFAs are Fe-Cr based ferritic stainless steels that contain an ultrahigh density of Y-Ti-O nanofeatures (NFs). The NFs provide outstanding high temperature properties and remarkable tolerance to irradiation induced displacement damage as well as the degrading effects of transmutation product helium. Indeed, the results of recent in situ injection experiments suggest that the NFs can be tailored to effectively transform helium from a liability to an asset. This is accomplished by trapping helium in ultrafine scale bubbles at the interfaces of the NFs, thereby increasing point defect sink strengths and proving deep trap reservoirs for very high concentrations of managed helium that protects grain boundaries and prolongs incubation doses for void and creep cavity formation. However, NFAs are in the very early stages of development. Important challenges and opportunities they face including fundamental issues of: a) determining the structures of the NFs and their interface with the matrix, as well as their compositions, that is their 'character'; b) relating the NF characteristics to their ability to provide sustained high temperature strength and irradiation tolerance; c) demonstrating and understanding the thermal and irradiation stability of far-from-equilibrium NFs and NFA microstructures. After a brief review of the status of these scientific issues, focus will be on a number of other engineering challenges including: a) identifying alloy compositionsynthesis designs and thermal mechanical processing paths that optimize the NFs and the balance of NFA microstructures; b) developing practical fabrication and joining methods that preserve optimal NFA microstructures, provide a balanced suite of outstanding and isotropic properties and yield defect free components; c) reducing costs; d) improving alloy homogeneity and reproducibility; e) establishing industrial scale supply sources; and, f) developing protocols needed to qualify new alloys for nuclear service.

11:00 AM

Microstructure and Creep Behavior of Nanocluster-Strengthened Ferritic Steels: *M Brandes*¹; Libor Kovarik²; Glenn Daehn¹; Joachim Schneibel³; Martin Heilmaier⁴; Michael Mills¹; Michael Miller³; ¹The Ohio State University; ²Pacific Northwest National Lab; ³Oak Ridge National Laboratory; ⁴University of Magdeburg

Mechanically-alloyed, nanostructured ferritic steels represent a class of alloys that can display high resistances to radiation and creep deformation. Their excellent high temperature creep performance derives from the presence of nanoclusters. The microstructure of a Fe-14YWT alloy was investigated by probe-corrected STEM imaging and electron energy loss spectroscopy. The structure of matrix and grain boundary nanoclusters are presented. The homogeneously-dispersed nanoclusters have faceted interfaces consistent with low index planes of the Fe matrix. The attractive interaction of dislocations with the nanoclusters was studied using bright-field STEM imaging. In light of these observations, a model of the creep response using a modified Frost-Ashby approach will be discussed. With this approach, it is possible to explain the low creep rates and small stress exponents that have been measured in these alloys. This research was sponsored by the U.S. Department of Energy, Materials Sciences and Engineering Division, Office of Basic Energy Sciences.

11:20 AM

On the High Temperature Creep and Crack Growth Studies of Nanostructured Ferritic Alloys: *E. Stergar*¹; M. Salston¹; G.R. Odette¹; K. Fields¹; D. Gragg¹; ¹UC Santa Barbara

Nano-structured ferritic alloys (NFAs) have high tensile and creep strength permitting service up to 800°C and manifest remarkable resistance to radiation damage. These outstanding properties derive from an ultrahigh density of Ti-Y-O enriched nano-features (NFs) that provide dispersion strengthening, help stabilize dislocation and fine grain structures, reduce excess concentrations of displacement defects and trap helium in fine, and relatively harmless, bubbles. The first part of the presentation summarizes an extensive database on the viscoplastic creep properties of the MA957 and other NFAs. The creep strength is anisotropic in extruded product forms with higher and lower strengths in the axial and transverse directions. Note the strong and weak directions for creep are opposite to those for fracture toughness of extruded NFAs, which are lower in the axial versus transverse directions. The second part of the presentation focuses on the low ductile tearing toughness of NFAs at elevated temperatures.

11:40 AM

Characterization of Nano-scale Features in Mechanically Alloyed and HIP-ed Oxide Dispersion Strengthened Steel U14YWT: Dhriti Bhattacharyya¹; Patricia Dickerson¹; Stuart Maloy¹; G. Robert Odette²; Michael Nastasi¹; Amit Misra¹; ¹Los Alamos National Laboratory; ²University of California, Santa Barbara

An Oxide-Dispersion-Strengthened ferritic steel with a high density of nano-features, designated U14YWT, is studied in order to understand the nature of the nano-features. This alloy has a composition Fe - 14Cr - 3W - 0.4Ti - 0.25Y2O3 (wt%), and was processed by Hot Isostatic Pressing. The authors examine the morphology, crystal structure and chemistry of the different nano-scale oxide particles existing in these alloys and their orientation relationship with the BCC-Fe matrix using conventional and high-resolution Transmission Electron Microscopy (TEM), Energy Dispersive X-Ray Spectroscopy (EDS) and Energy Filtered TEM (EFTEM). Three different types of precipitates or features were observed – (a) 50-300 nm, irregular shaped faceted particles, (b) 10-50 nm square shaped particles, and (c) small, spherical particles <5nm in diameter. The study revealed nanofeatures with hitherto unobserved crystal structures and varying chemical compositions, which, because of their relative abundance, may influence the radiation damage resistance of these ferritic alloys.

Characterization of Minerals, Metals and Materials: Characterization of Polymers, Composites and Natural Materials

Sponsored by: The Minerals, Metals and Materials Society, TMS Extraction and Processing Division, TMS/ASM: Composite Materials Committee, TMS: Materials Characterization Committee *Program Organizer:* Sergio Monteiro, State University of the Northern Rio de Janeiro - UENF

Thursday AM	Room: 14B
March 3, 2011	Location: San Diego Conv. Ctr

Session Chairs: Fernando Rizzo, PUC Rio de Janeiro; Jian Li, CANMET-MTL

8:30 AM

Characterization of Tensile Properties of Piassava Fiber Reinforced Polyester Composites: Denise Nascimento¹; Isabela da Silva¹; *Felipe Lopes*¹; Sergio Monteiro¹; ¹State University of the Northern Rio de Janeiro - UENF

The piassava fiber is one of the most rigid natural lignocellulosic fibers, which has since the last decade been investigated as possible reinforcement for polymeric composites. In the present work, the tensile properties of polyester composites reinforced with piassava fibers with different diameters were investigated. Composites with volume fractions up to 30% of continuous and aligned piassava fibers were tensile tested at room temperature to evaluate the ultimate strength, elastic modulus and total strain. For each volume fraction, separated fibers with smaller larger diameters were tested. The results indicated that the tensile properties tend to improve with increasing volume fraction of the thinnest piassava fibers. The role played by the fiber/matrix interaction was analyzed by scanning electron microscopy.

TMS2011 140th Annual Meeting & Exhibition

8:45 AM

Characterization of Tensile Tested Continuous Bamboo Stripped Fiber Reinforced Epoxy Composites: Lucas da Costa¹; Romulo Loiola¹; Sergio Monteiro¹; ¹State University of the Northern Rio de Janeiro - UENF

Composites with DGEBA/TETA epoxy matrix reinforced with thinner and continuous bamboo fibers stripped from culms were mechanically characterized by tensile tests. Specimens with up to 30% in volume of aligned fibers were tensile ruptured at room temperature. The results showed a steady increase in both the ultimate strength and the elastic modulus of the composites with the amount of incorporated bamboo fibers. The fractographic analysis by scanning electron microscopy showed evidence of moderate adhesion between the bamboo fiber and the epoxy matrix. This fiber/matrix adhesion by interaction mechanism apparently justifies the improved tensile properties of the composites.

9:00 AM

Characterization of Thermal Behavior of Polyester Composites Reinforced with Curaua Fibers by Differential Scanning Calorimetry: Ailton Ferreira¹; *Felipe Lopes*¹; Sergio Monteiro¹; Teresa Castillo¹; Ruben Rodriguez¹; ¹State University of the Northern Rio de Janeiro - UENF

Polyester composites reinforced with natural lignocellulosic fibers have, in recent times, been gaining attention in engineering areas as lighter and cheaper alternatives for traditional composites such as the "fiberglass". One of the strongest, the curaua fiber, is today being considered as reinforcement of composites for automobile interior parts. In fact, several research works are currently being dedicated to curaua fiber composites since physical and mechanical properties are required for practical uses. In this work, the thermal behavior of polyester composites reinforced with up to 40% in volume of curaua fibers was investigated by differential scanning calorimetry, DSC. The results showed endothermic events associated with water release and possible molecular chain degradation. Comparison with similar composites permitted to propose mechanisms that explain this DSC thermal behavior.

9:15 AM

Characterization of Thermogravimetric Behavior of Polyester Composites Reinforced with Coir Fiber: *Helvio Santafë*¹; Sergio Monteiro¹; Ruben Rodriguez¹; Teresa Castillo¹; ¹State University of the Northern Rio de Janeiro - UENF

The coir fiber extracted from the husk of the coconut fruits are worldwide available in tropical regions as a low cost lignocellulosic by-product for many applications including composite filler in automobile parts. Possible uses above room temperature require information on the thermal behavior of coir fiber composites. Therefore, the objective of this work was to perform thermogravimetric, TGA and DTG, analysis on polyester matrix composites incorporated with coir fiber with different intervals of diameter. In general, it was found that thermal degradation associated with weight loss occurred in two stages. Changes were also observed in the DTG peaks for the different diameters investigated.

9:30 AM

Characterization of Aluminum Composite Reinforced with ZrO2 Nanoparticles Produced by Mechanical Alloying and Sintering Process: *Jose de Jesus Cruz Rivera*¹; Jorge Garcia Rocha¹; Luis Salvador Hernandez Hernandez¹; Esperanza Elizabeth Martinez Flores¹; Roberto Martinez Sanchez¹; Hector Javier Dorantes Rosales¹; ¹Instituto de Metalurgia

Because of their high specific strength and elastic modulus, aluminum matrix composites have been studied extensively and are regarded as light weight / high strength materials. The Mechanical Alloying (MA) technique belong is process in that a solid state reaction takes place when the nanometric size is arise and the contact between the fresh powder surfaces of the reactant materials at room temperature. In this work it have been tried to take the advantages of using powder metallurgy processes to produce 2024 aluminum composite starting from alloy in powders and dispersing ZrO2 nanoparticles as reinforcement with the aim to increase mechanical properties and to avoid the drawbacks of liquid processes. The composite was obtained through mechanical alloying, sintering and hot extrusion

processes. The characterization was made using X ray diffraction, scanning electron microscopy and transmission electron microcopy.

9:45 AM

Flexural Mechanical Characterization of Polyester Composites Reinforced with Continuous Buriti Fibers: Tammy Portela¹; *Lucas da Costa*¹; Rômulo Loiola¹; Sergio Monteiro¹; ¹State University of the Northern Rio de Janeiro - UENF

The fibers extracted from the petiole of the buriti palm tree are relatively strong as compared to other lignocellulosic fibers, with a potential for composite reinforcement. In this work, polyester matrix composites incorporated with these fibers were investigated for their flexural behavior. Specimens with up to 35% in volume of continuous and aligned buriti petiole fibers were bend-tested until rupture. The results showed an increase in the composite mechanical strength and stiffness with incorporation of these fibers. A fractograph analysis by scanning electron microscopy disclosed an effective adhesion mechanism between the buriti petiole fiber and the polyester matrix. This mechanism is apparently responsible for the improved performance of the composites.

10:00 AM Break

10:15 AM

 Tensile Failure Characterization of Polymer Matrix Composites:
 Jeongguk Kim¹; Sung Cheol Yoon¹; Jung-Seok Kim¹; Hyuk-Jin Yoon¹; Sung-Tae Kwon¹; ¹Korea Railroad Research Institute

In this investigation, the failure behavior of glass fiber reinforced epoxy polymer matrix composites (PMCs) was characterized during tensile testing. The PMCs have been used for railway bogie materials application. Through tensile testing, the fracture initiated at the epoxy matrix, and the brittle failure mode was observed. In order to monitor tensile damage evolution of PMC sample, a high-speed infrared camera was used to measure surface temperature changes during tensile testing. Through the thermographic image analysis, crack initiation and propagation were qualitatively monitored. Moreover, the thermographic images were helpful to provide the information on fracture mode and mechanisms in PMC sample. In this investigation, an IR camera was used to facilitate a better understanding of damage evolution and failure mode of PMC materials during tensile testing.

10:30 AM

Rheological and Dynamic Strain Rate Studies of Wax-Coated Granular Composites Used in Sports Surfaces: *John Bridge*¹; Alper Kiziltas²; Douglas Gardner²; Michael Peterson²; Wayne McIlwraith³; ¹Maine Maritime Academy; ²University of Maine; ³Colorado State University

Dynamic mechanical thermal analysis (DMTA) tests were conducted on high-oil content, paraffin-based wax used in wax-coated granular These composites make up the surface of synthetic composites. Thoroughbred horse racetracks used in North America. The modulus and damping response from the DMTA tests were correlated with the dynamic triaxial shear strength response of the bulk track material taken at two different operational temperatures and at four strain rates. The purpose of these tests is to understand the mechanisms of shear strengthening of the bulk track material as the wax is heated through the first crystalline solid to liquid nominal transition temperature. Previous work using differential scanning calorimetry confirmed that under common operational surface temperatures, the wax coatings undergo distinct thermal transitions. The resulting increase in triaxial shear strength values affects the consistency of the racetrack which, in turn, can potentially affect Thoroughbred racing performance and safety of the track surface.

10:45 AM

Characterization of Plastic Materials Used by Automotive Industry (**Impact-Stress**): *Alejandro Rojo*¹; Nora Ramirez¹; Jorge Salgado¹; ¹ITESM Toluca

This work gives a different procedure to characterize the plastics used in the car body interior and improve its design process to be able to predict its behavior when subjected to impact tests involving human casualties. The standard Izod configurations are used on unnotched specimens for characterization by impact tests. From these tests we obtain the movement curves and the absorption energy estimations. Through stress analysis at high speeds and a video camera set-up, the area reduction of the specimen is obtained from the image analysis, allowing us to get the stress-strain real curve of the material. The proposed testing procedure allows the acquisition of force and displacement data through time at various strain rates, which are indispensable for the characterization of dynamic events. A specimen with a special configuration is used that shows the more detailed dynamic behavior resulting in more accurate numerical analysis in the design process.

11:00 AM

Dynamic-Mechanical Characterization of Polyester Matrix Composites Reinforced with Banana Fibers: Nathalia Rosa¹; Lucas Martins¹; *Felipe Lopes*¹; Lucas da Costa¹; Sergio Monteiro¹; Rubén Rodriguez¹; ¹State University of the Northern Rio de Janeiro - UENF

The fibers extracted from the stem of the banana plant are relatively stronger and have been used as reinforcement of polymer matrix composites. In addition to quasi-static mechanical properties, there is a need to characterize the dynamic behavior of banana fiber composites under thermal constraints. In this work, the temperature variation of the dynamic-mechanical parameters of polyester composites incorporated with up to 30% in volume of banana fibers were investigated by DMA tests. The storage and loss moduli as well as then tan delta were measured from 20 to 200°C in a TA Instrument operating with the flexural mode at 1 Hz. The results showed that the incorporation of banana fibers tends to increase the viscoelastic stiffness of the polyester matrix. It was also observed changes in the Tg and the structure dumping capacity of the composites with increasing fraction of banana fibers.

11:15 AM

Characterization of Thermal Properties of Curaua Fibers by Photothermal and Photoacoustic Techniques: *Felipe Lopes*¹; Leonardo Mota¹; Marcelo da Silva¹; Helion Vargas¹; Sergio Monteiro¹; ¹State University of the Northern Rio de Janeiro - UENF

Natural fibers, as a class of materials, are attracting the interest of engineering sectors owing to specific advantages such as lower cost and density as well as environmental benefits associated with renewability and biodegradability. For industrial applications, thermal properties, among others, are required especially in the case of an insulating natural fiber. In the present work, thermal properties of the curaua fibers were investigated by photothermal techniques, i.e., the open photoacoustic cell and a method based upon the monitoring of the temperature evolution as a function of time. This investigation, in turn, permitted to evaluate two important thermal properties (thermal diffusivity and specific heat capacity) of the curaua fibers. Indirectly, by means of simple mathematical relations, thermal conductivity and thermal effusivity were obtained. The results were compared with other materials and characterize the curaua fiber as an efficient insulator.

11:30 AM

Photoacoustic Thermal Characterization of a Natural Biofoam Extracted from the Buriti Palm Tree: *Lucas da Costa*¹; Leonardo Mota¹; Marcelo da Silva¹; Tammy Portela¹; Helion Vargas¹; Sergio Monteiro¹; ¹State University of the Northern Rio de Janeiro - UENF

A natural biofoam extracted from the buriti palm tree (Mauritia flexuosa) has shown characteristics for potential substitution of synthetic foams. In the present work, a photoacoustic thermal characterization was performed on buriti biofoam samples. An open photoacoustic cell technique and a photothermal rise method under continuous laser illumination were employed in order to determine the thermal diffusivity and the specific heat capacity of such material. Beyond their intrinsic values (finger print), these physical parameters represent the light-into-heat conversion efficiency and the amount of heat stored per unit volume, respectively. The results showed that the buriti biofoam presents thermal properties that permit its use as an effective insulation material.

11:45 AM

Pullout Test of Jute Fiber to Evaluate the Interface Shear Stress in Polyester Composites: Isabela da Silva¹; Alice Bevitori¹; *Felipe Lopes*¹; Sergio Monteiro¹; ¹State University of the Northern Rio de Janeiro - UENF

Jute fibers have in the past decades being investigated as possible reinforcement of polymer composites. However, information is still needed on the fiber interaction with a polymeric matrix for a complete evaluation of the capacity of load transference inside the composite. The present work investigated the interaction of jute fibers with polyester matrix by means of the critical length assessment through pullout tests. Tensile tests of polyester sockets embedded with different fiber lengths allowed the critical length to be determined and then the interface shear stress to be calculated. It was found a relatively low interfacial strength indicating a weak adhesion between the ramie fiber and the polyester matrix. The SEM analysis of pulled out fibers corroborates this result.

12:00 PM

Thermal Analysis Characterization of Ramie Fibers with Different Diameters: Ruben Rodriguez¹; Alice Bevitori¹; Isabela da Silva¹; *Felipe Lopes*¹; Sergio Monteiro¹; ¹State University of the Northern Rio de Janeiro - UENF

The fibers extracted from the stem of the ramie plant are among the strongest natural lignocellulosic fibers with potential to be used as reinforcement of polymer matrix composites. Characterization of the ramie fiber has recently been conducted for physical and mechanical properties. However, the effect of increasing temperature on the ramie fiber behavior has not yet been fully investigated. Therefore, the objective of this work was to perform a thermal analysis on ramie fibers with different diameters within the naturally found range in practice. The analysis was conducted by thermogravimetric, TGA and DTG, as well as differential scanning calorimetric, DSC, techniques. It was found that the ramie fibers present thermal stability up to 200°C and then suffer a sharp deterioration between 300 and 500°C, resulting in characteristic peaks.

12:15 PM

Characteristics of Cementious-Based Materials When Subjected to Microwave Energy: Natt Makul¹; ¹Phranakhon Rajabhat University

In this study, microwave energy at a frequency of 2.45 GHz with a multi-mode applicator was used to accelerate early-age hydration reaction of Portland cement pastes with/without pozzolan materials. Influences of water-to-cementtious ratios (w/c), pozzolan materials and aggregates were investigated. Delay time (30 minutes after mixing), microwave power (390 watt) and time of application (45 minutes), the phases and microstructural characteristics scanning electron microscope (SEM) with dispersive X-ray (EDX), X-ray diffraction (XRD) and thermal analysis (TG). Furthermore, the efficiency of curing procedures was evaluated by comparing the compressive strengths with the pastes that were cured by soaking in lime-saturated deionized water. From test results it can be concluded that water-to-cementtious strongly affect to rise in temperatures inside the pastes to be process, and to develop microstructures and to gain higher compressive strengths.

Characterization of Nuclear Reactor Materials and Components with Neutron and Synchrotron Radiation: Mechanical Characterization and Modeling

Sponsored by: The Minerals, Metals and Materials Society, TMS Structural Materials Division, TMS/ASM: Nuclear Materials Committee

Program Organizers: Matthew Kerr, US Nuclear Regulatory Commission; Meimei Li, Argonne National Lab; Jonathan Almer, Argonne National Laboratory; Donald Brown, Los Alamos National Lab

Thursday AM	Room: 4
March 3, 2011	Location: San Diego Conv. Ctr

Session Chairs: Matthew Kerr, US Nuclear Regulatory Commission; Don Brown, Los Alamos National Lab

8:30 AM Invited

Studies of Deformation Modes in Zirconium Alloys for Nuclear Power Applications by Diffraction: *Mark Daymond*¹; Fei Long¹; Don Brown²; Rick Holt¹; ¹Queen's University; ²Los Alamos National Lab

Understanding the performance of materials in the complex stresstemperature-radiation damage environment of a reactor requires predictive capabilities, and hence micromechanical models for prediction of material behaviour. Diffraction experiments, both texture and strain measurement, play a key role in the validation of such models. Internal stresses, generated between differently oriented grains, or between phases, greatly affect the mechanical performance of zirconium alloys. A study of the development of internal stresses by diffraction, coupled with micromechanical models, can provide insights into the deformation mechanisms operating as a function of applied strain and/or temperature. Radiation damage changes the dislocation structures present in a material, and hence the subsequent micromechanics of deformation. This paper demonstrates the application of the technique in understanding deformation modes operating in a zirconium alloy at room temperature. Results obtained on un-irradiated material are compared with those obtained from material irradiated over several years of service in a commercial reactor.

9:00 AM

In-Situ Observation of the Dissolution and Precipitation of Hydridesin Zircaloy-4: *Olivier Zanellato*¹; Michael Preuss²; Fabienne Ribeiro¹; Jean-Yves Buffiere³; Jean Desquines¹; Axel Steuwer⁴; ¹IRSN Cadrache, France; ²The University of Manchester; ³INSA Lyon; ⁴ESSS

Zircaloy-4 is used for fuel assemblies in Pressurised Water Reactors. In the reactor core, the material corrodes and picks up hydrogen that leads to precipitation of hydrides. These hydrides can impair the integrity of the structure, especially after temperature transients. This paper presents observations of in-situ temperatures cycles using synchrotron x-ray diffraction carried out on Zircaloy-4 plates charged to different levels of hydrogen content. The diffraction experiment allowed following the evolution of phase fractions, crystallographic structures and lattice strains during the heating cycle. The presence of a strong solubility/precipitation hysteresis of hydrides during temperature cycling was confirmed, as observed by some authors using more indirect methods. It was also possible to study the precipitation kinetics of the hydrides and solve some controversies found in the literature. Self consistent modelling was performed to understand the evolution of the elastic strain in the matrix and the hydrides.

9:20 AM

Effects of Altering Bulk Hydride Phase and Orientation on DHC Behaviour in Zr-2.5wt% Nb: *Eric Tulk*¹; Matthew Kerr²; Mark Daymond¹; ¹Queen's University; ²US Nuclear Regulatory Commission

Delayed Hydride Cracking (DHC) is a time dependant fracture mechanism that has caused both compromise and failure in zirconium reactor core

components. DHC entails the repeated formation, growth and fracture of a brittle hydrides at a notch tip. Although there is extensive experimental data collected on DHC, there is still no consensus on the mechanism of hydride precipitation and growth at the notch tip. A study is presented of how the hydride orientation (affected by the microstructure/texture and by applied stress) and phase (delta vs gamma; affected by quench rate and quantified with synchrotron techniques) of the bulk hydrides affects subsequent DHC behaviour. The different hydride phases have different volume expansions compared to the parent matrix, while a hydride precipitated under stress, and hence in a non-microstructure favoured orientation, presumably has a higher energy than a hydride precipitated under no stress. Initial results indicate that DHC behavior is affected.

9:40 AM Invited

Validation of Models and Simulations of Nuclear Fuels: Marius Stan¹; Bogdan Mihaila²; Mark Bourke²; ¹Argonne National Laboratory; ²Los Alamos National Laboratory

In the reactor, nuclear fuels are subjected to extreme radiation, temperature, and chemical environments that can severely damage their properties. Multi-scale theoretical models and computer simulations are often used to predict these effects. We discuss recent simulations of coupled heat transfer, chemical species diffusion and thermal expansion of UO2+x fuel elements with metallic clad. The simulations demonstrate that accounting for the dependence of thermal conductivity and density on local composition leads to changes in the predicted temperature profile that exceed 5%. Such predictions are difficult to validate due to the uncertainty associated with the models and the challenges related to the in situ measurements of the temperature profile in the fuel element. Recent developments and demonstration experiments at synchrotron X-ray and neutron user facilities are discussed to evaluate their potential for model validation. We also speculate on what future facilities might offer for making in situ measurements, including temperature profiles.

10:10 AM

Chemical Segregation of U-10wt.% Mo Fuel Foils during Simulated Bonding Cycles: *Sven Vogel*¹; Donald Brown¹; Maria Okuniewski²; Jan-Fong Jue²; Blair Park²; ¹Los Alamos National Laboratory; ²Idaho National Laboratory

The mission of the Global Threat Reduction Initiative of the National Nuclear Security Administration in the U.S. DOE is to reduce and protect vulnerable nuclear and radiological material located at civilian sites worldwide by providing support for countries' own national programs. The GTRI Reactor Convert program converts research reactors from the use of highly enriched uranium to low enriched uranium. The baseline fuel for conversion of high performance research reactors is monolithic uranium-10wt.% molybdenum, encased in an aluminum cladding. During fabrication, the aluminum cladding is hot isostatic pressed so that it bonds to the rolled U10Mo foil. However, the final crystal structure of the U10Mo foil is dependent on the HIP'ing temperature and profile. The γ phase is preferred for the fuel application and it is stable in U10Mo above ~560°C. However the fuel transforms to a, γ , and γ' crystal structures if held at temperatures below this point.

10:30 AM

Microstructure Characterization and Processing of U-Mo Alloy Fuels for Nuclear Reactors: *Amy Clarke*¹; Robert Field¹; Deniece Korzekwa¹; Robert Aikin¹; Duncan Hammon¹; David Alexander¹; Kester Clarke¹; Ann Kelly¹; Pallas Papin¹; Rodney McCabe¹; Carl Necker¹; Robert Forsyth¹; Joel Katz¹; David Dombrowski¹; ¹Los Alamos National Laboratory

Monolithic, low enriched uranium (LEU)-10 wt.% molybdenum (Mo) fuels have been identified as a potential replacement for highly enriched uranium (HEU) dispersion fuels in high performance research reactors. The microstructures of cast and rolled U-Mo alloys were characterized using optical and electron microscopy to understand the influence of processing on microstructure evolution during the production of monolithic foils. The ascast microstructure was examined using light optical microscopy (LOM) and electron backscatter diffraction (EBSD) and Mo segregation was quantified using electron microprobe analysis (EMPA). Homogenization heat-

treatments of the as-cast material were performed to evaluate possible time/ temperature combinations to reduce the extent of Mo segregation. EBSD of rolled microstructures was also performed to determine the influence of processing and chemical banding on microstructure evolution and texture. The results from this work support the Global Threat Reduction Initiative (GTRI) Convert Fuel Development Program.

10:50 AM Break

11:00 AM

Dissimilar Metal Weld Residual Stress Mappings by Neutron and X-ray Diffraction and Incremental Hole Drilling Methods: Camden Hubbard¹; Josh Schmidlin¹; Matthew Klug²; James Pineault³; Shane Van De Car³; Zhili Feng¹; Fei Ren¹; Wei Zhang¹; ¹Oak Ridge National Laboratory; ²Dominion Engineering, Inc.; ³PROTO Manufacturing

The US Nuclear Regulatory Commission (NRC) and the Energy Power Research Institute (EPRI) are conducting a weld residual stress validation program aimed at both (1) refining computational procedures for residual stress simulations in dissimilar metal welds, and (2) developing and categorizing the uncertainties in the resulting residual stress predictions. This program currently consists of four phases, with each phase increasing in complexity from lab size specimens to component mock-ups. The US NRC and EPRI are working cooperatively on this effort under a memorandum of understanding, with this talk focusing on the characterization of residual stresses in dissimilar metal welds by by the incremental hole drilling (IHD), X-ray diffraction (XRD) and neutron diffraction (ND) methods conducted by Oak Ridge National Laboratory (ORNL). The three methods provide stress maps at the surface (XRD), near surface (IHD) and through thickness ND).

11:20 AM

2D Mapping of Weld Residual Stresses Using the Contour Method: *Adrian DeWald*¹; Michael Hill²; ¹Hill Engineering, LLC; ²University of California, Davis

Residual stresses play a significant role in the performance of welded joints, which are often critical locations in nuclear reactor components. Accurate information regarding the magnitude and distribution of residual stress in welded joints is required for assessment of structural integrity. The contour method has become a useful tool for generating two-dimensional maps of residual stress in weldments. This paper provides a description of the contour method and presents the results of recent contour method measurements on weld joints. Comparisons with residual stress data obtained using complementary techniques (e.g., neutron diffraction and slitting) are also provided.

11:40 AM

Eliminating Do in Neutron Diffraction Weld Residual Stress Measurement: *Zhili Feng*¹; Wei Zhang¹; Paul Crooker²; Howard Rathbun³; David Rudland³; Raj Iyengar³; Xun-Li Wang¹; Ke An¹; Camden Hubbard¹; ¹Oak Ridge National Laboratory; ²Electric Power Research Institute; ³U.S. Nuclear Regulatory Commission

Neutron diffraction is a unique tool for non-destructive measurement of residual stresses of welded structures. The conventional approach generally requires the knowledge of stress-free lattice spacing a priori. For multiplepass dissimilar metal welds, the stress-free lattice parameter is a complex function of position due to the chemistry inhomogeneity in the weld region that can be challenging to determine experimentally. This paper presents a new approach to determine the weld residual stress field without the use of the stress-free lattice parameter and any presumption of the residual stress conditions. The theoretical basis is presented first. The new approach is applied to a multi-pass dissimilar metal weld consisting of a stainless steel base metal and a nickel alloy filler metal. The residual stress results as determined from the new approach are compared with finite element modeling results. The general applicability of the new approach for neutron diffraction residual stress measurement is discussed.

12:00 PM Invited

Neutron Diffraction Measurements in Thick Section Nuclear Reactor Piping Systems: *Thomas Holden*¹; D.W. Brown²; T. Sisneros²; M. Kerr³; 'Northern Stress Technologies; ²Los Alamos National Laboratory; ³US Nuclear Regulatory Commission

Time-of-flight neutron diffraction measurements were conducted at the SMARTS diffractometer at Los Alamos National Laboratory on a welded pressurizer safety nozzle which had been retired from service and decontaminated. Thick sections present experimental difficulties due to long neutron path lengths, difficult scattering geometries, and alloy concentration gradients at the weld interface. The safety nozzle studied was composed of carbon steel, stainless steel, and nickel based Alloy 182 weld metal with a large neutron absorption and scattering cross sections. This talk describes the efforts made to measure the stresses in the safety nozzle, specifically the use of a method akin to the $\sin^2\Psi$ method to minimize the neutron path length and recommendations are given for attempting problems of this kind. Finally comparisons will be made to measurements in a smaller plate specimen, fabricated from similar material and characterized with multiple techniques (neutron diffraction, contour method, incremental hole drilling, and a finite element weld model).

Coatings for Structural, Biological, and Electronic Applications II: Metallic, Semiconducting, Insulating Coatings - Applications

Sponsored by: The Minerals, Metals and Materials Society, TMS Electronic, Magnetic, and Photonic Materials Division, TMS: Thin Films and Interfaces Committee

Program Organizers: Nuggehalli Ravindra, New Jersey Institute of Technology; Choong Kim, University of Texas at Arlington; Nancy Michael, University of Texas at Arlington; Gregory Krumdick, Argonne National Laboratory; Roger Narayan, Univ of North Carolina & North Carolina State Univ

Thursday AM	Room: 6E
March 3, 2011	Location: San Diego Conv. Ctr

Session Chairs: Choong-un Kim, University of Texas at Arlington; Sudhakar Shet, National Renewable Energy Laboratory

8:30 AM Introductory Comments

8:35 AM Invited

Thin Film Coatings for Silicon Solar Cells: Requirements and Challenges: *Bhushan L. Sopori*¹; ¹National Renewable Energy Laboratory Abstract not available.

9:00 AM Invited

Effect of Gas Ambient on the Synthesis of Al and N Co-Doped ZnO:(Al,N) Films and Their Influence on PEC Response for Photoelectrochemical Water Splitting Application: *Sudhakar Shet*¹; Le Chen¹; Houwen Tang¹; Todd Deutsch¹; Heli Wang¹; Nuggehalli Ravindra²; Yanfa Yan¹; John Turner¹; Mowafak Al-Jassim¹; ¹National Renewable Energy Laboratory; ²New Jersey Institute of Technology

Al and N co-doped ZnO thin films, ZnO:(Al,N), are synthesized by radiofrequency magnetron sputtering in mixed Ar and N2 and mixed O2 and N2 gas ambient at 100°C. The ZnO:(Al,N) films deposited in mixed Ar and N2 gas ambient did not incorporate N, whereas ZnO:(Al,N) films grown in mixed O2 and N2 gas ambient showed enhanced N incorporation and crystallinity as compared to ZnO:N thin films grown in the same gas ambient. As a result, ZnO:(Al,N) films grown in mixed O2 and N2 gas ambient showed higher photocurrents than the ZnO:(Al,N) thin films deposited in mixed Ar and N2 gas ambient. Our results indicate that the gas ambient plays an important role in N incorporation and crystallinity control in Al and N co-doped ZnO thin films.

9:25 AM Invited

Viscoplastic Deformation in Porous Low-k Dielectrics: *Nancy Michael*¹; Emil Zin¹; Woong Ho Bang¹; Sean King²; Todd Ryan³; Choong-Un Kim¹; ¹University of Texas at Arlington; ²Intel; ³Global Foundries

One of the key advances in microelectronics technology is the implementation of porous low-k dielectrics (PLK) in interconnect structures. The use of PLK is necessary to increase the device operation speed, yet its implementation has been seriously delayed due mainly to the reliability failure of interconnects integrated with PLK. While several reliability failure mechanisms instigated by PLK have been identified, the linkage between those mechanisms and properties of PLK itself has been illusive. In recent investigation, we find that the root cause of those failures is related to viscoplasticity of PLK. According to theoretical silicate structure properties, PLK should not show plasticity at interconnect processing temperatures, yet our experiment produces evidence showing the opposite. A significant level of viscoplasticity occurs under a mild mechanical and thermal load. The mechanism of such deformation and its linkage to pore structure and molecular bond properties will be discussed in this paper.

9:50 AM

Nanostructured Zinc Oxide Coatings Developed Via Solution Precursor Plasma Spray Technique: *Raghavender Tummala*¹; Ramesh Guduru¹; Pravansu Mohanty¹; ¹The University of Michigan - Dearborn

Zinc Oxide (ZnO) is a wide band gap semiconducting material that has various applications including optical, electronic, biomedical and corrosion protection. It is usually synthesized via processing routes, such as vapor deposition techniques, sol-gel, spray pyrolysis and thermal spray of presynthesized ZnO powders. However, production of ZnO coatings using an inexpensive and a single step process which is also capable of producing nanostructures is of technological importance. Here, we report synthesis of nanostructured ZnO coatings directly from a liquid solution precursor in a single step using plasma spray technique, for the first time. Adherent and nanostructured ZnO coatings were deposited from the solution precursor prepared using zinc acetate and water/isopropanol. An axial liquid atomizer was employed in a DC plasma spray torch to create fine droplets of precursor for faster thermal treatment in the plasma plume to form ZnO. The microstructures of coatings revealed ultrafine particulate agglomerates. X-ray diffraction confirmed polycrystalline nature and hexagonal Wurtzite crystal structure of the coatings. Transmission electron microscopy studies showed fine grains in the range of 10-40 nm. Observed optical transmittance (~65-80%) and electrical resistivity (48.5-50.2 mO-cm) of ZnO coatings are attributed to the ultrafine particulate morphology of the coatings.

10:05 AM Break

10:15 AM

Thin Al Doped ZnO Films for Si Heterojunction Solar Cells: Sudhakar Shet¹; Bhushan L. Sopori; ¹National Renewable Energy Laboratory

Ga-N co-doped ZnO thin films with reduced bandgaps were deposited on F-doped tin-oxide-coated glass by radio-frequency magnetron sputtering at different substrate temperatures in mixed N2 and O2 gas ambient. We found that Ga-N co-doped ZnO films exhibited enhanced crystallinity compared to undoped ZnO films grown under the same conditions. Furthermore, Ga-N co-doping ensured enhanced N-incorporation in ZnO thin films as the substrate temperature is increased. As a result, Ga-N co-doped ZnO thin films exhibited much improved photoelectrochemical (PEC) response, compared to ZnO thin films. Our results therefore suggest that the passive co-doping approach could be a means to improve PEC response for bandgap-reduced wide-bandgap oxides through impurity incorporation.

10:40 AM Invited

Spin Coated Er2O3-SiO2 Films on Silicon Substrates: Sufian Abedrabbo¹; Bashar Lahlouh¹; Anthony Fiory²; Nuggehalli Ravindra²; ¹University of Jordan; ²New Jersey Institute of Technology

Optically active Er+3 in silica films, which are suitable for siliconbased optical applications, have been produced by a sol-gel deposition process with high Er atomic concentrations of 6 and 12 %, followed by furnace annealing. Films were characterized for their thickness, index of refraction, and photoluminescence at room temperature. Photoluminescence yield is strongly enhanced for vacuum annealing in the temperature range 500 – 750°C. Reasonable room-temperature photoluminescence is also observed for annealing at 1000°C. These results demonstrate the viability of incorporating Er at high concentrations.

11:05 AM

Magnetic Material Interactions for the Method of Magnetic Field Directed Assembly: *Rene Rivero*¹; Michael R. Booty¹; Anthony T. Fiory¹; Nuggehalli M. Ravindra¹; ¹New Jersey Institute of Technology

Magnetic Field Directed Assembly is a method that offers a nonstatistical solution to the problem of assembly via parallel processing. The method requires the use of magnetic layers on top of devices and in recesses within wafers where they need to be located. We have developed a model that allows us to select magnetic materials that minimize their total weight contribution to the system while maximizing magnetization. We apply the model to a range of magnetic materials of high permeability that are often used as magnetic layers on semiconductors.

11:20 AM Invited

Bioactive Hydroxyapatite Coatings on Titanium Implants: Hadeer Ibrahim Mohammed¹; *Adele Carrado*²; Thierry Roland³; Genevieve Pourroy²; Wafa Abdel-Fattah⁴; ¹Biophysics Department, Ain-Shams University; ²IPCMS; ³INSA; ⁴NRC

This study presents an alternative coating method based on biomimetic techniques which are designed to form a crystalline hydroxyapatite (HA) layer very similar to the process corresponding to the formation of natural bone. The deposition route is electroless and based on redox reaction having several advantages of controlled conditions, application to complicated shapes, without adverse effect of heating besides being cost effective. The oxidant, alkaline (pH 9.2 at 60 °C)and acidic (pH 5.3 at 80 °C) baths were performed. The HA formations on the surface of titanium alloy pre-treated were investigated by means of Scanning Electron Microscopy (SEM) and Energy Dispersive Spectroscopy (EDS), FT-IR (Fourier Transform Infrared) Spectroscopy, Atomic Force Microscopy (AFM) and Simulated Body Fluids (SBF) for several periods. The data suggest that the method utilized in this study can be successfully applied to obtain deposition of uniform coatings of crystalline hydroxyapatite on titanium substrates.

11:45 AM Invited

Flame Spray Deposition of Composite Titanium Alloy and Bioactive Glass Coatings: *Greg Nelson*¹; Andre McDonald¹; John Nychka¹; ¹University of Alberta

Flame spray deposition development and characterization of a composite coating for use in bone fixation implants is described. The composite coating was deposited using a mixture of TiAl64V and bioactive glass 45S5 powders to produce a porous coating. Porosity, phase distribution, and in vitro bioactivity will be discussed for these promising biomaterial coatings.

Sponsored by: The Minerals, Metals and Materials Society, ASM International, TMS Structural Materials Division, TMS/ASM: Composite Materials Committee Program Organizers: Meisha Shofner, Georgia Institute of

Technology; Carl Boehlert, Michigan State University

Thursday AM	Room: 6A
March 3, 2011	Location: San Diego Conv. Ctr

Session Chairs: Meisha Shofner, Georgia Institute of Technology; Erica Corral, University of Arizona

8:30 AM Invited

Characterization of Composite Materials: Thermal Analysis of ROMP-Based Thermosets: *Michael Kessler*¹; Xia Sheng¹; Timothy Mauldin¹; Wonje Jeong¹; Jong Lee²; ¹Iowa State University; ²Kumoh National Institute of Technology

Ring-opening metathesis polymerization (ROMP) has become a powerful tool for producing linear and networked polymers and their composites. In this work, we describe various monomers and catalysts that are being developed for ROMP-based thermosets for applications ranging from adhesives to structural composites. Differential scanning calorimetry and oscillatory shear rheology experiments are used to describe the kinetics of cure and gelation, as well as catalyst dissolution, for various ROMP-active monomers. The influence of multifunctional crosslinking agents, surface modified carbon nanotubes, and structurally modified vegetable oils on the cure behavior of the resins and the resulting thermo-mechanical properties of the cured thermosets are examined in detail using various thermal analysis techniques.

9:10 AM

Nanoparticle Shape Effects in Polymer Composites: Meisha Shofner¹; Ji Hoon Lee¹; Jasmeet Kaur¹; ¹Georgia Institute of Technology

Polymer nanocomposites have been widely studied in the past 20 years in order to elucidate and exploit changes in polymer behavior at the particlepolymer interface. The excess specific surface area of nanoparticles provides increased opportunity for polymer-particle interactions and changes to polymer morphology in the interfacial zone. The quantity and structure of interfacial material is influenced by many nanoparticle attributes such surface chemistry and size. In this research, the effect of nanoparticle shape was studied. Nanocomposites containing chemically similar calcium phosphate nanoparticles with different shapes have been synthesized and characterized to further understand how particle shape affects nanocomposite structure and properties. Three nanoparticle shapes have been used: near-spherical, nanofiber, and platelet. When blended into the same polymer matrix, trends in thermal and mechanical properties showed different sensitivities to changes in nanoparticle shape that may be understood in terms of aspect ratio and specific surface area.

9:30 AM

Effect of Piassava Fiber Incorporation In Morphological, Thermal and Viscoelastic Behavior of HDPE Composites: *Esperidiana Moura*¹; Thiago Luiz Souza¹; Anne Chinellato²; Walker Drumond³; Beatriz Nogueira¹; ¹Instituto de Pesquisas Energeticas e Nucleares - IPEN-CNEN/SP; ²Mash: Tecnologia em Compostos e Masters; ³Departamento de Engenharia Metalúrgica e de Materiais da Universidade de São Paulo

In the present work, the morphological, thermal and viscoelastic behavior of high-density polyethylene (HDPE) matrix composites were investigated. HDPE reinforced with the piassava fiber weight fractions varying to 10 % to 40 % were prepared and characterized by means of scanning electron microscopy (SEM), differential scanning calorimetry analysis (DSC), thermogravimetric analysis (TGA) and melt flow index (MFI) tests. The

results showed that there were significant changes (p < 0.05) in surface morphology, melting enthalpy, crystallinity percentage variation and initial degradation temperature of the HDPE and HDPE/fiber composites content different piassava fractions. HDPE MFI values presented a significant reduction around 60 %, due to piassava fiber incorporation, confirming that fiber addition significantly affects the dynamic viscoelastic melt.

9:50 AM

Thermo-Mechanical Behavior of HDPE/Sugarcane Bagasse Fiber/ Organoclay Nanocomposites: Anibal V Castillo¹; Alejandra Teran¹; Anne Chinellato²; Maria de Fátima Nascimento³; *Francisco Rolando Díaz*⁴; Esperidiana Moura³; ¹Laboratorio Tecnologico del Uruguay; ²Mash: Tecnologia em Compostos e Masters; ³Instituto de Pesquisas Energeticas e Nucleares - IPEN-CNEN/SP; ⁴Universidade de São Paulo

In recent years, studies have shown that the addition of natural fiber or proper filler is an effective strategy for achieving improved properties in polymer composites. Moreover, is especially important if such fibers are residues of agro-industrial processes. In this work a promising technique to develop HDPE matrix nanocomposites by addition natural fibers and clay nanoparticles prepared by extrusion process is described. The HDPE with 20 % (w/w) of sugarcane bagasse fiber from agro-industrial residues and 3 % (w/w) of bentonite chocolate organophilic nanoclay (Brazilian smectitic organophilic clay) addition were obtained using a twin-screw extruder machine type. After extrusion process, the composites were characterized by tensile and flexural tests, SEM, Vicat and HDT tests. The MFI tests were determined to evaluate the effects of fiber and organoclay addition on dynamic viscoelastic melt of the HDPE. The results showed that the thermomechanical properties of nanocomposites obtained were superior to those of the pure HDPE.

10:10 AM Break

10:30 AM Invited

Three Dimensional (3D) Microstructure Visualization and Modeling of Deformation in Composites by In situ X-ray Synchrotron Tomography: Jason Williams¹; Vijesh Tanna¹; Vaidehi Jakkali¹; *Nikhilesh Chawla*¹; Xianghui Xiao²; Francesco De Carlo²; ¹Arizona State University, School of Mechanical, Aerospace, Chemical, and Materials Engineering; ²Advanced Photon Source, Argonne National Laboratory, Argonne, IL

Characterization of composite materials is often conducted by mechanical testing followed by laborious cross-section, characterization, etc. X-ray tomography provides a wonderful means of characterization damage in composites non-destructively. In this talk, we report on a methodology that addresses the critical link between microstructure and deformation behavior, by using a three-dimensional (3D) microstructure obtained by x-ray synchrotron tomography. The approach involves capturing the microstructure by sophisticated in situ tensile testing in an x-ray synchrotron, followed by x-ray tomography and image analysis, and 3D reconstruction of the microstructure. Incorporation of the microstructure into a powerful finite element modeling code for simulation was also conducted. We will present a case study based SiC particle reinforced Al alloy matrix composites, as an illustration of how this technique can be used for a variety of composites. The evolution of damage in the form of particle fracture, interfacial debonding, and void growth will be described.

11:10 AM Invited

Spark Plasma Sintering of Ultra-High Temperature Ceramic Composites: Erica Corral¹; ¹The University of Arizona

The development of next generation hypersonic flight vehicles requires new thermal protection system (TPS) materials that are capable of withstanding extreme aerothermal heating loads. Transition metal borides are attractive materials for use in harsh environments due to their high temperature properties. However, the application of diboride-based ceramics has been limited due to poor sinterability using conventional sintering techniques. Therefore, our approach couples using spark plasma sintering (SPS) and high temperature sintering additives in order to reduce the sintering temperature of ZrB2-SiC composites from 1900 to 1700°C, while maintaining density

values >99% of theoretical density. The effect of adding small amounts sintering additives on the densification and refinement of the ZrB2-SiC microstructure using SPS will be discussed. In addition, high temperature oxidation behavior of ZrB2-SiC composites will be presented up to, 1650°C.

Computational Plasticity: Dislocations Structures and Dynamics during Plasticity

Sponsored by: The Minerals, Metals and Materials Society, TMS Materials Processing and Manufacturing Division, TMS Structural Materials Division, TMS/ASM: Computational Materials Science and Engineering Committee, TMS: High Temperature Alloys Committee *Program Organizers:* Remi Dingreville, Polytechnic Institute of NYU; Koen Janssens, Paul Scherrer Institute

Thursday AMRoom: 1AMarch 3, 2011Location: San Diego Conv. Ctr

Session Chair: To Be Announced

8:30 AM Invited

Plasticity at Small Scales: *Richard LeSar*¹; Caizhi Zhou²; ¹Iowa State University; ²Ames Laboratory

Deformation in small systems offers a unique environment in which to apply computational methods of plasticity at the mesoscale, specifically, in our case, discrete dislocation dynamics. The number of dislocations is relatively small, making the simulations tractable on modest computational platforms. The increasing number of experiments at this scale make it possible to use discrete dislocation simulations to first verify the calculations and then to provide important details that add to the understanding of the fundamental physical processes. In this talk, we will review the computational approaches for applying discrete dislocation mechanisms (e.g., cross slip), etc. We will then discuss the applicability of these methods to the plasticity in small pillars and single-crystal and polycrystalline thin films.

9:00 AM Invited

Applications of Phenomenological Mesoscale Field Dislocation Mechanics: Armand Beaudoin¹; Koenraad Janssens²; ¹University of Illinois at Urbana-Champaign; ²Paul Scherrer Institute

Phenomenological Mesoscale Field Dislocation Mechanics (Acharya & Roy, JMPS 2006) provides a platform for introducing constitutive theories for plastic deformation into a continuum setting. The continuum formulation provides for evolution and transport of the excess (geometric) dislocation density and continuity of the plastic strain rate. In this work, we present examples of dislocation evolution at the mesoscale in the compression of pillars, and in the cyclic loading of layered structures.

9:30 AM

Binary and Ternary Interaction Coefficients and Strain Hardening in BCC Single Crystals: *Ronan Madec*¹; Ladislas Kubin²; ¹CEA, DAM, DIF; ²LEM (CNRS/ONERA)

Dislocation dynamics simulations have now reached a stage where they are able to tackle such problems as the formation of dislocation microstructures and forest hardening in bulk single crystals. The connection between mesoscopic and continuum approaches of plasticity is based on the knowledge of the interaction matrix between slip systems and of the dislocation mean free paths, from which a hardening matrix can be derived. The objective of the present work is to establish this connection in the case of BCC crystals, using a dislocation dynamics simulation that is briefly described. Emphasis is put on the determination of the interaction matrix in the high temperature regime, above the so-called "athermal temperature" at which the lattice friction vanishes. Results on binary and ternary dislocation reactions are discussed. Preliminary crystal plasticity computations using these coefficients and stress vs. strain curves for various orientations are presented and discussed.

9:50 AM Invited

140th Annual Meeting & Exhibition

Continuity Constraints at Interfaces and Scale Dependence of the Mechanical Behavior of Crystalline Materials: Claude Fressengeas¹; Thiebaud Richeton²; Guofeng Wang³; ¹University Paul Verlaine - Metz / CNRS; ²CNRS / Arts et Metiers ParisTech; ³Harbin Institute of Technology

We analyze the implications on the mechanical behavior of metal matrix composites of tangential continuity conditions on the elastic distortion obtained from the balance of lattice incompatibility across a material surface of discontinuity by using both conventional crystal plasticity, appended with this continuity condition, and a field dislocation dynamics model. The latter features the long-range interactions due to the presence of geometrically necessary dislocations and the short range interactions arising from dislocation transport. Solution of the boundary value problems is obtained via a mixed finite element approach where balance of momentum is solved via a Galerkin scheme, while the transport problem is solved by a Galerkin-Least Squares method. The results in the simple shear of a Al-SiC particle strengthened composite demonstrate the effects of particle size, shape and distribution on the hardening behavior of the composite, as well as the role of the continuity constraints at the matrix-inclusion interfaces.

10:20 AM Break

10:35 AM Invited

Entropic Effect on Dislocation Nucleation: *Wei Cai*¹; Seunghwa Ryu¹; Keonwook Kang¹; ¹Stanford University

Dislocation nucleation plays an important role in the plasticity of submicron and nano-scale samples. However, the prediction of the dislocation nucleation rate from atomistic simulations by computing the nucleation free energy barrier at finite temperature has been lacking. Here we present the first atomistic predictions of the free energy barrier and nucleation rate for homogeneous and heterogeneous nucleation of dislocations in EAM Cu. The data exhibits anomalously large entropy, the neglect of which would cause an underestimate of the nucleation rate by many orders of magnitude. The origin of this entropic effect is discussed.

11:05 AM Invited

On Particle Size Effects: An Internal Length Mean Field Approach Using Field Dislocation Mechanics Simulations: Vincent Taupin¹; *Stephane Berbenni*¹; Claude Fressengeas¹; Olivier Bouaziz¹; ¹LPMM, CNRS, Univ Metz, ENSAM

A mean field approach including an internal length scale is developed in order to capture the particle size effects on the overall material's behavior of particle-reinforced alloys. A generalized self-consistent scheme (with coated particles) is employed, with a new "phase" representing the coatings where orderly dislocations between the matrix and the particles are present. The thickness of these "layers" is supposed constant and constitutes the internal length scale [1]. It is determined dynamically by field dislocation mechanics [2], where orderly dislocations accommodate lattice incompatibility between matrix and inclusions. The beneficial influence of this scheme, as compared to classical mean field approaches, is shown from comparisons with experimental data on the particle size effects in Al/SiC composites. [1] V. Taupin, S. Berbenni, C. Fressengeas, O. Bouaziz. Acta Materialia, In Press, 2010.[2] A. Acharya, A. Roy, J. Mech. Phys. Solids 54, 1687, 2006.

11:35 AM

Interaction between Edge Dislocations and Voids in bcc Iron Investigated Thanks to a Multiscale Approach: *Sylvain Queyreau*¹; Brian Wirth¹; Jaime Marian²; Anastasios Arsenlis²; ¹University of California at Berkeley; ²Lawrence Livermore National Laboratory

This work focuses on the strengthening associated to nanometer-sized vacancy clusters, or voids, which are formed in bcc Iron under irradiation. We propose a new Dislocation Dynamics (DD) modeling for dislocation – void interactions based on complementary atomistic calculations. The following mechanisms are assumed to control the void strengthening: (i) the surface step creation, (ii) the removal of dislocation segments inside voids and (iii) the distant interaction between the stress field of the dislocation and the voids. A coupling with Boundary Element Method is performed for this

last mechanism. The DD model is able to reproduce the effect of void size and the temperature dependence on the strengthening obtained in atomistic simulations. The strengthening contribution related to the line energy of the removed dislocation segments is twice larger than the surface energy contribution. However, the temperature dependence appears to be mainly controlled by the decrease in the surface energy.

11:55 AM

3-Dimensional Dislocation Dynamics Simulation of Low-Angle Grain Boundary Migration: *Adele Lim*¹; Wei Cai²; Mikko Haataja¹; David Srolovitz³; ¹Princeton University; ²Stanford University; ³Institute of High Performance Computing

Using dislocation dynamics simulations, we investigate the migration of a mixed low-angle grain boundary (LAGB) composed of a network of two intersecting dislocation arrays. The migration of this boundary was examined as a function of applied stress, dislocation climb mobility, and misorientation between grains adjacent to the boundary. Under an applied stress that gives rise to boundary migration, the dislocation network that comprises the boundary also translates along the boundary plane, i.e., migration normal to the boundary plane is coupled to tangential motion in the plane of the boundary. From the simulations, we find the boundary migration velocity to be directly proportional to the applied stress. At the same applied stress, the migration velocity increases with increasing dislocation climb mobility. We derive analytical expression for the mobility as well as the ratio of tangential to normal motion for a mixed LAGB having a simple and well-defined dislocation structure.

12:10 PM

Discrete Dislocation Simulations of Plasticity of Polycrystalline Thin Films: Caizhi Zhou¹; Richard LeSar¹; ¹Iowa State University

The mechanical properties of metallic thin films are of great importance in determining the reliability of microelectronic devices and have thus attracted much attention in materials research. One of the most important phenomena is that their strength differs significantly from that of the corresponding bulk materials when their dimensions become comparable to the length scales of the underlying dislocation microstructures. In our study, 3-D discrete dislocation dynamics (DDD) simulations have been used to investigate the size-dependent plasticity of polycrystalline thin films. We consider both cross-slip of dislocations and stress relaxation at grain boundaries. In this talk, we will relate the plastic deformation of polycrystalline thin films to such quantities as thin film thickness, grain size and dislocation density. In addition, we will compare the simulation results to experiment to guide the development of simple, accurate models for predicting thin film behavior.

Computational Thermodynamics and Kinetics: Thermodynamics and Microstructure Evolution in Soft Matter

Sponsored by: The Minerals, Metals and Materials Society, ASM International, TMS Electronic, Magnetic, and Photonic Materials Division, TMS Materials Processing and Manufacturing Division, TMS: Alloy Phases Committee, TMS: Chemistry and Physics of Materials Committee, TMS/ASM: Computational Materials Science and Engineering Committee, ASM: Alloy Phase Diagrams Committee *Program Organizers*: Raymundo Arroyave, Texas A & M University; James Morris, Oak Ridge National Laboratory; Mikko Haataja, Princeton University; Jeff Hoyt, McMaster University; Vidvuds Ozolins, University of California, Los Angeles; Xun-Li Wang, Oak Ridge National Laboratory

Thursday AM	Roo
March 3, 2011	Loca

Room: 9 Location: San Diego Conv. Ctr

Session Chairs: Mikko Haataja, Princeton University; James Morris, Oak Ridge National Laboratory

8:30 AM Invited

Continuum-Level Simulations of Two-Phase Lipid Membranes Coupling Composition with Deformation: Chloe Funkhouser¹; Francisco Solis²; *Katsuyo Thornton*³; ¹University of Michigan - Department of Biomedical Engineering; ²Arizona State University West - Division of Mathematical and Natural Sciences; ³University of Michigan - Department of Material Science & Engineering

We examine the formation and evolution of lipid raft-like domains in twophase lipid membranes using a continuum-level simulation method. Our model couples composition with membrane deformation using a modified Helfrich free energy. The compositional evolution is modeled with a phasefield method and is described by a Cahn-Hilliard-type equation, while the shape changes are described by relaxation dynamics in which surface area is conserved. Our objective is to investigate how various physical input parameters such as spontaneous curvature, bending rigidity, and phase fraction affect the dynamics and equilibrium morphological phases formed in lipid membrane vesicles and tubules. We find that the compositional and shape evolution are significantly altered when mechanical coupling is present by comparing the results with those of systems where this coupling is absent. Both dynamics and equilibria are examined to elucidate the link between the morphologies of the membranes with their physical properties.

9:10 AM Invited

Lateral Segregation in Lipid Bilayer Membrane Modulated by Curvature: *Tobias Baumgart*¹; ¹University of Pennsylvania

Lateral segregation of lipids and proteins in lipid bilayer membranes lies at the heart of fundamental biological phenomena such as organelle homeostasis, membrane signaling, and trafficking. Our research is directed at understanding how membrane curvature affects lateral segregation in both weak and strong segregation limits in the phase diagram of mixed model membranes. We will discuss the biophysical method of micropipette aspiration of giant unilamellar vesicles, which are bilayer membranes with spherical topology. These vesicles can be used to generate tubular membranes with adjustable radius that allow quantitatively investigating the role of curvature in modulating local membrane composition. In the strong segregation limit we introduce the phenomenon of curvature-induced nucleation and growth of lipid phases. In the weak segregation limit, we observe segregation with qualitative differences along two roughly orthogonal directions in the lipid mixing phase diagram. 140th Annual Meeting & Exhibition

9:50 AM

Modeling the Self-Assembly of Arbitrary-Shaped Ferro-Colloidal Particles in Bulk Liquid and at Fluid Interface: Tianle Cheng¹; Yu Wang¹; Paul Millett²; ¹Michigan Technological University; ²Idaho National Laboratory

Development of a novel diffuse interface field approach to modeling and simulation of self-assembly of ferro-colloidal particles in bulk liquid (e.g. uncured polymer melt) and at fluid interface (e.g. multi-phase fluid) is presented. The model employs diffuse interface fields to describe arbitrary particle shapes and sizes as well as dipole and charge properties. Particle interactions of long-range (electrostatic) and short-range (contact) as well as with fluid interface (capillary) are taken into account. In particular, electrostatic force is accurately treated (conventional point-dipole/charge approximation is not applicable due to non-spherical particle shapes and small inter-particle distances). Evolving microstructures of particle selfassembly and fluid interfaces with/without applied external field (used to tune self-assembling forces and control particle microstructures) are simulated without explicitly tracking the boundaries of arbitrary-shaped particles and multi-phase fluid. Various simulation examples are presented to demonstrate the new model's capability and potential to engineer advanced material microstructures.

10:10 AM Break

10:20 AM Invited

Lipid Rafts Reach a Critical Point: Sarah Veatch¹; Benjamin Machta²; ¹University of Michigan; ²Cornell University

Multicomponent lipid bilayer membranes can contain two coexisting liquid phases, named liquid-ordered and liquid-disordered. Recently, we demonstrated that large (micron-scale) and dynamic critical fluctuations are found in ternary lipid bilayer membranes prepared with critical compositions. Remarkably, robust critical behavior is also found in compositionally complex vesicles isolated directly from living cell plasma membranes. This finding strongly suggests that cells tightly regulate plasma membrane protein and lipid content to reside near a critical point and that critical fluctuations provide a physical basis of functional membrane heterogeneity in living cells at physiological temperatures. We are currently probing for signatures of critical fluctuations in intact cells using high resolution imaging techniques (scanning electron microscopy and super-resolution fluorescence localization microscopy). In addition, we are investigating possible structural and functional consequences of plasma membrane criticality using computational approaches.

11:00 AM Invited

Mesoscale Computational Studies of the Compositional and Morphological Heterogeneties of Biomembranes: Mohamed Laradji¹; ¹University of Memphis

Biomembranes are complex quasi-two dimensional fluids composed of various types of lipids and proteins. Experiments showed that plasma membranes of animal cells exhibit compositional and morphological organization. These include, nanoscale lipid domains, known as rafts, which are rich in saturated lipids and cholesterol. Lipid rafts are implicated in signaling, recruitment and endocytosis. Reasons for the finite size of lipid rafts remain elusive. This emphasizes the importance of understanding both the phase behavior and kinetics of multicomponent membranes while incorporating as many ingredients present in the plasma membrane. In this talk, I will review some of the computational work done by us for studies of both compositional and morphological heterogeneties in lipid membranes using mesoscale modeling either explicit or implicit solvent. This work is supported by NSF (DMR 0812470 and DMR 0755447) and the Research Corporation (CC6689).

11:40 AM Invited

Solid Domains on Fluid Lipid Vesicles Induced by pH: Stavroula Sofou¹; ¹Polytechnic Institute of New York University

Lipid bilayer membranes in the form of giant unilamellar vesicles (GUVs) were prepared. Lipid mixtures were composed of two lipid types - a lipid

with a titratable headgroup and a non-titratable headgroup - and variable levels of cholesterol. GUVs were prepared using the gentle hydration method and were imaged at room temperature using fluorescence microscopy. We show that lowering pH induces increase of the extent of formation of phase separated solid (gel) domains with size, shape and number that depend on the final pH value and the cholesterol content. Phase separation with lowering pH seems to be mostly driven by hydrogen bonding among the titratable lipid headgroups. At the lowest pH studied all mixtures exhibit formation of "florets". We suggest that this is mostly driven by the decrease of the overall membrane area per GUV arising from the shrinkage of the area in the gel phase domains at lower pH.

Electrode Technology for Aluminium Production: Cathode Materials and Wear

Sponsored by: The Minerals, Metals and Materials Society, TMS Light Metals Division, TMS: Aluminum Committee Program Organizers: Alan Tomsett, Rio Tinto Alcan; Ketil Rye, Alcoa Mosjøen; Barry Sadler, Net Carbon Consulting Pty Ltd

Thursday AM	Room: 16B
March 3, 2011	Location: San Diego Conv. Ctr

Session Chair: Frank Hiltmann, SGL Carbon GmbH

8:30 AM Introductory Comments

8:35 AM

Measurement of Cathode Surface Wear Profiles by Laser Scanning: Egil Skybakmoen1; Stein Rørvik1; Asbjorn Solheim1; Knut Ragnar Holm2; Priska Tiefenbach²; Oyvind Ostrem²; ¹SINTEF Materials and chemistry; ²NTNU

The service life time for high amperage aluminium reduction cells with graphitized cathodes is limited by cathode wear. The wear is normally very non-uniform, and it is commonly documented by photography and/or point measurements by levelling. In an attempt to record the wear surface in a much more detailed way, a laser scanning procedure was developed. A laser scanner with an accuracy of ± 0.5 cm has been used to produce a 3D model based on three overlapping scans with an average resolution of about 1 cm. The same cathodes was also measured with a leveller for comparison. The method developed gives detailed information regarding the wear at different positions within the cell, and it may become a valuable tool for investigating the influence of different parameters on the cathode wear.

9:00 AM

Coke Selection Criteria for Abrasion Resistant Graphitized Cathodes: Raymond Perruchoud¹; Werner Fischer¹; Markus Meier¹; Ulrich Mannweiler²; ¹R&D Carbon Ltd.; ²Mannweiler Consulting

The high abrasion rate of the graphitized cathodes became a major limitation of the pot lining life time for high amperage cells. This is related to the usage of low Sulfur anode grade petroleum coke resulting in too soft a cathode after graphitization. A review of the effects of the coke characteristics on the cathode abrasion and on the other pot lining relevant properties has been performed on a pilot scale. The selection of more isotropic calcined coke prepared by delayed coking of appropriate soft pitches allowed to decrease the abrasion rate by four times. No detrimental effects on the graphitization behaviour nor on the cathode relevant properties have been observed. Dedicated tar pitch feedstocks in optimized delayed coking have the potential, together with shaft kiln calcinations, to solve the W shaped wear of graphitized cathodes responsible of the short pot life time.

9:25 AM

Determination of the Effect of Pitch-Impregnation on Cathode Erosion Rate: Pretesh Patel1; Yoshinori Sato2; Pascal Lavoie1; 1Light Metals Research Centre; 2SEC Carbon, Ltd

In recent years, a number of smelters have adopted or trialed higher density, pitch impregnated cathode blocks as a measure to counter the decreasing cell life trend due to line current increases. To date, the true benefits of pitch impregnated cathode blocks are not fully understood. A collaboration between SEC CARBON Limited and the Light Metals Research Centre has therefore endeavored to understand the effects of pitch impregnation on cathode block performance. It was previously reported that pitch impregnated materials were found to have detrimental effects in regards to electrochemical wear resistance, and it was proposed that pitch impregnation increases reactivity of the cathode material. This paper will concentrate on recent work which was carried out firstly to characterize the difference between the pitch impregnation phase and the bulk cathode matrix and secondly to determine the reactivity of these phases under electrolysis conditions.

9:50 AM

Simplifying Protection System to Prolong Cell Life: Maryam Al Jallaf¹; Margaret Hyland²; Barry Welch³; Ali Al Zarouni¹; ¹DUBAL; ²University of Auckland; ³Welbank Consulting Ltd.

Cathode materials are mainly deteriorated by physical erosion, chemical and electrochemical corrosion. The wear patterns are characterised by "W-shaped wear" and localised potholes. A variety of materials such as alpha alumina and refractory hard materials have been used for protecting conventional cathodes.TiB2 based refractory hard materials are well suited for this. They satisfy the electrical conductivity requirements, have a very low solubility in molten aluminium and are wetted by aluminium providing potential benefit. The focus of study was to explore the potential of increasing life of graphitised cathodes using TiB2 grains without compromising on metal purity or cell performance and lining design. Statistical tools were used to determine the significance of erosion rate in operating cells. The study revealed that cathode life could be increased by at least 2 years. Increase in Ti and B impurities in pot metal was within the tolerance limits of the casthouse.

10:15 AM Break

10:25 AM

Aluminate Spinels as Sidewall Linings for Aluminum Smelters: Xiao Yan¹; Reiza Mukhlis²; M. Rhamdhani²; *Geoffrey Brooks*²; ¹CSIRO; ²Swinburne University of Technology

There is a need for ledge-free sidewalls due to about 30% energy savings for the Hall-Heroult process. However, this approach poses great material challenges because such sidewalls are in direct contact with oxidizing, corrosive and reducing environments at different cell locations. Here, NiAl₂O₄, MgAl₂O₄ and Ni_{0.5}Mg_{0.5}Al₂O₄, were identified and tested in cryolite-based baths at 980 °C under air and CO₂. Both specimens and baths were characterized using XRD, XRF and SEM-EDS methods. This study revealed that the NiAl₂O₄ and MgAl₂O₄ spinels had good corrosion resistances towards a molten cryolite-AlF₃-Al₂O₃-CaF₂ bath under CO₂, with solubility of Ni from NiAl₂O₄ being 100ppm and Mg from MgAl₂O₄ being 700ppm. Dissolutions of Ni and Mg into the bath were lowered to 70ppm Ni and 500ppm Mg by forming a Ni_{0.5}Mg_{0.5}Al₂O₄ solid solution due to reduced activities of NiO and MgO in the spinel solution. The corrosion behaviour of the Fe spinels is also discussed.

10:50 AM

A New Ramming Paste with Improved Potlining Working Conditions: *Bénédicte Allard*¹; Régis Paulus¹; Gérard Billat²; ¹Carbone Savoie - Vénissieux - France; ²Carbone Savoie - Aigueblanche - France

The ramming paste used in the aluminium electrolysis pots has long been a concern regarding health, safety and environment. While the situation has improved over the last 20 years, pastes on the market today still contain either carcinogenic products as PaH components or phenol, or other hazardous components. Health regulations in many regions require substitution of these hazardous components as soon as an acceptable alternative becomes available. A new paste, NeO², has been developed which contains no hazardous component, according to the present regulations. Standard physico-chemical properties of the paste have been studied, with some specific characterizations which will be detailed. This paper will provide a summary of paste developments and provide the latest results achieved with the NeO² paste.

11:15 AM

Towards a Better Understanding of Carburation Phenomenon: Martin Lebeuf¹; *Marc-André Coulombe*¹; Bénédicte Allard²; Gervais Soucy¹; ¹Université de Sherbrooke; ²Carbone Savoie

Cathode wear in aluminum electrolysis cells is an undesirable phenomenon which decreases potlife. Although it has been the subject of many studies, it is not yet satisfactorily understood. One major factor of this wear is the formation and dissolution of aluminum carbide, for which the mechanisms still remain to be thoroughly explained. Laboratory scale electrolysis experiments were performed under different operating conditions, namely the current density, the presence or absence of an aluminum metallic layer on the cathode surface and the atmosphere type. The aluminum carbide formation was then studied using X-ray Photoelectron Spectroscopy (XPS), Scanning Electron Microscopy-Energy Dispersive Spectroscopy (SEM-EDS), X-Ray fluorescence (XRF) and optical microscopy. In particular, the XPS analysis permitted further investigation of the chemical species present in bath-penetrated veins of the carbon cathode.

11:40 AM

Characterization of Sodium and Fluorides Penetration into Carbon Cathodes by Image Analysis and SEM-EDS Techniques: *Yuanling Gao*¹; Jilai Xue¹; Jun Zhu¹; Kexin Jiao¹; ¹Unversity of Science and Technology Beijing

The porous structure in carbon cathodes is materials dependent, which can provide channels for sodium and fluorides penetration during aluminum electrolysis. This work is aimed to develop a better digital method for characterization of the pores and the penetration resistance of the cathode products. The profiles of penetrated Na, F, Al vs. penetration depth in the cathode samples after aluminum electrolysis were obtained using SEM-EDS analysis. The internal porosity, pore size distribution, pore shape and direction, pore connectivity, etc. were also characterized by image analysis. It was found that the pore connectivity, not the total porosity, contribute the most to Na and F penetration varied with change in cathode materials (from semi-graphitic, full graphitic to graphitized carbons). Other detailed information about the correlation between the pore structures and Na-fluoride penetration will be presented.

Friction Stir Welding and Processing VI: Friction Stir Spot Welding

Sponsored by: The Minerals, Metals and Materials Society, TMS Materials Processing and Manufacturing Division, TMS: Shaping and Forming Committee

Program Organizers: Rajiv Mishra, Missouri University of Science and Technology; Murray Mahoney, Retired from Rockwell Scientific; Yutaka Sato, Tohoku University; Yuri Hovanski, Pacific Northwest National Laboratory; Ravi Verma, General Motors

Thursday AM	Room: 5B
March 3, 2011	Location: San Diego Conv. Ctr

Session Chairs: Tony Reynolds, University of South Carolina; Michael West, South Dakota School of Mines and Technology

8:30 AM Invited

Fatigue Behavior of Dissimilar Friction Stir Spot Welds between Aluminum and Steel Sheets: Van-Xuan Tran¹; Jwo Pan¹; ¹University of Michigan

Fatigue behavior of dissimilar friction stir spot welds in lap-shear specimens of aluminum 6000 series alloy and coated steel sheets is investigated based on experiments, analytical solutions and three-dimensional finite element analyses. The Al/Fe welds were tested under cyclic loading conditions.

TMS2011 140th Annual Meeting & Exhibition

Optical micrographs of the failed welds show that the Al/Fe welds mainly fail along the interfacial surface between the aluminum and steel sheets. Three-dimensional finite element analyses were conducted to obtain the stress intensity factor and J integral solutions for the welds with complex geometry, bend and gap. Analytical solutions for the equivalent welds with consideration of the bend and gap were also derived. The computational and analytical solutions suggest that the J integral and in-plane effective stress intensity factor solutions at the critical locations of the welds can be used as fracture mechanics parameters to correlate the fatigue crack growth patterns of the Al/Fe welds in lap-shear specimens.

8:55 AM

Material Flow and Temperature Distribution in Friction Spot Welding of Al and Steel: Yingchun Chen¹; Phil Prangnell¹; ¹The University of Manchester

The material flow in friction spot welding of Al to steel has been investigated by differential etching after welding a split top sheet consisting of two Al-alloys with similar mechanical properties, but different copper contents. The temperature distribution was studied using an infrared thermal camera and thermocouples. The effect of rotation speed, plunge depth, dwell time, surface condition of steel sheet (un-coated and galvanized), and tool coupling on the material flow and temperature distribution are systematically discussed. The aim of the work was to better understand the effect of coupling with the spot welding tool and, between the top and bottom sheets, as a function of the tool geometry and the welding conditions, on the relationship between material flow and the temperature distribution, and the formation of weld defects and intermetallic reaction layers at the joint interface during welding.

9:15 AM

Continued Development of Friction Stir Spot Welding for Advanced High Strength Steels

: Yuri Hovanski¹; Michael Santella²; Glenn Grant¹; ¹Pacific Northwest National Laboratory; ²Oak Ridge National Laboratory

With successful research in friction stir spot welding of advanced high strength steel alloys demonstrating that tool materials do exist that can be utilized to rapidly produce spot joints in a variety of high strength automotive sheet materials, heightened interest continues to further development of process parameters and tooling for production ready applications. As such a specific list of targeted alloy and thickness combinations were investigated for joinability by means of friction stir spot welding. Combinations of hotstamp boron steels, transformation induced plasticity steels and dual-phase alloys were utilized to investigate spot joints between dissimilar alloy and thickness combinations. Mechanical properties of the lap joints along with an investigation of the sheet interfaces are presented. Low cost versions of both polycrystalline cubic boron nitride and silicon nitride tools were used during the evaluation, and their potential for high volume production is reported.

9:35 AM

Structure-Property Relationships of Fatigue in Friction Stir Spot Welding of AZ31 Mg Alloy: *J Jordon*¹; ¹Mississippi State University

In this present work, structure-property relations are quantified in regards to fatigue performance of friction stir spot welding. Lap-shear coupons of AZ31 magnesium alloy were spot welded using two sets of tooling and welding parameters. Optical microscopy of the initial state of the microstructure of each set of spot welds revealed differences in the weld interface in both size and shape. Both sets of welds were fatigue tested in load control until failure at various load ratios. Fractography analysis revealed differences in the failure modes and the number of cycles to failure for the two sets of coupons. Direct correlations were made between the structure of the weld interface and the number of cycles to failure.

9:55 AM

Mechanical and Microstructural Investigation of Dissimilar Resistance and Friction Stir Spot Welds in AA5754-H22 and AA6082-T6 Aluminium Alloys and 22MnB5 Hot-Stamped Boron Steel: *Antonio da Silva*¹; Egoitz Aldanondo¹; Pedro Alvarez¹; Alberto Echeverría¹; Martin Eiersebner²; ¹Research Centre LORTEK; ²FRONIUS International GmbH

The aim of this investigation is to evaluate and compare two distinct spot joining processes suitable for dissimilar welding aluminium and steel for mass production applications in the automotive industry: Friction Stir Spot Welding (FSSW) and Resistance Spot Welding (RSW). The effect of joining parameters on the mechanical and microstructural properties of dissimilar 1 mm-thick aluminium alloys (AA5754-H22 and AA6082-T6) and 22MnB5 hot-stamped boron steel joints produced by both processes has been investigated. Microstructural features of FSSW and RSW connections have been analysed; while mechanical performance has been investigated in terms of hardness and shear testing. Failure modes of shear specimens have been also investigated. Maximum failure loads close to 3 kN have been obtained in RSW connections; while FSSW has shown lower failure loads. Interfacial failure mode has been observed in RSW conditions; while a mixture of interfacial and nugget pullout failure modes have been found for FSSW connections.

10:15 AM

Effect of Coating on Mechanical Properties of Magnesium Alloy Friction Stir Spot Welds: *Wei Yuan*¹; R.S. Mishra¹; B. Carlson²; R. Verma²; R. Szymanski²; ¹Missouri University of Science and Technology; ²General Motors R&D Center

Magnesium alloy AZ31 sheets with a 25 um coating layer were friction stir spot welded. Compared to bare AZ31 sheet, the coated material exhibited lower tool plunge force for similar process parameters. Lap-shear tests indicated a much lower separation load for the coated AZ31 spot welds. The coated specimens separated in a nugget pull-out mode as a result of bottom-sheet cracking in the thermomechanically affected zone adjacent to the nugget. The initial crack started from the under surface of the bottom sheet and appeared to be dependent on thermal stress and strain gradient. The length of the crack varied as the tool rotation rate changed, and the crack moved away from the weld center as nugget size increased.

10:35 AM Break

10:45 AM Invited

Process-Properties Relationship in Friction Spot Welds on Aircraft Al-Alloys: Gabriel Pieta¹; *Jorge dos Santos*¹; Ana Paula Camilo²; Sergio Amancio¹; Marcelo Beltrao¹; Sebastiao Kury²; Nelson de Alcantara; Nelson de Alcantara²; ¹GKSS Forschungszentrum; ²Federal University of Sao Carlos

Friction Spot Welding (FSpW) is a new solid-state joining process able to produce similar and dissimilar overlap connections in different classes of materials. Advantages of this new technique are: short production cycles, high performance joints, absence of filler materials and good surface finishing supported by material refilling in the spot area. Although few authors have addressed the microstructural and mechanical behavior of friction spot welds of Aluminum alloys, there is still a lack of a systematic evaluation on the process-properties relationship. In this work aircraft aluminum alloy (rolled sheets) were investigated. Design of experiment (DOE) and analyses of variance (ANOVA) techniques were applied to evaluate joint shear strength under static loading. Sound joints with elevated shear strength were achieved and the influence of the main process parameters on joint strength evaluated.

11:10 AM

Retractable vs. Fixed Probe Tools in Swept Friction Stir Spot Welding: *Jeremy Brown*¹; James Gross¹; Jeff Buller¹; Dwight Burford¹; ¹Wichita State University

Swept Friction Stir Spot Welding is a variation of Friction Stir Spot Welding (FSSW). In contrast to conventional plunge and retract FSSW, in swept FSSW the tool is programmed to travel along a closed path following the plunge. The advantages of swept FSSW over the conventional FSSW

include a larger joint shear area and the minimization of hooking defects. A disadvantage of creating a FSSW joint with a Fixed Probe Tool (FPT) is the exit hole left in the joint. A potential method for removing the exit hole is to use a Retractable Probe Tool (RPT) where the probe may be retracted from the workpiece during welding. In this study the relative advantages and disadvantages of using RPT technology instead of FPT technology in swept FSSW have been examined by comparing the lap shear strength and fatigue life of joints produced by both technologies in 1mm thick AA7075 on AA2024.

11:30 AM

Friction Stir Spot Welding of Magnesium to Aluminum Alloys with a Cold Sprayed Interlayer: *Dustin Blosmo*¹; Todd Curtis¹; Timothy Johnson¹; Nicholas Procive¹; Christian Widener¹; Blair Carlson²; Robert Symanski²; Michael West¹; ¹South Dakota School of Mines and Technology; ²General Motors

The research focus is to join thin sheet magnesium to aluminum. Magnesium AZ-31 alloy was joined to Al 5754 alloy using both plunge spot welding and refill friction stir spot welding. A design of experiments was conducted to study the affect of welding parameters including plunge rate, plunge depth, and rotation speed on the joint strength and failure mode. Welds made on bare metal were compared to welds using different interlayers deposited using the cold spray process. Microstuctural analysis was also performed to characterize grain size and intermetallic formation.

11:50 AM

Swept FSSW in Aluminum Alloys through Sealants and Surface Treatments: *Karin Witthar*¹; Jeremy Brown¹; Dwight Burford¹; ¹Wichita State University

The objective is to investigate the effects that surface treatments have on the faying surface of 7075-T73 to 2024-T3 friction stir spots welds. The effects studied include mechanical properties and corrosion resistance. This experiment generates Friction Stir Spot Welded aluminum sheets of 0.040" thick 2024-T3 to 7075-T73. The dissimilar alloy sheets are treated with Alodine 600, and a sealant placed on the faying surface of the welds. The sealants chosen for this experiment are PRC-DeSoto PR-1432 GP and PRC-DeSoto PS 870 GRV. Coupons without sealants are also evaluated to establish a baseline statistical comparison. Four pin tools are used for these experiments. These pin tools have varying flow direction relative to the shoulder – neutral, additive, subtractive, and mixed. Mechanical properties of coupons with a guided 4-spot configuration are tested through ultimate lap shear and fatigue testing. Corrosion tested coupons are welded in a single spot configuration.

General Abstracts: Light Metals Division: Metal Matrix Composites

Sponsored by: The Minerals, Metals and Materials Society, TMS Light Metals Division, TMS: Aluminum Committee, TMS: Aluminum Processing Committee, TMS: Energy Committee, TMS: Magnesium Committee, TMS: Recycling and Environmental Technologies Committee

Program Organizers: Alan Luo, General Motors Corporation; Eric Nyberg, Pacific Northwest National Laboratory

Thursday AM	Room: 17A
March 3, 2011	Location: San Diego Conv. Ctr

Session Chair: Alan Luo, General Motors Global Research & Development

8:30 AM

Preparation and Characterization of Cast Hypereutectic Al-20wt.%Si-4.5wt.%Cu Nanocomposites with Al₂O₃ Nanoparticles: *Hongseok Choi***¹; Xiaochun Li¹; ¹University of Wisconsin-Madison**

Hypereutectic Al-20Si-4.5Cu nanocomposites were cast with various percentages of γ -Al₂O₃ nanoparticles that were dispersed by an ultrasonic

method. The as-cast Al-20Si-4.5Cu-Al₂O₃ nanocomposites showed marked enhancements in both strengths and ductility when compared with those of the original alloy without the nanoparticles. The ductility was significantly increased for more than 10 times with an addition of 0.5wt.% γ -Al₂O₃ nanoparticles. Microstructural analysis with optical and scanning electron microscopy (SEM) revealed that both the primary and eutectic silicon phases were significantly refined. The primary silicon phases were refined from star shapes to polygon or blocky shapes, and their edges and corners were much smoother. The large plate eutectic silicon phases were also modified into the fine fibrous ones.

8:55 AM

An Investigation of Nanoparticle Wetting, Grain Refinement and Mechanical Property Enhancement in Aluminum Matrix Nanocomposites: *Michael De Cicco*¹; Dake Wang¹; Xiaochun Li¹; ¹University of Wisconsin-Madison

Nanoparticle wettability and incorporation during ultrasonic processing was studied in a pure aluminum (Al) matrix with TiC_{0.7}N_{0.3} and Al₂O₃ nanoparticles. Additions of wetting elements of magnesium (Mg) and titanium (Ti) were used to enhance nanoparticle incorporation and wetting. In the pure Al without wetting elements significant $TiC_{0,7}N_{0,3}$ incorporation was observed however there was no observed incorporation of the Al₂O₃ nanoparticles. Additions of 0.2% Ti and 0.8% Mg (weight %) did not improve the incorporation of the $TiC_{0.7}N_{0.3}$ nanoparticles however with 10% Mg addition there was improvement in $TiC_{0.7}N_{0.3}$ nanoparticle incorporation. Additions of 0.2% Ti resulted in good incorporation of Al₂O₃ nanoparticles. Adding Mg resulted in Mg containing oxides in the samples due to reaction with the Al₂O₃ nanoparticles. The Al-10Mg+TiC_{0.7}N_{0.3}, which had the most significant nanoparticle incorporation, showed significant grain refinement and mechanical property enhancement. This grain refinement and mechanical property enhancement was maintained when pieces of the original 1.5% $\rm TiC_{0.7}N_{0.3}$ nanocomposites were added to additional Al-10Mg for a final 0.5% TiC_{0.7}N_{0.3} nanocomposite. This illustrates the potential of a master nanocomposite approach for metal matrix nanocomposite (MMNC) processing.

9:20 AM

Influence of Processing Parameters on Distribution of Fibers in Cast Aluminium Matrix: Pengfei Yan¹; Guangchun Yao¹; Jianchao Shi¹; Xiaolan Sun¹; *Hongjie Luo*¹; ¹School of Materials & Metallurgy, Northeastern University

In this paper, 5% short carbon fibers reinforced aluminium matrix composites were prepared by stir casting method, using different stirring times and stirring speeds. The microstructure of the composites was observed through optical microscope and scanning electron microscopy (SEM), the tensile test was carried out. The results demonstrated that stirring time and stirring speed influence the microstructure and mechanical properties of the composites. The higher stirring time and stirring speed make the distribution of the fibers uniform and improved the mechanical properties. But beyond certain parameter, the fibers culster and breakage, and the mechanical properties falles.

9:45 AM

In Situ Fabrication of Ceramic Containing Metal Matrix Composite onto a TC4 Ti Alloy by Laser Cladding: *Kemin Zhang*¹; Jianxin Zou²; ¹Shanghai University of Engineering Science; ²National Engineering Research Center of Light Alloy Net Forming, Shanghai Jiao Tong University

In the present work, a Ti based ceramic containing composite was successfully produced onto a TC4 Ti alloy by using laser surface cladding. TiC and Ti powders were mixed with a ratio of 1:3 and were put onto the TC4 alloy samples. They were then treated by laser beam with different scanning speed. The microstructure and composition modifications of the surface layer were investigated in details by using SEM, EDX and XRD techniques. The results have shown that, the laser clad layers have graded microstructures and compositions originated from the rapid heating, melting and cooling during laser processing. The maximum hardness of the laser

clad layer can research as high as 4.5 times of the initial one while the wear resistance was significantly improved after laser cladding.

10:10 AM Break

10:40 AM

Stability of Nanoparticle Dispersion and Property Enhancement in Aluminum Matrix Nanocomposites during Repeated Casting Cycles: Dake Wang¹; Michael De Cicco¹; Xiaochun Li¹; ¹University of Wisconsin-Madison

It was shown that aluminum metal matrix nanocomposites (MMNCs) can be simply recast and maintain good nanoparticle dispersion and property enhancement. Pure aluminum nanocomposites with 1.5 volume % $TiC_{0,7}N_{0,3}$ nanoparticle addition were produced by ultrasonic dispersion and cast in a permanent mold. The initial castings showed a significantly refined grain structure as well as 20% enhancement in yield strength, 24% enhancement in tensile strength and 7% enhancement in elongation. The materials were then remelted and cast four additional times. Scanning electron microscopy (SEM) analysis showed the nanoparticles remained well dispersed, and tensile testing showed maintained mechanical property enhancement.

11:05 AM

Study of Sputtering Deposition of Aluminum Boride-Based Composite: *Glorimar Ramos*¹; O. Marcelo Suárez¹; ¹University of Puerto Rico-Mayaguez Campus

New polymer/Al-based hybrid composites were proposed for device fabrication, which require precise formulation of sputtered Al/AlB₂ composite layers due to their tunable elastic modulus. Two methods were investigated to this purpose. In the first one the sputtering targets utilized were cast via centrifugal casting with added silicon to improve the part (target) castability. Particle gradient concentration allowed fabricating several sputtering targets in just one centrifugal casting process. In the second method, deposition of alternating Al and AlB₂ layers were analyzed. The deposited films obtained through both methods were compared and investigated using atomic force microscopy to observe surface grain morphology while a stylus profiler allowed measuring the film roughness and overall topography.

11:30 AM

Corrosion Behavior of Metal-Matrix Composite AlMg-SiCp: M.A. Hernandez¹; *S. Valdez*²; ¹E.T.S.E.I., Universidade de Vigo; ²UNAM-ICF

The AlMgSiC metal-matrix composite, obtained by Vortex Technique and the AlMg unreinforced alloy, have been studied in order to know their electrochemical response. The Vortex technique, generate a material composite with homogenous distribution of SiC particles and less casting porosity. The specimen tests were conducted in NaCl solution at 3.5 wt % for both the weight loss and potentiodynamic polarization measurements. The corrosion phenomena in unreinforced AlMg alloy were inhibited by the addition of silicon carbide particles, due to a slowing down the oxygen reduction reaction and the limiting cathodic current in function of time. The anodic dissolution in the alloy was proved by the formation of a nonstable oxide layer exhibiting partial protection having small resistance to polarization conditions.

11:55 AM

Preparation Process of Aluminum Foam Reinforced by Carbon Fibers: *Hongjie Luo*¹; Yihan Liu¹; ¹Northeastern university

In this paper, it shows the fabrication process of aluminum foam reinforced by carbon fibers, and effects of mass percentage and length of carbon fiber on aluminum foam structure and properties in detail. The results show that aluminum foam with uniform structure was prepared by copper-coated carbon fibers as the stabilizer, and the apparent density of aluminum foam gradually decreases along with increasing the copper-coated carbon fiber content. The apparent density and porosity were not influenced by carbon fiber length regularly. The compression performance results indicate that the quantity of carbon fiber has a remarkable influence on plateau stress and the platform width of aluminum foam. The plateau stress increases with the addition of carbon fiber obviously. The compressive strength of aluminum foam reinforced by carbon fiber is more than 5MPa generally, which is much higher than that of ordinary aluminum foam.

Hydrometallurgy Fundamentals and Applications: Session I

Sponsored by: The Minerals, Metals and Materials Society, TMS Extraction and Processing Division, TMS: Hydrometallurgy and Electrometallurgy Committee *Program Organizer:* Michael Free, University of Utah

Thursday AMRoom: 16AMarch 3, 2011Location: San Diego Conv. Ctr

Session Chair: Michael Free, University of Utah

8:30 AM Keynote

2011 EPD DISTINGUISHED LECTURER: The Removal of Arsenic, Selenium and Metals from Aqueous Solution by Iron Precipitation and Reduction Techniques: Larry Twidwell¹; ¹Montana Tech of The University of Montana

The removal of arsenic, selenium, and metal species from hydrometallurgical solutions and waste water has been and continues to be an important research topic. This presentation includes a discussion of the research conducted at Montana Tech of the University of Montana during the past twenty years and current literature studies. The discussion will be focused on removal of arsenic by co-precipitation with Fe(III) and Fe(II), co-precipitation with Fe(III) and Al(III), reduction using elemental iron; the removal of selenium by elemental iron and catalysed iron; and the removal of cadmium, copper, nickel, zinc by co-precipitationwith Fe(III) and Al(III).

9:10 AM

Enhanced Pressure Dissolution of Enargite Using Pyrite or Ferrous Sulfate: *Maria Ruiz*¹; Oscar Jerez¹; Jonathan Retamal¹; Rafael Padilla¹; ¹University of Concepcion

Enargite (Cu₃AsS₄) is hard to leach mineral in acid media, which requires high oxygen overpressures and high temperatures for fast dissolution rates. To improve the leaching kinetics of enargite in milder conditions, additions of pyrite or ferrous sulfate has been proposed. In this research, mixtures of enargite/pyrite, with 10 to 50 weight percent of pyrite, were leached in H_2SO_4 - O_2 media, while pure enargite was leached in H_2SO_4 - O_2 and H_2SO_4 - $FeSO_4$ - O_2 media. The results showed that mixtures of enargite/ pyrite leached faster than pure enargite and the rate enhancement increased with higher pyrite content. For a mixture with 50% pyrite, size 46 µm, complete dissolution could be obtained in 20 min at 180 °C and 690 kPa P_{O2} . In the same conditions, the dissolution of pure enargite was less than 15 %. Similarly, adding FeSO₄ to the leaching solution augmented the enargite leaching rate and again the rate enhancement increased with larger additions.

9:35 AM

Model and Simulation of Ion Exchange of Antimony: *Gerardo Cifuentes*¹; Jaime Simpson²; Cesar Zúñiga¹; Leoncio Briones¹; Alejandro Morales³; ¹USACH; ²ProPipe S.A.; ³UCN

A model is proposed for the removal of Sb by ion exchange from copper refining electrolytes that fits the data from the literature. The correction factors for the MX-2, UR-3300S and Duolite C-467 resins were 0.5531; 0.2839 and 0.5455, respectively. The following variables were studied: volume of resin (bed height), volumetric matter transfer coefficient, and initial antimony concentration in the solution. The model's average percentage error was 3.01%.

HURSDAY AM

10:00 AM Break

10:15 AM

Analysis of the Adsorption of Gold and Silver on Magnetic Species Formed in the Electrocoagulation Process: *Jose Parga*¹; Jesus Valenzuela²; ¹Institute Technology of Saltillo; ²University of Sonora

In metallurgical operations, cyanidations is the predominant process by which gold and silver are recovered from their ores and it is recognized that the Carbon in Pulp, Merrill-Crowe process or the Ion Exchange resins are used for the concentrations and purification of gold and silver from cyanide solutions. Among several options are available for recovery precious metals from cyanide solutions, Electrocoagulation (EC) is a very promising electrochemical treatment technique that does not require high concentrations of gold and silver in solutions.First, this study will provide an introduction to the fundamental concepts of the EC method for recovery precious metals fro cyanide solutions. In this research, X-ray Diffraction, SEM and Transmission Mossbauer Spectroscopy were used to characterize the solid products formed at iron electrodes during the EC process. The results suggest that magnetite particles and amorphous iron oxyhydroxides present in the EC products remove gold and silver in 5 minutes.

10:40 AM

Characterization and Performance of Smart Anode for Cobalt Electrowinning: *Masatsugu Morimitsu*¹; Katsuya Kawaguchi¹; ¹Doshisha University

Smart anodes for cobalt electrowinning were developed by thermal decomposition of a precursor solution containing ruthenium and titanium compounds. Low temperature decomposition produced less crystalline composite oxide on a titanium substrate, and the oxide showed a high catalytic activity for chlorine evolution and suppressed the anodic deposition CoOOH in cobalt electrowinning solutions. These properties were effective to reduce the cell voltage of cobalt electrowinning and the sludge as deposited on the crystalline oxide surface.

11:05 AM

Treatment of Acid Mine Drainage by Electrodialysis: *Daniella Buzzi*¹; Lucas Viegas²; Flávia Silvas¹; Marco Antônio Rodrigues³; Ivo André Schneider²; Andréa Bernardes²; Denise Espinosa¹; Jorge Alberto Tenório¹; ¹Universidade de São Paulo; ²Universidade Federal do Rio Grande do Sul; ³Universidade Feevale

One of the major impacts caused by coal mining activity is water pollution from acid mine drainage (AMD). AMD is produced by the reaction of pyrite, water and oxygen, that is intensified in the acidophilic bacteria presence. This solution acts as a leaching agent of minerals present in the residue, producing a solution with dissolved metals and sulfuric acid. Conventional treatment of AMD consists of neutralization and precipitation of heavy metals, but is technically deficient. The electrodialysis (ED) has emerged as an attractive process for effluents treatment since it does not need reagents addition and generates no waste polluting in the environment. The ED used to treat the AMD is a membrane process that consists in the separation of cations and anions by the application of an electric field on a process cell. In this study the possibility of using ED to the AMD treatment was evaluated aiming water reuse.

Magnesium Technology 2011: New Applications (Biomedical and Other)

Sponsored by: The Minerals, Metals and Materials Society, TMS Light Metals Division, TMS: Magnesium Committee Program Organizers: Wim Sillekens, TNO Science and Industry; Sean Agnew, University of Virginia; Suveen Mathaudhu, US Army

Research Laboratory; Neale Neelameggham, US Magnesium LLC

Thursday AM	Room: 6F
3	Location: San Diego Conv. Ctr

Session Chairs: Norbert Hort, Helmholtz-Zentrum Geesthacht; Michele Manuel, University of Florida

8:30 AM

Current Research Activities of Biomedical Mg Alloys in China: *Yufeng Zheng*¹; ¹Peking University

The potential biomedical application of Mg alloys as bioabsorable/ biodegradable implant in human body had been extensively studied worldwide, and becomes a emerging and promising application direction. Based on the presentations at a symposium on Biomedical Mg alloys in December 2009 at the 12th Annual Conference on Biomaterials, Chinese Society of Biomedical Engineering, and a symposium on Biodegradable Metallic Materials in May 2010 at Peking University, in these two conference the present author served as the Chairman and the abstract numbers are about 50 for each conference, the frontier research activities of biomedical Mg alloys in China as the orthopedic and cardiovascular implants will be systematically summarized and comprehensively reviewed in this paper. The research highlights on the alloying system design, novel structure, degradation rate control, surface modification methods of Bio-Mg will be demostrated via plenty of in vitro and in vivo study data.

8:50 AM Invited

Design Considerations for Developing Biodegradable Magnesium Implants: *Harpreet Brar*¹; Benjamin G. Keselowsky²; Malisa Sarntinoranont³; Michele V. Manuel¹; ¹University of Florida, Department of Materials Science and Engineering; ²University of Florida, Department of Biomedical Engineering; ³University of Florida, Department of Mechanical and Aerospace Engineering

The integration of biodegradable and bioabsorbable magnesium implants into the human body is a complex undertaking that faces major challenges. The complexity arises from the fact that biomaterials must meet both engineering and physiological requirements to ensure the desired properties. Historically, efforts have been focused on the behavior of commercial magnesium alloys in biological environments and their resultant effect on cell-mediated processes. Developing causal relationships between alloy chemistry and microstructure, and its effect on cellular behavior can be a difficult and time intensive process. A systems design approach driven by thermodynamics has the power to provide significant contributions in developing the next generation of magnesium alloy implants with controlled degradability, biocompatibility, and optimized mechanical properties, at reduced time and cost. This approach couples experimental research with theory and mechanistic modeling for the accelerated development of materials. The aim of this article is to enumerate this strategy, design considerations and hurdles for developing new magnesium alloys for use as biodegradable implant materials [1].

9:10 AM

Coating Systems for Magnesium-Based Biomaterials - State of the Art: Mark Staiger¹; Jay Waterman¹; ¹University of Canterbury

Magnesium and its alloys have the potential to be used for biodegradable orthopedic implants. However, the corrosion rate in physiological conditions is too high for most applications. For this reason, surface modification to slow the corrosion rate is of great interest. Such modifications must remain biologically compatible as well as protective in corrosive environments. What follows is a brief review of recent research in inorganic coatings and surface modifications to create coatings for magnesium-based biomaterials.

9:30 AM

Corrosion, Surface Modification and Biocompatibility of Mg and Mg Alloys: *Sannakaisa Virtanen*¹; Ben Fabry¹; ¹University of Erlangen

Mg-based materials corrode in aqueous biological environments and are of growing interest for use as biodegradable implants. For a successful and biologically safe application, a thorough understanding of the corrosion behavior in vivo is required but is currently lacking. In particular, the effects of proteins and cells on Mg corrosion are unknown. Moreover, the effect of Mg dissolution on the biological environment needs to be characterized, as the corrosion reaction is coupled with H2 gas evolution and surface alkalization. The aim of our study was to elucidate the interactions between corroding Mg (alloy) surfaces and cells, by an interdisciplinary approach of electrochemistry, surface modification and analysis, and cell culture testing. Of a special interest is the development of novel chemical and biological surface functionalization, to tailor the corrosion rate and biocompatibility.

9:50 AM

Magnesium Alloys for Bioabsorbable Stents: A Feasibility Assessment: *Charles Deng*¹; Rajesh Radhakrishnan¹; Steve Larsen¹; Dennis Boismier¹; Jon Stinson¹; Adrienne Hotchkiss¹; Jan Weber¹; Torsten Scheuermann¹; ¹Boston Scientific

Cardiovascular disease is the leading cause of the death in US. Stents are used to keep arteries open preventing cardiovascular disease related deaths. Presently, most stents consist of a stainless steel or other permanent metal alloy framework. Bioabsorbable stents are expected to provide scaffolding for the vessels for 3-6 months and then get fully absorbed within 1-2 years. They should ideally leave nothing behind, except the healed natural vessel, allowing restoration of healthy vessel properties. In this way, late stent thrombosis is unlikely, and prolonged anti-platelet therapy is not necessary. Also, bioabsorbable stents can be used as a delivery device for drugs such as Everolimus or Paclitaxel. Magnesium is a suitable candidate for bioabsorbable stent material. This presentation includes mechanical and electrochemical properties of magnesium alloy stents. In addition, it provides correlation between in vivo animal study and in vitro corrosion testing.

10:10 AM Break

10:30 AM

Processing Aspects of Magnesium Alloy Stent Tube: Robert Werkhoven¹; *Wim Sillekens*¹; Koos van Lieshout¹; ¹TNO Science and Industry

Biomedical applications are an emerging field of interest for magnesium technology, envisioning biodegradable implants that dissolve in the human body after having cured a particular medical condition (such as clogging of arteries or bone fractures). This challenges research in a sense that the materials to be used need to dissolve in vivo in a controlled fashion without leaving harmful remainders and while maintaining sufficient strength and other (mechanical) attributes as long as necessary. To comply to the requirements, magnesium alloys as well as their processing routes into implants need to be tailored. While new alloy compositions are receiving ample attention, the paper at hand addresses the latter issue. The application of choice is the (cardio)-vascular stent. The different steps in manufacturing magnesium AZX-alloy stent tube are considered, including extrusion and subsequent drawing operations. Strategy for development is that the microstructure of the stent tube should be rendered possibly fine.

10:50 AM

Ballistic Analysis of New Military Grade Magnesium Alloys for Armor Applications: *Tyrone Jones*¹; Katsuyoshi Kondoh²; ¹U.S. Army Research Laboratory; ²Joining and Welding Research Institute

Since 2006, the U.S. Army has been evaluating magnesium (Mg) alloys for ballistic structural applications. While Mg-alloys have been used in military structural applications since WWII, very little research has been done to improve its mediocre ballistic performance. The Army's need for ultra-lightweight armor systems has led to research and development of high strength, high ductility Mg-alloys. The U.S. Army Research Laboratory (ARL) and the Joining and Welding Research Institute (JWRI) of Osaka University collaborated through International Technology Center-Pacific (ITC-PAC) Contract Number FA-5209-09-P-0158 to develop the next generation of high strength, high ductility Mg-alloys using a novel Spinning Water Atomization Process (SWAP) for rapid solidification. New alloys AMX602 and ZAXE1711 in extruded bar form are characterized for microstructure, mechanical, corrosion, and ballistic response. Increases in ballistic performance and favorable corrosion resistance were evident when compared to the baseline alloy AZ31B.

11:10 AM

Mg17Al12 Intermetallic Prepared by Bulk Mechanical Alloying: Kenji Sakuragi¹; *Masashi Sato*¹; Takamitsu Honjo¹; Toshiro Kuji¹; ¹Tokai University

The properties of the metal hydrides are traditionally controlled by the nature and relative amount of the constituent elements. However, this straight forward way does not affect the thermodynamic properties of Mgbased hydrides in all cases, because the thermodynamic stability of Mgbased alloy is governed by the strong Mg-H bonding. In a last decade, nanocrystallised materials are widely investigated. The nano-crystalline provides other directions for solving many issues in the field of materials science. Ball milling process is general tool for preparing the nano-structured materials. The samples, however, show the fine powder form and the most of those are very sensitive against circumstance around. The bulk-form samples are desirable. In this study, it will be demonstrated that Mg17Al17 phase was prepared by newly developed Bulk Mechanical Alloying.

11:30 AM

Corrosion Behaviour of Mg Alloys in Various Basic Media: Application of Waste Encapsulation of Fuel Decanning from UNGG Nuclear Reactor: *David Lambertin*¹; Adrien Blachere¹; Fabien Frizon¹; Florence Bart¹; ¹CEA Marcoule

The dismantling of UNGG nuclear reactor generates a large volume of fuel decanning. These materials are based on Mg-Zr alloy. The strategy could be to encapsulate these wastes into an ordinary Portland cement (OPC) or geopolymer (aluminosilicate material) in a form suitable for storage. Studies have been performed on Mg or Mg-Al alloy in basic media but no data are available on Mg-Zr behaviour. The influence of representative solution of OPC and geopolymer with Mg-Zr alloy has been studied on corrosion behaviour. Electrochemical methods have been used to determine the corrosion densities at room temperature. Results show that the corrosions densities of Mg-Zr alloy in OPC solution is one order of magnitude more important than in geopolymer solution environment and effect of inhibiting agent has been undertaken with Mg-Zr alloy. Evaluation of encapsulation of Mg-Zr alloy in OPC and geopolymer has been done in term of corrosion hydrogen production.

Magnetic Materials for Energy Applications: Other Magnets

Sponsored by: TMS Electronic, Magnetic, and Photonic Materials Division, TMS: Energy Conversion and Storage Committee, TMS: Magnetic Materials Committee; JSPS 147th Committee on Amorphous and Nanocrystalline Materials; Lake Shore Cyrotronics, Inc.; AMT&C

Program Organizers: Victorino Franco, Sevilla University; Oliver Gutfleisch, IFW Dresden; Kazuhiro Hono, National Institute for Materials Science; Paul Ohodnicki, National Energy Technology Laboratory

Thursday AM	Room: 11A
March 3, 2011	Location: San Diego Conv. Ctr

Session Chair: Iver Anderson, Ames Laboratory

8:30 AM Invited

Nanoscaling like Noodles — A Novel Approach to Fabrication Nanocomposite Magnets with High Energy Density: *J.Ping Liu*¹; Chuanbing Rong¹; Ying Zhang¹; M.J. Kramer²; ¹University of Texas-Arlington; ²Ames Laboratory

Exchange-spring hard/soft phase nanocomposite magnets have extremely high energy density owing to the inter-phase exchange coupling. The precondition for the effective exchange coupling is the nanoscale soft phase grains homogenously distributed in the hard-phase matrix. Recently we found that by severe plastic deformation, the soft phase a-Fe grains in a SmCo/Fe composite system with the Fe concentration up to 35% can be "selfnanoscaled" to ~10 nm from the original particle size of 10 μ m. The ~1000 times size reduction is a result of a brittle/ductile composite deformation that leads to the elongation of the ductile component into noodle-like grains. The "noodles" then breakdown into nanoscale grains with further deformation. Subsequent warm compaction processing of the deformed nanocomposite particles produces fully dense bulk magnets with retained nanoscale morphology of the hard/soft phase composites. The energy density of the composite magnets is as double higher as the single-phase counterparts.

8:55 AM Invited

IntergranularDiffusioninExchange-CoupledSm-Co/FeNanocomposites and Thin Films:Matthew Kramer¹; Ying Zhang¹; J Liu²;Chuanbing Rong²;Ichiro Takeuchi³; Debjani Banerjee³; ¹Ames Lab/ISU;²University of Texas at Arlington; ³University of Maryland

The nanostructural features, especially grain sizes, soft phase distribution and their grain boundaries are critical features to be controlled in exchange coupled permanent magnets. Using advanced microscopy techniques, we have investigated the Co-Fe interchange in SmCo_5 +Fe and Sm_2Co_7 +Fe nanocomposites and thin films. We find that the behavior of the interdiffusion between the bcc soft phase and the magnetically hard phases are similar in thin films and bulk samples under similar annealing conditions: Co and Fe interdiffuse forming a $\text{Co}_{40}\text{Fe}_{60}$ bcc soft phase while the balance of the Fe forms a ternary Sm-Co-Fe phase of the initial phase. If the initial bcc phase has optimal Co content, substantial interdiffusion of Fe into the Sm-Co phases is not observed nor was the initial phase distributions retained. The magnetic properties of these alloys are inferior suggesting that optimal grain boundary chemistry is dependent on the appropriate local chemical driving forces.

9:20 AM

Hard Magnetic PrCo₃ Structural and Magnetic Properties: *Lotfi Bessais*¹; Khedidja Younsi¹; Vincent Russier¹; Jean-Claude Crivello¹; ¹CNRS

The structure and magnetic properties of nanocrystalline PrCo3 obtained from high energy milling technique and investigated by X-ray diffraction. Curie temperature determination and magnetic properties measurements are reported. The as-milled samples have been annealed in a temperature range of 1023K to 1273K for 30mn to optimize the extrinsic properties. The Curie temperature is 349K and coercive fields of 55kOe at 10K and 12kOe at 293K are obtained on the samples annealed at 1023K. A simulation of the magnetic properties in the framework of micromagnetism has been performed in order to investigate the influence of the nanoscale structure. A composite model with hard crystallites embedded in an amorphous matrix, corresponding to the as-milled material, leads to satisfying agreement with the experimental magnetization curve. The microscopic scale is also considered from DFT calculations of the electronic structure of RCo_x compounds where R=(Y,Pr) and x=2,3 and 5.

9:35 AM

Directional Annealing Induced Texture in Melt-Spun Sm-Co Based Alloys: *Tanjore Jayaraman*¹; Paul Rogge¹; Jeffrey Shield¹; ¹University of Nebraska

Developing texture in nanocrystalline permanent magnet alloys is important for continued development in permanent magnet materials. This paper reports texture development in melt-spun alloys using directional annealing, a novel approach that utilizes anisotropic grain growth for texture development. Melt spinning of $(Sm_{88}Co_{12})_{100-x-y}Nb_{x}C_{y}$ (x, y = 5) alloys produced isotropic grain structures of the SmCo, phase. The conventional and directional annealing formed the equilibrium Sm2Co17 phase. While conventional annealing resulted in random crystallographic orientations, directional annealing with appropriate combinations of annealing temperature and translational velocity resulted in the development of (0006) in-plane texture as determined by x-ray diffraction analysis. Magnetization measurements along different directions corroborate the texture development, and suggested that the degree of texture was on the order of 25-40 percent. Coercivity values above 2 kOe were maintained. The texture development via directional annealing while minimizing exposure to elevated temperatures provides a promising route to anisotropic high-energy permanent magnets.

9:50 AM

Magnetic Hardening of Nanocrystalline Sm-Fe-Mo Synthesized by Mechanical Alloying: Lotfi Bessais¹; Salwa Khazzan¹; *Najeh Mliki*²; Gustaaf Van Tendeloo³; ¹CNRS; ²University of Tunisia; ³EMAT, University of Antwerp

Materials based on rare-earth and iron have drawn much attention due to their high performance properties for permanent magnet application. The structural and magnetic properties of Sm2(Fe,Mo)17, its out of equilibrium precursor and their carbides are investigated by means of powder X-ray diffraction, magnetic measurements and HRTEM. In this work, the Rietveld analysis shows that the stoichiometry for the hexagonal phase is 1/9. Moreover, it points out a lattice expansion along the c axis after Mo substitution for Fe and reveals 2e preferential occupation for Mo atoms the out of equilibrium hexagonal precursor. Upon carbonation, the lattice expansion favors the Curie temperature increase up to 49% for the metastable 1/9C carbide. The Curie temperature and the coercive field of the 1/9 carbides are higher than those of 2/17 ones. This makes the hexagonal precursor a competitive candidate for use as permanent magnet.

10:05 AM

Understanding and Control of Coercivity in Non-Rare Earth Alnico Permanent Magnets: *Scott Long*¹; Iver Anderson²; R.W. McCallum²; Matthew Kramer²; Wei Tang²; Yaqiao Wu²; ¹Iowa State University; ²Ames Lab

Due to expanding Chinese markets & manufacturing capacity and subsequent decline in rare earth (RE) exports from this dominant RE source (97% world market), suitable alternatives to rare earth magnets are desired. Alnico alloys were the premier permanent magnet material before the development of Sm-Co and, especially Nd-Fe-B. Although coercivities are relatively low, Alnico magnets have the highest remanence of commercially available non-RE permanent magnets. Alnico magnets have superior thermal properties to Nd-Fe-B and, with modest improvements in coercivity, could be a viable alternative in many electric motor and generator applications. Alnico alloys rely on shape anisotropy of nano-scale precipitates as a main coercivity mechanism. The effects on coercivity of precipitate shape/ spacing and alignment of parent grains (prior to precipitation) will be investigated. Characterization methods will include SEM, TEM, and SQUID TMS2011 140th Annual Meeting & Exhibition

magnetometry and the results will be presented. Funding provided by DOE-EERE-FCVT Office through Ames lab Contract DE-AC02-07CH11358.

10:20 AM Break

Magnetic Materials for Energy Applications: Requirements of Magnetic Materials for Current Technological Applications

Sponsored by: TMS Electronic, Magnetic, and Photonic Materials Division, TMS: Energy Conversion and Storage Committee, TMS: Magnetic Materials Committee

Program Organizers: Victorino Franco, Sevilla University; Oliver Gutfleisch, IFW Dresden; Kazuhiro Hono, National Institute for Materials Science; Paul Ohodnicki, National Energy Technology Laboratory

Thursday AM	Room: 11A
March 3, 2011	Location: San Diego Conv. Ctr

Session Chair: Paul Ohodnicki, National Energy Technology Laboratory

10:30 AM Invited

The Transformational Potential of Magnetic Materials: ARPA-E Investment: *Rajeev Ram*¹; ¹ARPA-E

Producing electricity is the largest sink of primary energy in the US consequently electricity production is the largest contributor to atmospheric carbon dioxide. The ARPA-E ADEPT program is focused on improvements in electrical energy efficiency from lower cost, more efficient, solid-state lighting to lighter weight electrical vehicles to a flexible electricity grid. Program targets include converters utilizing magnetic materials with high operating flux exceeding 0.5T (15x greater than MnZn) with electrical resistivity exceeding 1mOhm-cm (5-10x MnZn) and high thermal conductivity. For chip-scale power conversion, novel magnetic materials deposited as CMOS compatible laminates or as ink-get printed and sintered nanocolloids are being developed. At the kW scale, module integrated converters employing advanced thick-film magnetic nanocomposites as well as transformer geometries are being explored. At MW scale, approaches include creating greater flexibility in grid assets such as transformers by employing advanced converter architectures that leverage bipolar SiC.

10:55 AM Panel Discussion

Requirements of Magnetic Materials for Current Technological Applications: *Moderator: Paul R. Ohodnicki*¹; ¹National Energy Technology Laboratory

Panelists:

Karl Gschneidner¹; ¹Ames Laboratory: Critical Parameters for the Utilization of First Order Magnetocaloric Regenerator Materials in Magnetic Cooling Machines

Takehisa Minowa¹; ¹Shin-Etsu Chemical Co. Ltd.: Application of Nd-Fe-B Magnets to the Megawatt Scale Generator for the Wind Turbine

Jinfang Liu¹; ¹Electron Energy Corporation: Industrial Requirements and Applications of Hard Magnetic Materials

*Aru Yan*¹; ¹Ningbo Institute of Material Technology and Engineering: **Current Status of Permanent Magnet Research and Market in China**

Francis Johnson¹; ¹General Electric Global Research: Industrial Needs and Applications for Soft Magnetic Materials

*Ryusuke Hasegawa*¹; ¹Metglas, Inc: **Soft Magnetic Materials in Energy Applications**

Sarah Bedair¹; ¹US Army Research Laboratory: Low Loss, High Power Density Magnetics in Inductor/Transformer Cores for Army Applications

12:35 PM

Industrial Requirements and Applications of Hard Magnetic Materials: *Jinfang Liu*¹; ¹Electron Energy Corporation

The selection of hard magnetic materials for industrial applications depends on many factors but is primarily determined by the trade off between cost and performance. Magnetic performance of interest includes residual induction (Br), coercivity (Hc) and intrinsic coercivity (Hci). Br and Hc are normally pre-determined by electromagnetic design. Application environment (temperature, humidity, and pH of the service environment) is a critical factor for the selection of hard magnetic materials. Applications of hard magnetic materials can be found everywhere, from cell phones, computers, automobiles, office appliances, to fighter jets, missiles, and space vehicles. In recent years, green technologies attracted a lot of attention. Hard magnetic materials play a significant role in many green technologies, such as electric or hybrid vehicles and wind turbines. Demand for hard magnetic materials is said to surge in the coming years.

12:45 PM

Low Loss, High Power Density Magnetics in Inductor/Transformer Cores for Army Applications: Sarah Bedair¹; Wesley Tipton¹; Damian Urciuoli¹; Brian Morgan¹; ¹US Army Research Laboratory

The Army Research Laboratory (ARL) currently has efforts in high efficiency power conversion for unique, military specific applications in the power ranges: 1) 1-100kW, 2)mW-10W. The former power requirements motivate high efficiency materials for use in bulk scale inductors and transformers. The magnetic material requirements include high B_{eat} with high operating temperatures (>120°C) and minimal switching losses (20-200kHz switching frequencies). There is also an ARL thrust for power conditioning units (mW-10W scale), where the vision is an ultra-miniature, mm³ scale, distributed power supply. Increasing the switching frequency (20-500MHz) of DC-DC converters would lead to size reduction of the magnetic passives which dominate the converter size. High inductance densities in a miniature form factor on integrated, single chip platforms necessitate novel, thin film (µm-10's µm thick), CMOS-process compatible (<400°C thin-film deposition) magnetic materials. The material requirements for high frequencies include low eddy current losses and minimization of µ" (complex permeability).

12:55 PM

Soft Magnetic Materials in Energy Applications: *Ryusuke Hasegawa*¹; ¹Metglas, Inc

In light of energy generation and efficient use of it, development of pertinent soft magnetic materials based on amorphous and nanocrystalline alloys is discussed. These materials have lower magnetic losses and faster flux reversal than crystalline counterparts. This increases devices' operating frequency, which enables smaller and more efficient devices. The impact of this is evidenced in magnetic switches and pulse generation and compression. Examples are pulse sources for lasers and charged-particle accelerators. The latter application is noteworthy as it could lead to nuclear fusion for energy generation. In the area of energy efficiency, these materials contribute considerably in reducing energy distribution system loss with the resultant reduction of CO2 emission at power plants. In power management, non-crystalline alloys are widely used in power electronics including switch-mode power supplies for e.g. PCs, inductors in inverters in wind/solar power generators and power supplies in hybrid cars.

1:05 PM

Industrial Needs and Applications for Soft Magnetic Materials: Francis Johnson¹; ¹GE Global Research

Research and development trends in soft magnetic materials will be discussed from the perspective of an industrial research organization. Key application drivers will be reviewed, included modular power electronic systems for mobile and stationary applications, traction motor systems, and power generation systems. Unique challenges are faced when selecting and engineering magnetic materials for operation in the kilohertz frequency band at Megawatt power levels as compared to the Megawatt frequency bands at the kilowatt power level. The impact of recently enhanced emphasis on materials sustainability, when applied to the value chain of components in an integrated power system, will be discussed.

1:15 PM

Critical Parameters for the Utilization of First Order Magnetocaloric Regenerator Materials in Magnetic Cooling Machines: Karl Gschneidner¹; 'Iowa State University

Materials which undergo a first order magnetic transition exhibit a number of properties which may prohibit or limit their utilization as regenerator materials for magnetic refrigerators, freezers, air conditioners, etc. These include hysteresis, time for the completion of the transition, adiabatic temperature change, ductility/brittleness, and magnetostriction. Other properties may include corrosion resistance, environmental concerns, vapor pressure, and friability. Since an operating cooling machine will undergo about a trillion cycles in its lifetime there are many challenges for the materials design engineer to ameliorate these obstacles for a reliable magnetocaloric refrigerant.

Microstructural Processes in Irradiated Materials: Nuclear Fuel Materials

Sponsored by: The Minerals, Metals and Materials Society, TMS Structural Materials Division, TMS/ASM: Nuclear Materials Committee

Program Organizers: Gary Was, University of Michigan; Thak Sang Byun, Oak Ridge National Laboratory; Shenyang Hu, Pacific Northwest National Laboratory; Dane Morgan, UW Madison; Yasuyoshi Nagai, Tohoku University

Thursday AM	Room: 3
March 3, 2011	Location: San Diego Conv. Ctr

Session Chairs: Dieter Wolf, Argonne National Laboratory; Maria Okuniewski, Idaho National Laboratory

8:30 AM Invited

Multi-Scale Modeling of Irradiation Effects on Nuclear Fuel Microstructure: Dieter Wolf⁺; ¹Argonne National Laboratory

In spite of the well-known existence of microstructural phenomena in nuclear materials, such as void swellingand fission-gas release, a comprehensive understanding of how microstructural processes control the thermo-mechanical behavior of nuclear materials remains to be developed. This lecture provides a vision on how a predictive nuclear fuel modeling capability can be developed by an atomistically-informed mesoscale approach. Two critical elements of the approach are: (i) capturing irradiation effects within an atomistically-informed mesoscale modeling framework, and (ii) developing a comprehensive theoretical and computational mesoscale approach that considers all the various, simultaneously occurring and highly coupled microstructural process within a unified framework. The critical need for experiments will be emphasized. Work supported by the Energy Frontier Research Center for Materials Science of Nuclear Fuels and by Argonne National laboratory's LDRD program.

9:10 AM

Formation and Incorporation Energies of Fission Gases He, Xe, and Kr in bcc Uranium: *Benjamin Beeler*¹; Benjamin Good¹; Chaitanya Deo¹; Sergey Rashkeev²; Michael Baskes³; Maria Okuniewski²; ¹Georgia Institute of Technology; ²Idaho National Laboratory; ³University of California-San Diego

Various metallic nuclear fuels are bcc alloys of uranium that swell under fission conditions, creating fission product gases such as helium, xenon and krypton. An analysis is performed on He, Xe, and Kr point defects in metallic uranium using two methodologies. Defects are investigated within a density functional theory framework utilizing projector augmented-wave pseudopotentials and also with Modified Embedded Atom Method potentials. Formation and incorporation energies of He, Xe, and Kr are calculated at various defect positions for the prediction of fission gas behavior in the bcc phase of uranium. The most likely position for dilute Xe and Kr atoms in bcc uranium is the substitutional site. Helium atoms are likely to be found in a wide variety of defect positions due to the comparable formation energies of all defect configurations analyzed. This is the first detailed study of the stability and incorporation of fission gases in uranium.

9:30 AM

Recent Results of Microstructural Characterization of Irradiated RERTR Fuels: *Dennis Keiser*¹; Jan-Fong Jue¹; Adam Robinson¹; Pavel Medvedev¹; ¹Idaho National Laboratory

The Reduced Enrichment for Research and Test Reactor (RERTR) program is developing low enriched U-Mo fuels for use in reactors that currently employ fuels containing highly enriched uranium. Two different fuel types are being developed: a dispersion fuel and a monolithic fuel. A large part of this fuel development involves irradiation testing in the Advanced Test Reactor. This presentation will discuss the microstructural development that occurs during the irradiation of these two types of fuel. Emphasis will be given to the recent results from the microstructural characterization of irradiated nuclear fuel plates using electron microscopy.

9:50 AM

Phase Field Modeling of Void Growth in Irradiated Two-Phase U-Zr Alloys: Ximiao Pan¹; Morral Morral¹; Y. Wang¹; ¹OSU

Void growth in irradiated, two-phase U-Zr alloys was investigated using a phase field model. The phase field model was linked to a thermodynamic and kinetic database that included vacancies (Va) to represent the U-Zr-Va system. The thermodynamic database was created from an established one for binary U-Zr alloys and by treating the U-Va and Zr-Va binaries as regular solutions with a 40 kJ/mole interaction energy. There were no ternary interaction parameters. A solute mobility database was created from experimental measurements and is composition dependent, while the vacancy mobility was taken as a constant. The phase field model predicts void growth under irradiation in two-phase, gamma + gamma prime alloys. The change in vacancy concentration with time due to irradiation was assumed to be a function of the local vacancy concentration. This assumption was suggested by a plume model prediction, as an alternative to using the mean field approximation for damage.

10:10 AM

Lanthanides Migration and Immobilization in U-Zr Based Nuclear Fuels: *Guillermo Bozzolo*¹; Gerard Hofman¹; Abdellatif Yacout¹; Hugo Mosca²; ¹Argonne National Laboratory; ²CNEA

Redistribution of fission products such as minor actinides and lanthanides leads to migration to the surface of U-Zr based fuels, generating concern due to their interaction with the cladding. The existing remedy for preventing this effect is the introduction of diffusion barriers on the cladding inner surface or by adding thermodynamically stable compound-forming elements to the fuel. Exploring this second option, in this work we introduce atomistic modeling using the BFS method for alloys to study the formation of lanthanide-rich precipitates in U-Zr fuel and the segregation patterns of all constituents to the surface. Surface energies for all elements were computed and, together with the underlying concepts of the BFS method and large scale simulations, the migration of lanthanides to the surface region in U-Zr fuels is explained. The role of additions to the fuel such as In, Ga, and Tl for immobilization of lanthanides is discussed.

10:30 AM Break

10:50 AM

Fission Induced Fuel Swelling, Creep and Sintering of U-Mo Alloy Fuel: Gerard Hofman¹; Yeon Soo Kim¹; ¹Argonne National Laboratory

U-Mo alloy fuel is currently under development for the use of high-power research and test reactors. Irradiation tests of this fuel have been conducted in the Advanced Test Reactor for the US GTRI-Convert program, formerly known as the RERTR (Reduced Enrichment for Research and Test Reactors) and worldwide. Detailed analysis of metallographic sections of irradiated U-Mo fuel plates has shown that the apparent fuel swelling contains a significant fuel creep component induced by high fission. Some of the 140th Annual Meeting & Exhibition

fuel particles with a high fission density and a fission rate show sintering with neighbour particles due to fission induced diffusion. Analysis results of fission induced swelling, creep and sintering of U-Mo alloy fuel are presented. A comparison with other ceramic fuels is also given.

11:10 AM

Simulation of Recrystallization in Uranium Dioxide Nuclear Fuels: Jonathan Madison¹; Veena Tikare¹; Elizabeth Holm¹; ¹Sandia National Laboratories

Uranium Dioxide (UO_2) high burn-up structures found in the rim of light water reactor fuels demonstrate marked differences in yield as well as a variety of additional microstructural markers such as Xe depletion, decreased hardness, increased porosity and extensive recrystallization. In an effort to more clearly understand the microstructural evolution in the formation and development of the rim structure, a kinetic Monte Carlo model incorporating a probabilistic cellular-automata approach has been developed. This model treats dynamic recrystallization while utilizing a position and time-dependent damage accumulation in both two and three-dimensional domains. Results will be provided offering insights into local percolation thresholds, mechanisms for damage migration and implications for continued irradiation of fuel materials beyond currently established NRC regulations.

11:30 AM

The Influence of Temperature on the Evolution of Irradiation-Induced Defect Structure in CeO₂: *Bei Ye*¹; Wei-Ying Chen¹; Mark Kirk²; James Stubbins¹; Abdellatif Yacout²; Jeffery Rest²; ¹U of Illinois at Champaign-Urbana; ²Argonne National Lab

Microstructure evolution of ceria (CeO₂) during irradiation has been investigated through transmission electron microscopy (TEM) under in-situ irradiation. Single crystal CeO₂, grown by molecular beam epitaxy, is used to simulate fluorite-structure UO₂, which is a very important nuclear fuel. 500 keV xenon ions were implanted into CeO₂ thin foils at a range of temperatures (room temperature, 600°C and 800°C) to reveal the temperature effects in defect structure development (to $5x10^{15}$ ions/cm²). Experiment results show a clear impact of temperature on irradiation damage production. At room temperature, defect clusters appear in irregular shapes, and gas bubbles are hardly observed. On the contrary, at elevated temperatures, defect clusters tend to form circular-shaped dislocation loops while gas atoms precipitate in high-density (~ $1.5x10^{17}$ ions/cm²) gas bubbles with a size of ~ 1 - 2 nm in diameter. The differences are attributed to the correlation between defect diffusion ability and temperature.

11:50 AM

Influence of Radiation Damage on Strontium Diffusion in Silicon Carbide: *Erich Friedland*¹; Nic van der Berg¹; Johan Malherbe¹; Elke Wendler²; Werner Wesch³; ¹University of Pretoria; ²Institute for solid state physics; ³Friedrich-Schiller-Universitaet

Fuel elements of gas cooled nuclear reactors and those studied under the International Generation IV Reactor Program are commonly based on TRISO fuel particles. These particles are encapsulated by pyrolitic carbon and silicon carbide layers to reduce fission product release. This study aims to obtain information on strontium diffusion in silicon carbide and the influence of radiation damage on it. For this purpose strontium was implanted in silicon carbide wafers at temperatures ranging from 300 to 900 K. Diffusion coefficients were obtained from the broadening of the implantation profile after thermal annealing studies up to 1700 K using ion beam analysis. Structural information was obtained by electron microscopy. Comparison of profile broadening in annealed single and poly-crystalline samples yielded information on the importance of volume and grain boundary diffusion. Information on the influence of radiation damage was extracted by comparing results from samples implanted at room and elevated temperatures.

12:10 PM

Atomistic Modeling of Fission Products Transport in SiC and ZrC TRISO Fuels: *Sungtae Kim*¹; David Shrader¹; Sarah Khalil¹; Andrew Heim¹; Dane Morgan¹; Izabela Szlufarska¹; ¹University of Wisconsin - Madison

SiC is used as the primary barrier layer to metallic fission product release in TRISO nuclear fuels, but release of Ag and Cs at higher temperatures has been reported. Some studies have suggested the ZrC can provide improved fission product retention compared to SiC and ZrC is presently under consideration for use with, or even in place of, SiC. We have used ab initio methods to determine the structure, mobility, and energetics of Ag and Cs defects in bulk, and to a lesser extent, grain boundaries of SiC and ZrC. We find an important role for impurity – vacancy clusters, charged defect states, and dramatic changes possible in comparing grain boundary and bulk diffusion. Predicted diffusion behavior agrees with measured values where comparisons can be made but solubility predictions suggest that other processes than those considered here may be playing a role in measured fission product release.

Neutron and X-Ray Studies of Advanced Materials IV: Dislocations, Strains and Stresses III

Sponsored by: The Minerals, Metals and Materials Society, TMS Structural Materials Division, TMS/ASM: Mechanical Behavior of Materials Committee, TMS: Chemistry and Physics of Materials Committee

Program Organizers: Rozaliya Barabash, Oak Ridge National Laboratory; Xun-Li Wang, Oak Ridge National Laboratory; Jaimie Tiley, Air Force Research Laboratory; Peter Liaw, The University of Tennessee; Erica Lilleodden, GKSS Research Center; Brent Fultz, California Institute of Technology; Y-D Wang, Northeastern University

Thursday AM	Room: 10
March 3, 2011	Location: San Diego Conv. Ctr

Session Chairs: Jaimie Tiley, Air Force research Laboratory; Peter Liaw, UTK

8:30 AM Invited

Development of Recrystallization Texture during Friction Stir Processing of Magnesium Alloy: Hahn Choo¹; Zhenzhen Yu¹; Wei Zhang²; Zhili Feng²; Sven Vogel³; Edward Kenik²; ¹Univ of Tennessee; ²Oak Ridge National Laboratory; ³Los Alamos National Laboratory

The influence of thermo-mechanical input during friction stir processing (FSP) on texture development was investigated for AZ31B Mg alloy. By varying key processing parameters systematically, i.e., rotation speed and travel rate of the tool, a series of FSP specimens were prepared with a wide range of thermo-mechanical input that can be represented in terms of Zener-Hollomon parameter (Z). Neutron diffraction results show a dramatic change in volume-averaged texture in the stir zone as Z parameter was increased, clearly indicating the influence of processing parameters on the deformation and recrystallization mechanisms. Using the neutron diffraction results, in combination with electron backscattering diffraction and three-dimensional transient modeling, the deformation and recrystallization mechanisms responsible for the microstructure development during FSP of Mg alloy were investigated.

8:50 AM

Neutron Diffraction Measurements of Residual Stresses in a 50-mm Thick Weld Plate: *Wanchuck Woo*¹; Vyacheslav EM¹; Jeong-Ung Park²; Gyu-Baek An³; Baek-Seok Seong¹; ¹KAERI (Korea Atomic Energy Research Institute); ²Chosun University; ³POSCO Steel

Most of the engineering neutron diffractometers have a difficulty in increasing their penetration capability over 25 mm thickness in plate. In order to decrease the beam attenuation, we optimized the configurations of the diffractometer. Specifically, the bent perfect crystal monochromator Si (111) at the take-off angle of 45° provides the wavelength of 2.4 Å and

the bcc ferrite (110) peak at the diffraction angle of 71.7°. It constitutes the wavelength located at the lower neutron cross-section of iron (avoid the 112 Bragg edge) and enables us to obtain the enhanced peak resolution and intensity. We have successfully determined through thickness variations of the residual stresses in the 50-mm thick, 300-mm width/length weld plate without any cutting. Used gauge volumes were 2x2x8 mm³(longitudinal) and 2x2x20 mm³(transverse/normal), and 'stress-free' do measurements were considered. Significant amounts of the tensile longitudinal stresses (over 300 MPa) were observed along the heat-affected zone.

9:05 AM

Deformation Behavior of Nanostructured Metals Over Different Strain Rates and Temperatures: *Ryan Ott*¹; Yinmin Wang²; Matthew Besser¹; Jonathan Almer³; Matthew Kramer¹; ¹Ames Laboratory (USDOE); ²Lawrence Livermore National Laboratory; ³Argonne National Laboratory

For most metals the length-scale of the microstructure can significantly affect both the bulk macroscopic mechanical response and the atomic-scale deformation mechanisms. Furthermore, the mechanical behavior can also depend on the strain rate and deformation temperature. We have examined the deformation mechanisms of different nanostructured metals (e.g. Ni, Cu) using real-time high-energy X-ray diffraction. We report on the effects of both strain rate and test temperature on the grain and twin-boundary stability, the lattice strain, and dislocation-mediated plasticity. From the experiments we find that the lattice strain and the peak broadening are dependent on the deformation conditions. The interconnection between the deformation mechanisms measured by in situ X-ray diffraction and the mechanical responses measured by bulk tests are discussed.

9:20 AM

Deformation Studies of a Creep Resistant Bainitic Steel Using Synchrotron and Neutron Diffraction: *Michael Weisser*¹; Alexander Evans¹; Steven Van Petegem¹; Stuart Holdsworth²; Helena Van Swygenhoven¹; ¹Paul Scherrer Institut; ²EMPA

Creep resistant bainitic steels are commonly used for power plant applications, experiencing both static and cyclic stresses at typical operating temperatures of 565°C. The strengthening mechanisms at both ambient and elevated temperatures are governed by the complex microstructure comprising ductile ferrite matrix and hard carbides. Synchrotron X-rays and neutrons provide an insight to the phase specific behaviours of the main microstructural components during deformation. Residual lattice strain measurements on ex-situ deformed samples with two different deformation histories have shown opposing trends for the ferrite matrix: i) large ferrite phase strain when tensile deformed at ambient temperature and ii) balanced phase strain when creep deformed at operating temperatures. This supports the operation of different deformation mechanisms. Complementary tensile loading tests performed in-situ at ambient temperature suggests that the residual ferrite phase strain originates from load-transfer of the plastifying ferrite matrix to a cementite phase with the onset of macroscopic plasticity.

9:35 AM

MikroGap Area Detector for Stress and Textures Analysis: *Bob He*¹; ¹Bruker AXS

Two-dimensional X-ray diffraction is an ideal method for examining the residual stress and texture. The most dramatic development in twodimensional x-ray diffractometry involves three critical devices, including x-ray sources, x-ray optics and detectors. The recent developments in brilliant X-rays sources and high efficiency X-ray optics provide high intensity X-ray beam with the desired size and divergence. Correspondingly, the detector used in such a high performance system requires the capability to collect large two-dimensional images with high counting rate and high resolution. This presentation introduces an innovative large area detector based on the MikroGap[™] technology and the diffraction vector approach for processing the data for stress and texture analysis. The fundamental equations for stress and texture analysis are derived from the unit vector expression. The stress is given by the distortion of the diffraction ring and the texture is given by the intensity variation along the diffraction ring.

9:50 AM

Micromechanical Behavior Evolution of Twinning-Induced Plasticity Steels Studied by Neutron Diffraction and Self-Consistent Modeling: *Xiaopeng Liu*¹; Ru Lin Peng²; Xiangyuan Wang¹; Yandong Wang³; Yongfeng Shen¹; Shuyan Zhang⁴; Xin Sun⁵; Sten Johansson²; ¹Northeastern University; ²Linköping University; ³Beijing Institute of Technology; ⁴Rutherford Appleton Laboratory; ⁵Pacific Northwest National Laboratory

TWIP (Twinning-Induced Plasticity) steels exhibit good ductility at a very high strength level and are therefore promising materials for making automotive parts with complex geometry. The enhanced formability of such steels is attributed to the formation of mechanical twins during plastic deformation. To understand the twinning-related micromechanical behaviors, in-situ time-of-flight (TOF) neutron diffraction experiments under tensile loading were performed at ISIS to study the change in lattice strains for different hkl-planes of a Fe-30Mn-4Si-3Al TWIP steel. The micromechanical behavior in the TWIP steel is further simulated by the self-consistent model considering both dislocation-slipping and twinning activities. The parameters used for describing the micromechanical behavior of the TWIP steels are directly derived from the TOF experiments and TEM observation. A reliable prediction on evolution of hkl lattice strains and grain orientation distribution is achieved while the interaction of slipping and twinning is considered in the studied material undergoing uniaxial tensile deformation.

10:05 AM

Study of Material Deformation at High Pressure Using Synchrotron X-Rays: Jiuhua Chen¹; Jennifer Girard¹; ¹Florida International University

Developments of high pressure apparatus in conjunction with ultrabrilliant third-generation synchrotron X-ray sources have significantly advanced our capability to study material properties under extreme conditions. Here we report some recent developments in characterization of mechanical properties of materials at high pressure and temperature. In these experiments, x-ray diffraction is used to measure the differential stress and x-ray radiograph imaging is used to determine the strain/strain rate of specimens. The maximum pressure and temperature generated by the deformation high pressure apparatus can reach above 10 GPa and 1300°C respectively. Accuracy of stress and strain rate measurements are about 50 MPa and 10⁻⁶. While experiments are routinely conducted on polycrystalline specimens, latest advances enable experiments on single crystalline samples as well. Pressure/water induced transitions of active slip system along different crystallographic orientations have been observed in recent experiments.

10:15 AM

Micromechanical and Neutron Diffraction Studies of Intergranular Strain Development near a Fatigue Crack Tip: *Lili Zheng*¹; Yanfei Gao¹; Rozaliya Barabash²; Sooyeol Lee³; Jinhaeng Lee¹; Ewen Huang¹; Hahn Choo¹; Peter K Liaw¹; ¹University of Tennessee; ²Oak Ridge National Laboratory; ³The University of British Columbia

The general deformation characteristics near a fatigue crack tip include a plastic zone in front of the crack tip and a plastic wake left behind, where the cyclic loading and fatigue crack growth lead to a compressive strain. The magnitude and distribution of the compressive strain in this plastic wake depend on the stress multiaxiality, material properties, and crack growth increment in each loading cycle. We compare lattice strain measurements by the neutron diffraction technique and simulations by an irreversible and hysteretic cohesive-interface model, which is developed to simulate the fatigue crack nucleation and growth. Crystal plasticity simulations have been conducted to relate the macroscopic and lattice strains. This method also allows us to quantitatively analyze the grain-orientation-dependent lattice strain. Excellent agreement between micromechanical models and neutron strain measurements has been reached. We also discuss implications on fatigue behavior of nanocrystalline or superplastic polycrystals where grain boundary plasticity dominates.

TMS2011 140th Annual Meeting & Exhibition

10:25 AM

In-Situ Observations of Martensitic Transformation and Precipitation in Blast Resistant Steel: *Xinghua Yu*¹; Sudarsanam Babu¹; John Lippold¹; ¹The Ohio State University

BlastAlloy 160 (BA160) is a Naval steel strengthened by lath martensite, Cu precipitates, and M2C carbides. Previous martensite morphology investigation shows that martensite sub-structure has a significant impact on the strength of BA160. In order to understand the martensitic transformation kinetic, time-resolved X-ray diffraction using synchrontron diffraction is performed at Spring-8 in Japan. The martensite morphology change during transformation is also in-situ observed laser scanning confocal microscope. Specimens are heated to different peak temperatures to achieve different prior austenite grain size. Results reveal prior austenite grain size has an influence on both martensitic transformation and amount of retained austenite. Cu Precipitates and carbides in steel are ex-situ characterized by 3D atom probe.

10:35 AM Break

10:45 AM Invited

High P-T nanoMechanics and Molecular Physics: Yusheng Zhao¹; ¹Los Alamos National Laboratory

Nano-crystalline materials show drastic differences in physical properties compared with their bulk counterparts under high pressure (P) and temperature (T) conditions. We show a model to explain the observed contrasts between nano-metals and nano-ceramics, in the sense that the surface tension and compression of nanocrystals are the underlying cause of the differences in elasticity, yield strength, and work hardening and weakening. This nanomechanics model has been tested by the comparative study of constitutive property and elastic modulus of nano-/micron- crystalline materials under high pressure and high temperature conditions. These studies provide fundamental understanding for metal/ceramics performances at nano-scales. Our study on molecular inclusion compounds consisting of host frameworks with guest hydrogen molecules trapped inside nano-scale cages reveals that a strong densification/pressurization effect that the nano-scale molecular cages may exert on the enclosed hydrogen molecules.

11:05 AM

Fast X-Ray Microdiffraction and X-Ray Phase-Contrast Imaging Studies of Self-Propagating Reactions in Nanolayered Metals: *Todd Hufnagel*¹; Stephen Kelly¹; Timothy Weihs¹; Sara Barron¹; Eric Dufresne²; Kamel Fezzaa²; ¹Johns Hopkins University; ²Argonne National Laboratory

Self-propagating exothermic reactions in nanoscale metallic multilayers occur as localized (~100 μ m wide) reaction fronts that propagate at velocities on the order of 10 m/s. These reactions are extremely challenging to study because they require experimental techniques with excellent spatial (<100 μ m) and temporal (<100 μ s) resolution. Here we describe two complementary techniques. In time-resolved x-ray microdiffraction we focus a high flux (~10¹⁴ ph/s) "pink" beam to a small (<10 μ m) spot and use a fast shutter to produce a short (<75 μ s) pulse of x-rays and collect the resulting diffraction patterns. With x-ray phase-contrast imaging we can examine the real-space structure of the reaction front with excellent spatial (~2 μ m) and temporal (~0.5 μ s) resolution. This research was supported by the U.S. Department of Energy, Office of Basic Energy Sciences, Division of Materials Sciences and Engineering under award DE-FG02-09ER46648.

11:20 AM

Strain Heterogeneity in Deformed Polycrystals Inferred from Neutrons, Synchrotron, and Laboratory Diffraction Experiments -- Application to a Duplex Steel: *Christophe Le Bourlot*¹; Olivier Castelnau²; Brigitte Bacroix¹; Thierry Chauveau¹; Marie-Hélène Mathon³; Veijo Honkimäki⁴; Thomas Buslaps⁴; Dominique Thiaudière⁵; ¹LPMTM; ²Arts et Métiers ParisTech; ³CEA-LLB; ⁴ESRF; ⁵Synchrotron SOLEIL

In order to investigate the local response of polycrystals, which is heterogeneous owing to elastic and plastic anisotropies of grains, and to validate mean- and full-field micromechanical models, we have performed elastic strain measurements using several diffraction techniques (neutrons, transmission and reflexion under synchrotron radiation, Laue microdiffraction, and laboratory X-ray) during which the specimen was tensile deformed in-situ. Those techniques are providing different spatial and instrumental resolution, and also different gauge volumes that can range from cubic micrometers up to cubic centimeters. Application has been performed on a duplex steel (ferrite and austenite) as an example of two-phase high-strength polycrystals. The uncertainty and relevance of the different measurements will be discussed and compared with simulations based on an elasto-viscoplastic self-consistent model.

11:30 AM

Mapping the Strain Distributions in Deformed Bulk Metallic Glasses Using Hard X-Ray Diffraction: *Jozef Bednarcik*¹; Hermann Franz¹; Lianyi Chen²; Xiaodong Wang²; Jianzhong Jiang²; ¹Deutsches Elektronen Synchrotron DESY; ²ICNSM, Zhejiang University and Laboratory of New-Structured Materials

Bulk metallic glasses (BMGs) represent relatively new class of materials which exhibit many interesting properties. Compared with crystalline counterparts, BMGs have some superior properties, such as high yield strength, hardness, large elastic limit, high fracture toughness and corrosion resistance, and hence are considered as promising engineering materials. It was recently demonstrated that X-ray diffraction utilizing high-energy photons can be used to measure the elastic strain under compression and tension. The main objective of this work was to follow the strain distribution within Cu-Zr-Al-Ti bulk metallic glass undergoing bend deformation using in-situ hard X-ray diffraction. The special emphasis was placed at the observation of differences between the strain distributions within Cu-Zr-Al-Ti bulk metallic glass when exposed to different levels of bending deformation. X-ray diffraction experiments using high-energy photons (100 keV) were performed at the BW5 wiggler beamline of DORIS III positron storage ring at DESY (Hamburg, Germany).

11:45 AM

X-Ray Diffraction Analysis of the Dislocation Structure of Cu-Nb Interfaces: Gábor Csiszár¹; Amit Misra²; Tamás Ungár¹; ¹Eötvös University Budapest; ²Los Alamos National Laboratory

The Burgers vector population and dislocation densities are determined in strongly textured Cu-Nb multilayers by the method of X-ray line profile analysis. In a high-resolution diffractometer dedicated for line profile analysis the specimens are mounted on a crystal-goniometer. For each hkl reflection the samples are oriented in such a manner that always the major texture component is in reflection conditions. The strain part of line broadening is evaluated in terms of individual measured dislocation contrast factors. The Burgers vector population is evaluated by matching the measured and the theoretically calculated contrast factors. When the total specimen thickness is less than about a few micrometers, the prevailing Burgers vectors are either within the plane parallel to the interface of close to these directions.

11:55 AM

Stress Field in Deformed Polycrystals at the Micron Scale: Johann Petit¹; *Olivier Castelnau*¹; Michel Bornert²; Christophe Le Bourlot³; Odile Robach⁴; Jean -Sébastien Micha⁴; Olivier Ulrich⁴; ¹PIMM-CNRS; ²Unité de Recherche NAVIER; ³LPMTM-CNRS; ⁴CEA-Grenoble

The overall elastic and plastic straining of polycrystals leads to the build up of strong stress and strain heterogeneities inside and between grains. These heterogeneities have to be considered for many issues, e.g. onset of microplasticity, crack propagation, phase transformation, ... The white beam X-ray Laue microdiffraction technique under synchrotron radiation is in principle perfectly adapted for stress field characterizations in deformed polycrystals at the micron scale. The shape of the resulting Laue diffraction patterns reveals many features relative to the specimen deformation including the elastic strain of interest. We will present new results obtained during in situ tensile tests on tungsten (for which the stress field is expected to remain homogeneous upon incremental loading) and duplex steel (in which strong heterogeneities arise). The presentation will focus on a new data treatment method making use of state-of-the-art image processing and allowing reaching a stress accuracy adapted to micromechanical investigations.

12:10 PM

Study of Microstrain Evolution during Creep of a Ferritic Superalloy: Shenyan Huang¹; Bjørn Clausen²; Donald Brown²; Zhenke Teng¹; Gautam Ghosh³; Morris Fine³; Peter Liaw¹; ¹University of Tennessee; ²Los Alamos National Laboratory; ³Northwestern University

In-situ neutron diffraction has been utilized to monitor the microstrain evolution during creep deformation of ferritic superalloys. The ferritic superalloy designed for ultra supercritical steam turbine applications at elevated temperatures was strengthened by a secondary phase of coherent coplanar ordered (Ni,Fe)Al B2-type precipitates. Isothermal creep experiments under constant loading were carried out at different stress levels for various compositions. The temporal evolutions of the elastic phase strain, plane-specific strain (intergranular strain), lattice misfit between the matrix and precipitates, and peak width as a representative of dislocation density were determined. Insights into the micromechanism of creep deformation were achieved with the microstructural information obtained by in-situ neutron diffraction measurements as well as scanning-electron microscopy and transmission-electron microscopy characterizations of grain boundaries, B2 precipitates, and dislocations.

12:20 PM

EXAFS Study of Local Atomic Environment in Annealed and Quenched Fe-27.5 at.% Ga Single Crystals: *Gavin Garside*¹; Sivaraman Guruswamy¹; ¹University of Utah

Extended x-ray absorption fine structure (EXAFS) measurements were made at the Advanced Photon Source at ANL on Fe-27.5 at % Ga single crystals that were long-term annealed and quenched. These EXAFS measurements were taken at the K-edges of Fe, and Ga to determine the Fe-Ga, Fe-Fe, and Ga-Ga atom distances and short range ordering pair correlations. The magnetoelastic coupling, the source of magnetostrictive strain, is sensitive to the interatomic spacing of the magnetic ion core. The measurements of local inter-atomic distances is therefore of interest to gain an improved understanding of how solutes influence magnetostriction in alpha-Fe-based alloys. Annealing was done at 1150 degree C for 70 days followed by quenching in water to room temperature. The paper presents estimated Fe-Fe, Fe-Ga and Ga-Ga near neighbor distances.

12:35 PM

SANS to Evaluate Precipitate Morphology Degradation in Creep Exposed Single Crystal Nickel Base Superalloy: *Jozef Zrnik*¹; Pavel Strunz²; Alexander Epishin³; Thomas Link³; ¹Comtes FHT, Inc.; ²Nuclear Physics Institute; ³Technical University Berlin

Turbine blades in gas turbines, fabricated of Ni base superalloys, operate under the creep and creep-fatigue conditions. One of the main changes which appear in microstructure during creep exposure is the directional coarsening (rafting) of originally cubic gamma prime (γ) precipitates embedded in gama (γ) matrix. For residual lifetime estimation, it is desirable to have a non-destructive method which could reliably evaluate the progress in γ' degradation in dependence on exposure time and relate these changes to the magnitude of stress the blade is experiencing. The available literature indicates that necessary information can be obtained form the analysis of geometrical parameters of the γ' microstructure and γ/γ' misfit [1, 2]. Using the bulk sensitive small-angle neutron scattering (SANS), morphological changes of γ phase resulting from the operation condition can be detected. SANS method [3] has proved to contribute successfully to the morphology assessment of γ in nickel base superalloys [4]. The aim of this investigation was to evaluate the morphological changes of γ' in creep-exposed singlecrystal Ni-base superalloy CMSX4 using SANS method and relate them to the various applied stress levels. The secondary aim of the experiment was to test a possibility to investigate the microstructural parameters using a new special sample design: a conic specimen. As a result of the diameter change along the longitudinal axis, a continuous change of applied stress magnitude acting during the creep test exists, which contributes substantially to γ morphology modification and causes different microstructural change at different positions along the specimen.

12:50 PM Invited

Investigation of Welding Residual Stresses Before and After Post-Weld Heat Treatment: *Anna Paradowska*¹; John W.H. Price²; Trevor R. Finlayson³; R. Ibrahim²; ¹ISIS, Rutherford Appleton Laboratory; ²Monash University, Department of Mechanical Engineering; ³The University of Melbourne, School of Physics

In welded structures residual stresses are formed primarily as the result of differential contractions which occur as the weld metal solidifies and cools to ambient temperature. RS have a significant effect on corrosion, fracture resistance, creep and corrosion/fatigue performance and a full understanding of these stresses is desirable. The aim of this paper is to investigate residual stresses in various weldments using the non-destructive neutron diffraction technique. This research is focused on characterization of the residual stress distribution: in the original weld and after conventional post-weld heat treatment. The focus of the measurements is on the values of the sub-surface strain/stress variations across the weld and through the thickness of the weld.

Pb-Free Solders and Other Materials for Emerging Interconnect and Packaging Technologies: Processing and Reliability Issues

Sponsored by: The Minerals, Metals and Materials Society, TMS Electronic, Magnetic, and Photonic Materials Division, TMS: Electronic Packaging and Interconnection Materials Committee *Program Organizers*: Indranath Dutta, Washington State University; Darrel Frear, Freescale Semiconductor; Sung Kang, IBM; Eric Cotts, SUNY Binghamton; Laura Turbini, Research in Motion; Rajen Sidhu, Intel Corporation; John Osenbach, LSI Corporation; Albert Wu, National Central Univ, Taiwan; Tae-Kyu Lee, Cisco Systems

Thursday AM March 3, 2011 Room: 7B Location: San Diego Conv. Ctr

Session Chairs: Kejun Zeng, Texas Instruments Inc; Andre Lee, Michigan State University

8:30 AM Invited

Impact of Isothermal Aging and Sn Grain Orientation on Long Term Reliability of SnAgCu Solder Interconnects in 5.0wt% NaCl Solution Environment: *Tae-Kyu Lee*¹; Bo Liu¹; Bite Zhou²; Thomas R. Bieler²; Kuo-Chuan Liu¹; ¹Cisco Systems, Inc.; ²Michigan State University

Understanding the sensitivity of Pb-free solder joint reliability on various environmental conditions becomes a critical topic while deploying Pb-free products in various markets and applications. The work reported here concerns the impact of marine environment to SnPb and SnAgCu interconnects. Both SnPb and SnAgCu solder alloy wafer level packages with and without 5% NaCl salt spray pre-condition with various isothermal aging are thermal cycled to failure. These tests consistently show three interesting results. First, the corrosion path in SnAgCu exactly aligned with a preferred Sn grain orientation. Second, the salt spray test didn't degrade the lifetime of SnPb solder joints but reduces the life of SnAgCu. Third, salt spray applied solder joints after thermal aging show an even further degradation, which turns out more than 50%. The potential mechanisms leading to these results are presented and dependency of the degradation on different solder alloys are discussed.

8:55 AM

In-Situ 2D X-Ray Study of Pb-Free Solder Joints and Next Generation Thermal Interface Material in Flip Chip Packages: Yan Li¹; Rahul Panat¹; Bin Li¹; Rose Mulligan¹; Purushotham Kaushik Muthur Srinatha¹; Arun Raman¹; ¹Intel Corp

In-situ observations of the soldering process in microelectronic packages can reveal the effect of input process parameters on the joint formation. A hot stage was placed inside a 2D X-ray machine to perform in situ X-ray study at temperature as high as 300°C. This apparatus was employed to understand the root cause of corner thermal resistance degradation of a next generation TMS2011 140th Annual Meeting & Exhibition

thermal interface material after temperature cycle B stress. First level interconnect solder bump bridging during chip attach in a flip chip package with large die area substrate warpage was also studied. Lastly, the in-situ X-ray system was used to analyze second level interconnects ball grid array solder joint bridging in a large die package with integrated heat spreader during surface mounting solder reflow. By being able to study failures in-situ at high temperatures, a new dimension to the package failure analysis has been presented in this paper.

9:15 AM

The Stability Window and Mechanical Properties of the Interfacial Intermetallic in Lead-Free Solder Joints: *Keith Sweatman*¹; Kazuhiro Nogita²; Hideaki Tsukamoto²; Tetsuro Nishimura¹; ¹Nihon Superior Co., Ltd.; ²University of Queensland

The trend to copper UBM for lead-free area array packages subjected to drop impact means that the properties of the intermetallic that forms at the solder/copper interface are major determinants of joint reliability. The transformation of the Cu6Sn5 from the close packed hexagonal η to the monoclinic η' at 186°C can reduce the impact resistance and long term reliability of the solder joint. In this paper the authors will report new studies on the effect of Ni over the range 0-9% on the stabilization of the η phase. The distribution of the Ni in the Cu6Sn5 and its crystal structure, lattice dimensions and thermal stability have been studied using SEM/EDS, TEM/EDS, synchrotron micro-XRF mapping techniques, synchrotron XRD, DSC and dilatometry. The mechanical properties of the intermetallic as a function of nickel content have been measured by nanoindentation. The data collected provides basis for lead-free alloy formulation for area array attachment.

9:35 AM

Effect of Temperature and Strain Rate on Flow and Fracture Behavior of Pb-Free Solder Joints: *Andre Lee*¹; Deep Choudhuri¹; K. Subramanian¹; ¹Michigan State University

Isothermal mechanical characterization of Pb-free solder joints was carried out at various temperatures between -55C and 150C at strain rates ranging from 0.001 s^-1 to 0.1 s^-1. Grain boundary sliding was the dominant mode of deformation at high temperatures and low strain rates, where as debonding at intermetallic compounds (IMC)/ solder interfaces was dominant at low temperatures and high strain rates. Shear banding was noted at the intermediate temperatures and strain rates. The extents of overlap between these modes of deformation depend on both temperatures and strain rates. Higher strain rates at a given temperature resulted in a mode of deformation representative at a lower temperature with a slower strain rate. These findings are significant with respect to thermomechanical fatigue reliability evaluation by accelerated tests since the range of temperatures and ramp rates encountered during service encompasses similar transitions between different modes of deformation.

9:55 AM

Printing of Functionally Graded, Pb-Free Braze Layers for Use in High Temperature Die Attach Applications: Jared McCoppin¹; Thomas Reitz²; Ryan Miller²; *Henry Young*¹; ¹Wright State University; ²Wright Patterson Air Force Base

Functional gradation of a die-attach has the potential to mitigate thermal stress in high temperature environments. Our current research uses an aerosol-based printing system to print functionally graded, Pb-free die attach layers.

10:15 AM Break

10:25 AM

Joule Heating Effect Caused by Continuous Al Trace Damage under Electromigration on Physical and Statistical Failure Analysis of Solder Joints: Jung Kyu Han¹; Daechul Choi¹; King-Ning Tu¹; ¹University of California Los Angeles

In reliability concerns of flip-chip Pb-free solder joint, under-bumpmetallization structure has a strong impact. To investigate physical failure mode and mean-time-to-failure of different under-bump-metallization structure, three different test vehicles were used: Pb-free solder with thick Cu (7.5 um), e-less Ni (5 um), and thin Cu (0.5 um) under-bump-metallization. In an accelerated test condition (> 7.5 x 10^3 A/cm^2), Al trace also has continuous damage with time while solder joint forms void at the interface. In order to correlate Joule heating effect with physical and statistical failure analysis, temperature change of the chip and resistance change of the solder was measured by in-situ monitoring. Joule heating due to Al trace finally leads to the melting of solder and affects the mean-time-to-failure. Focused-ion-beam images give good understanding of the behavior.

10:45 AM

Erosion Behavior of Stainless Steels in Molten Lead-Free Solder: *Hiroshi Nishikawa*¹; Songai Kang¹; Tadashi Takemoto¹; ¹Osaka University

The dissolution of iron and stainless steel during soldering presents a serious issue for manufacturing equipment such as wave soldering baths and soldering-iron tips. Severe erosion damage of stainless steel wave solder equipment has been encountered in operation. Therefore, it is necessary to study the erosion mechanism of stainless steel by molten lead-free solders. A method for evaluating the erosion depth of stainless steel by molten lead-free solder has been investigated using micro-focus X-ray systems for fluoroscopic and computed tomography (CT) to establish a method for measuring the maximum erosion depth. In this study, the effect of immersion test parameters and surface condition of the test sample on the erosion behavior of 304 and 316 stainless steels into a molten solder was investigated and the interface reaction between the lead-fee solder and stainless steel was studied.

11:05 AM

Influence of Solder Microstructure and Cu₆Sn₅ Interfacial Intermetallic on Mechanical Shock Resistance of Sn-rich Solders: *Kyle Yazzie*¹; Huiyang Fei¹; Hanqing Jiang¹; Nikhilesh Chawla¹; ¹Arizona State University

Pb-free solder alloys are routinely subjected to mechanical shock and drop conditions in service. While these solder alloys are susceptible to dynamic loading, a fundamental understanding of mechanical shock is lacking. Quantifying the contributions of intermetallic layer thickness and solder microstructure to the mechanical shock behavior of the solder specimen is extremely important and needs to be studied. In this study, dynamic strength of Sn-3.9Ag-0.7Cu solder joints was quantified as a function of strain rate, solder microstructure, and intermetallic layer thickness. The morphology and distribution of intermetallic precipitates in Pb-free solder joints was observed using X-ray tomography and radiography. Digital image correlation was used in conjunction with high-speed video, and nanoindentation of Sn grains in solder joints, to measure constitutive data for high-fidelity finite element models. The mechanisms for deformation and the interplay between soldercontrolled and intermetallic controlled fracture will be discussed.

11:25 AM

Interdiffusion of Aluminum/Germanium Bi-Layer Thin Film: Chao-Nan Yeh¹; Kewin Yung¹; Albert T. Wu¹; ¹National Central University

Al/Ge bi-layer thin film is a possible candidate for hermetic sealing in the application of MEMS devices. Al/Ge thin film was deposited on Si substrates by sputter. The interdiffusion coefficient of Al/Ge film that was annealed at 200°C, 300°C, 400°C for various duration of times was calculated by Boltzmann-Matano analysis with depth profiling distributions. The diffusivities have the values in the range of 10^-22, 10^-21, 10^-20 (m^2/s) for the found that the diffusivity decreased as the annealing time heat treatment temperatures of 200°C, 300°C, and 400°C, respectively. We increased annealing times at the same annealing temperature. The depth profile showed layer-exchange phenomenon for the samples that were annealed at 300°C for 10 days. Two glass substrates were bonded by Al/ Ge thin film along the edges of the substrates and immersed in red ink for several days, and the results showed that Al/Ge film provides good hermetic sealing property.

11:45 AM

Influence of Dynamic Recovery and Recrystallization on the Fatigue Fracture Mechanics of Lead-Free Solder Joint: *Huili Xu*¹; Woong Ho Bang¹; Choong-un Kim¹; Tae-Kyu Lee²; Hongtao Ma²; Kuo-Chuan Liu²; ¹University of Texas Arlington; ²Cisco Systems, Inc.

The mechanism of solder joint failure under various fatigue conditions has emerged as one of the critical research subjects in device packaging industry. While recent studies address a few failure mechanisms, it is not yet clear how fatigue failure interacts with dynamic microstrctural changes possible in solder joint. With low homologous temperature, solder has an ability of releasing the fatigue damage, yet its influence on the failure mechanism is not well understood. Utilizing high cycle bending and shear fatigue tester, we have conducted series of investigations to better understand such mechanism. This study reveals that dynamic recovery is the most active form of damage relaxation at room temperature while recrystallization is at higher temperature and that such mechanism is effective only when their kinetics can keep up with the rate of damage accumulation. This paper presents our findings along with mechanistic analysis of fatigue fracture process.

Phase Stability, Phase Transformations, and Reactive Phase Formation in Electronic Materials X: Phase Equilibria and Transformation of the Pb-Free Solders and Thermoelectric Materials

Sponsored by: The Minerals, Metals and Materials Society, TMS Electronic, Magnetic, and Photonic Materials Division, TMS: Alloy Phases Committee

Program Organizers: Chih-Ming Chen, National Chung Hsing University; Hans Flandorfer, University of Vienna; Sinn-Wen Chen, National Tsing Hua University; Jae-ho Lee, Hongik University; Yee-Wen Yen, National Taiwan Univ of Science & Tech; Clemens Schmetterer, TU Bergakademie Freiberg; Ikuo Ohnuma, Tohoku University; Chao-Hong Wang, National Chung Cheng University

Thursday AM	Room: 7A
March 3, 2011	Location: San Diego Conv. Ctr

Session Chairs: Hyuck Mo Lee, Korea Advanced Institute of Science and Technology; Albert T. Wu, National Central University

8:30 AM Invited

Ni-Sb-Sn Alloys as Possible High-Temperature Solders: Phase Equilibria and Thermochemistry: *Herbert Ipser*¹; Ratikant Mishra¹; ¹University of Vienna

Ternary Sb-Sn alloys are being considered as high-temperature solders where the liquidus temperature can be adjusted by varying amounts of a third element. Therefore, the ternary Ni-Sb-Sn phase diagram, with particular emphasis on the Sn-rich corner, was investigated by X-ray powder diffraction, electron microprobe analysis and thermal analyses. A number of isothermal sections, different isopleths, as well as the liquidus projection will be presented. Partial pressures of Sb were determined by an isopiestic vapor pressure method along three sections through the ternary system. From these measurements it was possible to derive partial Gibbs energies (i.e. thermodynamic activities) of Sb, and from their temperature dependence the other partial thermodynamic properties could be obtained. All these experimental data will provide an input for a CALPHAD-type optimization of the ternary Ni-Sb-Sn system.

8:55 AM Invited

The Effect of Sb Addition on Sn-Based Alloys for High-T Lead-Free Solders: An Investigation of the Ag-Sb-Sn System: Simona Delsante¹; Dajian Li¹; Gabriella Borzone¹; Andy Watson²; ¹University of Genoa; ²University of Leeds

Today there is a renewed interest in alloys belonging to Sb-Sn-X (X = Cu, Ag, Bi) ternary systems and their phase equilibria, phase transformation and thermodynamic properties because of their possible use as high temperature

lead-free solders in the electronic industry. The integral mixing enthalpy of Ag-Sb-Sn liquid alloys has been measured along five different sections (25Ag75Sn, 50Ag50Sn, 30Sb70Sn, 50Sb50Sn and 70Sb30Sn) at 530, 600 and 630°C using a high temperature Calvet calorimeter by dropping pure elements (Ag or Sb) in the binary liquid bath. The ternary extrapolation models of Kohler, Muggianu and Toop were used to calculate the integral enthalpy of mixing and to compare measured and extrapolated values. Selected ternary alloys have been prepared for a thermal investigations by using a differential scanning calorimeter at different heating/cooling rate in order to clarify the temperature of the invariant reactions and the crystallization path.

9:20 AM

Phase Field Simulations of Growth and Coarsening in the Interdiffusion Zone of Lead Free Ag-Cu-Sn/Cu Joints: *Nele Moelans*¹; ¹Katholieke Universiteit Leuven, Belgium

Solute transport and the growth of intermetallic layers, precipitates and voids in the interdiffusion zone of solder joints is highly affected by temperature and solder and substrate compositions, but also by the current size, shape and arrangement of the grains and precipitates. A quantitative phase-field model for multi-component alloys is developed that distinguishes different phases and grain orientations and considers the effect of both bulk and grain boundary diffusion. CALPHAD expressions for the bulk Gibbs energy and diffusion mobilities of the ternary Ag-Cu-Sn system are directly used in the phase-field model. The effect of temperature, composition and grain and precipitate size and spatial distribution on the growth and coarsening of intermetallic layers and precipitates in polycrystalline solder joints are studied by means of phase-field simulations. This work fits within the activities of COST MP0602 "Advanced Solder Materials for High Temperature Application".

9:35 AM

Phase Equilibria in the Au-Ag-X (X= Sn and Zn) Systems: *Yoshikazu Takaku*¹; Eri Sato¹; Ikuo Ohnuma¹; Toshihiro Omori¹; Ryosuke Kainuma¹; Kiyohito Ishida¹; ¹Tohoku University

Au as well as Ni is usually plated on the surface of the Cu substrate to prevent it from being oxidized due to atmospheric exposure. Therefore, the equilibrium relationship between Au and Pb-free solders, such as Sn-Ag-Cu and Sn-Zn-Bi alloys, are of practical importance. In this study, the phase equilibria of the Au-Ag-X (X=Sn and Zn) systems were investigated experimentally. Making use of experimental results, the thermodynamic assessment was carried out based on the CALPHAD (Calculation of Phase Diagrams) method. In the Au-Ag-Sn system, experimental results have shown that the stability of the ε -Ag₃Sn is enhanced by Au, which was taken into account in the thermodynamic evaluation. In the Au-Ag-Zn system, an A2/B2 order-disorder transition boundary was determined. Now, 11 elements, namely, Sn, Ag, Cu, Pb, Sb, Bi, Zn, In, Ni, Al and Au, are available in the thermodynamic database ADAMIS (Alloy Database for Micro-Solders), which we developed in 1999.

9:50 AM

Thermodynamic Modeling of the Ag-Cu-In-Sn System: *Wojciech Gierlotka*¹; Kai-chien Zhang¹; ¹YuanZe University

The binary Cu-Sn system is the basis for various emerging Pb-free solders and for most of the important solder-related materials systems. With the increasing demand for Pb-free solders and more advanced applications of soldering technology in electronic products, the Cu-Sn system has become one of the most important material systems. The ternary Ag – Cu – Sn system is promising replacement of classic Pb-Sn solder due to favorable solder ability and wetting properties. Unfortunately, the temperature of melting of ternary Ag – Cu – Sn eutectic (217oC) is much higher than lead solder eutectic (183oC). Some other elements, like In or Bi can decrease temperature of the eutectic point. The Calphad method has been used for thermodynamic modeling of the Ag – Cu – Sn – In quaternary system. The set of thermodynamic parameters were obtained and good agreement between experimental results and calculation was found.

10:05 AM Break

10:20 AM Invited

High Temperature Lead-Free Solder: Phase Relations in (Cu,Ni)-Sn-Zn: *Clemens Schmetterer*¹; Hans Flandorfer²; Divakar Rajamohan²; Herbert Ipser²; ¹TU Bergakademie Freiberg; ²University of Vienna

The issue of lead-free high temperature solders with melting temperatures > 230 °C, which are required for e.g. die-attach, chip scale package and multi-chip modelling, remains unsolved. Alloys of the systems Cu-Sn-Zn and Ni-Sn-Zn have been contemplated as promising solders. Phase diagrams of these systems provide detailed information to the solidification behavior and formation of intermetallic compounds, which is necessary for the control of the microstructure of alloys and alloy interfaces. The systems Cu-Zn, Ni-Zn and Ni-Sn-Zn have been investigated by means of XRD, DTA and metallography including EPMA. In the binary systems significant changes of the phase relations compared to previous versions were found. The ternary system has been investigated above 700 °C; the phase relations have been represented as isothermal and vertical sections, as well as a liquidus surface and reaction scheme. Furthermore, the crystal structures of three ternary compounds were determined and compared to neighboring phases.

10:45 AM

Sn-Bi-Te Phase Equilibria and Interfacial Reactions in the Sn/Bi2Te3 Couples: Chen-nan Chiu¹; *Chia-ming Hsu*¹; Sinn-wen Chen¹; ¹National Tsing Hua University

This study investigates the phase equilibria of the ternary Sn-Bi-Te system and interfacial reactions in the Sn/Bi2Te3 reaction couples. The Bi2Te3 is an important thermoelectric compound, and Sn is the primary constituent element of electronic solders. Various Sn-Bi-Te alloys were prepared and equilibrated at 160 and 500°C, and the equilibrium phases were determined. In addition to the already known SnBi2Te4 and SnBi4Te7 compounds, three new ternary compounds were found in the Sn-Bi-Te system. Interfacial reactions between Sn and Bi2Te3 at 150 and 160°C were studied. A Sn-Bi liquid layer was formed between Sn and Bi2Te3 at 150 and 160°C. The reaction path is Sn/L/SnTe+L/SnTe+Bi/Bi2Te3, and could be well illustrated with the determined isothermal Sn-Bi-Te isothermal section.

11:00 AM

Microstructures and Liquidus Projection of the Ternary Ag-Sb-Te System: *Hsin-jay Wu*¹; Sinn-wen Chen¹; ¹National Tsing Hua University

Ag-Sb-Te alloys are important for thermoelectric applications. Fifty-one Ag-Sb-Te ternary alloys were prepared, and their primary solidification phases were analyzed. The liquidus troughs of the liquidus projection of the ternary Ag-Sb-Te system are determined based on the experimental results and the phase diagrams of the three binary constituent systems. There are thirteen primary solidification phase regions. In addition to the three terminal solid solution phases and nine binary compounds, there is one ternary compound, AgSbTe2. A unique microstructure with bright spherical phases uniformly dispersed in a matrix caused by a miscibility gap in the liquid phase is found in the γ -Ag2Te primary solidification phase regime. A very fine microstructure with nanometer size Ag2Te is also observed, resulting from the class I reaction, liquid= δ +Ag2Te+AgSbTe2, at 496.5°C, and the liquid composition of Ag-40.0at%Sb-36.0at%Te.

11:15 AM

A Study on the Phase Transformation and Microstructure Evolution of Sputtered Bi-Te Thermoelectric Films with Different Compositions during Post-Annealing: *Minsub Oh*¹; Seong-jae Jeon¹; Seungmin Hyun²; Hoo-jeong Lee¹; ¹Sungkyunkwan University; ²Korea Institute of Machinery and Materials

This study examined the fundamental aspect of the phase transformation and the microstructure evolution of Bi-Te films during post-annealing. Bi-Te Films of various compositions were grown by co-sputtering deposition and annealed at 200°C for different durations. We examined the microstructure of the films using X-ray diffraction and transmission electron microscopy and also measured the electrical and thermoelectric properties. The effects of the post-annealing on the thermoelectric properties and their variations with the film composition were found remarkable: The film with a composition close to that of Bi2Te3 shows the very sensitive improvement of the Seebeck coefficient (56 μ V/K to 250 μ V/K) with the annealing while the films with a composition away from that of Bi2Te3 show little changes in Seebeck coefficient. Our careful characterization using XRD and TEM disclosed that such interesting behavior is a direct consequence of a phase transformation involving a metastable phase and the stable Bi2Te3 phase.

11:30 AM

Fabrication Process of Half-Heusler Compound TiNiSn Based on the Solid-Liquid Reaction: *Shinya Otani*¹; Yoshisato Kimura¹; Yaw-Wang Chai¹; Yoshinao Mishima¹; ¹Tokyo Institute of Technology

Half-Heusler compound TiNiSn is one of the most promising thermoelectric materials which can be used to directly convert waste heat into clean electric energy at around 1000K. The objective of this work is to establish the basis of new fabrication process for both n-type TiNiSn and p-type doped Ti(Ni,Co) Sn. We have proposed to apply the solid(TiNi)/liquid(Sn) reaction for the powder metallurgy process focusing on the low melting of Sn. The formation behavior of Ti(Ni,Co)Sn phase was observed using diffusion couples. We have found that Ti(Ni,Co)Sn phase layer forms at the Ti(Ni,Co)(S)/Sn(L) interface not only as continuous layers but also as faceted grains growing toward the liquid Sn phase. Nearly single-phase Ti(Ni,Co)Sn alloys can be fabricated by the proposed process which is based on the reactive sintering between Ti(Ni,Co) and Sn powders, where Ti(Ni,Co)powders with averaged grain size of 30µm were prepared by gas atomization.

11:45 AM

Formation of Intermetallic Compounds between Lead-free Solder Systems and Thermoelectric Materials: *Tai-Yin Lin*¹; Chien-Neng Liao²; Albert Wu¹; ¹National Central University; ²National Tsing Hua University

SnTe intermetallic compound rapidly formed at the interfaces between p-type bismuth telluride (Bi0.5Sb1.5Te3) thermoelectric materials and lead-free solders. The intermetallic compound affects the mechanical and electrical properties of the joints. Different lead-free solder alloys, Sn-3.5Ag, Sn-3Ag-0.5Cu, Sn-0.7Cu, were used. Bi0.5Sb1.5Te3 slices were immersed in the molten solder baths when the reaction temperature was at 250oC for various duration of time. The results suggested that the joints of Sn-Ag solder had thinner interfacial compounds than those of Sn-Cu and Sn-Ag-Cu solders. Furthermore, the existence of antimony in p-type thermoelements affected the growth rate of the interfacial compounds. Solid state aging was conducted to investigate the stability of the inetermetallic compound. Electroless nickel is plated at the interfaces to serve as diffusion barrier. The results could provide the understanding of the growth kinetics of the intermetallic compounds in the thermoelectric material systems.

Physical and Mechanical Metallurgy of Shape Memory Alloys for Actuator Applications: Applications of Shape Memory Alloys

Sponsored by: The Minerals, Metals and Materials Society Program Organizers: S. Raj, NASA Glenn Research Center; Raj Vaidyanathan, University of Central Florida; Ibrahim Karaman, Texas A&M University; Ronald Noebe, NASA Glenn Research Center; Frederick Calkins, The Boeing Company; Shuichi Miyazaki, Institute of Materials Science, University of Tsukuba

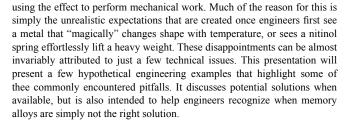
Thursday AM	Room: 11B
March 3, 2011	Location: San Diego Conv. Ctr

Session Chairs: F. Calkins, The Boeing Company; Santo Padula II, NASA Glenn Research Center

8:30 AM Invited

Shape Memory Actuation: Pitfalls and Opportunities: Tom Duerig¹; ¹Nitinol Devices and Components

More than 50 years after the discovery of shape memory alloys, and after investments of millions of dollars, there are very few successful examples of



8:50 AM Invited

Selected Applications of Aeropropulsion Actuation and Shape Control Devices Using HTSMAs: *Todd Quackenbush*¹; Robert McKillip¹; ¹Continuum Dynamics, Inc.

Recent research has seen the relatively rapid development of High Temperature Shape Memory Alloys (HTSMAs), materials that combine useful work output with transition temperatures well in excess of the range of typical binary NiTi SMAs. The proposed paper will describe recent demonstration applications of HTSMAs in devices representative of mechanisms useful for a variety of aeropropulsion applications. The work to date has chiefly featured application of Pt-doped NiTi alloys in wire form, though some data on Pd- and Hf-doped alloys will also be presented. The paper will describe bench top and wind tunnel experiments of demonstration devices employing HTSMA wire actuators. The test results validate operation at 300+ C and document the force and strain capability of the new alloys. Ongoing and projected work in pertinent areas will also be described.

9:10 AM

Optimization of Ferromagnetic Shape Memory Alloys for Strain Detection: *Terryl Wallace*¹; John Newman¹; William Leser²; Patrick Leser²; Michael Horne²; ¹NASA Langley Research Center; ²North Carolina State University

The safety of aerospace vehicles is largely dependent on the ability of modern nondestructive evaluation (NDE) tools to detect structural damage before it reaches a critical size. However, existing NDE technologies are inherently limited by the physical response of the structural material being inspected and are therefore not generally effective at the identification of small discontinuities, making the detection of incipient damage difficult. One innovative solution to this problem is to add particles or coatings of a second material with an enhanced NDE response to damage. Ferromagnetic shape-memory alloys (FSMAs) are an ideal material for this application as they undergo a uniform and repeatable change in both magnetic properties and crystallographic structure (martensitic transformation) when subjected to strain and/or temperature changes which can be detected using conventional NDE techniques. In this study, the NDE response of a FSMA as a function of composition and processing was investigated.

9:25 AM

Fabrication and Characterization of Porous Meta-Magnetic Shape Memory Alloys: James Monroe¹; Josue Perez¹; Ibrahim Karaman¹; Kohei Ito²; Ryosuke Kainuma²; ¹Texas A&M University; ²Tohoku University

NiMn based meta-magnetic shape memory alloys (MMSMAs) exhibit reversible magnetic field induced martensitic phase transformation due to the differences between the austenite and martensite magnetic saturation levels. Most mechanical experimentation on these alloys has been confined to single crystals due to the low fracture toughness caused by intergranular incompatibility. Powder metallurgy techniques, such as pressureless and spark plasma sintering, have been used on NiCoMnSn to introduce small pores between grains that relax the geometric constraints improving both the toughness and shape memory recovery. Introducing pores can also make these alloys attractive for micropump and magnetocaloric applications. Space holders and Ni43Co7Mn39Sn11 pre-alloyed powders are used to create a bi-modal pore size distribution with small pores <50µm to improve ductility and large interconnected pores 300-500µm to allow the transport of fluids. The effects of porosity and processing on the MMSMA foam's magnetic, thermal and mechanical response are then characterized.

9:40 AM

New Concepts for Shape Memory Actuator Systems: *Sven Langbein*¹; Konstantin Lygin¹; Tim Sadek¹; ¹Ruhr University Bochum

The existing actuator systems based on shape memory alloys (SMA) are characterized mainly by the alignment to specific applications. The adoption of the solutions for other applications is admitted in only a few cases. In order to improve the flexibility and the critical properties of actuators that are based on SMA, different kinds of concepts can be found. Beyond the conventional form of an actuator there is the possibility to create integrated or adaptive shape memory actuator systems for example by using agonist-antagonist principle or other adaptive resetting principles. Another emphasizing feature of SMAs is their potential to produce different functional effects, for example thermal shape memory or superelasticity, in one component. Separated from the former point of view a new perspective with extreme integral and standardized set up is opened up. The aim of this study is to show and to analyze such integrated and adaptive SMA components.

9:55 AM Break

10:05 AM Invited

A Hyper-Elastic Thin Film Nitinol Flow Diverter for Brain Aneurysms: Greg Carman¹; Y.J. Chun¹; K.P. Mohanchandra¹; D. Levi¹; C. Kealey¹; C.S. Hur¹; D. DiCarlo¹; F. Vinuela¹; ¹UCLA

This presentation describes the fabrication of a hyperelastic thin film (~5 microns) Nitinol material attached to a stent for use a flow diverter in the treatment of brain aneurysms. The thin film Nitinol is sputter deposited with transformation temperatures at or near body temperature (37C). The thin film Nitinol is micromachined using a lift off method to produce a film containing fenestrations of different sizes. The geometry of the fenestrations are chosen with a finite element model to produce a film providing a 400% recoverable elongation. The film is attached to a commercially available stent and tested both in vitro and in vivo. Particle image velocimetry data demonstrate that the flow diverter dramatically reduces the flow into a simulated aneurysm sac. In vivo data using a swine with surgically created aneurysm demonstrate occlusion of the aneurysm sac within as little as 2 minutes.

10:25 AM

Development of a SMA-Based Drive Unit for Prehension Orthoses to Support Disabled People: Yukiharu Yoshimi¹; Shunji Moromugi²; Kazuhiro Kitamura³; Tsunaki Ikeda²; Takakazu Ishimatsu²; ¹Yoshimi,Inc.; ²Nagasaki University; ³Aichi University of Education

Most conventional assistive devices use hydraulic motors or pneumatic rams in order to assist the human bodily motion. Their structures are robotic and mechanical, making the devices heavy and tricky to put on. We believed by replacing the motor, a widely used traditional driving source, with shapememory alloy, we can utilize shape-memory alloy's super-elastic property and shape memory property to improve assistive devices and create a more silent, compact device that allows more natural movements. Devices that use super-elastic material operate according to the strength applied by the user. This makes the device very safe. The other characteristic of shape-memory alloy, which is its shape memory property, is activated by electrical heating. This means operation speed can be adjusted by controlling the current.

10:40 AM

Antagonistic SMA Actuator with Bowden Cable Housing for Orthosis Systems: *Hyung-Min Son*¹; Dong-Hyun Jeong¹; Yun-Jung Lee¹; ¹Kyungpook National Univ.

This paper proposes an orthosis system driven by a new antagonistic SMA actuator with bowden cable housing. Many attempts on the actuator of orthosis have been researched to overcome the limitation of electric motordriven orthosis which is usually bulky and heavy. In contrast to conventional approaches, the SMA actuator has attractive features such as light weight, high power density, and silent actuation. In terms of the mechanical configuration, there have been winding-type, weaving-type, straight-line-type, coil-type, and bowden-cable-type actuators. Among these alternatives of the SMA actuation, the winding-type is superior with respect to force generation, amount of displacement within a restricted volume. The mechanical design 140th Annual Meeting & Exhibition

including new winding method of the SMA wire and control system are investigated in this study. The proposed SMA actuator is applied to an arm orthosis and its performance is verified through experiments.

10:55 AM

Modeling of Improved Frequency Shape Memory Alloy Actuation Structures: *Aaron Stebner*¹; James Mabe²; Joseph Kreuger¹; Frederick Calkins²; L. Catherine Brinson¹; ¹Northwestern University; ²The Boeing Company

While SMA actuators have proven a successful means for creating adaptive aerospace structures in many demonstrations, including live flight tests, maximum operational frequencies have been identified as a property that could inhibit their commercial implementation in some circumstances. The maximum cyclic frequency of aerospace actuation structures is primarily limited by cooling time, thus several approaches to increase the surface area and reduce the mass of existing actuator forms are being examined. To understand these approaches and enhance their design processes, actuator performance is being modeled using a 3D SMA constitutive law that has been developed and implemented into ABAQUS via a user subroutine. The resulting characterization of the work capability-cooling time relationships of the different approaches is presented.

11:10 AM

Control Loops of Shape Memory Actuators by Detection of the Electrical Resistance: Horst Meier¹; *Alexander Czechowicz*¹; ¹Ruhr-University Bochum

Due to their ability to change into a previously imprinted actual shape through the means of thermal and electrical activation, shape memory alloys (SMA) are suitable as actuators. To apply these smart materials to a wide range of industrial applications, a simple method of controlling the actuator effect is required. The detection of inner electrical resistance allows to gauge the actuator's movement. By usage of a microcontroller a smart system without any hardware sensors can be realized. Changing outer boundary conditions and the material fatigue (affecting the control loop) can be compensated by software. The paper gives an overview about different controling methods for SMA-actuators, experiments concerning the resistance behaviour of SMA and the development of automotive actuator systems using a resistance control feedback signal.

11:25 AM

Computer-Aided Development and Simulation Tools for Shape Memory Actuator Systems: Horst Meier¹; *Alexander Czechowicz*¹; ¹Ruhr-University Bochum

This paper deals with the dynamic properties of SMA-actuators (Shape Memory Alloy) -characterized by their rate of heating and cooling procedures- that today can only be described insufficiently for different boundary conditions. Based on an analysis of energy fluxes into and out of the actuator, a numerical model, implemented in MATLAB/SIMULINK is presented. Besides the fluxes, the time variable parameters like the latent heat of transformation or the influence of stress on the transformation temperatures are also included in the model. These parameters, depending on the actuator-geometry and temperature, the fraction of martensite and the environmental conditions are considered in the simulation in real time. The SMA-wire based actuation system, can be configured by drag and drop tools and finally simulated and graphically displayed for different actuator-systems. The development of such tools, from the theoretical equations to the verification on real elements, is the main topic of this article.

11:40 AM

Problems and Solutions for Shape Memory Actuators in Automotive Applications: Sven Langbein¹; Konstantin Lygin¹; Tim Sadek¹; ¹Ruhr University Bochum

The increased automation of technical applications in automobiles requires the use of simple and effective actuator components. The interior of vehicles offer numerous opportunities where mechanical actuators can be or have already been replaced by electrical actuators, e.g. unlocking functions for cup holders or glove boxes. The growing application range of electrical actuators leads to new problems. The need for optimisation can be located in fields of weight, sounds and costs. Because of the high power density, the simple design and the noiseless actuation of shape memory alloys, they are a solution for this problem. But the use of SMAs leads to new problems, too. The requirements of a short reactivation time, of a high durability and for an operability in ambient temperatures between -40 and +80°C have been identified as critical for SMA actuators. Therefore, ways to increase these properties by technical means are presented in this study.

11:55 AM Conclusion of Symposium

Polycrystal Modelling with Experimental Integration: A Symposium Honoring Carlos Tome: Emerging Polycrystal Models with Experimental Integration II

Sponsored by: The Minerals, Metals and Materials Society, TMS Structural Materials Division, TMS Materials Processing and Manufacturing Division, ASM-MSCTS: Texture and Anisotropy Committee, TMS/ASM: Mechanical Behavior of Materials Committee, TMS/ASM: Computational Materials Science and Engineering Committee

Program Organizers: Ricardo Lebensohn, Los Alamos National Laboratory; Sean Agnew, University of Virginia; Mark Daymond, Queens's University

Thursday AM	Room: 6C
March 3, 2011	Location: San Diego Conv. Ctr

Session Chairs: Anthony Rollett, Carnegie Mellon University; Craig Hartley, El Arroyo Enterprises; Philip Eisenlohr, Max-Planck Institut fuer Eisenforschung

8:30 AM Invited

Full-Field Modeling with Experimental Integration of 3-D Polycrystalline Materials Deforming in Different Regimes Using Fast Fourier Transforms: *Ricardo Lebensohn*¹; ¹Los Alamos National Laboratory

We present a recent extension of a numerical formulation based on Fast Fourier Transforms to obtain the evolution of micromechanical fields in 3-D polycrystals during the elastoplastic transition. This formulation, originally developed [1] as a fast algorithm to compute the elastic and elastoplastic response of composites using input from a digital image of their microstructures, has been in turn adapted to deal with 3-D polycrystals deforming either elastically or by dislocation glide in a rigid-viscoplastic regime (e.g [2]). The present extension to elasto-viscoplasticity allows us to predict, e.g., the evolution of the full stress field in polycrystalline microstructures, with intragranular resolution. The relevance of this formulation to the interpretation of 3-D space-resolved measurements obtained with emerging experimental methods will be discussed. [1] H. Moulinec, P. Suquet, Comput. Methods Appl. Mech. Eng. 157, 69 (1998). [2] R.A. Lebensohn R. Brenner, O. Castelnau, A.D. Rollett, Acta Mater. 56, 3914 (2008).

8:55 AM Invited

Solving Finite-Deformation Crystal Elasto-Viscoplasticity with a Fast Fourier Transformation-Based Spectral Method: *Philip Eisenlohr*¹; Martin Diehl¹; Franz Roters¹; Ricardo Lebensohn²; ¹Max-Planck-Institut für Eisenforschung; ²Los Alamos National Laboratory

We extend the spectral framework introduced by Lebensohn (Acta Materialia 49, 2001, pp. 2723--37) to the case of finite-deformation hyperelasticity. Here, the connection between the total deformation gradient and its work-conjugate (first Piola--Kirchhoff) stress is found at each Fourier grid point by invoking a crystal plasticity framework which internally decomposes deformation into elastic and plastic parts. The partitioning between both contributions is established by implicit integration of a state variable-based constitutive material law and associated update of its internal state. This flexible framework is applied to the problem of curling, which

occurs in wire drawing of body-centered cubic polycrystals, and is contrasted to the purely viscoplastic infinitesimal-strain solution.

9:20 AM Invited

Problem Solving with Viscoplasticity: *Anthony Rollett*¹; ricardo lebensohn²; Francis Wagner³; David Field⁴; ¹Carnegie Mellon University; ²los alamos national laboratory; ³University of Metz; ⁴Washington State Univ

Carlos Tomé has made many contributions to the problem of relating mechanical response to microstructure but it remains an interesting challenge. Euclidean distance maps have proven to be a useful tool for quantifying the proximity of hot spots to grain boundaries, for example. We report on recent results that show that the development of local misorientation is also strongly related to the presence of grain boundaries. In this case, the relationship between local misorientation around each point and distance to the nearest boundary is monotonic: the largest misorientations are found close to boundaries. No direct relationship, however, emerged between misorientation development and grain size. Both simulation with the FFT model and EBSD maps of lightly deformed IF-steel show this trend in a very similar way. These findings are intended to illustrate the general way in which the study of viscoplasticity can help one to understand microstructure-property relationships.

9:45 AM

Modeling Slip and Twinning Induced Plastic Deformation: Comparison between a Crystal Plasticity Finite Element and a Self Consistent Approach: Hamidreza Abdolvand¹; Charles Mareau¹; Mark R. Daymond¹; ¹Queen's University

Results from a crystal plasticity finite element (CPFE) code used to model elasto-plastic deformation in an HCP material are compared to those obtained from self-consistent (SC) approach. In the constitutive equations of both models, it is assumed that slip and twinning deformations can be described using a rate dependent formulation. The predictions of both models in terms of average strain-stress response, lattice strain and texture development, and twinning volume fraction for uniaxial compression loading along the axial direction of a magnesium alloy AZ31 rod are compared with experiment. Excellent agreement is achieved. Due to different grain geometry assumptions, the results of the CPFE model are softer than that of the SC model if the same material constitutive law parameters are used. The inclusion of more realistic grain-grain interactions in the CPFE approach resulted in better prediction of texture development than with the SC model.

10:05 AM Break

10:20 AM Invited

Modeling Non-Conservative Deformation in Crystal Plasticity: Craig Hartley¹; ¹El Arroyo Enterprises LLC

Restricting crystal plasticity models to conservative deformation is inadequate to describe situations where dislocation climb can occur in addition to glide. Both occur in response to a virtual force due to the local effective stress due to mechanical sources and an excess or deficit of point defects. It is convenient to express these forces in terms of the projections of the local effective stress tensor onto the slip plane in the slip direction, using the Schmid Tensor, and onto the extra half plane of edge and mixed dislocations, using a similar construct called the Climb Tensor. Because this latter quantity only acts on the edge components of mixed dislocations, it depends on the character of the dislocation population in a manner that is conveniently described by a Dislocation Density Vector. These concepts can be employed in a natural manner to develop expressions that expand crystal plasticity models to include creep.

10:45 AM Invited

Improving Texture Predictions by Introducing Microstructurally Based Spin Continuity on Grain Boundaries: *Raúl Bolmaro*¹; Andrea Fourty¹; Javier Signorelli¹; ¹IFIR

Texture evolution predictions are usually assertive on the description of components and general trends but lack a proper quantitative output for their severity. Moreover, if we attempt to rationalize the results in function of modern quantitative experiments describing grain fragmentation and misorientations, the limitations of the models become evident. The current paper presents an implementation of certain rules stemming from continuity of spin on grain boundaries in an FCC polycrystal subject to large deformations. Continuity of spins together with shear stress continuity and strain assumptions on a pair of grains are further used on a Taylor like homogenization scheme. The main results of experiments, accumulated along the last decade, describing misorientations at fragment boundaries, distribution of misorientations for selected texture components and misorientation evolution vs. deformation are remarkably well reproduced. The model can also give hints on the process of development of dislocation arrays on geometrically necessary dislocation boundaries.

11:10 AM

Grain-Scale Interactions and Correlations: Effects on Yield Strength and Flow Stress: James Stolken¹; Bryan Reed¹; Mukul Kumar¹; ¹LLNL

The influence of micro-plasticity phenomena on yielding and subsequent work hardening is considered in the context of Grain-Boundary Engineered microstructures. Samples of commercial purity copper and nickel where subjected to thermal-mechanical processing that produced microstructures with varying fractions of low "Sigma" grain-boundaries over a modest range of grain size and with nearly identical (random) crystallographic texture. A four-fold variation in grain-boundary effectiveness (Hall-Petch effect) is observed. Finite element simulations were performed to specifically access the role of stress concentrations and cooperative slip near grain boundaries. Conventional crystal plasticity calculations coupled with high resolution EBSD data are ideally suited to address these two issues and thereby deduce some of the unique grain-scale phenomena upon comparison with experiments. Nearest neighbor and larger-scale twin-related domain correlations are examined and new directions in model development are identified.

11:30 AM

Grain Boundary Engineered Materials as Correlated Networks: Bryan Reed¹; Ming Tang¹; James Belak¹; Joel Bernier¹; Vasily Bulatov¹; Thomas LaGrange¹; Mukul Kumar¹; ¹Lawrence Livermore National Laboratory

This presentation will describe an emerging viewpoint that considers the extended network of grain boundaries as an entity unto itself. Especially in grain boundary engineered materials, these networks exhibit correlations that can extend over many grain diameters, and these correlations are very important for the clustering and percolation properties that determine the ability of the microstructure to withstand a variety of insults. We will describe ongoing efforts to capture the mathematical essence underlying grain boundary network correlations in a way that translates well into computer simulation. Prior work has shown that purely mathematical models can reproduce these correlations surprisingly well, producing microstructures that look much like real grain boundary engineered materials, provided they correctly represent the network constraints governing the formation, growth, and interaction of twins. Now we have implemented phase field simulations built on these same mathematical models, showing the importance of special boundary mobility in controlling coarsening.

11:50 AM

Multiscale Modeling of the Mechanical Response of Dislocation Structures Developed Using High Straining at Low Deformation Temperatures: *Krzysztof Muszka*¹; Janusz Majta¹; ¹AGH University of Science and Technology

Metals subjected to high deformation at low temperature are characterized by ultrafine/nano structure, high volume fraction of high-angle grain boundaries and high fraction of dislocation structure in the form of cells and/or subgrains. The stored energy present in such materials, as elastic energy in dislocation structure and as boundary energy in the high-angle grain boundaries, affects in a complex way annealing processes leading to more stable structures. Upon annealing, both dynamic recovery, and recrystallization can take place, as well as structural (abnormal) coarsening. All of these mechanisms lead to dislocation structures' rearrangements into more stable high angle grain boundaries. In the present work, FEM multiscale physically-based model is proposed to predict the mechanical behavior 140th Annual Meeting & Exhibition

of ultrafine-grained materials developed using severe plastic deformation process (MaxStrain deformation) with or without subsequent annealing. An approach, relating macroscopic stress to dislocation cell size and dislocation density at submicron scale, is used.

12:10 PM

Study Microstructure Evolution in FCC Polycrystalline Materials Using a New Eulerian Continuity Model: Sadegh Ahmadi1; Brent Admas1; David Fullwood¹; ¹Brigham Young University

A new model for predicting the evolution of microstructure in FCC polycrystalline materials is presented. The proposed model was developed based upon the continuity relations by which motion of grain particles in the mass space and rotation of orientations in the orientation space are monitored in an Eulerian framework. To study the accuracy of the proposed model, rolling process of a commercially pure nickel material was simulated using this model. Then, textural and statistical analyses of the experimental and simulated microstructures were carried out. Based on the obtained results, it was found that the new model predicts the statistical features of the microstructure for low and intermediate levels of rolling reductions, but for deformations above 70% because of not including complicated physical phenomena (i.e. grain fragmentation and inhomogeneities) in simulations, the accuracy of the continuity model on predicting the statistics of the real microstructure was decreased.

12:30 PM Invited

Strain Hardening Behavior of HPDC Mg-Al Alloys at Low Strains: K. Vanna Yang1; C. H. Caceres1; A. V. Nagasekhar2; M. A. Easton3; 1ARC Centre of Excellence for Design in Light Metals, The University of Queensland; ²Carpenter Technologies; ³CAST Co-operative Research Centre

The Kocks-Mecking method of analysis was applied to quantify the contribution of the eutectic microstructure to the strain hardening behaviour of high pressure die cast Mg-Al and Mg-RE alloys at low strains. The strain hardening rate was proportional to the volume fraction of the eutectic phases for 7 binary Mg-Al and 3 Mg-RE binary alloys. The results indicate that a large share of the specimens remains elastic at low strains, suggesting that the softer core yields first. The strain hardening rate of each alloy is commensurate with the amount of intermetallic in the eutectic.

Recycling General Session: Waste Utilization

Sponsored by: The Minerals, Metals and Materials Society, TMS Extraction and Processing Division, TMS Light Metals Division, TMS: Recycling and Environmental Technologies Committee Program Organizer: Joseph Pomykala, Argonne National Laboratory

Thursday AM	Room: 12
March 3, 2011	Location: San Diego Conv. Ctr

Session Chair: Jeffrey Spangenberger, Argonne National Laboratory

8:30 AM Introductory Comments

8:35 AM

Designing a Collaborative System for Socio-Environmental Management of Industrial Waste: Marisa Borges1; Fabio Baldini2; 1Universidade Federal do Paraná: ²Excel Solutions

The proposed method emphasizes the optimization of waste management with regard to the exploitation of raw materials incorporated in the remains of industry, as well as the economics of natural resources as an environmental impact assessment. This system [tool] allows: (a) the conversion of an environmental liability into an asset by finding a line of appropriate research for each type of waste and the development of new materials applicable to other industries, (b) performs internal control of the waste generated (production, storage, final destination) as well as legal conformity.

8:55 AM

Analysis of Carbon Fiber Recovered from Optimized Processes of Commercial Scale Recycling Facilities: Joseph Heil¹; Davis Litzenberger¹; Jerome Cuomo¹; ¹North Carolina State University

Carbon fiber reinforced polymer composites (CFRPs) are highly desired materials exhibiting superior strength to weight properties. Aerospace grade carbon fiber, once recycled, is still a valuable material. By evaluating properties of carbon fibers from commercial facilities, target applications in both the aerospace industry and within consumer goods such as automobiles and sporting goods can be identified. In 2009 NC State University characterized fibers recovered from initial production batches of commercial recycling facilities; in 2010 characterization of carbon fibers recovered from optimized processes was conducted. Special attention was paid to recycled intermediate modulus (IM) fibers versus virgin standard modulus (SM) fibers; as previous work as shown better or comparable mechanical properties from recycled IM fibers compared to virgin SM fibers. Characterization focuses on morphology by using scanning electron microscopy, surface chemistry (derived from x-ray photoelectron spectroscopy analysis), and mechanical testing on the tow and filament level.

9:15 AM

Analysis and Control of Light Hydrocarbon Gases in the Pyrolysis/ Combustion Process of Several Solid Wastes: Joner Alves1; Chuanwei Zhuo2; Yiannis Levendis2; Jorge Tenório1; 1University of Sao Paulo; ²Northeastern University

The disposal of wastes is a serious environmental problem, since available landfill space is dwindling. Their treatment by pyrolysis or combustion has merit, and the corresponding fuel or power production is of technological interest. However, such processes need a rigid control of emissions. This work addresses the gaseous light hydrocarbons (LHCs) generated during sequential pyrolysis and partial oxidation of unserviceable tires, PET bottles, corn wastes (DDGS) and sugarcane bagasse in a two-stage laminar-flow horizontal furnace, kept at 1000°C. Gas chromatography was used to identify and quantify the components of the emitted gaseous light hydrocarbons. The results showed that the biomass residues generated the highest emissions of aliphatic hydrocarbons, whereas PET generated the most aromatic hydrocarbons. When stainless steel meshes were inserted in the exhaust flow, it was found that hydrocarbon emissions were curtailed; as such meshes catalyzed partial conversion of these carbon-bearing gases to carbonaceous nanomaterials.

9:35 AM

Reduction Properties of Iron Ore Composite Pellets Bearing Waste Plastics: Burak Birol1; Muhlis Saridede1; 1Yildiz Technical University

Plastic wastes become a huge problem day after day due to the growth of plastic industry. Hence, plastic wastes are used as a raw material for other industries to eliminate this problem. Polyethylene Terephthalate (PET), which is a commonly used for plastic bottles, may be used as a reductant for iron production because of its C and H content. In this study, composite pellets containing iron ore concentrate, flux and reductant were prepared. Crystallized PET bottles and coke were used as reductant after ground. The prepared pellets were reduced at 1400°C for 30 min. and iron nuggets were produced successfully. Usage of waste PET purely as reductant in composite pellets gives a higher metallization degree and proper carbon content than coke or PET and coke mixture.

9:55 AM

Recycling Charge and Subsidy for Waste Packaging Containers in Taiwan: Esher Hsu1; Chen-Ming Kuo2; 1National Taipei University; 2I-Shou University

Under the 4-in-1 recycling system, Taiwan producers and importers who using packaging containers have the responsibility to pay the recycling fees for recycling the waste packaging containers they produced or imported, while the collectors/recycling plants who collect/sort/recover waste packaging containers receive subsidy for conducting recycling. A reasonable pricing for recycling charge and subsidy is a way for sustainability of the recycling. The objective of this study is to provide an amending mechanism for product charge and recycling subsidy in response to the social economic changes. This study employs a regression analysis and cost adjusting model to link the factors used for calculating product charge and recycling subsidy on recycling waste packaging containers with socio-economic indicators, raw material prices, wholesale prices, and secondary material prices. Study results provide estimated models to EPA in Taiwan for amending product charge and recycling subsidy in response to the social economic changes.

10:15 AM Break

10:25 AM

Treatment of Waste Leaching Liquor of a SHS Produced Tungsten Boride: M. Seref Sonmez¹; Sertac Yazici¹; *Bora Derin*¹; ¹Istanbul Technical University

In this study, the recycling conditions of waste liquor obtained after the production of tungsten boride powder from calcium tungstate by self-propagating high temperature synthesis (SHS) and the following hydrochloric acid leaching were investigated in detail. Environmentally unfriendly and extremely acidic (pH \sim -0.3) liquor consisting of calcium, magnesium, and boron ions was treated with 1 M sodium carbonate solution to precipitate magnesium carbonate and calcium carbonate phases. The obtained amorphous precipitates were heated up to the temperature of 400°C for re-crystallization. As a result, MgO, CaCO3 and CaMg(CO3)2 phases were obtained, while sodium, boron, chlorine ions were remain in the solution. The present study is still in progress.

10:45 AM

The Effect of CO2 Carbonation Reaction on the Behavior Leaching of Heavy Metals and Chlorine in the Industrial Waste Incineration Ash: *Ji-Whan Ahn*¹; Kwangsuk Yoo¹; Seong-Young Nam¹; ¹Korea Institute of Geoscience and Mineral Resources

Industrial waste incineration ash(IWIA) is the residue generated during the incineration of municipal solid waste. In Korea, approximately 100 thousand tons of IWIA ash was generated in 2008, with nearly 93.7% of the generated bottom ash landfilled. The ash consists of glasses, ceramics, ferrous metals and slag typically including a small amount of unburnt, non ferrous metals such as aluminum and copper. Many studies have found that the physical properties of the ash are suitable for aggregate substitutes in road materials. Environmental problems, however, such as the leaching of heavy metals and salts must be also considered. In this study, it has been researched to the behaviors of ferrous and non-ferrous materials, heavy metals, and chlorine in the ash under recycling process including carbonation system.

11:05 AM

Study on the Treatment of Wastewater Containing High Concentration of Ammonia Nitrogen: *Ding Lichao*¹; Chen Yunnen¹; ¹Jiangxi University of Science and Technology

With the development of industrial production, more and more wastewater containing high concentration ammonia nitrogen was discharge into the environment, which caused serious harm to the environment. Treating the wastewater has great significance to protect water resources. Using air-stripping combined with oxidation to uptake high concentration of ammonia nitrogen wastewater. The influence of operating parameters was investigated. Experimental results revealed that pH of solution, aeration time and aeration strength showed heavy influence on ammonia nitrogen removal. Air-stripping combined with oxidation can be considered as an alternative approach for the removal of high concentration of ammonia nitrogen from practical metallurgical wastewater. When pH was 11, aeration time 20 min, aeration strength 1040 L/h, and oxidation with 10 % NaCIO solution 10 min, the initial ammonia nitrogen 2130 mg/L could reduce to 12 mg/L. Other items could also be removed to meet the "Integrated wastewater discharge standard (GB8978-88)".

Sponsored by: The Minerals, Metals and Materials Society, TMS Structural Materials Division, TMS: Refractory Metals Committee *Program Organizers:* Omer Dogan, DOE National Energy Technology Laboratory; Jim Ciulik, University of Texas, Austin

Thursday AM	Room: 19
March 3, 2011	Location: San Diego Conv. Ctr

Session Chairs: S.K. Varma, University of Texas at El Paso; Panos Tsakiropoulos, University of Sheffield

8:30 AM Invited

N

Computational Design of Oxidation and Creep-Resistant Ductile Refractory Alloys for High Temperature Applications: *Abhijeet Misra*¹; ¹QuesTek Innovations LLC

Computational materials design integrates targeted materials processstructure-property models within a systems framework to meet specific engineering needs. A key component to design models is a basis on fundamental thermodynamics, phase equilibria, and diffusion, implemented in a multicomponent framework applicable to real systems. The application of computational materials design is especially advantageous to systems that must operate in environments or for lifetimes that are difficult to validate in a laboratory setting. QuesTek Innovations LLC is applying its Materials by Design® technology to the computational design and development of oxidation- and creep-resistant ductile multicomponent refractory-based superalloys for use at 1300°C and above. Fundamental design tools have been developed and used to design microstructural concepts with the potential of achieving critical performance requirements simultaneously. The computational design approach for these systems will be discussed along with some results from QuesTek's DOE-NETL and DARPA-funded programs on the development of niobium and molybdenum-based refractory alloys.

8:50 AM

First-Principles Calculation and Thermodynamic Modeling of Cr-Al-Ni-Ti Quaternary System: *Michael Gao*¹; Omer Dogan¹; ¹National Energy Technology Laboratory

Enhancement of creep resistance of structural alloys for high-temperature applications largely rely on presence of finely dispersed high-strength second phase particles that are resistant to oxidation. In this study, the phase stability in Cr-Al-Ni-Ti system was investigated using first principles calculations, CALPHAD modeling, and characterization tools such as SEM and TEM. There are several technologically important strengthening compounds in this system, namely, Laves C15-Cr2Ti, Heusler L21-AlNi2Ti, and B2-AlNi. The alloying partitioning behavior of these compounds in the ternaries and quaternary were theoretically studied using DFT calculations. Their elastic constants and theoretical strength were also predicted. Phonon calculations were carried out to predict the temperature dependence of their structural, thermodynamic, elastic, and plastic properties, for example, heat capacity and coefficient of thermal expansion. Based on the present DFT calculations, previous thermodynamic assessment, and available experimental data, the thermodynamic descriptions of the quaternary system was optimized using CALPAHD approach.

9:10 AM

Effect of Various Ternary Additions on Cr-Cr₂Ta Based Alloys: *Ayan Bhowmik*¹; Howard Stone¹; ¹University of Cambridge

Alloys based upon Cr-Cr₂X (X being Ta, Nb, Hf etc) have been considered for a while as alternative materials for high temperature service. In this study, we present the effect of alloying additions of Mo, Al and Si on Cr-Cr₂Ta two phase alloys. The ternary additions have been made in 5 and 10 atomic percents to a master alloy of Cr-10at% Ta. Mo has been added for increased strength, Al for superior oxidation resistance and Si for improved HURSDAY AM

140th Annual Meeting & Exhibition

toughness and oxidation resistance. The binary Cr-10at% Ta alloy comprises of Cr₂Ta dendrites and a eutectic mixture of Cr(Ta) solid solution and Cr₂Ta. The composition and stability of the individual phases upon alloying have been determined using electron probe microanalysis and scanning electron microscopy. The microhardness and room temperature fracture toughness of the alloys have also been determined using three point bend tests.

9:30 AM

Microwave Sintering of Nb/Nb5Si3 Composite Material: Yi Liu¹; Huimin Lu¹; Jingru Dai¹; ¹Beihang University

Based on the high melting point, low density, a balance of high-temperature strength and room-temperature toughness, Nb/Nb5Si3 composite material has become a super-alloy for the next generation of aircraft engine. Nb/Nb5Si3 composite material was sintered by the method of direct microwave heating and SiC auxiliary heating, and the effects of peak sintering temperature and sintering time on the density and microstructure of the material were investigated. Compared with conventional sintering, microwave sintering time is only its 20%, and the energy consumption has been reduced by about 70%. Nb5Si3 phase appears in the sample and the grain size is between $1{\sim}2$ µm, after sintering at 1600° for 5 min. In the meantime, the mechanism of microwave sintering was systematically studied.

9:50 AM Break

10:10 AM

Oxidation Behavior of Nb-25Cr-20Si-15Mo-5B and Nb-25Cr-20Mo-15Si-10B in Air from 700 to 1300°C: *Benedict Portillo*¹; Shailendra Varma¹; ¹University of Texas El Paso

Nb-25Cr-20Si-15Mo-5B and Nb-25Cr-20Mo-15Si-10B (at.%) have been subjected to oxidation in air for 24 hours and 168hrs of cyclic oxidation in a range of temperatures from 700 to 1300°C. The as cast microstructures of both alloys contained a molybdenum rich solid solution, Nb₅Si₃, and NbCr₂. The 10%B alloy exhibited better oxidation resistance than the 5%B alloy after 24hrs of oxidation. Samples were characterized by XRD, x-ray mapping, and EDS on SEM. A semi continuous intermediate oxide layer containing molybdenum was found to develop in both alloys at high temperature and was not observed to spall after cooling. The 10%B alloy was also found to have significantly better performance after long term cyclic oxidation test.

10:30 AM

Study of the Effect of Al, Cr, Mo and Ta Additions on the Microstructure and Properties of Nb Silicide Based Alloys: *Panayiotis Tsakiropoulos*¹; ¹The University of Sheffield

Niobium silicide based alloys could replace Ni based superalloys in some structural applications at high temperatures. Alloy development must address the improvement of environmental behaviour and mechanical properties at room, intermediate and high temperatures. Alloying and processing have sought to enhance the performance of the Nbss, to identify optimum microstructures in terms of phase selection, stability and microstructural architecture and to understand how the latter affect performance. In this work, the role of Al, Cr and Mo and Ta in the microstructures of Nb-24Ti-18Si (at %) based alloys has been studied. The phases observed in the alloys were the Nbss, the Nb3Si and aNb5Si3 and BNb5Si3 silicides and Laves phase. The role of the alloying elements on the stability of Nb3Si, the structure of Nb5Si3and on the Nb3Si > Nbss + aNb5Si3 and betaNb5Si3 > alphaNb5Si3 + (Nb,Ti)ss transformations and the formation of the C14-Cr2Nb Laves phase will be discussed.

10:50 AM

Thermomechanical Processing and Microstructure Evolution in Nb-Si-Ti-Al-Cr-X Alloys for High Temperature Aeroengine Applications: *Raghvendra Tewari*¹; Hyojin Song²; Amit Chatterjee³; Vijay Vasudevan²; ¹Bhabha Atomic Research Centre; ²University of Cincinnati; ³Rolls-Royce Corporation

The present paper reports the development of selected Nb-Si-Ti-Cr-Al-X alloys subjected to various conditions. Detail microstructural investigations have revealed a strong tendency for solute partitioning and the formation of the laves phases. Thermomechanical processing was quite effective in breaking down the cast-structure and refining microstructure. The morphological distribution, structure and chemical composition of the various phases were investigated. The β phase exhibits B2 ordering. Dissolution and re-precipitation of the Laves phase, which has been encountered during various heat treatments, has been studied in detail and characterized in terms of elemental distribution in the phase and mechanistic aspects. The results reveal that additional strengthening of the β matrix can be achieved by precipitation of the Laves phase. Mechanical properties of these alloys in different conditions were also evaluated and interesting results were obtained. The role of microstructure, in particular the Laves phase, in controlling mechanical properties is discussed.

11:10 AM

Consolidation of Tantalum Materials by the Cold Spray Process: *Matthew Trexler*¹; Robert Carter¹; Victor Champagne¹; ¹U. S. Army Research Laboratory

Cold spray is a novel process used to consolidate metal powders to which ceramic particulates may be added to form both thin coating and large bulk materials. Cold spray relies on the large deformation that occurs when small particles that have been entrained in a super sonic gas stream impact upon a substrate. Cold spray eliminates the need for more complex methods of forming parts such as liquid infiltration and/or sintering, which can be difficult given the high processing temperatures needed to form refractory metals. This work examines the use of cold spray as it pertains to the consolidation of refractory Ta powder for use as structural components. Cold spray was able to create fully dense near-net shaped powder parts that exhibit excellent tensile properties with limited post-processing.

11:30 AM

Ta/Al2O3 Based Coatings Produced by Thermal Spraying: *Marcio Mendes*¹; Eraldo Souza²; Narayanna Ferreira²; Clodomiro Alves, Jr.²; ¹Universidade Federal do Rio Grande do Norte ; ²Universidade Federal do Rio Grande do Norte

Thermal spraying is a group of processes in which metallic or nonmetallic particles are deposited on a substrate properly prepared, provided or semimolten melt, thus forming a surface coating. The heating necessary for the operation is generated by a spray torch using a combustible gas, electrical arc or plasma. The aim of this paper is soaking, using a plasma torch arc not transferred, particulate mixture of tantalum oxide and aluminum prepared in a stoichiometry manner and with excess of Al +5% and +10%, with flows of 10, 20 and 30 1/min on a 316 stainless steel substrate, producing a coating with high microhardness composed of nanometric particles of tantalum in an alumina matrix. The products of the sprays were characterized by XRD, SEM and electron temperature of the plasma jet was obtained by optical emission spectroscopy.

11:50 AM

Micropillar Compression of Nanocrystalline and Ultra-Fine-Grained BCC Metals Processed by Severe Plastic Deformation: Jonathan Ligda¹; *Brian Schuster*²; Qiuming Wei¹; ¹University of North Carolina Charlotte; ²U. S. Army Research Laboratory

We report on the mechanical properties of nanocrystalline (NC) and ultra-fine-grained (UFG) tantalum and other bcc metals processed using high pressure torsion (HPT). HPT samples have an inherent gradient in structure and properties along a radius of a bulk platen; grains are UFG near the center and NC near the edge. Using site-specific FIB we have examined the properties of micro-compression and tension specimens with grain sizes ranging from tens to hundreds of nanometers and have probed the balance between specimen strength, toughness, strain rate sensitivity and the deformation mode (e.g. homogenous or localized plastic deformation). Observations of the proposed mechanism will be supported through microstructural examinations with transmission electron microscopy. This study will aid in the understanding of how the deformation occurs in bcc metals when the grain size is reduced to the nanoscale.

Sensors, Sampling, and Simulation for Process Control: Temperature-Related Process Monitoring Systems

Sponsored by: The Minerals, Metals and Materials Society, TMS Extraction and Processing Division, TMS: Process Technology and Modeling Committee, TMS: Solidification Committee *Program Organizers:* Brian Thomas, University of Illinois at Urbana-Champaign; Andrew Campbell, WorleyParsons; Srinath Viswanathan, University of Alabama; Lifeng Zhang, Missouri University of Science and Technology; James Yurko, 22Ti LLC; Thomas Battle, Midrex Technologies

Thursday AM	Room: 13
March 3, 2011	Location: San Diego Conv. Ctr

Session Chairs: Hani Henein, University of Alberta; Srinath Viswanathan, University of Alabama

8:30 AM

Dynamic Run-Out Table Cooling Simulator and Temperature Controllers: *Nicolas Pethe*¹; Kai Zheng¹; Didier Huin¹; Christian Moretto¹; Evgueni Poliak¹; ¹ArcelorMittal

Intense competition in steel market has led to the development of a number of high strength steel grades which pose new serious challenges in their manufacturing. One of the major challenges lies in the control of strip cooling after hot rolling, which has become a key step in delivering products with desired microstructure and mechanical properties. To meet this need, SimROT, a dynamic run out table cooling simulator has been developed. Based on a coupling between physical principle based thermal and metallurgical models, SimROT is able to predict temperature and mechanical property accurately over a wide range of products. In addition, a control system has been developed by introducing adaptation to compensate for unmodeled dynamics and a model-based dynamic controller. Implementation has been carried out in the ArcelorMittal USA Riverdale plant to have replaced the old commercial system. Production data have shown significant performance improvement for the entire product mix.

8:55 AM

Real-Time Model-Based Spray-Cooling Control System for Steel Continuous Casting: *Bryan Petrus*¹; Kai Zheng²; X. Zhou¹; Brian Thomas¹; Joseph Bentsman¹; ¹University of Illinois at Urbana Champaign; ²Mittal Steel Company

A new system to control secondary cooling water sprays in continuous casting of steel slabs, CONONLINE, is presented. It features use of a realtime numerical simulation of heat transfer and solidification within the strand as a software sensor in place of unreliable pyrometer sensors. The one-dimensional finite-difference model, CON1D is adapted to create the real-time predictor of the slab temperature and solidification state. During operation, the model is updated with data collected by the caster Level 2 automation system, including measured mold heat flux. A decentralized controller configuration based on a bank of PI (Proportional-Integral) controllers with antiwindup is developed to maintain the shell surface temperature profile at a desired setpoint. A user-friendly monitor accepts setpoint changes from the caster operator and visualizes the state of the caster for the operators. Example simulations demonstrate how better shell surface temperature control is achieved. The system has been implemented to control the Nucor Steel casters in Decatur, Alabama.

9:20 AM

Measurement of the Solidification Front inside a Metallurgical Reactor: *Clement Bertrand*¹; Marc-Andre Marois¹; Martin Desilets¹; Gervais Soucy¹; ¹University of Sherbrooke

Recent amperage increase programs in aluminium smelters generally aim at boosting the metal production using a slightly modified design of an electrolytic cell while keeping its thermal equilibrium unchanged. It is sometimes difficult to evaluate the dynamic cell behaviour with regards to those changes in design and operating point. Sensors are thus needed to diagnose and control the thermal state of modern electrolysis cells. Due to the aggressiveness of the electrolytic bath and high temperatures, solidification front thickness measurements are tedious, imprecise and time consuming. A new measurement technique intended at the evaluation of the solidification front inside an experimental phase change reactor close to a typical aluminium reduction cell is developed. The study of its thermal behaviour is used here to show the possibilities and challenges brought by this new technique. Direct measurements and numerical simulations support the development of such a sensor.

9:45 AM

Inverse Prediction and Control of the Bank Thickness in High Temperature Metallurgical Reactors: *Marc LeBreux*¹; Martin Désilets¹; Marcel Lacroix¹; ¹Université de Sherbrooke

An inverse heat transfer procedure for predicting the time-varying bank thickness in high temperature metallurgical reactors is presented. A Kalman filter coupled with a recursive least-square estimator (inverse method) is employed to estimate the time-varying solidification front position from the data collected by a temperature and/or heat flux sensor located in the reactor wall. The inverse method, known also as a virtual sensor, is then combined to a proportional-integral (PI) controller in order to control the bank thickness by regulating the air forced convection cooling of the reactor external wall. The inverse prediction and the control strategy are thoroughly tested for typical phase change conditions that prevail inside industrial facilities. It is seen that the discrepancy between the exact and the estimated bank thickness remains smaller than 5% at all times, and that the controller performance is much better when the virtual sensor uses a heat flux sensor at the wall/bank interface.

10:10 AM Break

10:25 AM

Online Imaging Pyrometer for Laser Deposition Processing: *James Craig*¹; Thomas Wakeman¹; Richard Grylls²; James Bullen³; ¹Stratonics, Inc.; ²Optomec, Inc. ; ³Optomec, Inc.

An online imaging pyrometer has been developed to monitor the temperature distribution of the melt pool in laser additive manufacturing processes. The imaging pyrometer uses two CCD cameras with "long and short" wavelength filters in the NIR waveband. The intensity ratio is formed and the two wavelength temperature is determined from a calibration, relating the ratio to the temperature. In the experiment, deposit strips are formed over a variation of laser power levels, ranging from standard levels for a superalloy to about half the initial level. As the power is lowered, the deposit efficiency is reduced, as is its dimensions. Melt pool temperature distributions are measured in the final 6 through 10 passes and their properties will be presented and described. Peak temperatures of about 1800 C are noted for standard power levels, and in general lower temperatures are observed at lower power levels.

10:50 AM

Optimization of Continuous Hot Dipped Galvanization Lines through the Addition of a Hot Coating Weight Sensor: *Christopher Burnett*¹; Andreas Quick¹; ¹Thermo Scientific

The ability to reliably measure the zinc coating directly above the pot allows for dramatic improvements in hot dipped galvanizing line performance. The feedback time for air knife control is nearly instantaneous. When coupled with intelligent control software in a complete coating weight Autocontrol system, a "hot" coating weight gauge can reduce overcoating to save raw materials, avoid overcoating and increase overall mill yield. While this location significantly improves coating weight autocontrol performance due to short dead time between air knife and measurement, the environment presents electrical, mechanical, and thermal challenges that must be considered in the final sensor design.

11:15 AM

Monitoring of Meniscus Thermal Phenomena with Thermocouples in Continuous Casting of Steel: *Brian Thomas*¹; Mary Wells²; Dianfeng Lee³; ¹University of Illinois at Urbana Champaign; ²Waterloo University; ³Belvac Metal Forming Company

Many steel quality problems are related to mold level fluctuations, stickers, deep oscillation marks, and other events at the meniscus, and can be detected by monitoring temperature signals in the wall of the copper mold. This work applies an inverse heat conduction model to investigate the potential capabilities of mould thermocouples to detect such phenomena by computing the sensitivity of the detected signal to heat flux variations at the meniscus. The model is first validated with temperature data recorded in a commercial slab casting mold, and in a previous laboratory measurement. The method is capable of monitoring meniscus level, and to detect large level fluctuations. However, its ability to detect temperature fluctuations decreases with the frequency of the fluctuations and the distance of the thermocouple from the hotface. Sensitivity calculations with the model are presented to quantify these detection limits.

11:40 AM

Implementation of Temperature and Strain Micro-Sensors into a Casting Mold Surface: *Brian Thomas*¹; Michael Okelman²; ¹University of Illinois at Urbana Champaign; ²ArcelorMittal Inc.

Microfabricated thin-film thermocouples (TFTCs) and Fiber Bragg Grating (FBG) sensors can be embedded in the coating layers of the mold to measure temperature, heat flux, and strain during continuous casting. Embedding sensors within 1mm near the surface has the advantages of sensitive real-time monitoring of thermal behavior without damping by the copper mold, and protection from hostile environments. A novel TFTC suited for use in continuous casting molds has been designed and a method to embed TFTCs in a coating layer was developed, as well as a computational model to quantify the effect of air gaps between the sensor strip and the copper mold on heat transfer and stress in the coating layer. Finally, a method to successfully embed FBG sensors has been proposed. The signal output by FBG sensors embedded in a nickel coating layer on a copper mold has been investigated and can be predicted with simple equations.

12:05 PM

Simulated Temperature Profile Control of a Laminar Cooling System Using the Genetic Algorithms: *Baher Bineshmarvasti*¹; J. Barry Wiskel¹; Amos Ben-Zvi¹; Hani Henein¹; ¹University of Alberta

The Genetic Algorithms optimization method, in conjunction with a finite element thermal model, was used to simulate control of the temperature profile (i.e. both cooling rate and coiling temperature) of a steel skelp during laminar cooling. Simulated optimization parameters include skelp velocity and laminar cooling configuration. As an example case, the Genetic Algorithms was used to obtain a simulated laminar cooling configuration for an imposed skelp cooling rate of 11.5°C/s and a coiling temperature of 600°C. The ability to achieve the desired skelp cooling profile was found to be sensitive to the control point location (e.g. temperature location inside skelp) used in the Genetic Algorithms.

Silicon Production, Purification and Recycling for Photovoltaic Cells: Session I

Sponsored by: The Minerals, Metals and Materials Society, TMS Extraction and Processing Division, TMS Light Metals Division, TMS: Energy Conversion and Storage Committee, TMS: Recycling and Environmental Technologies Committee

Program Organizers: Anne Kvithyld, SINTEF; Gregory Hildeman, Consultant; Gabriella Tranell, Norwegian University of Science and Technology (NTNU); Arjan Ciftja, SINTEF; Shadia Ikhmayies, Al Isra University

Thursday AM March 3, 2011 Room: 14A Location: San Diego Conv. Ctr

Session Chair: Gabriella Tranell, Norwegian University of Science and Technology

8:30 AM

Polysilicon in Photovoltaics: Market Conditions & Competing PV Technologies: *David Lynch*¹; Byron Cocilovo²; Mario Marquez²; Akram Amooali²; Andrew Shroads²; Scott De Valle²; Rochellee Manygoats²; Chad Munich²; ¹Solar Technology Research Corporation; ²University of Arizona

Material requirements and technical issues impacting several photovoltaic (PV) technologies are examined. That data, along with projections regarding the growth in installed PV capacity, are used to predict demand the solar industry will place on materials used in producing solar cells. Those figures are compared to current production figures and available reserves.

8:50 AM

Agglomeration as a Minor Mechanism for Polycrystalline Silicon Grown in a Fluidized Bed Reactor: *Mohamad Zbib*¹; Uttara Sahayam¹; Wayne Osborne²; Grant Norton¹; David Bahr¹; ¹Washington State University; ²REC Silicon

Polycrystalline silicon, grown using fluidized bed reactors, produces crystalline granular beads, as well as fine (sub 100 nm) amorphous nanopowders. The microstructure of this material was analyzed using scanning and transmission electron microscopy to determine if agglomeration of the nanopowders in the granular material is a significant growth mechanism, in part due to concerns regarding pores in the material. The granular material is primarily crystalline with a high twin density, but some amorphous regions appear around 100-500 nm sized pores, while the porosity larger than 1000 nm exhibits a crystalline structure to the edge of the pore. Total volume fraction of porosity varied between 1.5-4%; pores less than 500 nm represent 0.3 volume %; therefore, it appears agglomeration of nanopowders to the granular beads exists, but is only a minor contributor to the total mass of silicon produced.

9:10 AM

Preparation of Polysilicon by the Reaction of Zinc and Silicon Tetra-Chloride: *Tao Zhang*¹; Huimin Lu¹; Jingbo Xu¹; ¹Beihang University

Polysilicon is the cornerstone of the photovoltaic industry as more than 80% of the solar cell chips are manufactured by the silicon material (monocrystalline silicon and polysilicon). In this paper, polysilicon is produced through a reaction between silicon tetra-chloride and zinc in a reaction furnace. The experiment results indicate that this method is promising and lays a good foundation for industrial application. The conditions of this reaction were studied including temperature, reaction time, reaction atmosphere and the ratio of zinc and silicon tetrachloride. The polysilicon produced meets the requirements of solar cells. The energy consumption of this method has been reduced by about 60%, as compared with traditional polysilicon production methods.

9:30 AM

Macrosegregation of Impurities during Solidification of Metallurgical Grade Silicon in a Vertical Bridgman Furnace: Marcelo Martorano1; João Ferreira Neto2; Theógenes Oliveira1; Tomoe Tsubaki2; 1University of São Paulo; ²Instituto de Pesquisas Tecnológicas do Estado de São Paulo

Directional solidification of metallurgical-grade Si was carried out in a vertical Bridgman furnace. The effects of a change in mold velocity on the macrosegregation of impurities were investigated. Macrostructures of cylindrical Si ingots consist mostly of columnar grains parallel to the ingot axis. Neither dendrites, nor cells, were observed although there is some indication of their presence in the microstructures obtained at the largest velocities. Measured concentrated profiles of impurities showed that ingot bottom and middle are purer than the metallurgical Si. Impurities accumulate at the ingot top creating the typical normal macrosegregation. When mold velocity decreases, macrosegregation and ingot purity increase, changing abruptly below 20µm⁻¹. A mathematical model of solute transport shows that, for mold velocities $\geq 20 \mu m^{-1}$, macrosegregation is caused mainly by diffusion in a stagnant liquid layer assumed at the solid-liquid interface, while for lower velocities, macrosegregation increases owing to convective solute transport.

9:50 AM Break

10:10 AM

Removal of Inclusions from Solar Grade Silicon Using Electromagnetic Field: Anping Dong¹; Lucas Damoah¹; Lifeng Zhang¹; ¹Missouri University of Science and Technology

SiC and Si3N4 are the main non-metallic particles in the solar grade silicon impair the conversion efficiency of the solar cell. Since the non-metallic particles and the metallic impurity elements are non- or less-conductive while the molten silicon is well conductive, under EM field, the Lorenz force will push the particles to the boundary layer, thus remove these inclusions. A laboratory-scale electromagnetic purification unit was used to remelt the silicon scraps and remove inclusions from the melt. The effects of frequency and the current on the inclusion removal are discussed.

10:30 AM

Effect of Calcium Addition and Microstructure of Metallurgical Grade Silicon on Its Leaching Behavior: Yulia Meteleva-Fischer1; Yongxiang Yang1; Rob Boom1; 1Delft University of Technology

Leaching is a very attractive method of purification for metallurgical grade silicon due to its low costs. However, quantitative published results and proposed treatment conditions remarkably differ from each other. The true reason for the various explanations is in the origin of silicon. Specific microstructure and impurities set result in specific leaching behavior of silicon. In present work leaching behavior has been analyzed based on microstructure of metallurgical grade silicon and concentration of calcium addition. It is shown that leaching behavior and efficiency of metallurgical grade silicon depends very much on microstructure of grain boundaries, which is affected by calcium content. It has been detected that increase of calcium concentration and slow cooling rate result in favorable microstructure of grain boundaries, which is possible to remove more easily by using only diluted hydrochloric acid.

10:50 AM

Effect of Solidification Conditions on Si Growth from Si-Cu Melts: Yosuke Ohshima1; Takeshi Yoshikawa1; Kazuki Morita1; 1University of Tokyo

To develop a new silicon refining process for solar cells, solidification refining of silicon with Si-Al melt has been investigated in our research group. This process is considered to be more effective than conventional solidification refining from thermodynamic prediction. However, refined Si with needle-like shape was highly dispersed in a directional solidification refining. Accordingly, the solidification conditions to obtain bulk Si crystal were investigated with various temperature gradients and cooling rates, and bulk Si crystal was obtained under limited conditions. Since cooling rates were still slow, further development was required for the practical process. In

this study, solidification conditions to obtain bulk Si crystal by solidification refining with Si-Cu melt were investigated under various conditions, such as temperature range, temperature gradient, solidification rate, etc. Bulk Si crystal was found to be obtained when the flat interface was observed. Also, the condition to obtain facet Si growth was discussed.

11:10 AM

Structure Silicon Deposits Obtained by Electrolytic Refining in Salt Melt: Oleg Chemezov¹; Oleg Vinogradov-Jabrov¹; Yuriy Zaikov¹; Aleksey Apisarov1; Andrey Isakov1; 1Russian Academy of Sciences

Silicon deposits containing up to 99.99 of main component were obtained by electrowinning from salt melts. Substrates were used from glass-carbon, graphite and nickel. The operating temperature was varied from 550 to 800C. Structure silicon deposits were investigated by ESM method.

11:30 AM

Silicon Electrodeposition Process in Molten Fluorides: Anne-laure Bieber1; Laurent Massot1; Laurent Cassayre1; Pierre Chamelot1; Mathieu Gibilaro1; Pierre Taxil1; 1Laboratoire de génie Chimique

With the exponential growth of solar industry for the photovoltaic panel, the silicon demand is exceeding the supply. So developing new processes able to produce Solar Grade Silicon (SoG-Si) is a major stake. Electrodeposition seems to present many advantages for the production of SoG-Si. The aim of this work is the achievement of an acceptable purity deposit of silicon suitable for the photovoltaic industry in molten salts between 700 and 900°C by electrochemical way in molten fluorides. First, the silicon ions reduction mechanism was studied using cyclic and square wave voltammetries. These experiments, correlated to a bibliography study, allow asserting that Si(IV) ions are reduced in a one-step process exchanging four electrons: Si(IV) + 4 e- = Si Deposits of silicon were obtained after electrolysis under different conditions (nature of the solvent, temperature, current density, cathode material) and characterized by scanning electron microscopy (SEM) and energy dispersive spectroscopy (EDS).

Size Effects in Mechanical Behavior: Combined Approaches Applied to Size Scale Dependent **Experimental Problems**

Sponsored by: The Minerals, Metals and Materials Society, Not Applicable, TMS: Nanomechanical Materials Behavior Committee Program Organizers: Erica Lilleodden, GKSS Research Center; Amit Misra, Los Alamos National Laboratory; Thomas Buchheit, Sandia National Laboratories; Andrew Minor, UC Berkeley & LBL

Session Chairs: Thomas Buchheit, Sandia National Laboratories; T. John Balk, University of Kentucky

8:30 AM

The Behavior of Nanoporous Au and Cu Foams with Controllable Pore Size: I-Chung Cheng1; Andrea Hodge1; 1University of Southern California

Monolithic nanoporous copper and gold foams prepared by dealloying processes are investigated. The pore and ligament size are controllable by using either free corrosion or electrochemically driven methods. The ligament size of the samples dealloyed by free corrosion is ~ 50 nm, while the ligament size of the samples dealloyed by electric driven method is \sim 15nm. Electron backscatter diffraction (EBSD) inverse pole figure maps show the grain morphology and orientation of the base alloy before and after dealloying. The mechanical behavior of nanoporous foams is tested by nanoindentation. Hardness and modulus values are compared in order to determine the effect of oxide formation to the overall material behavior.

8:50 AM Invited

Nanoporous FCC Metals: Effects of Nanoscale Structure on Mechanical Behavior: *T. John Balk*¹; ¹University of Kentucky

Nanoporous metals with nanoscale ligaments offer a unique opportunity to explore the deformation behavior of highly confined metallic volumes. The ligaments provide an extreme constraint on the motion of dislocations. This presentation will discuss several FCC metals in nanoporous form that were mechanically tested. Thin film and bulk samples of nanoporous Au, Pd, Ir and Ni exhibit mechanical properties much different from those of their fully dense counterparts. Hardness testing of nanoporous Au suggests equivalent strength values that may approach the theoretical level. While the measured stress in thin films corresponds to an equivalent stress of one-half the theoretical shear strength, the equivalent elastic modulus appears to be underestimated for porous materials. In nanoporous Pd films, hydrogen was absorbed more quickly than in dense Pd films, leading to large compressive stresses and a gradual phase transformation. These measurements will be interpreted in light of the nanoporous structure of each metal.

9:20 AM

Scaling Behavior of Nanoporous Bcc Materials: *Ralph Spolenak*¹; Flavio Mornaghini¹; ¹ETH Zurich

The scaling behavior of fcc metals, with regard to yield strength, has been well established, whereas the sub 100 nm regime has been explored by including nanoporous gold into the scaling plots of solid pillar geometries. Recently, bcc materials have also been explored in pillar geometry, and their scaling behavior has been found to be less sensitive to pillar diameter than fcc systems. Pillar geometries, however, are difficult to fabricate below 100 nm diameters. Here, we present a study on nanoporous tungsten as fabricated by a novel thermal dealloying process. Stud sizes of below 20 nm exhibit strength levels close to the theoretical yield strength.

9:40 AM

Internal Friction Measurements in Nanocrystalline and Nanoporous Metals: Nicolas Briot¹; ¹University of Kentucky

Several mechanisms have been proposed to account for internal friction in metals at various temperatures, including interactions between dislocations and point defects, nucleation of kink/antikink pairs and grain boundary diffusion. In this study, damping properties of free-standing cantilever samples were investigated using a home-built system composed of a vacuum chamber and a laser vibrometer connected to an acquisition system. The cantilever's deflection was observed in real time, and the evolution of logarithmic decrement of free decay was determined between -150°C and +150°C. Internal friction peaks were observed for nanocrystalline and coarse grain nickel samples, as well as for nanoporous metals obtained by dealloying. The damping peaks for nanocrystalline Ni appear to arise from interactions between dislocations and point defects. Because the ligament size of the nanoporous structure (between 5 and 15 nm) makes dislocation nucleation more difficult, different relaxation mechanisms may be involved.

10:00 AM

Measurement and Analysis of Internal Friction in Sputtered Thin Films of Aluminum: *Guruprasad Sosale*¹; Luc Frechette²; Srikar Vengallatore¹; ¹McGill University; ²Universite de Sherbrooke

Measuring internal friction in deposited thin films can provide useful insight into the effects of scale and confinement on the mechanisms of anelasticity and guide the design of high-performance microresonators used in microelectromechanical systems for sensing and communications. To this end, we have developed a new approach for accurate measurement of internal friction based on a silicon microcantilever platform that uses thermoelastic damping for calibration. This approach has been implemented to measure the effects of thickness (50–500 nm), frequency (100–1500 Hz), and adhesion layers (15 nm thick chromium) on internal friction in sputtered films of aluminum at room temperature. Our measurements suggest that damping is dominated by mechanisms within the film, rather than at the interface or free surface. We have used our results to critically evaluate previously proposed theories for damping due to grain-boundary sliding in thin Al films. Results from measurement and modeling will be presented.

10:20 AM Break

10:40 AM

Augmentation of Micro-Tension Testing Methods: New Parallelized Sample Fabrication Techniques and Development of Elevated Temperature Micro-Heater Grips: Paul Shade¹; Robert Wheeler²; Sang-Lan Kim²; Michael Uchic³; Sabyasachi Ganguli⁴; Jianjun Hu²; ¹Universal Technology Corporation; ²UES Inc.; ³AFRL; ⁴UDRI / AFRL

Mechanical testing of micron-size samples provides distinct advantages over macroscopic testing for quantifying selected fundamental processes that govern plastic flow. However, the application and utilization of micron-scale tension testing methods has been paced by a number of factors. One factor is that sample fabrication can be both slow and expensive if an extensive amount of focused ion beam (FIB) milling is required. Another factor is a lack of suitable methods that can locally heat the micro-scale test samples while keeping temperature-sensitive components on a micro-mechanical test frame at room temperature. The present study aims to address these two deficiencies. We demonstrate a novel technique for parallelized specimen fabrication that utilizes high-aspect-ratio Si stencil masks in conjunction with a broad ion beam milling system. Furthermore, we present progress toward the development of MEMS-based microheater grips that can be used to conduct high temperature micro-tensile experiments within a scanning electron microscope.

11:00 AM

Casting and Testing of Cast metallic Microsamples: *Jerome Krebs*¹; Csilla Miko¹; Nadja Marxer¹; Andreas Mortensen¹; ¹EPFL

Under pressure, molten metal can be made to fill cavities significantly smaller than one micrometer in width. Pressure casting processes may, therefore, offer an alternative approach towards preparing net-shape metallic samples having dimensions sufficiently small for plasticity size effects to be manifest. We present results of a project aimed at the production of microsamples by pressure infiltration of molten metal into shaped micrometric cavities produced within salt-based molds, followed by directional solidification and leaching of the mold. Our goal is to define a new class of small-scale monocrystalline samples different from micromachined "nanopillars", or vapor-grown whiskers, that can be tested for mechanical behavior on the scale of plasticity size effects. Recent results on microcast samples of aluminum and copper will be presented, with focus on their processing and mechanical properties.

11:20 AM

Understanding Mechanical Behaviors of Indium Nanostructures through Synchrotron Laue X-Ray Microdiffraction: Michael Burek¹; *Arief Budiman*²; Gyuhyon Lee¹; Ju-Young Kim³; Nobumichi Tamura⁴; Martin Kunz⁴; Julia Greer³; Ting Tsui¹; ¹University of Waterloo; ²Los Alamos National Laboratory; ³California Institute of Technology; ⁴Lawrence Berkeley National Laboratory

Indium is a key material in lead-free solder applications for microelectronics due to its ductility, wetting properties, and high electrical conductivity. With electronic devices continuing to shrink and the promise of indiumbased nanotechnologies, it is important to develop an understanding of the mechanical properties of indium nanostructures. Studying how dislocation configurations and densities evolve in particular during deformation will be crucial in understanding the mechanical behaviors of indium nanostructures and this is enabled by the synchrotron Laue x-ray microdiffraction (µSXRD) technique. Using this approach, we found significant Laue peak broadening of indium after the deformation which indicates accumulation of dislocations much like in bulk metals during deformation. These observations, coupled with post-compression scanning electron microscopy, as well as in situ uniaxial compression tests, suggest thermally activated deformation processes in low-melting temperature indium, such as diffusion and dislocation climbs act to suppress the size effect commonly reported in other metal nanostructures.

2011 Functional and Structural Nanomaterials: Fabrication, Properties, Applications and Implications: Nanomaterials-Characteristics

Sponsored by: The Minerals, Metals and Materials Society, TMS Electronic, Magnetic, and Photonic Materials Division, TMS: Nanomaterials Committee

Program Organizers: Jiyoung Kim, Univ of Texas; David Stollberg, Georgia Tech Research Institute; Seong Jin Koh, University of Texas at Arlington; Nitin Chopra, The University of Alabama; Suveen Mathaudhu, U.S. Army Research Office

Thursday PM	Room: 8
March 3, 2011	Location: San Diego Conv. Ctr

Session Chairs: Seong Jin Koh, University of Texas at Arlington; Nitin Chopra, U. of Alabama

2:00 PM Introductory Comments

2:05 PM

Engineered Electronic Transport in Assembled Carbon Nanotube (CNT) Thin Films: Role of CNT-scale Properties and Network Topology: *Moneesh Upmanyu*¹; Hailong Wang¹; Yung Jung¹; Myung Hahm¹; ¹Northeastern University

Nanoelectronic devices that rely on the superior electronic transport in individual CNTs are typically beleaguered by reliability and scalability issues, the primary reason for the ongoing paradigm shift towards CNT thin films as active elements. In this talk, we present coarse-grained computations on understanding the role CNT-scale mechanics and assembled network topology on the form of electronic transport across the thin films. In particular we explore the effect of nanoscale confinement that arises during template-assisted directed assembly of CNT solutions. Our results show that the width and thickness of the nanoscopic trenches result in a topology that acts to alleviate the effect of the electrical heterogeneity in the networks. We also presents results on the effect of extrinsic deformation, via densification or prescribed strain, on the electronic transport. Validation of the results is achieved through electrical characterization of fluidic assembly of ultra-thin CNT thins films on micropatterned silica substrates.

2:20 PM

Calculating the Relative Density of Nanoporous Metal Structures: Ran Liu¹; Antonia Antoniou¹; ¹Georgia Institute of Technology

In cellular materials the relative density controls different material properties, from mechanical response to resistivity. We report on a simple phenomenological model that can predict the relative nanoporous metal density using a geometrical consideration. The dependence of relative density on ligament diameter and length is also examined. We finally report on the dependence of yield strength on relative density for isotropic nanoporous platinum structures.

2:35 PM

Fundamental Interactions between Au Nanoparticles and Deoxyribonucleic Acid: Govind Mallick¹; *Mlleshree Karna*²; Shashi Karna¹; ¹Army Research Laboratory; ²University Southern California

In recent years, there has been increased interest in the application of semiconductor quantum dots (QDs) and metal nanoparticles (NPs) in biomedical research as fluorescent labels and sensors. The optical properties of QDs and NPs allow them to be effective imaging agents and also allow them to bind with target biomolecules, such as the deoxyribonucleic acid (DNA) through a linker, followed by change in color and/or electrical conductivity. The focus of this research is the understanding of fundamental interactions between gold (Au) NPs and single-strand (ss) DNA. Spectroscopic and surface probe microscopic techniques were used to investigate and understand fundamental interactions between Au NPs and ss-DNA. Uv-Vis spectra suggest complexation between Au NPs and ss-

DNA, which is also validated by Atomic force microscopic images. Further analysis of the results will be discussed.

2:50 PM

Large 3D Oxides with Length Scale Dependent Magnetic Properties: J. Morales¹; J. Garay¹; ¹UC Riverside

Materials with length scale confinement have been shown to have very different magnetic properties than traditional materials. Polycrystalline bulk materials usually have the advantage of lower costs required for synthesis, but bulk materials with grain sized in the true nanoscale have been notoriously difficult to fabricate. A processing method is presented for the production of macroscopic nanocomposites that display length scale dependent magnetic properties. Depending on the composition, the nanocomposites have soft or hard magnetic hysteresis, display exchange bias or have antiferromagnetic/ferrimagnetic (AFM/fM) coupling. Possible applications of our nanocrystalline oxides are permanent magnets, magnetic sensors and in magneto-optical devices. The results are discussed in terms of length scale and composition of magnetic phases.

3:05 PM

Thermoelectric Circuits Based on Single Bismuth Telluride and Bismuth Nanowires as Bolometric Detectors: *Tito Huber*¹; K. Owusu.¹; ¹Howard University

Bismuth and Bismuth Telluride compounds are thermoelectrics of high efficiency. Films and nanowires of these materials are interesting as building blocks of thermoelectric circuits that can that measure the incident electromagnetic energy, such as infrared light and X-rays. We will discuss our method for the fabrication of individual nanowires and the preparation of thermoelectric circuits based on them. Our fabrication method is based on several steps, namely, synthesis of nanowire array composites, isolation of the individual nanowires in solution, deposition of the nanowires on patterned electrodes, and contact making using focused ion beam and other techniques. Results of measurements of the electronic transport and thermoelectric properties of the circuits will be presented. The implication of these technology advances in the field of bolometric detection will be discussed.

3:20 PM

Crystallization Kinetics and Giant Magneto Impedance Behavior of FeCo Based Amorphous Wires: *Rajat Roy*¹; Partha Sarkar¹; Satnam Singh¹; Ashis Panda¹; Amitava Mitra¹; ¹National Metallurgical Laboratory

The effects of Nb addition on crystallization kinetics and giant magneto impedance (GMI) properties of $Fe_{39}Co_{39}Si_8B_{14}$ amorphous wires prepared by in-water quenching system have been investigated. Thermal behaviors of the wires have been investigated by thermal electrical resistivity measurement and differential scanning calroimetry. The substitution of 4 at% Nb for Fe and Co increases crystallization temperature and merges two crystallization peaks into one peak, leading to a significant increase in thermal stability against crystallization for $Fe_{37}Co_{37}Nb_4Si_8B_{14}$ wire. The formation of Fe_2Nb phase due to addition of Nb increases the activation energy for crystallization from 425 to 550 kJ/mol. The GMI properties of the alloys are evaluated at driving current amplitude of 10 mA and a frequency of 400 kHz. The alloys show the single peak behavior in the GMI profile. The change in GMI properties increases from 10% at 0 at% Nb to 25% at 4 at% Nb.

3:35 PM Break

3:50 PM

Utilization of Fe-Based Nanocomposite Materials for Industrial Applications: *Ryan Dehoff*¹; Andrew Klarner¹; Wei Chen¹; Peter Blau¹; Louis Aprigliano²; Dave Novotnak³; William Peter¹; ¹Oak Ridge National Laboratory; ²Strategic Analysis, Inc.; ³Carpenter Powder Products

Nanomaterials are typically not utilized for structural applications due to size scale limitations and difficulty producing bulk quantities of material. The current research examines the production of Fe-based amorphous or nanocrystalline powder materials via the gas atomization process and subsequent utilization of these powder materials for the production of bulk components and coatings. High cooling rates associated with the gas

atomization process allow for increased quantities of Boron and Carbon to be incorporated into the material than would be tolerable during conventional alloy processing such as casting. Devitrification of the amorphous material resulted in a nanoscale or submicron distribution of complex carbides and borides distributed in an iron based matrix. The resulting material is extremely hard and abrasion resistant, making it an ideal material for high wear applications. The microstructure and mechanical behavior of the material is discussed including material function in field applications.

4:05 PM

Silicon Coated Vertically Aligned Carbon Nanotubes as High Capacity Anodes for Lithium Ion Batteries: *Kara Evanoff*¹; Thomas Fuller¹; W. Jud Ready²; Gleb Yushin¹; ¹Georgia Institute of Technology; ²Georgia Tech Research Institute

The development of thick, high specific capacity anodes with long cycle lifetime is an attractive route to increase the energy and power storage characteristics of Li-ion batteries with reduced cost and weight. Silicon (Si) has a theoretical capacity nearly ten times greater than graphitic anodes. However utilizing Si in a non-destructive manner has been a challenge due to the large volume changes that occur during Li insertion and extraction. Without sufficient mechanical robustness of Si-based anodes and without free space available in the electrode for Si volume expansion during electrochemical alloying with Li, the significant stresses generated during cell operation commonly lead to rapid mechanical degradation of the anode. Here, we present a novel, robust anode architecture consisting of Si coated vertically aligned carbon nanotubes to achieve a high specific capacity, large thickness, and greatly improved anode stability.

4:20 PM

Engineering Shapes in Nanotechnology: Helicity on Demand: *Zi Chen*¹; Carmel Majidi²; David Srolovitz³; Mikko Haataja¹; ¹Princeton University; ²Harvard University; ³Institute of High Performance Computing

The formation of helical nanostructures continues to be a subject of intense fundamental and applied research. Though usually modeled as onedimensional space curves, natural and synthetic helices often exhibit behavior that can only be captured with two-dimensional models. In this work, the pitch angles, chiralities, and radii of such helices are determined within a novel theoretical framework combining continuum mechanics and differential geometry. The theory can be specialized to study a broad range of natural and engineered helical shapes. As a concrete example, the deformation of a thin, elastically isotropic ribbon under prescribed surface stress on one or both surfaces is resolved, with the morphology of resulting helix quantitatively related to the surface stresses. Furthermore, the theoretical predictions are shown to be in excellent quantitative agreement with table-top experiments. In more general terms, we anticipate this framework will enable the design of engineered helical structures in, e.g., biology and nanotechnology.

4:35 PM

Nanoimprinting and Piezoresponse Force Microscopy of Ferroelectric Poly(Vinylidene Fluoride-Trifluoroethylene) Copolymer Films: *Yuanming Liu*¹; Dirk Weiss¹; Jiangyu Li¹; ¹University of Washington

Patterned poly(vinylidene fluoride-trifluoroethylene) [P(VDF-TrFE)] ferroelectric films with feature size down to nanometer scales have their scientific and technological significances. In this talk, we demonstrate an enhanced rapid nanoimprinting process on P(VDF-TrFE) copolymer films with feature size down to 100nm in just 3 minutes. The structure and crystallinity of the thin film were measured by scanning electron microscope, and atomic force microscope. The ferroelectricity of the imprinted films was investigated by surface potential measurement and piezoresponse force microscopy. Electrical properties of P(VDF-TrFE) films were also studied utilizing switching spectroscopy PFM (SSPFM) mode, which allowed real-space mapping of switching behavior and electromechanical activity. The SSPFM measurements were carried out at different temperatures. The effects of imprinting conditions have been investigated, and the optimal imprinting parameters for excellent pattern transfer have been identified.

4:50 PM

Synthesis of Vertical Ultra-long Platinum Nanolawns via Thermally Assisted Photoreduction: *You-Lin Shen*¹; Shih-Yun Chen¹; Jenn-Ming Song²; Tzu-Kang Chin²; Chu-Hsuan Lin²; In-Gann Chen³; ¹National Taiwan University of Science and Technology; ²National Dong Hwa University; ³National Cheng Kung University

Among the Pt nanostructures, nanowires attract more attention becaused of their great potential as 3D electrodes for highly active electrocatalysts. Several methods have been reported to synthesize Pt nanowires, but there is no template and surfactant-free routes available so far for obtaining Pt nanowires whith the aspect ration higher than 50. In this study, the thermally-assisted photoreduction process, is developed to prepare vertically grown ultra-long Pt nanowires via the photocatalytic ability and semiconductor characteristics of the TiO2 substrate. The remarkable aspect ratio of up to 200 is the greatest value reported. TEM analytical results suggest that the Pt nanowires are single-crystalline with a preferred <111> growth direction. The ultra-long Pt NWs can also be prepared on TiO2 coated carbon fibers. The results of electrochemical tests indicate that such a Pt NWs/TiO2 hybrid structure could be applied as the electrocatalyst for methanol oxidation, which provides high catalytic activity and CO tolerance.

5:05 PM Concluding Comments

Advances in Mechanics of One-Dimensional Micro/ Nano Materials: Nanomechanics: Multilayers, Composites, Wires, and Sensors

Sponsored by: The Minerals, Metals and Materials Society, TMS Materials Processing and Manufacturing Division, TMS Electronic, Magnetic, and Photonic Materials Division, TMS: Nanomechanical Materials Behavior Committee

Program Organizers: Reza Shahbazian-Yassar, Michigan Technological University; Seung Min Han, Korea Advanced Institute of Science and Technology; Katerina Aifantis, Aristotle University

Thursday PM	Room: 1B
March 3, 2011	Location: San Diego Conv. Ctr

Session Chairs: Ali Shokuhfar, K.N.T University; Seung Min Han, Korea Advanced Institute of Science and Technology

2:00 PM

Plasticity in the Nanoscale Cu/Nb Single Crystal Multilayers as Revealed by Ex Situ Synchrotron X-Ray Microdiffraction: *Arief Budiman*¹; Seung-Min Han²; Patricia Dickerson¹; Martin Kunz³; Nobumichi Tamura³; John Hirth¹; Amit Misra¹; ¹Los Alamos National Laboratory (LANL); ²Stanford University; ³Advanced Light Source (ALS), Berkeley Lab

There is much interest in the recent years in the nanoscale metallic multilayered composite materials due to their unusual mechanical properties such as very high flow strength and stable plastic flow to large strains. These unique mechanical properties have been proposed to result from the interface-dominated plasticity mechanisms in nanoscale composite materials. Studying how the dislocation configurations and densities evolve during deformation will be crucial in understanding the mechanics of the nanolayered materials. To shed light on these topics, uniaxial compression experiments on nanoscale Cu/Nb single crystal multilayer pillars using ex situ synchrotron Laue X-ray microdiffraction technique were conducted. Using this approach, we found significant Laue peak broadening in the Cu phase after deformation while none was observed in the Nb phase. These observations suggest that the plasticity here is achieved by storage and recovery of dislocations by the many interfaces in the multilayers during the course of the deformation.

2:20 PM

Enhanced Tensile Strength and Ductility in Nano-Multilayer: Ju-Young Kim¹; Julia Greer¹; ¹Caltech

We have performed the in-situ tensile and compressive testing and microstructural characterizations of nano-multilayer of Cu-Zr metallic glass and nanocrystalline (nc) Cu. They show enhanced strength and ductility at the nano-scale compared to single amorphous Cu-Zr layer. We found nc Cu layers play a key role in attaining ductility in these composites by preventing shear bands from transferring into the neighboring Cu-Zr layer. The initial films were deposited via RF magnetron-sputtering, and dog-bone shaped one-dimensional micro-tensile/compressive samples were patterned using photolithography, directional ion milling, and undercutting of Si substrate by selective dry etching. We analyze the specific deformation mechanisms leading to the nano-multilayers' improved mechanical properties by focusing on the non-trivial contribution of interfaces to defect activity during deformation with TEM images.

2:40 PM

In-Situ Observation of Ultra-Strong but Ductile Deformation Behavior of Single Crystalline Metallic Nanowires: Jong Hyun Seo¹; Youngdong Yoo²; Sang Won Yoon¹; Tae-Yeon Seong³; *In-Suk Choi*⁴; Kon Bae Lee⁵; Bongsoo Kim²; Jae-Pyoung Ahn⁴; ¹Korea Institute of Science and Technology - and - Korea University; ²KAIST; ³Korea University; ⁴Korea Institute of Science and Technology; ⁵Kookmin University

We experimentally observed ultra-strong but ductile deformation behavior of single crystalline Au, Pd and PdAu nanowires resulting from deformation twinning process. In-situ tensile tests were performed using Nanomanipulator and AFM force measurement equipped in FEI DualBeam system. Microstructural change was also characterized using TEM at different deformation stages. The real time observation of twin nucleation and twin migration of metallic nanowires was accomplished with quantitative stress-strain measurement. The yield stress of a <110> rhombic Au nanowire reaches up to 1.54 GPa at 4% elastic strain and then twin nucleation occurs with a sudden load drop down to 200 MPa. Followed by twin migration, structural reorientation of the <110> rhombic nanowires into the <100> square nanowires results in ductile elongation at about 41% at the constant stress of 200 MPa. The ultra-strong but ductile deformation by twinning process was also observed for Pd and PdAu nanowires.

3:00 PM

Artificial Neural Network for Solving Large Deflection of Micro/ Nano-Beams: Payam Heidary¹; Ali Shokuhfar¹; ¹K.N.Toosi University of Technology

A technique based on artificial neural network (ANN) is developed for solving large deflection of micro/nano beams. The proposed method is designed to be simple and is accessible to users with minimal experience with multi-layer feed forward ANN. Additionally, this ANN method produces a continuous solution, which can be evaluated at any point within the domain and satisfies the boundary conditions. Traditional training methods of ANN for solving nonlinear Euler Bernoulli beams consisting a system of Fourth order nonlinear boundary value problem are inappropriate and those cannot reach to best approximation. In this paper, to overcome the limitation associated with the current training algorithm, a hybrid of two optimization methods, i.e. sequence quadratic programming (SQP) and particle swarm optimization (PSO) have been used for training adjustable parameters in approximation function. Some of the numerical results are described to validate the proposed technique and to compare with finite difference method.

3:20 PM

Geometric Nonlinear Effects on the Micro/Nano-cantilever Biosensors: Ali Shokuhfar¹; *Payam Heidary*¹; ¹K.N.Toosi Univ. of Technology

In this study the influence of geometrically nonlinear deformation on the response of microsensors based on tension or displacement detection was investigated. Although the large deflection of micro/nano-scale sensor can improve the signal to noise ratio, it can be expected that nonlinear response create poor scale factor linearity. Nonlinear Euler-Bernoulli beams theory

for the geometrically nonlinear deformation was utilized. The introduced nonlinear model has been compared with the effect of behavior on the performances of the microsensors with tension or displacement detector. Based on the introduced model for both silicon and polymeric sensors, the opportunities and challenges of nonlinear microsensors and the designed guidelines are discussed. The results were compared with exiting simulation data and the sources of errors were discussed.

3:40 PM Break

4:00 PM

Synthesis and Mechanical Properties of AL/γ-Al12Mg17 Nanocomposite **Prepared by Ball Milling and Hot Pressing**: *Ali Shokuhfar*¹; Ashkan Zolriasatein¹; Narguess Nemati²; Abbas Sabahi²; ¹Advanced Materials and Nanotechnology Research Laboratories, Department of Mechanical Engineering, K.N.Toosi University of Technology; ²Sahand University of Technology

Aluminium based metal matrix composites reinforced with γ -Al12Mg17 intermetallic nano particle were prepared by mechanical milling and hot pressing methods. γ -Al12Mg17 intermetallic nano particle was synthesized by mechanical milling (MM) of Pre-alloyed β -Al3Mg2 intermetallic compound ingot in attritor ball mill. The content of reinforcement in the composite was varied from 0 to 15% (by weight). Powders were mixed by planetary ball mill for 10 hour. Hot pressing of milled samples was executed at 380°C under 800MPa pressure in a uniaxial die. Nanocomposite samples were prepared in sizes 10 mm in diameters and 20 mm in height. Investigation of density, hardness and compression test properties has carried out on the nano composite sample to study the effect of particles concentration on mechanical properties. The γ -Al12Mg17 reinforcement remarkably improves the mechanical properties of pure Al.

4:20 PM

Effect of Intermetallic Reinforcement Particle Size on Wear Behaviour of Al/γ-Al12Mg17 Nanocomposite Prepared by Ball Milling and Hot Pressing: Ashkan Zolriasatein¹; *Ali Shokuhfar*¹; Narguess Nemati²; ¹Advanced Materials and Nanotechnology Research Laboratories, Department of Mechanical Engineering, K.N.Toosi University of Technology; ²Sahand University of Technology

In this work, the wear behaviour of aluminium matrix composites reinforced with γ -Al12Mg17 intermetallic particles was evaluated. Composite samples were manufactured by ball milling and hot pressing method using different amounts of γ -Al12Mg17 intermetallic particles having various sizes (nano and micro particles) were mixed with micrometric Al powder particles. Attrition milling time of prealloyed intermetallic powder particles was optimized to prepare nano and micro γ -Al12Mg17 intermetallic particles. Hot pressing of milled samples was executed at 380°C under 800MPa pressure in a uniaxial die. After the manufacturing, samples were tested in terms of wear.Volumetric wear rate was determined by the measurement of difference in weight of the pin sample before and after the test using a high precision balance. The effects of intermetallic reinforcement particle size on wear behaviour of nanocomposite were investigated. Based on the SEM observation of the worn surfaces the plausible wear mechanisms were discussed.

Aluminum Reduction Technology: Energy Savings by Cell Design Improvements

Sponsored by: The Minerals, Metals and Materials Society, TMS Light Metals Division, TMS: Aluminum Committee, TMS: Aluminum Processing Committee

Program Organizers: Mohd Mahmood, Aluminium Bahrain; Abdulla Ahmed, Aluminium Bahrain (Alba); Charles Mark Read, Bechtel Corporation; Stephen Lindsay, Alcoa, Inc.

Thursday PM	Room: 17B
March 3, 2011	Location: San Diego Conv. Ctr

Session Chair: Bjorn Moxnes, Hydro Aluminium AS

2:00 PM

Experimental Investigation of Single Bubble Characteristics in a Cold Model of a Hall-Héroult Electrolytic Cell: Subrat Das¹; Yos Morsi¹; *Geoffrey Brooks*¹; William Yang²; John Chen³; ¹Swinburne University od Technology; ²CSIRO Light Metals National Research Flagship; ³University of Auckland

Understanding the characteristics of the bubbles generated within a Hall-Héroult electrolytic cells, can assist greatly in the optimization and the operation of the process. One of the significant factors that greatly influence the bubbles formation is the vertical walls formed by the anodes. In this paper we used a high speed camera to investigate the effect of vertical walls on the shape of a single bubble rising in two liquids of high and low viscosity namely glycerol and water respectively under various offsets of the vertical wall and gas injection rates. The images of the bubble rising were recorded at the speed of 5000 frames per second and subsequently processed using the classical image-processing algorithms incorporated with MATLAB. The data related to various parameters such as aspect ratio, equivalent diameter of the bubble and bubble distance from the vertical wall are presented and discussed for various flow rate regimes. The findings showed that the presence of a vertical wall on one side of the bubble has a significant effect on the bubble shape, orientations and the trajectory path. In addition, it was found that as the bubble moved away from the wall, the velocity of the fluid between the bubble and the wall increased relative to the surrounding fluid, which created an asymmetric flow field around the bubble. Still the aspect ratios of the bubbles were found to be a function of the rate of gas injection as well as wall offset.

2:20 PM

Large Gas Bubbles under the Anodes of Aluminum Electrolysis Cells: Alexandre Caboussat¹; *Laszlo Kiss*²; Jacques Rappaz³; Klára Vékony⁴; Alexandre Perron⁵; Steeve Renaudier⁶; Olivier Martin⁷; ¹Ycoor Systems SA; ²Universite du Quebec a Chicoutimi; ³École Polytechnique Fédérale de Lausanne; ⁴Universitat Polytècnica de Barcelona; ⁵Rio Tinto Alcan - CRDA; ⁶Rio Tinto Alcan - LRF; ⁷7Rio Tinto Alcan - LRF

The gas bubble laden layer under the anodes during the electrolysis of alumina plays an important role in the hydrodynamics and the voltage balance of the reduction cells. Under certain geometrical and operational conditions, very large gas pockets can be formed. The particular shape of these large gas bubbles was first described by Fortin et al in 1984. In the present paper the results of a combined experimental and numerical approach are described. In the experiments, the shape and the kinematics of the Fortin bubbles were analyzed by videography and Particle Image Velocimetry (PIV). A finite element method (FEM) combined with a Volume of Fluid (VOF) method was used to reproduce the experimentally observed phenomena, with particular attention to the reduction of the numerical diffusion of the liquidgas interfaces. The morphology of the large bubbles and their movement including the velocity field around them are described.

2:40 PM

Initiatives To Reduction Of Aluminum Potline Energy Consumption Alcoa Poços De Caldas/Brazil: André Abreu¹; Mauro Salles¹; Ciro Kato¹; ¹Alcoa

Energy is one of the most important inputs for aluminum production and is responsible for approximately 40% of the cost of aluminum production (CAP) in Soderberg pots. Facing the 2008/09 global economic downturn, Alcoa Poços de Caldas Plant, Brazil, has focused its efforts on a planned project, counting on its personnel's potential, to reduce the energy consumption. Main initiatives taken along this process were: workshops on energy (thermal balance and energy consumption), STAR Probe measurements (pot control focused on thermal balance), new cathode design, financial model development and changes in automatic pot control. Through this project a reduction of 77mV/pot and 0.30 kWh/kg Al were achieved, the best ever result reached at the plant at the present load level. In financial terms, in 2008/09, US\$ 1 million was saved without any extra investment.

3:00 PM

Electrical Conductivity of the KF-NaF- AlF3 Molten System at Low Cryolite Ratio with CaF2 Additions: Alexander Redkin¹; *Alexander Dedyukhin*¹; Alexei Apisarov¹; Pavel Tin'ghaev¹; Yurii Zaikov¹; ¹Institute of High Temperature Electrochemistry

Calcium fluoride is brought to cryolite-alumina melts with alumina. The CaF2 content does not exceed 5 wt.%. It increases density and depress the electrical conductivity of cryolite-alumina melts. The influence of calcium fluoride on physicochemical properties is investigated only for high cryolite ratio (2.5-3.0). At lower CR the electrical conductivity of cryolite melts containing CaF2 was not investigated yet. The electrical conductivity of the NaF-KF-AIF3 system at CR=1.3-1.7 was investigated depending on the CaF2 content and [KF]/([NaF]+[KF]) molar ratio. The CaF2 concentration did not exceed 16 wt. %. The [KF]/([NaF]+[KF]) molar ratio was varied from 0 to 0.5. The electrical conductivity was found to decrease with calcium fluoride addition at all electrolytes under investigation. The cryolite ratio effect on the electrical conductivity of NaF-KF-AIF3-CaF2 melts has been discussed.

3:20 PM Break

3:30 PM

Study of ACD Model and Energy Consumption in Aluminum Reduction Cells: *Tian Yingfu*¹; Wang Hang¹; ¹Chongqing Tiantai Aluminum Industry Co., Ltd

A model of anode-cathode distance (ACD) is built according to actual production in traditional reduction cells. And the limit ACD is study in this paper. Based on the ACD model and the limit ACD it can be described why some cells can normal produce under low cell voltage at present aluminum industry. And it is possible that only 9500kW•h/t of the DC energy will be required at 2.0 cm of ACD and 0.8 A/cm² of anode current density.

3:50 PM

Cell Voltage Noise Reduction Based on Wavelet in Aluminum Reduction Cell: *Binchuan Li*¹; Jianshe Chen¹; ¹Northeastern University

For line current fluctuation, cell voltage signals collected in aluminium electrolysis process are with high noise, which have a significant impact on the electrolyzer cell voltage and precision of alumina feeding amount. Based on wavelet de-noising theory, this paper analyses and compares different wavelet bases and threshold conditions for signal de-noising effect by application of MATLAB modeling simulation and field research. Simulation and processing results of field data show that 5-step Harr Wavelet is a good choice for filtering cell voltage signal, with better prospects.

Bulk Metallic Glasses VIII: Mechanical and Other Properties II

Sponsored by: The Minerals, Metals and Materials Society, TMS Structural Materials Division, TMS/ASM: Mechanical Behavior of Materials Committee

Program Organizers: Gongyao Wang, University of Tennessee; Peter Liaw, Univ of Tennessee; Hahn Choo, Univ of Tennessee; Yanfei Gao, Univ of Tennessee

Thursday PM	Room: 6D
March 3, 2011	Location: San Diego Conv. Ctr

Session Chairs: Dongchan Jang, California Institute of Technology; Yuri Petrusenko, National Science Center - Kharkov Institute of Physics & Technology

2:00 PM Invited

Transition from Strong-Yet-Brittle to Stronger-and-Ductile by Size Reduction in Metallic Glasses: *Dongchan Jang*¹; Julia Greer¹; ¹California Institute of Technology

A combination of high strength and extended deformability of materials is favorable for engineering applications, as the former assures optimal performance under extreme environments while the latter increases the reliability by protecting the system from a sudden breakdown. In this work we report the attainment of both high strength and superior deformability in Zr-based metallic glass by using sample dimensions as key propertycontrolling parameter. We report that once the lateral dimension is decreased to 100 nm, the formation of shear bands seizes, and the material shows significant homogeneous plasticity (25%) while maintaining its high strength (2.25 GPa). Furthermore, unlike in other engineering materials, we observe a distinct difference between the transition from lower, bulk-like strength to higher one and that from brittle to ductile deformation, as strength and ductility appear to be de-coupled in these metallic glass nano-pillars. A phenomenological model for size dependence and brittle-to-homogeneous deformation is provided.

2:20 PM Invited

Local Structures of Supercooled Ni-Nb, Cu-Zr, and Cu-Hf Melts at Eutectic and Bulk Metallic Glass-Forming Compositions: Victor Wessels¹; Kevin Laws²; Kisor Sahu¹; Nicholas Mauro³; Anup Gangopadhyay³; Kenneth Kelton³; Jörg Löffler¹; ¹ETH Zurich Laboratory of Metal Physics and Technology; ²University of New South Wales; ³Washington University in St. Louis

The development of stable, efficiently-packed clusters has been proposed to form the basis of improved glass-forming ability in certain alloy compositions. The observation of similar cluster formation in supercooled liquids of binary eutectic compositions may provide a solution to the longstanding puzzle of Stockdale, Hume-Rothery and Anderson regarding the preferential occurrence of eutectics at certain whole-number composition ratios. Recently, a rapid chemical and topological ordering in a supercooled Cu46Zr54 liquid was measured using the beamline electrostatic levitation (BESL) technique, consistent with the results of MD simulations that predict the development of atomic-scale ordered clusters in supercooled melts prior to the glass-forming compositions in Ni-Nb, Cu-Zr, and Cu-Hf alloys. By comparing the results of the BESL analysis with predictions from a stable cluster packing model, the influence of atomic-scale clustering on liquid stability and glass-forming ability was studied.

2:40 PM

Sliding Wear Behavior of Cu50Hf41.5Al8.5 Bulk Metallic Glass: *Rainer Hebert*¹; Dharma Maddala¹; ¹University of Connecticut

The sliding wear and friction behavior of Cu50Hf41.5Al8.5 bulk metallic glass has been studied at different devitrification stages. Hardness and wear volume loss are linearly related for the fully amorphous condition and the early devitrification stage. For longer annealing times, the crystallization

products remain below about 50-80 nm in size, the wear behavior improves marginally while the hardness increases about twice as much for samples annealed at 515°C for between 60 min and 300 min annealing than for the first 60 min. Fracture toughness measurements suggest that the wear behavior changes from hardness controlled to fracture toughness controlled with devitrification. Transmission electron microscopy studies showed moreover that nanocrystals developed during sliding for as-cast sample and structurally relaxed samples. The results of this study suggest that wear behavior of the Cu50Hf41.5Al8.5 metallic glass can be improved with careful annealing treatments and then exceeds the wear behavior of 304 stainless steel.

2:50 PM Invited

Residual Stresses Induced by Laser Shock Peening on Zr-Based Bulk Metallic Glass and Its Effect on Plasticity: *Yunfeng Cao*¹; Xie Xie²; Bartlomiej Winiarski³; Gongyao Wang²; Yung Shin¹; Philip Withers³; Peter Liaw²; ¹Purdue University; ²University of Tennessee; ³University of Manchester

Zr-based bulk metallic glasses (BMGs) are a new family of attractive materials with good glass-forming ability and excellent mechanical properties. However, BMGs typically show near-zero ductility in tension and limited plasticity in compression, which significantly impedes the wide industrial application of BMGs. It was recently reported that the plasticity of BMG can be improved by controlling the residual stress in BMGs. In this study, laser shock peening (LSP) under a water-confinement configuration is employed to impart compressive residual stresses into the BMG material and hence to improve the plasticity of BMG. An improvement of plasticity is demonstrated via static compression tests. A complete LSP model, while considering the LSP-induced plasticity, is employed to predict the residual stresses by LSP for the first time, which are compared with the experimental data measured by the focused-ion-beam micro-slitting method. A reasonable agreement is obtained, especially in the region close to the workpiece surface.

3:10 PM

Relaxation and Nanocrystallization of Bulk Amorphous Niti Processed by Severe Plastic Deformation: *Martin Peterlechner*¹; Joachim Bokeloh²; Gerhard Wilde²; Thomas Waitz¹; ¹University of Vienna, Faculty of Physics; ²University of Münster

Metallic glasses can be obtained by processing routes that drive an initial crystalline phase far from thermal equilibrium. In the present work, bulk amorphous NiTi alloys were processed by severe plastic deformation. At relatively low degrees of the deformation, specimens contain a mixture of crystalline and amorphous phases. The crystalline volume fraction decreases with increasing degree of deformation until an almost completely amorphous structure is obtained. Upon heating, nanocrystallization occurs by three-dimensional growth at a constant rate. The overall activation energy of the crystallization is significantly lower than that observed in the case of thin ribbons of amorphous NiTi processed by sputter deposition or melt spinning. The results of the crystallization obtained from isothermal calorimetry were modelled in terms of the Johnson-Mehl-Avrami theory. This requires a careful analysis of the data with respect to the overall exothermic heat flow caused bycrystallization and relaxation of the amorphous phase.

3:20 PM Break

3:30 PM Invited

Manifestation of the Bulk Metallic Glass Structure Features in the Compression-Compression Fatigue Experiments: Yuri Petrusenko¹; Alexander Bakai¹; Ivan Neklyudov¹; Sergij Bakai¹; Peter K. Liaw²; Gongyao Y. Wang²; Lu Huang³; Tao Zhang³; ¹National Science Center - Kharkov Institute of Physics & Technology; ²The University of Tennessee; ³Beihand University

We have performed extensive experiments using the electron irradiation and fatigue technique, which study the bulk metallic glass (BMG) structuredefect stability and their role in the anelastic and plastic deformations. These data in combination with results of the field emission microscopy lead to a conclusion that BMGs possess stable points and extended structure defects. This conclusion is important for the interpretation of results of the low (10

Hz) and high (20 kHz) frequency compression-compression fatigue and fracture experiments. The low-frequency fatigue has comparatively large fatigue-endurance limits, and the fracture is controlled by the initiated from the surface catastrophic crack propagating at a direction of 45° to the applied stress. At the high-frequency fatigue the BMG fracture is a result of several stages, which includes anelastic boundary slip, slip-layers formation and propagation, branching and development of the inner nano-cracks, resulting in the catastrophic crack formation mainly along the applied stress direction.

3:50 PM

Structural Characterization of Iron Based Bulk Metallic Glass by Dilatometric Measurements: Fatemeh Saeidi¹; *Mahmoud Nili-Ahmadabadi*¹; Amir Seifoddini¹; ¹University of Tehran

Bulk metallic glasses (BMGs) are a relatively new class of materials with a specific combination of interesting properties. Understanding the structure of BMGs is an attractive issue in material science, due to its close connection with glass forming ability and mechanical properties. The structural inhomogeneous nature and the structural stability of BMGs greatly affect their mechanical properties. In the present study, dilation measurements were conducted on samples of a Fe-Co-Cr-Mo-Y-C-B bulk metallic glass to calculate the structural stability and the activation energy of the alloy by heating samples with different heating rates and routs. Dilation curves and thermal behavior of the samples are analyzed based on the structural relaxation and free volume theory. In addition some thermal parameters such as glass transition temperature and crystallization temperatures are obtained by dilatometric curve and compared with temperatures derived from differential thermal analysis (DTA).

4:00 PM

Effect of Li on the Microstructure and Mechanical Properties of an Mg-Based BMG: *Ignacio Figueroa*¹; John Plummer²; Iain Todd²; ¹National Autonomous University of Mexico; ²University of Sheffield

Though Mg-based glassy alloys typically fail in a brittle manner, with cracking often occurring before yielding, they display high specific strengths making them a potential option for engineering applications. Li has the ability to lower the density of the alloy further though limited data is present in the literature as to the effect it has on structure, with no reports of its impact on mechanical response. Here, between 3-15 at% Li is added to a base Mg-Cu-Gd BMG with XRD and TEM implemented to characterise the structural response to the alloying addition. Adding Li in increasing proportions is found to favour the formation of a glass-crystal composite and induce plastic flow. Finally, a fully crystalline alloy results with maximum plastic flow, whilst retaining the high failure strength of the base alloy. It is thus illustrated that amorphous pre-cursors can lead to crystalline alloys with improved mechanical properties.

4:10 PM Invited

Selective Nanocrystallization of Metallic Glasses Induced by Nanoindentation: Jordi Sort¹; Jordina Fornell¹; Aïda Varea¹; Emma Rossinyol¹; Luiz Bonavina²; Carlos Souza²; Walter Botta²; Claudemiro Bolfarini²; Claudio Kiminami²; Santiago Suriñach¹; Josep Nogués³; *Maria D Baró*¹; ¹Universitat Autònoma de Barcelona; ²Universidade Federal de Sao Carlos; ³ICREA/ICN-CSIC

Nanocrystallization of $Zr_{c_2}Cu_{18}Ni_{10}Al_{10}$ and $Fe_{67,7}B_{20}Cr_{12}Nb_{0.3}$ (at %) metallic glasses can be locally induced by nanoindentation. While in the first alloy this phenomenon causes significant increases in hardness and plasticity, nanocrystallization of the Fe-based alloy constitutes an effective magnetic patterning procedure. Indeed, periodic arrays of micrometer-sized ferromagnetic structures with perpendicular-to-plane magnetic anisotropy and enhanced saturation magnetization are obtained at the surface of the Fe-based glassy ribbon (initially showing in-plane magnetic anisotropy) after nanoindentation. Detrimental effects caused by the dipolar/exchange interactions between the dots and the matrix can be avoided by heating the indented ribbon beyond T_c of the glass (340 K), since the crystallized regions (consisting of α -Fe) remain ferromagnetic up to very high temperatures. The inverse magnetostriction effect seems to be the main factor contributing to the observed perpendicular anisotropy. Our results pave the way for new

strategies to fabricate miniaturized magnetic devices or patterned magnetic recording media.

4:30 PM

Phase Formation and Mechanical Properties of Cu-Zr-Co alloys: *Fatemeh A. Javid*¹; Norbert Mattern¹; Simon Pauly¹; Jürgen Eckert¹; ¹Leibniz Institute for Solid State and Materials Research Dresden

Cu50Zr50 B2 phase is a stable phase at temperatures above 715oC. On the other hand Co50Zr50 is a B2 phase which is stable at room temperature. It seems that adding cobalt to binary Cu-Zr stabilizes Cu50Zr50 B2 phase at room temperature. In this work the effect of cobalt on phase formation and mechanical properties of Cu-Zr alloy is investigated. Rods with composition of Cu50-xZr50Cox (x=2, 5, 10, 20 at.%) and 3mm Ø were suction casted into a copper mould. X-ray analysis showed a martensite CuZr phase for 2 & 5 at.% Co compositions, while compositions with 10 & 20 at.% Co had stabilized B2 phase. DSC measurements declared a martensitic transformation for 2 & 5 at.% Co samples in which increasing the Co content, decreased the transformation temperatures. Under compression test 10 & 20 at.% Co compositions showed deformation-induced martensitic transformation and plastic strains up to 15%.

4:40 PM

Temperature Effects on Flow of Several Metallic Glasses: *Lisa Deibler*¹; John Lewandowski¹; ¹Case Western Reserve University

Several different test techniques were utilized to examine the effects of changes in test temperature and/or prior thermal exposure on the flow behavior of a variety of different amorphous metal alloys. Melt spun ribbons of magnesium-, iron-, and zirconium- based metallic glasses were evaluated as well as zirconium-based bulk metallic glasses. The effects of changes in test temperature and strain rate on the flow/viscosity were determined at temperatures approaching Tg for the various systems. Fracture surface morphologies for the different metallic glasses and test conditions were also characterized. The results will be reviewed in the light of ongoing work on the behavior of amorphous systems.

4:50 PM

Study of Activation Parameters of Deformation by Broadband Nanoindentation Creep in Structural Relaxed Zr-Cu-Al Bulk Metallic Glasses: Zenon Melgarejo¹; Joseph Jakes²; Jonathan Puthoff¹; Hongbo Cao¹; Chuan Zhang¹; Donald Stone¹; Paul Voyles¹; ¹University of Wisconsin-Madison; ²Performance Enhanced Biopolymers, United States Forest service, Forest Products laboratory

Models of plastic deformation in BMGs hypothesize shear transformation zones (STZs) as the elementary units of plastic deformation. Activation energy for shear of an STZ depends on stress; activation parameters should vary systematically with atomic structure including short and medium range order and should be sensitive to composition, quenching rate, and annealing. In the present work we employ broadband nanoindentation creep (BNC) to characterize activation volume and energy for plastic deformation in Zr-Cu-Al BMGs. BNC measures hardness across 5-6 decades of strain rate, and is therefore capable of mapping out the shape of the activation barrier. BMGs studied include Zr54Cu38Al8, Zr45Cu49Al6, and Zr36Cu58Al6. STZ sizes estimated from activation volume measurements vary between 170 and 600 atoms depending on composition and annealing. Annealing generally increases both activation energy and STZ volume. Structural relaxation of Zr54Cu38Al8 is studied in detail by measuring BNC in specimens annealed in a differential scanning calorimeter (DSC).

5:00 PM

Enhanced Plasticity of a Zr-Cu-Ni-Al Bulk Metallic Glass by Micro Nb Additions: Shuang-shuang Chen¹; John Plummer¹; Iain Todd¹; ¹The university of Sheffield

Zr-based bulk metallic glasses have been extensively studied because of their high glass forming ability and prominent mechanical properties. In this work, the effect of micro Nb additions on plasticity of a Zr-Cu-Ni-Al bulk metallic glass is explored. In compression testing, the base alloy showed limited plasticity of 2.2%; however, this significantly increased to 19.7% upon addition of 0.5 at.% Nb, with the alloy exhibiting typical strain softening during deformation. The large plasticity was attributed to shear band interaction with a phase separated structure.

5:10 PM

A Study on Crystalline Phases Present in the As-Solidified and Crystallized Microstructures in $Zr_{s3}Cu_{21}Al_{10}Ni_{8}Ti_{8}$ Alloy: *Raghvendra Tewari*¹; Suman Neogy¹; Gautam Dey¹; Srikumar Banerjee²; S. Ranganathan³; ¹Bhabha Atomic Resrach Centre; ²Department of Atomic Energy; ³ Indian Institute of Science

In the present study the as-solidified and subsequently crystallized microstructures of $Zr_{s3}Cu_{21}AI_{10}Ni_{8}Ti_{8}$ alloy have been examined in detail using transmission electron microscopy. Solidification was carried out by melt spinning, suction casting and copper mould casting techniques. The last technique yielded a partially crystalline microstructure comprising 'big cube phase' in dendritic morphology and bct Zr_2Ni phase, whereas the other two techniques resulted in amorphous microstructures. The crystallography of the dendritic growth and that of the instabilities at the crystal/liquid interface has been examined and it has been established that the dendrites grew by the formation of atomistic ledges. The bct- Zr_2Ni phase formed during solidification also appeared during crystallization and showed various types of internal faults depending upon the crystallite size, crystallography of which has been examined. The present study also brought out the role of oxygen in controlling the degree of medium range order and crystallization behavior of glasses.

Carbon Dioxide and Other Greenhouse Gas Reduction Metallurgy - 2011: CO2 and GHG Reduction in Metal Industries

Sponsored by: The Minerals, Metals and Materials Society, TMS Extraction and Processing Division, TMS Light Metals Division, TMS: Energy Committee

Program Organizers: Neale Neelameggham, US Magnesium LLC; Ramana Reddy, The University of Alabama; Maria Salazar-Villalpando, National Energy Technology Laboratory; James Yurko, 22Ti LLC; Malti Goel, INSA

Thursday PM	Room: 15B
March 3, 2011	Location: San Diego Conv. Ctr

Session Chairs: Maria salazaar - Villapando, National Energy Technology Laboratory; Malti Goel, Jawaharlal Nehru University

2:00 PM Introductory Comments

2:05 PM

Vacuum Distillation of Aluminum and Silicon via Carbothermal Reduction of Their Oxides with Concentrated Solar Energy: *Peter Loutzenhiser*¹; Enrico Guglielmini¹; Alwin Frei; Aldo Steinfeld¹; ¹ETH Zurich

Using concentrated solar radiation as the energy source of high-temperature process heat, the carbothermal reductions of Al2O3 to Al and SiO2 to Si were examined thermodynamically and demonstrated experimentally at vacuum pressures. Reducing the system pressure favors Al(g) and Si(g) formation, enabling their vacuum distillation and avoiding contamination by carbides and/or oxycarbides. Exploratory experimentation in a solar reactor was performed with mixtures of charcoal with alumina and silica in the ranges of 1300-2000 K and 1997–2263 K, respectively, at 10-3 bar by direct exposure to concentrated thermal radiation. Distilled samples contained up to 19 wt% of Al in Al-Al2O3 mixtures and 79 wt% of Si in Si-SiO2 mixtures. When the reducing agent is derived from a biomass source, the solar-driven carbothermal processes are CO2 neutral.

2:25 PM

The Alkali Roasting of Complex Oxide Minerals for High Purity Chemicals – Beyond Le Chatelier into 21st Century: Animesh Jha¹; ¹University of Leeds

It was in 1855 when Le Chatelier invented the alkali roasting and leaching process for the extraction of alumina from natural minerals. However, his process was replaced by the Bayer process since 1888. Was the aluminium industry short-sighted to reject Le Chatelier in favour of Bayer's process? This paper critically examines the impact of Le Chatelier's proposal for the extraction two important inorganic chemicals, alumnium hydroxide from bauxite and gibbsite and sodium chromate from chromite minerals. The paper reviews past research in alumina and chromium chemicals and adds new dimension to the chemicals processing, by considering Le Chatelier's approach for the extraction of very high purity aluminium hydroxide, chromium chemicals and titanium dioxide, using high-temperature alkali roasting followed by leaching. The emphasis of new research is on zero-waste process, including CO2 sequestration, which was the beautiful characteristic of Le Chatelier's process chemistry but lost through the generations.

2:45 PM

The Alkali Roasting and Leaching of Ilmenite Minerals For the Extraction of High Purity Synthetic Rutile and Rare-Earth Oxides: Animesh Jha¹; *Graham Cooke*¹; ¹University of Leeds

CO2 reduction by alternative energy devices such as wind-power, electric vehicles utilize rare-earth elements (REE) in several forms; such as in piezoelectric devices, batteries and magnetic materials. In 2010, the 95% of Rare Earth supply is controlled by China, compared to USA being dominant supplier in the 1980s. The dependence upon a single source of lanthanides has prompted the utilization of lower grades of titaniferous mineral concentrates, which often have rich seams of REE. We propose a new methodology, which utilizes the low-grade minerals for the extraction of synthetic rutile and also significant quantities of REE. We demonstrate the alkali roasting of lower grades of mineral concentrates and subsequent leaching in an aqueous medium for preferential flocculation of REE during the extraction of synthetic rutile. Changes in mineral structure during alkali roasting and leaching determine flocculation of REE and permit their separation at the front end of unit process.

3:05 PM

Hydrogen-Rich and Carbon-Neutral Gas as Reducing Agent for Heavy Metal Containing Residues: *Thomas Griessacher*¹; Jürgen Antrekowitsch¹; ¹University of Leoben

Heavy metal containing residues are typically hazardous wastes why on the one hand side a deposition gets more and more complicated and on the other hand side the large amounts of metals like Zn, Cu, Fe and Pb represent a significant value. So a post-treatment of these materials with the recovery/recycling of the metals and stabilization of the waste is not even ecological but often also economical. The therefore typically applied recycling processes utilize pyrometallurgical steps, where carbon or carbon monoxide from fossil coal and coke is used as reducing agent, which results in large amounts of CO_2 -emissions. An alternative option is the application of a hydrogen-rich gas emitted at biomass utilization processes as carbonneutral reducing agent. Investigations at a retort process which were done at different temperatures and times showed excellent results concerning the achievable reduction rates and final contents of the heavy metals for various residues.

3:25 PM

Bauxite Residue Use to Remove SO2 from Gas Effluents: *Luis Venancio*¹; Paulo Santos¹; José Antonio Souza¹; Emanuel Macedo¹; Wanderson Rodrigues¹; ¹Federal University of Pará

The production of alumina from bauxite using the Bayer process generates 0.7 to 2.0 ton of the residue known by red mud per ton of alumina. This material has no large scale current use and is usually stored. This paper shows that it can be used in a suspension with water as a gas effluent cleaner with high efficiency to remove SO2. It can substitute other materials currently

140th Annual Meeting & Exhibition

used reducing the overall environmental impact and potentially reducing the cost of gas treatment.

3:45 PM

Greenhouse Gas Emission Reduction from Aluminum Industry in India: Challenges and Prospects: Malti Goel¹; ⁻¹INSA

Ferrous and non-ferrous metals industries are source of both direct and indirect greenhouse gas (GHG) emissions. Indian metal industry accounted for 29.7% of the total GHG emitted from the industry sector in 2007 and is moving towards low carbon economy. Aluminum is second largest contributor after steel. Indian Aluminum industry is growing and is adopting several effective measures for better efficiencies through process change and waste utilization. Improvement in the energy efficiency is expected to optimize energy use and realize material efficiencies as well. It can form the basis of monitoring reduction in emissions. National Mission for Enhanced Energy Efficiency (NMEEE) seeks to upscale the efforts to unlock the market for energy efficiency on a public private partnership (PPP) basis to achieve up to 25% saving in energy. In this paper an attempt is made to overview recent developments in Indian Aluminum industry as well as summarizes challenges and prospects.

4:05 PM Break

4:15 PM

Dissolution Kinetics of Steelmaking Slag and Its Promotion for the Growth of Algae: Chunfang Zi¹; Kai Huang¹; Lianyun Liu¹; Xiaohui Li¹; *Hongmin Zhu*¹; ¹University of Science and Technology of Beijing

In this study, the dissolution kinetics of steelmaking slag in water was studied. It was found that the silicon extraction increases with temperature, and decreasing in the particle size of slag enhanced silicon dissolution. A simple dissolution model was proposed to describe and explain the dissolution behavior of the slag particles in water. The external film diffusion was determined to be the controlling step of the whole dissolution process. The model described experimental data well in the whole process of dissolution. The apparent activation energy determined to be 4.8 kJ/mol, and the concentration of silicon produced a linear relationship with the specific surface area of slag, which also supports the assumption of external film diffusion control. Further experiments by using pH meter to monitoring the pH variation for the slag particle samples showed more proofs that the leaching behavior observed the physical dissolution process.

4:35 PM

Life Cycle Assessment of China's Alumina Manufacturing by Bayer Process: *Li Hongxu*¹; Duan Ge¹; Bai Hao¹; Cang Daqiang¹; ¹University of science and technology, Bejing

In this paper LCA was newly used to evaluate the environmental impact of alumina manufacturing by Bayer process in china from two aspects of matter and energy flow, Gabi software acted as analysis tools with evaluation model established, and five environmental impact assessment criteria were selected based on the actually typical date of manufacturing. Evaluation results show that alumina manufacturing has a great impact on the global warming and human health of respiration, even roasting process gives rise to the greatest impact of winter fog index. Scenario analysis has proposed possible ways of reducing environmental load caused by Bayer process including: (1) the economic and efficient use of mineral processing technology; (2) optimization of energy use, saving power consumption or the use of new more economical source of energy; (3) actively promote the use of innovated technology and equipment in alumina manufacturing and waste such as red mud utilization process.

4:55 PM

Analysis of Carbon Emission Reduction of China's Integrated Steelworks: *Hao Bai*¹; ¹University of Science and Technology Beijing

Coal, as the main energy in ferrous metallurgy, is consumed on a large scale and great amount of CO2 is emitted likewise. In this paper, a model, based on carbon balance, was developed for CO2 emission analysis, with data obtained from a typical integrated steelworks in China. The result shows that, CO2 emissions increase almost constantly with the growth of

steel production. However, coals of different classes and product variety in the steelworks exerted an influence on CO2 emissions. Furthermore, three scenarios, including natural gas instead of coal for power generation, EAF process partly replacing integrated steelmaking, and feasible techniques applied to achieve lowest process energy consumption (LPEC), were assumed to seek possible ways of carbon emission reduction. The result proves that the second scenario is most effective. If 40% of the steel product could be from EAF process, CO2 emissions would be reduced by 45.07%.

Challenges in Mechanical Performances of Materials in Next Generation Nuclear Power Plants: Session II

Sponsored by: The Minerals, Metals and Materials Society, American Nuclear Society, ASM International, Japan Institute of Metals, National Science Foundation, TMS Materials Processing and Manufacturing Division, TMS Structural Materials Division, ASM Materials Science Critical Technology Sector, TMS: Advanced Characterization, Testing, and Simulation Committee, TMS/ASM: Composite Materials Committee, TMS: Energy Committee, TMS: High Temperature Alloys Committee, TMS/ASM: Nuclear Materials Committee

Program Organizer: Faramarz Zarandi, CANMET-Materials Technology Laboratory

Thursday PM	Room: 5A
March 3, 2011	Location: San Diego Conv. Ctr

Session Chairs: G. Robert Odette, University of California, Santa Barbara; Laura Carroll, Idaho National Laboratory

2:00 PM

Simplified Powder Processing of ODS Ferritic Stainless Steels: Joel Rieken¹; Iver Anderson²; Matthew Kramer²; ¹Iowa State University; ²Ames Laboratory

Precursor ferritic stainless steel powders (i.e., Fe-16.0Cr-(0.2-0.4)(Ti,Hf)-0.2Y at.%) were oxidized in situ using a novel gas atomization reaction synthesis technique. During this process, a metastable Cr-enriched oxide layer formed and enveloped the rapidly solidified powder particles. Upon consolidation, this metastable oxide phase was used as an internal oxygen reservoir, which was continuously dissolved during elevated temperature heat treatment, through oxygen exchange reactions with Y and other reactive alloying additions (i.e., Ti or Hf). These exchange reactions resulted in the formation of nano-metric mixed oxide dispersoids (i.e., Y-Ti-O or Y-Hf-O) throughout the alloy microstructure. Subsequent thermal-mechanical processing was then used to develop fine dislocation sub-structures for increased alloy strengthening. Transmission electron microscopy coupled with high-energy X-ray diffraction was used to evaluate phase evolution and thermal stability of the dispersoids within these ODS ferritic stainless steel alloys. Support from the USDOE-FE (ARM program) through Ames Laboratory contract no. DE-AC02-07CH11358 is gratefully acknowledged.

2:20 PM

Degradation of High Temperature Mechanical Performance in Ferritic-Martensitic Steels: *Meimei* Li¹; Saurin Majumdar¹; Ken Natesan¹; ¹ANL

Ferritic-martensitic steels are the lead structural materials for nextgeneration nuclear energy systems. Due to increased operating temperatures required in advanced high-temperature reactor concepts, the high temperature performance of the alloys and reliable high temperature structural design methodology have become increasingly urgent issues. This paper discusses the critical code qualification issues identified for applications of advanced ferritic-martensistic steels with the focus on extension of design allowables to the 60-year design life and need for an improved creep-fatigue design rule. Efforts in developing a fundamental understanding of microstructural evolution and associated mechanical property change during long-term aging processes to assist development of mechanism-based predictive models for reliable data extrapolation will be discussed. Detailed analysis of archive fatigue and creep-fatigue data of ferritic-martensitic steels to improve the understanding of creep-fatigue interaction and establishment of improved creep-fatigue models will also be addressed.

2:40 PM

Optimized Thermomechanical Treatment for High Strength 9Cr Ferritic-Martensitic Steels: *Lizhen Tan*¹; Edward Kenik¹; Jeremy Busby¹; ¹Oak Ridge National Laboratory

Ferritic-martensitic (F-M) steels, e.g., 9-12 wt.%Cr, are important structural materials for use in advanced nuclear reactors due to their tolerance of irradiation and swelling resistance. However, their strength is less than that of other candidate alloy systems. Many efforts have focused on controlling alloying compositions during the development of such steels. Recently, thermomechanical treatment (TMT) showed significant improvement in mechanical properties on several high-Cr F-M steels by introducing high density of dislocations and fine precipitates. This work primarily studies the effect of TMT on a commercial 9Cr F-M steel NF616. The NF616 in an optimized TMT condition showed more than 35% enhancement in strength, which had strength comparable and ductility superior to PM2000 oxidedispersion-strengthened (ODS) steel. A variety of characterization techniques were employed to elucidate the strengthening mechanism induced by the TMT. Additionally, model 9Cr F-M steels were developed with the guidance of computational thermodynamics. Preliminary results of the model steels in TMT conditions showed significant enhancement in strength.

3:00 PM

Nitride-Strengthened Reduced Activation Martensitic Steels: *Yiyin* Shan¹; Ping Hu¹; Wei Yan¹; Wei Wang¹; Wei Sha²; Ke Yang¹; ¹Institute of Metal Research; ²Queen's University of Belfast

Two nitride-strengthened reduced activation martensitic (RAFM) steels with different Mn contents were investigated. The experimental steels were designed, based on the Eurofer 97 steel, but the C content was reduced to an extremely low level. The steel with low Mn content (0.47 wt.%) could not obtain a full martensitic microstructure due to the inevitable d-ferrite independent of cooling rate after soaking. This steel showed similar room temperature strength and higher strength at 600°C, but lower impact toughness, compared with Eurofer 97 steel. Fractography of the Charpy-V notch (CVN) impact specimen revealed that the low room temperature toughness should be related to the Ta-rich inclusions initiating the cleavage fracture. The large amount of V-rich nitrides and more dissolved Cr in the matrix could be responsible for the similar strength to Eurofer 97 steel. In the second steel the Mn content was increased to 3.73 wt.% and obtained a full martensitic microstructure.

3:20 PM

Inclusion Initiated Cleavage Fracture in a Nitride-Strengthened Reduced Activation Martensitic Steel: *Wei Yan*¹; Wei Wang¹; Ping Hu¹; Lifeng Deng¹; Yiyin Shan¹; Ke yang¹; ¹Institute of Metal Research

The nitride-strengthened reduced activation martensitic steel is a novel and promising heat-resistance structural steel for the future fusion reactor. The experimental steel in this work contained much Mn element and showed high strength at both room temperature and 600°. The inclusion morphology analysis in the steel revealed that the inclusions mainly consisted of Al2O3 and MnS. Fractography on the surface of the broken Charpy V-notch (CVN) specimens showed that the inclusions in this steel initiated cleavage fracture, which should be responsible for the poor impact toughness. The inferior tolerance of the steel to inclusions is explained from the views of the high strength enhanced by the addition of too much Mn and the detrimental characteristics of the inclusions.

3:40 PM Break

4:00 PM

Determination of Ion Bombardment, in Reactor Irradiation and Post Irradiation Fatigue Properties: *Z. W. Zhang*¹; Suiqiong Li¹; Wen Shen¹; C. T. Liu¹; Xun-Li Wang¹; Xun-Li Wang²; Bryan Chin¹; ¹Auburn University; ²Oak Ridge National Laboratory

Energetic neutron irradiation and associated transmutation reactions cause significant damage and deterioration in material properties. Any one of a number of material properties may limit the reactor performance and lifetime. Because of the cyclic nature of reactors and because cracks will inevitably be present, fatigue crack propagation as well as the influence of irradiation on fatigue behavior become one of the concerns for the designing of the fusion devices. With the development of experimental reactor and accelerator-based irradiation facilities world-wide, the development of testing technology, particularly for scoping properties of irradiated materials is of particular significance in light of the current fusion reactor materials development program. In this paper, we concentrate on some of the advance on fatigue properties testing of irradiated materials, as they conduct under the conditions of ion bombardment, in reactor irradiation and post irradiation. Some example test module designs and limitations were discussed.

4:20 PM

Oxidation and Diffusion Investigation of the Carbides Used as Cladding Materials in TRISO-Coated Fuel Particles: *John Youngsman*¹; Brian Gorman²; Ivar Reimanis²; Darryl Butt¹; ¹Boise State University; ²Colorado School of Mines

The continued development of Generation IV nuclear reactors is dependent upon advancing the fundamental understanding of TRISO-coated particle fuels under various working conditions. The present work investigates the interaction of cesium, palladium, and silver with silicon carbide and zirconium carbide in order to suggest a kinetic model for the behavior. The metals are urania fission products and the carbides are used as cladding materials that form the containment vessel in the TRISO particle. Ion implantation is used to deposit the metals into the carbide substrates which are then subjected to high temperatures. Diffusion properties and microstructure development are characterized with SIMS, EBSD, XRD, SEM, and TEM. Thermogravimetric analysis of the carbides at elevated temperatures under CO-CO₂ environments is used to supplement the diffusion and microstructural data to propose a kinetic model for the degradation of the SiC and ZrC substrates.

4:40 PM

Forming 6061 Al HIP-Clad DU10Mo Monolithic Fuel Plates: *Kester Clarke*¹; David Alexander¹; Cheng Liu¹; Hunter Swenson¹; ¹Los Alamos National Laboratory

A significant goal for the Global Threat Reduction Initiative (GTRI) is converting high performance research reactors from highly enriched (HEU) to low enriched (LEU) uranium, requiring development, qualification, and production of high-density, monolithic LEU10Mo foils. These foils are to be co-rolled with Zr and clad with 6061Al using hot isostatic pressing (HIP). Some reactor designs, for example the Advanced Test Reactor (ATR), require a forming/bending operation after HIP processing. The selected method for bending fuel plates is press brake forming with solid punches and flexible bottom dies. Small scale trials with multi-layer 6061 Al HIPclad DU10Mo (depleted uranium), co-rolled with Zr, have been performed. Important results include springback evaluation in the multi-layer plates and examination of the interaction/diffusion zone integrity as a function of strain. Experiments also provided samples for evaluation of radius measurement techniques and plate relaxation as a function of time and temperature.

Characterization of Nuclear Reactor Materials and Components with Neutron and Synchrotron Radiation: Irradiated Materials and Technique Development

Sponsored by: The Minerals, Metals and Materials Society, TMS Structural Materials Division, TMS/ASM: Nuclear Materials Committee

Program Organizers: Matthew Kerr, US Nuclear Regulatory Commission; Meimei Li, Argonne National Lab; Jonathan Almer, Argonne National Laboratory; Donald Brown, Los Alamos National Lab

Thursday PM	Room: 4
March 3, 2011	Location: San Diego Conv. Ctr

Session Chairs: Jonathon Almer, Argonne National Lab; Don Brown, Los Alamos National Lab

2:00 PM Invited

Characterization of Radioactive Materials Using the MARS Beamline at the Synchrotron SOLEIL: *Bruno Sitaud*¹; Pier Lorenzo Solari¹; Sandrine Schlutig¹; ¹Synchrotron SOLEIL

Since 2004 numerous efforts have been done at the new French synchrotron SOLEIL to construct a beamline for studying radioactive matter in general and nuclear materials in particular. This Multi Analyses on Radioactive Samples beamline (MARS) has been designed and built thanks to a close partnership with CEA. The optics and the experimental stations has been optimized for performing X-ray characterizations (diffraction, scattering, absorption spectroscopy, fluorescence imaging) for a very large variety of radioactive elements. The special infrastructure of this beamline has been defined to be in accordance with the safety regulations for analysing of relatively high activity samples (up to 2 GBq for gamma emitters and 18.5 GBq for other emitters). Several relevant results obtained during the commissioning of the experimental end stations are presented and discussed in the frame of the near future characterisations of nuclear materials from X-ray diffraction and absorption spectroscopy.

2:30 PM

Neutron Imaging for Non-Destructive Testing of Nuclear Materials: *Peter Vontobel*¹; Eberhard Lehmann¹; Yong Dai¹; Mirco Grosse²; ¹Paul Scherrer Institut; ²Forschungszentrum Karlsruhe

Unlike X-rays thermal neutrons transmit heavy metals like UO_2 or lead easily and provide high sensitivity for small amounts of hydrogen containing compounds like ZrH₂. Neutron radiography is therefore an ideal probe for non-destructive, post-irradiation examination of fuel rods from nuclear power plants or lead target rods from a spallation neutron source. After irradiation such samples are strong γ sources themselves. At the spallation neutron source SINQ of the Paul Scherrer Institute operates a unique neutron imaging facility allowing highly radioactive samples to be positioned in a neutron beam for radiography. The main advantage of this method is to highlight regions in a sample with peculiar material changes e.g. cracks or fissures, cladding corrosion, material swelling, etc.. Well-directed destructive investigations in a hot cell can subsequently be applied to such material zones. The capabilities of our facility will be demonstrated with selected results.

2:50 PM Invited

From In-Core to BOP to Waste, Neutrons Characterize Nuclear Materials and Components: Ron Rogge¹; ¹National Research Council

From the advent of materials engineering applications of neutron scattering, the Canadian Neutron Beam Centre has been applying neutron scattering techniques for the nuclear industry. Over this period stress mapping, powder diffraction, texture and other neutron scattering techniques have been employed to study materials from in the reactor core to the balance of plant (BOP). Studies have characterized in-core component materials, nuclear fuels, studied hydrogen ingress/egress, examined components of heat transport system and evaluated materials used for waste storage. The presentation will present how results have been used to further fundamental understanding of the materials, aid failure analysis, evaluate fitness-for-service and predict component lifetime.

3:20 PM

SANS and TEM Investigation of Phase Precipitation in HT-9 at High Neutron Irradiation Dose Levels: *Joris Van den Bosch*¹; Osman Anderoglu¹; Tobias Romero¹; Patricia Dickerson¹; Robert Dickerson¹; Peter Hosemann¹; Rex Hjelm¹; Stuart Maloy¹; ¹LANL

Phase precipitation caused by neutron irradiation is known to strongly influence the mechanical properties of the structural materials and forms one of the lifetime limiting factors for high Cr steel cladding. Most phases can be analyzed using TEM but fully coherent, isostructural phases such as alpha prime are very difficult to image with TEM and more easily observed using small angle scattering measurements. Therefore, TEM and SANS specimens of ferritic-martensitic alloy HT-9 were taken from a duct irradiated in the FFTF reactor up to 155 dpa at a temperature of 380-510°C. In this presentation we will discuss the microstructure of the HT9 steel duct after long term irradiation based on Small Angle Neutron Scattering (SANS) and TEM results from 5 different locations along the length of the duct.

3:40 PM

Synchrotron Radiation Study of Unirradiated and Irradiated Ferritic-Martensitic Steels: *Meimei Li*¹; Jonathan Almer¹; Yang Ren¹; Jeff Terry²; Stuart Maloy³; Ken Natesan¹; ¹ANL; ²Illinois Institute of Technology; ³Los Alamos National Lab

Ferritic-martensitic steels are the lead structural materials for various types of advanced fission and fusion energy systems. The high performance of this class of alloys heavily relies on complex dislocation and subgrain structure and second-phase precipitate particles. The stability of these microstructual features is the key for maintaining the superior properties over an extended reactor service life. To develop a quantitative understanding of microstructural evolution and mechanical property degradation during long-term thermal aging, unirradiated mod.9Cr-1Mo and NF616 were investigated by in situ synchrotron x-ray diffraction (XRD) under thermal and thermo-mechanical loading and by ex situ thermal and mechanical testing and microstructural characterization by synchrotron radiation and electron microscopy. Microstructural change under irradiation was characterized by synchrotron extended x-ray absorption fine structure (EXAFS) spectroscopy in irradiated mod.9Cr-1Mo to understand the different roles of alloying elements in the evolution of local atomic environments during irradiation.

4:00 PM Break

4:10 PM

X-ray Absorption Spectroscopy Study of Irradiated ZrC and ZrN: *Daniel Olive*¹; Yong Yang²; Jeff Terry¹; ¹Illinois Institute of Technology; ²University of Wisconsin-Madison

In complex alloys, radiation-induced segregation and the creation of other stable phases can lead to irradiation hardening and embrittlement. The mechanisms of radiation damage are much less clear in simple, stable binary compounds. Samples of ZrC and ZrN were irradiated to 1 dpa at 800 °C in the Advanced Test Reactor, and shipped to the MRCAT beamline for XAS measurements. The data indicates that no new phases formed in the material. The ZrC retained the overall cubic NaCl structure, with no detectable expansion of the lattice. The number of nearest neighbors remained saturated, as extra carbon in the grain boundaries, adventitious carbon, etc. will find and repair unterminated Zr caused by irradiation. However, at larger interatomic distances, the coordination was significantly reduced indicating that defect sites have resulted in smaller regions of perfect crystallinity. The measurements on ZrN showed similar results to that of ZrC.

THURSDAY PM

4:30 PM

Cold Neutron Prompt-Gamma Activation Analysis of Hydrogen Pickup during Zirconium Alloy Corrosion: *Adrien Couet*¹; Arthur Motta¹; Robert Comstock²; Rick Paul³; ¹Penn State University; ²Westinghouse Electric Company; ³National Institute of Standards and Technology

Zirconium alloy fuel cladding corrosion and the associated hydrogen pickup is a critical life-limiting degradation mechanism for nuclear fuel in existing and advanced nuclear reactors, since the ingress of hydrogen can cause embrittlement. Past studies used destructive techniques, such as hot vacuum extraction, to measure hydrogen but knowledge of the pickup variation with corrosion and the pickup mechanism is lacking. This research investigates the mechanistic link between hydrogen pickup, oxidation rate, alloy chemistry, and microstructure on a wide selection of zirconium alloys. With the usual destructive techniques, we combine the non destructive technique of Cold-Neutron Prompt-Gamma Activation Analysis. This technique allows precise determinations of hydrogen content, (and thus the hydrogen pickup fraction at various stages of corrosion), and the ability to perform several measurements on a single sample, thus removing the sample-to-sample variability. The results obtained are discussed and related to the overall corrosion kinetics and to the oxide structure.

4:50 PM

Comparison of Proton, Benchtop X-Ray and Synchrotron X-Ray Radiography of Surrogate Urania and Thoria/Ceria Composite Fuel Samples: *Mark Bourke*¹; Donald Brown¹; Darrin Byler¹; Christopher Chen¹; Jeremy Kropf²; James Hunter¹; Fesseha Mariam¹; Christopher Morris¹; Andrew Saunders¹; ¹Los Alamos National Laboratory; ²Argonne national laboratory

Two surrogate nuclear fuel types were examined with three radiographic probes. The samples were rods (a few cm long) of urania and thoria-ceria that were 5mm and 10mm in diameter respectively. Spatial and density heterogeneities were introduced with inclusions during sintering and by altering the sintering conditions during powder consolidation. Three radiographic tools were used; benchtop (425 KeV) X-rays, synchrotron (225KeV) X-rays and 800 MeV protons. Tomographic reconstructions were produced. The spatial and density resolutions achieved with the different techniques are compared as well as the potential for their improvement. The potential application of the different techniques to highly radioactive samples will also be considered.

5:10 PM

Crystallographic Texture Contrast in Neutron Radiography of Zirconium Based Components: Javier Santisteban¹; Sven Vogel²; Anton Tremsin³; Winfried Kockelmann⁴; Eberhard Lehmann⁵; ¹Comision Nacional de Energia Atómica; ²Los Alamos National Laboratory; ³University of California at Berkeley; ⁴Rutherford Appleton Laboratory; ⁵Paul Scherrer Institut

The microstructure and crystallographic texture of metal objects affect the transmission of thermal neutrons. As a result the Bragg edges departs largely from those found on isotropic polycrystalline materials, with some Bragg edges even absent along certain specimen directions. A clear understanding of the wavelength dependence of the neutron transmission of textured materials can be directly exploited in energy-resolved neutron imaging. Here, we present the wavelength-dependent transmission of different Zr-based components of nuclear reactors such as pressure tubes, rolled plates and welds, in order to interpret the intensity variations observed in neutron radiographies of such components. The discussion is based on energy-resolved transmission measurements and radiographies taken at ISIS (UK) and PSI (Switzerland), and theoretical calculations of the elastic coherent total cross section from the orientation distribution function (ODF) of the crystallites composing a sample.

5:30 PM

Spatially Resolved Strain Fields in Nuclear Fuel Plates Determined by Synchrotron X-Ray Diffraction: *Maria Okuniewski*¹; Don Brown²; Levente Balogh²; Jeff Terry³; Daniel Olive³; Yulia Trenikhina³; John Okasinski⁴; Pavel Medvedev¹; Hakan Ozaltun¹; Soenke Seifert⁴; Soma Chattopadhyay³; Tomohiro Shibata³; Hasitha Ganegoda³; Jan-Fong Jue¹; Barry Rabin¹; Glenn Moore¹; Blair Park¹; ¹Idaho National Laboratory; ²Los Alamos National Laboratory; ³Illinois Institute of Technology; ⁴Argonne National Laboratory

The U.S. Reduced Enrichment for Research and Test Reactors program converts research reactors which utilize highly enriched uranium fuel to low enriched uranium fuel in order to prevent proliferation. The fuel that is utilized for the conversion of the high performance research reactors is U-10wt.%Mo (U10Mo) alloy foil encased in an Al-6061 cladding. Hot isostatic pressing (HIP'ing) is used to fabricate the reactor fuel. During the fabrication process, residual stresses are introduced to the plates via the difference in thermal expansion coefficients in the U10Mo and Al. Synchrotron x-ray diffraction was utilized to measure the spatially resolved residual strain in two HIP cooling processes. Diffraction measurements were calculated from the fractional change in the lattice parameter of the HIP'ed specimen to the bare U10Mo foil. Finite element calculations are compared to the strain results obtained from the diffraction experiments.

5:50 PM

Diffraction Studies of Irradiated Cladding and Duct Reactor Materials: *Tarik Saleh*¹; Stuart Maloy¹; Tobias Romero¹; Joris Van Den Bosch¹; Sara Perez-Bergquist¹; Donald Brown¹; ¹Los Alamos National Laboratory

Qualifying materials for use in reactors with fluences greater than 200 dpa requires development of advanced alloys and irradiations in fast reactors to test these alloys. Research into the mechanical behavior of these materials under reactor conditions is conducted under the Fuel Cycle Research and Development program. Specimens of a ferritic/martensitic alloy (HT-9) from a duct previously irradiated in the FFTF reactor to doses of up to 155 dpa at temperatures from 370 to 510°C are presently being tested. In order to probe deformation mechanisms in these materials, samples of HT-9 were tested in tension in situ on the SMARTS beamline at the Los Alamos Neutron Science Center. Results showed load sharing between the carbides and parent phase of the steel beyond yield, displaying the critical role of carbides during deformation. Complimentary measurements of radiation induced microstructural effects using Pair Distribution Function and Orientation Imaging Microscopy will also be discussed.

Computational Plasticity: Multiscale Modeling in Plasticity

Sponsored by: The Minerals, Metals and Materials Society, TMS Materials Processing and Manufacturing Division, TMS Structural Materials Division, TMS/ASM: Computational Materials Science and Engineering Committee, TMS: High Temperature Alloys Committee *Program Organizers:* Remi Dingreville, Polytechnic Institute of NYU; Koen Janssens, Paul Scherrer Institute

Thursday PM	Room: 1A
March 3, 2011	Location: San Diego Conv. Ctr

Session Chair: To Be Announced

2:00 PM Invited

Effective Elastic Properties of Solids Containing Imperfectly Bonded Nano-Inhomogeneities Based on Atomistic-Continuum Interphase Model: *Mohammed Cherkaoui*¹; Bashkar Paliwal¹; ¹Georgia Institute of Technology

The classical micromechanics is revised to study elastic properties of heterogeneous materials containing nano-inhomogeneities. Contrary to the previous studies, this work introduces the concept of interphase instead of sharp interface to account for the surface/interface excess stress effect

at the nano-scale. The interphase's constitutive properties are derived within the continuum framework from atomistics. These properties are then incorporated in micromechanics-based interphase model to compute the effective properties of the nanocomposite. This approach bridges the gap between discreet systems (atomic level interactions) and continuum mechanics. An advantage of this approach is that it combines atomistic with a three-phase micromechanical model that considers inhomogeneity shape, thereby enabling both the shape and anisotropy of the nano-inhomogeneity and nano-interphase to be simultaneously accounted for in computing overall properties.

2:30 PM

Kinetics of Deformation Mechanisms in Nanocrystalline Copper: Mathieu McPhie¹; Stéphane Berbenni²; Mohammed Cherkaoui¹; ¹Georgia Tech Lorraine, GT-CNRS UMI 2958; ²Laboratory of Physics and Mechanics of Materials (LPMM), CNRS, ENSAM

A multiscale micromechanical model is developed to describe the new physics present in the deformation behaviour of nanocrystalline materials, in particular the breakdown of the Hall-Petch law. This model includes the effects of the emission and absorption of dislocations from grain boundaries, and the coupled grain boundary sliding and migration.Numerical input for this model is given by atomistic simulations of bicrystal layers of fcccopper using the nudged elastic band technique. Using this technique, zero-temperature, stress-dependent activation energies and saddle point configurations are found for a wide variety of grain boundary misorientations. Additionally, the effect of defects in the grain boundary structure (voids, ledges, dislocations) is studied.

2:50 PM

Experimental and Microstructurally Based Computational Investigation of the High Strain-Rate Behavior of High Strength Aluminum Alloys: *William Lee*¹; Khalil El-Khodary¹; H. Salem²; Mohammed Zikry¹; ¹North Carolina State University; ²American University of Cairo

The objective of this study is to identify the dominant microstructural and dislocation-density mechanisms related to the high strength and ductile behavior of high strength aluminum alloys, and how high strain-rate loading conditions would affect the overall behavior. Characterization techniques and specialized microstructurally-based finite-element (FE) analyses based on a dislocation-density based multiple-slip crystalline plasticity formulation that accounts for an explicit crystallographic and morphological representation of different precipitates and their rational orientation relations was conducted. As the microstructural FE predictions have indicated, and consistent with the experimental observations, the interrelated effects of precipitates, dispersoids, and grain-boundaries acting on different crystallographic orientations, enhance the strength, the ductility, and reduce the susceptibility of 2139-Al to shear strain localization and dynamic crack propagation.

3:05 PM Break

3:20 PM Invited

Lengthscale, Orientation and Morphology Effects in Fatigue Crack Nucleation in Polycrystals: *Fionn Dunne*¹; ¹University of Oxford

A crystal plasticity model for near-alpha hcp titanium alloys embodying a quasi-cleavage failure mechanism is presented and employed to investigate the conditions necessary in order for facet nucleation to occur in cold-dwell fatigue. A model polycrystal is used to investigate the effects of combinations of crystallographic orientations, lengthscale effects, and the essential role of (cold) creep during hold periods in the loading cycle. Direct comparisons of model predictions are made with dwell fatigue test results. The crystal model for faceting is found to be consistent with a range of experimental observations.

3:50 PM Invited

Quantifying the Microstructure-Induced Uncertainty in Strain Concentrations at Engineered Defects: Corbett Battaile¹; Luke Brewer²; John Emery¹; Brad Boyce¹; ¹Sandia National Laboratories; ²Naval Postgraduate School

Materials properties are usually assumed to be either independent of the details of the materials' microstructure, or perhaps sensitive only to the structure's average characteristics (e.g. the Hall-Petch effect in metals). However, this assumption is sometimes inadequate. In particular, when the length scale of the relevant mechanism(s) is comparable to that of the microstructure itself, the resulting properties can depend strongly on the particular, local, microstructural environment in which the relevant mechanism(s) operate. To illustrate this, we have used electron backscatter diffraction and digital image correlation to measure the influence of microstructure on deformation near engineered defects in brass, and polycrystal plasticity finite element analysis to simulate the statistical dependence of local deformation on microstructure. We will present the results of this study, and discuss the concept of microstructure-induced uncertainty in materials properties in general.

4:20 PM

Modeling the Evolution of the Microstructure in Magnesium by Means of Incremental Energy Minimization: *Joern Mosler*¹; Malek Homayonifar¹; ¹GKSS-Forschungszentrum Geesthacht

Magnesium alloys exhibit a relatively poor formability for traditional metal forming processes. This is directly related to the complex interplay between slip and twinning observed in magnesium single crystals. In the present contribution, slip and twinning as well as the evolution of the subgrain microstructure in magnesium are analyzed by means of a variational principle. Within the proposed model, every single aspect is driven by energy minimization, i.e., the energetically most favorable microstructure is obtained. In contrast to previous approaches, the twinning's interface energy as well as an energy related to the misfit of the crystal in a boundary layer is also considered. This introduces implicitly a size effect within the model allowing to determine the thickness of the aforementioned twin lamellas. The novel approach is verified by comparing numerically computed results to their experimental counterparts observed within the channel die.

4:40 PM

Studying Dislocation Nucleation from Different Shaped Notches Using a Multiscale Model: *Steffen Brinckmann*¹; Dhiraj Mahajan¹; Alexander Hartmaier¹; ¹ICAMS

Engineering materials have rough surfaces. This surface roughness acts as stress concentrator and dislocations nucleation site. The dislocations move into the material and might lead to irreversible plastic deformation, which may trigger fracture of the engineering material. While the dislocation dynamics model has been used to study dislocations motion and free surface interaction, that model is a continuum representation. Molecular dynamics, on the other hand, accurately describe dislocation - notch interaction. However, molecular dynamics alone might lead to numerical artifacts. We present a novel approach that combines molecular dynamics and dislocation dynamics in a domain separating concurrent approach. The notch domain is simulated using molecular dynamics while the outer domain is simulated with dislocation dynamics. We study how dislocations are nucleated repeatedly at the notch and how they propagate into the surrounding area. Furthermore, we investigate how the notch shape influences the incipient irreversible deformation.

5:00 PM

A Microstructure Sensitive Crystal Plasticity Model for a-Iron: Alankar Alankar¹; David Field²; ¹Max-Planck Institute for Iron Research; ²Washington State University

A dislocation density based crystal plasticity finite element model (CPFEM) is developed for a-iron which tracks dislocation densities on 12 no. of {112} slip systems. Based upon the kinematics of crystal deformation and dislocation interaction laws, dislocation generation and annihilation laws are modeled. Screw dislocations velocity is modeled such as they move in

kink-pairs. This leads to capture the typical phenomenon of low mobility of screw dislocations as compared to their edge counterparts in bcc metals. The CPFEM model is calibrated using literature data of single crystals oriented with tensile axis along [-111], [001], and [011] directions. Simulation results of texture evolution and slip activity in a multicrystal show reasonably good agreement with experimental observations.

5:20 PM

Statistical Modeling of Elastic Strain, Lattice Rotation and Dislocation Density Tensor in FCC Crystals: Mamdouh Mohamed¹; Jie Deng¹; Anter El-Azab¹; *Ben Larson*²; ¹Florida State University; ²Oak Ridge National Laboratory

A computational technique to characterize the statistics of internal elastic fields of 3D dislocation systems in deforming crystals is presented. The internal elastic fields are computed based on 3D dislocation realizations generated by the method of dislocation dynamics. The results show that the elastic strain components exhibit nearly symmetric probability density functions with zero mean values, which depend on the level of crystal strain. The probability density function for the lattice rotation, however, is found to be non-symmetric. The correlation of all elastic field components are found to be highly anisotropic and tend to be enhanced as the crystal strain is increased. The importance of the current analysis is demonstrated by the relevance of the simulations to the development of a mesoscale plasticity theory, and the direct comparison of the simulations with spatially resolved 3D X-ray microscopy measurements of lattice rotation and the dislocation density tensor at the mesoscale.

Electrode Technology for Aluminium Production: Inert Anodes and Wettable Cathodes

Sponsored by: The Minerals, Metals and Materials Society, TMS Light Metals Division, TMS: Aluminum Committee Program Organizers: Alan Tomsett, Rio Tinto Alcan; Ketil Rye, Alcoa Mosjøen; Barry Sadler, Net Carbon Consulting Pty Ltd

Thursday PM	Room: 16B
March 3, 2011	Location: San Diego Conv. Ctr

Session Chairs: Veronique Laurent, Rio Tinto Alcan; Jilai Xue, Department of Nonferrous Metallurgy

2:00 PM Introductory Comments

2:05 PM

Pressureless Sintering of TiB2–Based Composites Using Ti and Fe Additives for Development of Wettable Cathodes: *Hamed Heidari*¹; Houshang Alamdari¹; Dominique Dubé¹; Robert Schulz²; ¹Université Laval; ²Hydro-Quebec

Titanium diboride is the most promising candidate material for development of wettable cathodes for aluminum smelting. It is considered as an alternative for carbon cathodes in order to reduce the anode cathode distance resulting in higher energy efficiency in electrolysis cells. In this work, TiB2-based ceramic specimens were consolidated using metallic additives followed by pressureless sintering. Different proportions of iron and titanium (= 10wt%) were used as low melting point sintering additives. Sintering was conducted at 1400-1650oC under controlled atmosphere. The effects of composition, sintering temperature, milling time and pre-alloying of the additives on densification, microstructure, and mechanical properties were investigated. It was found that pre-alloying and milling time have significant influence on densification, microstructure uniformity and bending strength. Uniform crack-free microstructure with even distribution of pores as well as maximum relative density of 91% and bending strength of 300 MPa were obtained using pre-alloyed additives, milling time of 30 min and sintering for 1 h at 1650°C.

2:30 PM

Furan Resin and Pitch Blends as Binders for TiB2-C Cathodes: *Hongliang Zhang*¹; Jinlong Hou¹; Xiaojun Lü¹; Yanqing Lai¹; Jie Li¹; ¹School of Metallurgical Science and Engineering, Central South University

Blends of furan resin and pitch were applied for the binder of TiB2-C cathodes. Some characteristic properties of binder and furan/pitch based TiB2-C cathodes were studied. The actual coking value of furan/pitch binder was higher than theoretical value that simply adding up. There was a synergistic effect between pitch and furan resin. Such synergistic effect leads to ameliorative TiB2-C cathode materials with lower open porosity, electrical resistivity and higher bulk density, compressive strength than those of pure pitch based TiB2-C cathode materials. In addition, the low-temperature electrolysis expansion of TiB2-C samples were tested also, furan/pitch based TiB2-C samples showed lower electrolysis expansion than pitch based TiB2-C samples (1.68% and 1.87%, respectively). Molecular structure (FTIR) and semicoke morphology (SEM) analysis results indicated that after adding appropriate amount of furan resin, the pitch binder was modified by furan resin effectively, the cohesion and flexibility of pitch binder were significant enhanced.

2:55 PM

Influence of Cobalt Additions on Electrochemical Behaviour of Ni-Fe-Based Anodes for Aluminium Electrowinning: Vivien Singleton¹; Barry Welch²; Maria Skyllas-Kazacos¹; ¹University of New South Wales; ²Welbank Consulting Ltd.

The anodic behaviour of surface-oxidised Ni-Fe-Co alloys was investigated over short-termperiods of aluminium electrolysis in an alumina-saturated bath. Additions of 10wt% Co were found to significantly improve the anodic wear resistance, due to suppression of Fe_xO formation. Anodes having cobalt contents =30wt% exhibited poor performance due to rapid outwards diffusion of cobalt to the reaction interface. In general, the protective ability of the pre-formed oxide scales was greatly affected by the level of porosity and surface adhesion. In electrolytes containing <4wt% Al₂O₃, catastrophic failure of the anodes was observed due to concentration polarisation at the reaction interface. Under these conditions, the metal was rapidly destroyed by a combination of dissolution and fluorination events.

3:20 PM Break

3:30 PM

Effects of the Additive ZrO2 on Properties of Nickel Ferrite Cermet Inert Anode: Xiao Zhang¹; Guangchun Yao¹; Yihan Liu¹; Jia Ma¹; Zhigang Zhang¹; ¹Northeastern University

The objective of this paper is to study a new attempt on preparing Cu-Ni-NiO-NiFe2O4 ceramic inert anodes by adding trace ZrO2 (0~1.50 wt%), carrying out high temperature solid-phase process. NiFe2O4 spinel, the matrix material, was prepared firstly with extra 18wt% NiO and Fe2O3 as the raw materials. The product was crushed to fines, and then mixed uniformly with Cu-Ni and ZrO2 powders to prepare Cu-Ni-NiO-NiFe2O4 ceramic inert anodes by cold-pressing sintering method. The impact of ZrO2 addition on the relative density, the bend strength and the corrosion resistance of Cu-Ni-NiO-NiFe2O4 ceramic inert anodes was investigated. The results show that, with the addition of 0.5% ZrO2, the relative density slightly increases and the corrosion resistance decreases a little while the bending strength improves remarkably from 55.50MPa of the sample without ZrO2 additive to 105.26Mpa.

3:55 PM

Effect of Sintering Atmosphere on Phase Composition and Mechanical Property of 5Cu/(10NiO-NiFe2O4) Cermet Anodes for Aluminum Electrolysis: Zhong Zou¹; Juan Wei¹; Liang Tian¹; Kai Liu¹; *Liang Zhang*¹; Qing Lai¹; Jie Li¹; ¹Central South University

5Cu/(10NiO-NiFe2O4) cermet anodes for aluminum electrolysis were prepared by the cold-pressing sintering method in different atmosphere, and their phase composition, microstructure and mechanical property were also investigated. The results reveal that 5Cu/ (10NiO-NiFe2O4) cermet can be obtained by sintering in the low vacuum or atmosphere with oxygen content

of 10ppm, 200ppm, 2000ppm, and 10000ppm respectively, and O2 content brings great effect on the content of phase composition of materials. Cermet tend to have a high content of NiO sintered under atmosphere with low O2 content, and a high content of metallic phase sintered under atmosphere with high content of O2. When O2 content in the atmosphere is 10ppm, the grain size of 5Cu/(10NiO-NiFe2O4) cermet is 5.43µm, the bending strength can reach 80.05Mpa at the room temperature.

Electrometallurgy Fundamentals and Applications: Session I

Sponsored by: The Minerals, Metals and Materials Society, TMS Extraction and Processing Division, TMS: Hydrometallurgy and Electrometallurgy Committee Program Organizer: Michael Free, University of Utah

Thursday PM	Room: 18
March 3, 2011	Location: San Diego Conv. Ctr

Session Chair: Michael Free, University of Utah

2:00 PM

Electrochemical Reduction of Tantalum Oxide in a CaCl2 – CaO Molten Salt Electrolyte: Roger Barnett¹; *Derek Fray*¹; ¹University of Cambridge

Tantalum is usually prepared by the sodium reduction of potassium heptafluorotantalate. However, this route is relatively expensive and this paper reports the direct electro-deoxidation of tantalum oxide (Ta2O5). When tantalum oxide is immersed in a melt of CaCl2 containing CaO, a series of calcium tantalum oxides formed with orientations in the direction of the CaO concentration gradient. These include CaTa4O11, Ca2Ta2O6 and Ca2Ta2O7. The morphology varied with the compound leading to a sample with reduced strength. Reduction experiments, where the tantalum oxide was made the cathode in a bath of CaCl2 – CaO resulted in a similar series of calcium tantalum compounds with Ca3(CaTa2)O9 as the final stage before the formation of tantalum. Final oxygen contents of 6700 ppm were achieved with carbon contamination in 1200 ppm range from the carbon anode. The use of inert anodes is discussed.

2:25 PM

Molten Oxide Electrolysis Application to Steelmaking: A New Approach of Slag Science?: Ghazal Azimi¹; *Antoine Allanore*¹; Donald Sadoway¹; ¹MIT

Molten oxide electrolysis (MOE) is a new steelmaking technique that does not rely on the use of carbon in the step of chemical conversion of iron oxide to metal. However, the fundamental chemical knowledge developed in slag science is of critical importance to design a mixture of molten oxides that is adapted to the development of an electrolysis operation with high selectivity. Starting from thermodynamic evaluation and discussion of available data on iron speciation in molten slag, the recent results and developments obtained by MOE will be presented. These show that a fundamentally new approach using iron oxide chemistry in molten oxide and the corresponding change in energy vector used for the conversion of iron oxide will not require the development of new science, but could help physico-chemists in the development of new characterization methods.

2:50 PM

Direct Electroreduction of Oxides in Molten Fluorides: *Laurent Cassayre*¹; Mathieu Gibilaro¹; Jacques Pivato¹; Laurent Massot¹; Pierre Chamelot¹; Olivier Dugne²; ¹Université de Toulouse; ²CEA Marcoule

In the last decade, a great amount of work has been dedicated to the study of the so-called direct reduction reaction, which aims at the conversion of a solid oxide into its metal by electrochemical reduction in a molten salt. The considered applications are for instance titanium production and conversion of spent nuclear oxide fuels in molten chloride salts (CaCl2 and LiCl respectively). However, up to now, the use of chloride salts is still problematic partially because of the anodic reaction. In the present work,

an attempt to use fluoride salts in replacement of chlorides was carried out in order to reduce SnO2, Fe3O4, TiO2, TiO and UO2 solid pellets. After intensiostatic electrolyses, metal conversion was obtained for all oxides except TiO, and the structure of the metal observed by SEM had a typical coral-like structure. An overview of the results is presented here.

3:15 PM

Thermodynamic Studies on the Preparation of Titanium Alloys by Molten Salt Electrolysis: *Du Jihong*¹; Shenghong Yang¹; Qingyu Li¹; Chengben Yang¹; Mingxia Sun¹; Zhengping Xi¹; ¹Northwest Institute for Nonferrous Metal Research

The high cost of raw materials limits more applications of the titanium and titanium alloys, However, preparation of titanium alloy by molten salt electrolysis has advantages of low cost and low pollution, by far, the formation mechanism of titanium alloy prepared by this method has not yet been studied in-depth. In this paper, we selected the binary titanium alloy preparation for research object, and the calculated results show that the decomposition voltage for the formation of titanium alloy not only relates to the Gibbs free energy for each oxide formed, but also relates to the Gibbs free energy for the alloying reaction. We gave the thermodynamic explanations for the experimental results of alloying process of different types of mixedoxide electrolysis, and concluded the deoxidation laws and alloying pathways during the electrolysis of mixed oxides which has theoretical predictability on the preparation of titanium alloys by molten salt electrolysis.

3:40 PM Break

3:55 PM

Preparation of TiFe Alloy by Electrolysis in Molten Salt: Hu Meilong¹; Bai Chenguang¹; Shi Ruimeng¹; *Lv Xuewei*¹; Liu Xuyang¹; ¹chongqing university

FeTi alloy was prepared directly by electrolysis in molten CaCl2 at 1173K and 3.1V using titanium concentrate as feed material, graphite rod as anode. The mechanism of electro-dexidiztion of titanium concentrate was studied preliminarily. The results showed that FeTi alloy can be prepared by electrolysis using titanium concentrate in molten salt. Fe is first deoxidize product and titanium oxides are deoxidized gradually. And temperature has great effect on the product. Fe2Ti was obtained at 1133K ands FeTi was obtained at 1173K.

4:20 PM

Recapturing Metals from Electrocoagulation Floc: Jewel Gomes¹; Md Islam¹; Paul Bernazzani¹; George Irwin¹; Dan Rutman¹; David Cocke¹; Mohammad Islam¹; ¹Lamar University

Electrocoagulation (EC) is an emerging technology mainly used for wastewater treatment. In this process, in situ coagulants are produced by passing electric current through a conductive aqueous media in presence of sacrificial electrodes. When iron is used as electrodes, layered double hydroxides (LDH) or green rust are formed as intermediates that turns into iron metallic oxides/hydroxides/oxyhydroxides with time. LDH has a very effective capacity to absorb different kinds of water contaminants, such as arsenic, lead, cadmium, and copper in its structure. In this study, we present our work to treat the EC-floc to recapture the metals, such as copper. Both thermal and electrochemical methods have been applied for the treatment. The floc and recovered metals have been characterized using XRD, SEM/ EDS, FTIR, and Moessbaur spectroscopy. A cost analysis is also presented for the treatment and recovery processes.

4:45 PM

Mechanism of Antimony Deposition in Alkaline Solution Containing Xylitol: *Wei Liu*¹; Tianzu Yang²; Qionghua Zhou¹; ¹Henan University of Science and Technology; ²School of Metallurgical Science and Engineering, Central South University

The mechanism of antimony deposition in alkaline solution containing xylitol was investigated by cyclic voltammetry, linear sweep voltammetry and alternating current impedance techniques. The theoretical kinetics equations of electrode reaction velocity were also derived. Cyclic voltammograms with different scan rates indicate that the antimony electrodeposition process



is an electrocrystallization which is an irreversible electrode process. The apparent activation energy, apparent transfer coefficient and exchange current density of cathodic electrode process are calculated to be 46.33 kJ mol-1, 0.64 and 4.40×10 -6 A m-2, respectively. The values of the kinetics parameters calculated from the theoretical kinetics equations are agreed well with the experimentally measured ones.

5:10 PM

Preparation of Ti-Al Intermetallic by Electrolytic Reduction from TiO2 and Al2 O3: Chengbeng Yang¹; *Du Jihong*¹; Zhengping Xi¹; ¹Northwest Institute for Nonferrous Metal Research

An investigation into preparation of Ti-Al intermetallic by electrolytic reduction from TiO2 and Al2O3. Electroanalysis process and thermodynamics mechanism was discussed. The results shows that, in 1223K and 3.1 V electrolytic conditions in molten salt of CaCl2. Electrolysis process can be divided into three stages: the initial reaction exist Ca3Al2O6, TiO and so on .Middle. exist Al2Ca, Ti2O and so on. At last, Al2Ca reacts with TixOy to form Ti-Al intermetallic. The main reaction is electrolytic reduction of TiO2 or Al2 O3, and metallothermic reduction of Al2Ca to form Ti-Al intermetallic. There is no oxygen and other impurities in reduction by SEM inspection. Current efficiency could be arrived 40%.

General Abstracts: Electronic, Magnetic and Photonic Materials Division: Session II

Sponsored by: The Minerals, Metals and Materials Society, TMS Electronic, Magnetic, and Photonic Materials Division, TMS: Alloy Phases Committee, TMS: Biomaterials Committee, TMS: Chemistry and Physics of Materials Committee, TMS: Electronic Materials Committee, TMS: Electronic Packaging and Interconnection Materials Committee, TMS: Energy Conversion and Storage Committee, TMS: Magnetic Materials Committee, TMS: Nanomaterials Committee, TMS: Thin Films and Interfaces Committee

Program Organizers: Long Qing Chen, Pennsylvania State University; Sung Kang, IBM Corporation; Mark Palmer, Kettering University

Thursday PM	Room: 9	
March 3, 2011	Location:	San Diego Conv. Ctr

Session Chair: To Be Announced

2:00 PM

Processing Parameter Optimization to Synthesize High Quality Single Phase CZTS Film: *Prashant Sarswat*¹; Michael Free¹; Ashutosh Tiwari¹; ¹University of Utah

Synthesis of Cu_2ZnSnS_4 (CZTS) photovoltaic absorber material from an electrodeposition-annealing route can be considered as promising production methodology. In the present work, single-phase Cu_2ZnSnS_4 thin film synthesis using a single-stage electrochemical deposition, followed by Sulfurization at elevated temperature, is reported. Electrodepositon of Cu-Zn-Sn was carried out on a conducting substrate using a platinum counter electrode and a saturated calomel reference electrode. Single phase CZTS is formed over a narrow range of bath concentrations, and a slight deviation may lead to formation of various secondary phases. The processing parameters are optimized to minimize the secondary phase formation and achieve high quality CZTS film. Detailed structural, morphological, electrochemical, and optical properties of film were investigated using several techniques including x-ray diffraction, Raman and UV-visible spectroscopy, electrochemical impedance spectroscopy and scanning electron microscopy.

2:20 PM

Tatalum Nitride For Efficient Visible-Light-Driven Photocatalyst: *Zheng Wang*¹; Jiangting Wang¹; Lianyun Liu¹; Kai Huang¹; Jungang Hou¹; Hongmin Zhu¹; ¹University of Science and technology Beijing

Tantalum nitride (Ta3N5) nanoparticles as a visible light photocatalytst were prepared by nitriding the amorphous tantalum nitride naoparticles under ammonia atmosphere at 1073 K. The production of well-crystallized Ta3N5 nanoparticles have primary particles 40-60 nm in size and a broad absorption band in the vicinity of 600 nm. The as-synthesized materials exhibit good activity for H2 and O2 evolution from pure water under visible light irradiation ($\lambda = 420$ nm).

2:40 PM

Failure Mechanism of Electrode in Crystalline Photovoltaics: *Oh Chulmin*¹; Park Nochang¹; Han Changwoon¹; Hong Won Sik¹; ¹KETI/ Reliability Physics Research Center

In this study, the electrode used for the path of electron generated by solar energy was subjected to identified the failure mechanism. the crystalline soler cell with electrode was prepared without EVA and backsheet to eliminate the effect of another parts. Several environment test were conducted with measuring various the solar parameters each constant interval time to monitor the degradtion of electrode performance affected by various environment condition. After environment test, the Auger analysis was conducted to identify failure site with various position of electrode. Therefore, we established the the failure mechanism of electrode and made an opportunity to build the acceleration test for reliability performance of photovoltaices electrode.

3:00 PM

Property–Structure Relations II Oxide Thin Films Used in Light Sensing Applications: J. Wilde¹; Y. Kodera²; C. Dames²; J. Garay²; ¹Raytheon Vision Systems; ²UC Riverside

Over the past few years, uncooled infrared bolometer arrays have been reaching performance levels previously thought possible only with the cooled detectors. One of the most important bolometer design parameter is the bolometer temperature sensing material. This material must necessarily have a high temperature coefficient of resistance (TCR) with low 1/f noise properties with a sufficiently low bolometer thermal time constant. One well known thermistor material is Vanadium Oxide (VOX). Although some important physical properties of bulk VOx are known, the effective properties of VOx thin films are not well understood. We present result of our on-going investigations of the effects of VOx thin film microstructure and composition on material properties (electrical and thermal conductivity). We discuss the results in light of grain morphology, grain size, defects and defect length scales.

3:20 PM

The Investigation of Chemical Vapor Deposited Antimony Doped SnO2 Thin Films by Synchrotron Grazing Incidence X-Ray: Yang Yi Lin¹; Albert T. Wu¹; ¹National Central University

In recent years, transparent conductive oxides (TCO) films have been widely used for the solar cell due to its high transmission, low sheet resistance and highly texture structure that could increase the efficiency of the solar cell. The purpose of this study is to investigate the amount of antimony that was doped into tin oxide thin films by synchrotron radiation grazing incidence X-Ray diffraction. The films were prepared by CVD deposition by using SnCl4 and SbCl5 as precursors. Films were deposited at 450 and 500° for various times. The results suggested that the lattice constant of the film varied with the amount of dopant. The measurement of opto-electrical properties indicated that the films would have higher transmittance and lower resisvitiy by doping antimony in tin oxide films.

3:40 PM Break

4:00 PM

Synthesis of Nano-sized Tantalum Nitrides with Various Morphology: Lianyun Liu¹; Chunhong Ma¹; Zheng Wang¹; Kai Huang¹; Shuqiang Jiao¹; *Hongmin Zhu*¹; ¹University of Science and Technology Beijing

Tantalum nitrides (TaNx) nanoparticles with different crystal phase and various morphology were synthesized through low temperature homogenous sodium reduction route with the subsequent assistance of heat-treatment process. X-ray diffraction and TEM results demonstrated that the tantalum nitrides had the morphology of sphere, rectangle or square with the average particle size below 100nm. The specific surface area of the tantalum nitrides powders measured by BET was around 9.87-13.49m2•g-1, which indicated such nano-sized tantalum nitrides are the promising candidate for capacitor with high specific capacitance.

4:20 PM

Properties of Perfect GaP Crystals: Sergei Pyshkin¹; John Ballato²; Andrea Mura³; ¹Academy of Sciences of Moldova; ²Clemson University; ³University of Cagliari

Here we discuss over 40 year evolution of GaP single crystal properties and their convergence to the behavior of GaP nanoparticles. We show that migration of host and impurity atoms to their proper equilibrium positions leads to creation of an impurity superlattice inside the host lattice. Essential role of the photomechanical effect in the final formation of perfect crystals also has been observed. We demonstrate that the highly ordered nature that develops throughout the decades facilitates stimulated emission, increases the radiative recombination efficiency and spectral range of luminescence. In GaP doped by N substituted P with the period of 10 nm we observe a new type of crystal lattice where nitrogen divides it in short P chains. Highly optically excited GaP:N single crystal turns into the crystalline bound exciton phase - a unique accumulator of optic energy and a prospective medium for non-linear optic phenomena.

4:40 PM

Development of New Transparent Conductive Material of Mg(OH1-xCx)2 (x = 0.1-0.35) by Magnetron Sputtering: *Takamitsu Honjo*¹; Toshiro Kuji¹; ¹Tokai university

It is well known that transparent conductive materials are key materials for FPD (Flat Panel Display). Indium Tin Oxide (ITO) consisting of indium - tin oxides have been widely used for practical applications. However, indium is a typical rare element so that the price has increased rapidly over the last several years. Therefore, many research works for developments of the alternative-material without including indium have been actively done. We are reporting that, Mg(OH1-xCx)2 (x = 0.1-0.35) is an excellent electrical conductor with high optical transparency. The compound has approximately 80% of optical transmission and conductivity of approximately 10-2 ohm cm. The compound was fabricated through two consecutive processes. First Mg-C films were prepared by magnetron sputtering. Then, post-treatment was done in the moist air. These processes yielded Mg(OH1-xCx)2 (x = 0.1-0.35). In this study, the fabrication processes, optical and electrical conductive properties of the compound.

5:00 PM

Synthesis of Ultrafine Single Crystals and Nanostructured Coatings of Indium Oxide from Solution Precursor: Nagaswetha Pentyala¹; Ramesh Kumar Guduru¹; Pravansu Mohanty¹; ¹University of Michigan Dearborn

Indium oxide (In2O3) has been widely used in sensors, solar cells and microelectronics. There are several techniques available for making In2O3 crystals and coatings. Here we present, for the first time, inexpensive and straightforward synthesis of micron/submicron size single crystals, as well as nanostructuted adherent coatings of In2O3 from InCl3 precursor via calcination and DC plasma spray technique, respectively. In2O3 crystals were made by heating the precursor on different substrates at different temperatures, whereas nanostructured films were deposited by feeding atomized liquid directly into the plasma plume. The coatings had ultrafine particles with grain size ranging between 40 - 75 nm. The crystallinity,

phase of the crystals and coatings were characterized by X-ray Diffraction. The coatings with a thickness of 25 micron showed 60% transmission in the visible region and the electrical resistivity(6.5mO-cm) was comparable to the literature. The nanostructured coatings with large surface area could be useful in sensors.

5:20 PM

Reliability of Wedge Wire Bonds Subjected to Ultrasonic Welding and Thermal Cycling: *Anil Saigal*¹; Michael Zimmerman¹; James Battaglia¹; ¹Tufts University

Ultrasonic welding is being increasingly used to attach plastic lids as part of integrated circuit packages to replace metal and ceramic lids in hermetic packages. This paper presents the effect of the ultrasonic welding lid attachment process on the reliability and mechanical strength of 1.0 and 1.5 mil gold wedge wire bonds in LDMOS integrated circuit packages. Theoretical modeling of the system including wirebonds and package geometry showed that the natural frequencies of the system were significantly different than the natural frequencies of the wirebonds. This indicates that the ultrasonic welding process does not cause significant stresses in the wirebonds, and therefore doesn't effect wire bond reliability. This hypothesis was tested by exposing the wirebonded packages to thermal air-to-air cycling of the MIL-spec temperature extremes of -65°C and +150°C. Results showed that thermal cycling caused degradation of wirebond pull strengths, but the lid attachments did not cause any deterioration.

General Abstracts: Light Metals Division: General Light Metals

Sponsored by: The Minerals, Metals and Materials Society, TMS Light Metals Division, TMS: Aluminum Committee, TMS: Aluminum Processing Committee, TMS: Energy Committee, TMS: Magnesium Committee, TMS: Recycling and Environmental Technologies Committee

Program Organizers: Alan Luo, General Motors Corporation; Eric Nyberg, Pacific Northwest National Laboratory

Thursday PM	Room: 14B
March 3, 2011	Location: San Diego Conv. Ctr

Session Chair: Alan Luo, General Motors Global Research & Development

2:00 PM

The Effect of Residual Chloride on the Sintering and Sintered Properties of Titanium and Its Alloys: *Ma Qian*¹; ¹The University of Queensland

The commercial production of titanium since 1948 has been based on the tetrachloride route. As a reaction product, residual MgCl2 or NaCl exists in most titanium products. Commercially available titanium powder can contain chlorine, for example, ranging from < 10 ppm to 2 wt.% (under-separated). This paper reviews the effect of the residual chloride on the sintering and sintered properties of titanium and its alloys. A detailed literature survey indicates that vacuum sintering is able to produce highly dense (> 98%TD) Ti-6Al-4V with tensile properties equivalent to wrought levels from titanium powders containing up to 0.36 wt.% chloride. This offers a potential cost-effective near-net shape fabrication route for many applications where fatigue is not critical. However, sintering in argon results in much inferior properties of chlorine. The effect of the residual chloride on titanium powder metallurgy is discussed.

2:20 PM

High Strain Rate Behavior of 2139-T8 Al Alloy: *Buyang Cao*¹; K. Ramesh¹; ¹The Johns Hopkins University

The high strain rate behavior of the age hardenable Al-Cu-Mg-Ag alloy known as Al 2139 has been measured over a wide range of strain rates. We obtain dynamic flow stresses of 450 MPa at quasi-static strain rates and flow stress of 550 MPa at dynamic strain rates. We explored the contributions of

several strengthening mechanisms to the total strength of the material, using quantitative TEM together with existing models for each mechanism. Using the results of atomistic calculations, we show that the O phase is the primary strengthening phase in this alloy.

2:40 PM

Determination of Heat Treatment Effect on 6XXX Series Aluminum Foams by Design of Experiment: *Deniz Polat*¹; B. Ozkal¹; O. Keles¹; ¹Istanbul Technical University

In recent years, there is a high demand for light-weight metals foams. Aluminum foams being one of the most commonly preferred metallic foam have been utilized in a wide ran-ge of sectors such as health, construction, defense and automotive due to its properties such as industrial advantages (raw material cost, availability and ability to be worked on), melting temperature, specific strength and corrosion resistance. In this work, first 6XXX series of aluminum alloy foams are produced from elemental powders via compact powder melting methods. The alloying elements, Si, Mg and foaming agent titanium hydride powders are added in aluminum powder. Each powder mixture's composition is determined by response surface methodology. 3 levels and 3 parameters are chosen in order to investigate the effects of alloving elements. Then, in order to evaluate their mechanical properties heat treatment is applied at 540°C for 40 min and aged naturally. The results are evaluated by microstructural analysis and hardness tests. A response surface methodology is employed to analyze the hardness results. OM (optical microscopy) and SEM (Scanning Electron Microscopy) are utilized to investigate their microstructures. The formation of AlFeSi and Mg2Si intermetallics are seen within the aluminum foam structure. Also, the hardness values of the samples are increased after heat treatment.

3:00 PM

Effect of Reacted Layer on Galvanic Corrosion Phenomenon at Interface between Ti Dispersion and Mg-Al Alloy: *Katsuyoshi Kondoh*¹; Nozomi Nakanishi¹; Rei Takei¹; Junko Umeda¹; ¹Osaka University

It was previously clarified pure titanium (Ti) particles were effective reinforcements of magnesium (Mg) composites because of their higher hardness, Young's modulus and suitable ductility. When Mg-Al alloy was used as matrix material, Ti-Al reacted layer was formed at the interface between Ti dispersoids and matrix. In general, standard electrode potential (SEP) of Ti is -1.63V, which is much larger compared to Mg (SEP; -2.363V), and results in galvanic corrosion at the interface between Ti and Mg due to the large difference of the SEP. In this study, the effect of the Ti-Al intermetallic layer on the galvanic corrosion of Mg-Al composites reinforced with Ti particles was investigated by salt immersion test. On the other hand, Scanning Kelvin Prove Force Microscopy (SKPFM) analysis was applied to directly measure the surface potential difference at the interface. By comparing these measurements, the galvanic corrosion phenomenon of the Mg composite was quantitatively investigated.

3:20 PM

Compressive Capacity and Fracture Mechanism of Aluminum Foam: *Hai Hao*¹; Guoqiang Lu¹; Mouhamadou Diop¹; Hanwei Dong¹; Xingguo Zhang¹; ¹Dalian University of Technology

The tests of compressive capacity of aluminum foam samples manufactured by the melt foaming method were carried out and the compressive curves of stress-strain were obtained. The behavior of deformation by compression and the energy absorption of the aluminum foam were studied. The test results show that there are three regions during the deformation: linear elastic deformation region, collapse region and densification region. As the porosity increases, the capacity of elastic strain resistance reduced significantly, and the specimen with a porosity of 75% has the highest energy absorption capacity. The aluminum foam failed due to a mixture mechanism of malleable tearing and brittle fracture, moreover the slit develops along the crystal border.

3:40 PM Break

4:00 PM

LiAl Alloy Prepared by Bulk Mechanical Alloying: *Takamitsu Honjo*¹; Toshiro Kuji¹; ¹Tokai University

LiAl alloy has a high potential as cathode materials of Li-ion battery. In this study we have successfully prepared LiAl alloy by newly developed Bulk Mechanical Alloying (BMA). This MA process has a great advantage for Ball-Milling type MA because everything was in a die and handling of fine powders are not necessary. In general, Ball-milling type MA is time consuming process. In this paper, we will demonstrate that BMA is effectively yielding alloying Li and Al elements compared to Ball-Milling MA even for active element like Li. Prepared alloy has a nano-sized morphology.

4:20 PM

Multistage Fatigue Model for High-Strength Textured Al Alloys: *Yibin Xue*¹; Chong Teng¹; Brian Jordon²; Mark Horstermeyer³; David McDowell⁴; Elias Anagnostou⁵; ¹Utah State University; ²University of Alabama; ³Mississippi State University; ⁴Georgia Tech; ⁵Northrop Grumman

Physically motivated mechanistic MultiStage Fatigue (MSF) model is extended for structural health prognosis to evaluate the extended fatigue life of aging aircrafts. Typically military airframes undergo variable loading conditions with certain severe overloads that induce plastic deformations at the rivet holes or the location of extreme geometry changes, which often serve as fatigue damage initiation sites. Therefore, the structural health prognosis requires an excellent cyclic plasticity, damage incubation and fatigue crackgrowth life prediction model that is capable of accurately accounting for the effects of 1) multiaxial loads, 2) notch effects, and 3) overload. The deformation gradient at the macroscopic notch root is integrated into the loading transfer function for fatigue damage incubation model. The overload effects to small-crack growth are further evaluated both experimentally and numerically. A high-order MSF model was developed consider uncertainty induced by the combination effects of microstructure and loading.

4:40 PM

Super Plasticity of Magnesium Alloys after Rolling and ECAP: Miroslav Greger¹; Radim Kocich¹; ¹VSB-Technical University Ostrava

The paper is focused on investigation of structure and properties of Mg alloys with fine-grained nano-structure. Forming of magnesium alloys with usual grain size 250 to 500 μ m is difficult as they are characterised by low plastic properties. Application of SPD processes (Severe Plastic Deformation) enables us to achieve in these alloys as well an ultra-fine grains – nano-grains – and thus also high mechanical properties. Influence of accumulation of deformation by the ECAP process on grain size and mechanical properties of the alloys AZ61 and AZ91 was determined experimentally. Application of the ECAP technology generated nano-structure with an average grains size around approx. d \sim 0.7 μ m. After the ECAP deformation e = 6 these alloys gained super-plastic behaviour. Ductility of the alloy AZ91 was around 420 %. Experiment proved influence of extreme plastic deformations on grain refinement and on final values of mechanical properties.

5:00 PM

Tomographic Reconstruction of Microstructures in Al-Ni-Y-Based Alloys: *Mauricio Gordillo*¹; Lichun Zhang¹; Thomas Watson²; Mark Aindow¹; ¹University of Connecticut; ²Pratt and Whitney Aircraft

Recently, there has been significant interest in the use of metastable vitreous intermediates in the development of new high strength Al alloys. Such intermediates have higher solubility limits than crystalline Al. Thus, by careful control of alloy composition and thermal history during devitrification, one can obtain fine-grained microstructures with higher volume fractions of precipitates than can be achieved in conventional Al Alloys. We have investigated Al-Ni-Y-based alloys that can be produced in the glassy state by gas atomization. These alloys devitrify to a give a matrix of FCC Al with laths of Al19Ni5Y3 and secondary Al3Ni or Al3Y precipitates. Here we report the use of serial section FIB tomography to study microstructural development in these alloys during powder consolidation and subsequent forging. It is shown that the Al19Ni5Y3 laths retain their integrity during

forging and rotate with the flowing Al matrix, rather than breaking up as one might expect.

5:20 PM

Improved Properties of Light Alloys Using Near-Nano and Nano-Based Materials in Bulk Consolidation Processing: *Robert Gansert*¹; Chris Melnyk²; David Grant²; David Lugan²; Brian Weinstein²; ¹Advanced Materials & Technology Services, Inc.; ²California Nanotechnologies, Inc.

Near-nano and nano-grained light alloys (Al, Ti, Mg) show great potential for applications in a variety of industries (e.g., energy, automotive and aerospace). The Hall-Petch relationship cites the strengthening of materials by reducing the average crystallite (grain) size. A study is proposed to investigate the increase in mechanical properties provided by near-nano and nano-grained powders used in powder metallurgical applications. Nanocrystalline powders of light alloys (aluminum, titanium, magnesium) will be produced from cryomilling operations. Consolidated forms of near-nano and nanocrystalline materials will be produced using Spark Plasma Sintering (SPS). The mechanical properties of the nearnano and nanocrystalline materials will be compared to consolidated forms of conventional materials. Initial testing of aluminum and titanium based materials shows a significant increase in hardness and shear from use of nearnano and nano- crystalline materials. Cryomilled powders and consolidated forms of these powders will be examined using microstructural analysis and mechanical property testing.

General Abstracts: Materials Processing and Manufacturing Division: Casting, Surface Modification. and Powder Processing

Sponsored by: The Minerals, Metals and Materials Society, TMS Materials Processing and Manufacturing Division, TMS/ASM: Computational Materials Science and Engineering Committee, TMS: Global Innovations Committee, TMS: Integrated Computational Materials Engineering Committee, TMS: Nanomechanical Materials Behavior Committee, TMS/ASM: Phase Transformations Committee, TMS: Powder Materials Committee, TMS: Process Technology and Modeling Committee, TMS: Shaping and Forming Committee, TMS: Solidification Committee, TMS: Surface Engineering Committee *Program Organizers:* Corbett Battaile, Sandia National Laboratories; Joy Forsmark, Ford Motor Company; Amit Misra, Los Alamos National Laboratory

Thursday PM March 3, 2011 Room: 2 Location: San Diego Conv. Ctr

Session Chair: To Be Announced

2:00 PM

Application of Thermodynamics in Nucleation of Secondary Graphite on Heat Treated Ductile Cast Iron: *Fabian Imanasa Azof*¹; Eung Ryul Baek¹; ¹Yeungnam University

Microstructure gives significant effect on the mechanical properties of ductile cast iron. Secondary graphite which occurs during the tempering of martensitic ductile cast iron can deteriorate the elastic modulus and hardness property of the material. Current research presents some application of thermodynamics in nucleation of secondary graphite on heat trated ductile cast iron. The nucleation of secondary graphite in 3.7C-3Si on several austenitization and tempering temperatures were examined using TGA-DTA analysis to ensure the validity of calculation.

2:15 PM

Evaluation of Microstructures and Mechanical Properties on the Effects of Build Orientation and Building Parameters on Manufactured Ti6Al4V Specimens by EBM: *Karina Puebla*¹; Sara Gaytan¹; Lawrence Murr¹; Ryan Wicker¹; ¹The University of Texas at El Paso

Titanium alloys are the preferred metallic biomaterials for implants due to their mechanical properties, biocompatibility, and corrosion resistance. Ti6Al4V is one of the employed metal powders in electron beam melting (EBM), an additive manufacturing technology capable of fabricating complex 3-dimensional end-use products layer-by-layer. The current investigation was performed to determine the effects of build orientation and scan rate on the microstructure and mechanical properties of EBM manufactured specimens. Microscopic characterization and mechanical testing was performed. Electron microscopy analysis demonstrated the existence of α and β phases and grain size variations in the microstructure. The different melt scan rate created dissimilarities and produced zones with defects such as porous and voids of non-melting or sintering of Ti6Al4V powder. These effects produced variations affecting physical and mechanical properties of the manufactured specimens. The suggestions to meet specific mechanical properties of EBM manufactured products will be discussed.

2:30 PM

140th Annual Meeting & Exhibition

Calciumsilicate-Graphite-Compound, a New Material for the Flow Control of Liquid Aluminium Alloys: *Wolf Huettner*¹; Tobias Hoelscher¹; Mark Quackenbush²; Rusty Smith³; ¹Calsitherm International; ²Prime Material Sales; ³Industrial Products International

Graphite and Calciumsilicate are standard materials in casting processes, especially in direct contact with liquid aluminium alloys. The new material is a compound of Calciumsilicate and various amounts of Graphite. It combines the advantageous properties of both materials. The thermal conductivity of the Calciumsilicate increases significantly, whereas the thermal expansion, especially in the plane of the graphite lattice orientation becomes small. The properties are dependend upon the amount of graphite and can be tailored close to required values. Both properties results in an improved thermal shock resistance. The graphite particles also reduce significantly the oil absorption without any additional coating, which is of importance for the use as transition-plate. Furthermore the graphite particles in the compound act as a self-lubricating agent, also at operational temperatures, as the graphite consists of a high oxidation resistance. The material has a high potential to reduce costs especially in the billet production.

2:45 PM

Influence of a Direct Current on the Solidification Behavior of Pure Aluminum: *Yunhu Zhang*¹; Changjiang Song¹; Liang Zhu¹; Hongxing Zheng¹; Qijie Zhai¹; ¹Shanghai University

To well understand the action mechanism of electric current on the solidification structures of metals and alloys, the effect of a direct current (DC) on the solidification behavior of pure aluminum was investigated experimentally. The experiments show that the measure accuracy of an unarmored K-Type thermocouple is clearly affected by the electric current, but an armored one is not. Therefore, an armored K-Type thermocouple was used to examine the effect of a DC on the solidification behavior of pure aluminum. The results reveal that the freezing temperature decreases by about 1.5° with the application of an 8A/cm2 DC during the solidification of pure aluminum. The reason for this change is simply discussed.

3:00 PM

Influence of Heating Effect on the Solidified Structure of Pure Aluminum by Electric Current Pulse: *Zhenxing Yin*¹; Bo Li¹; Yongyong Gong¹; Qijie Zhai¹; 'Shanghai University

This paper investigated the effect of electric current pulse (ECP) on solidification structure of pure aluminum under different pulse parameters. The results exhibit that the area ratio of equiaxed zone increases sharply with the increase of peak value of electric current; however the area ratio varies slowly with the increase of pulse frequency. Additionally, the effect of ECP on solidification structure of aluminum under slower cooling rate was studied, which was attained by imposing thermal insulator on the top of ingot. The results show that the shrinkage cavities of ingots become smaller to varying extents, especially under high current peak value. The structure refinement effects however all weaken too. Based on these findings above, the conclusions can be drawn that current peak value plays a more important role in the refinement of solidified structure than pulse frequency and Joule heat effect isn't the main cause for structure refinement.

3:15 PM

Influence of Silicon to (Fe,Si)Al Island Formation in Fe2Al5 Aluminide Layer during Heat Treatment of Al-Si Coated Steel Sheets: *Nandyo Alpalmy*¹; Baek Eung-Ryul¹; Kim Tai-Ho²; ¹Yeungnam University; ²POSCO

Aluminide layers (i.e. Fe3Al, FeAl, FeAl2, Fe2Al5, FeAl3) grew between the melt and the surface of steel sheets coated with Al-Si alloy during heat treatment. It is assumed that silicon affects the morphology of these aluminide layers. (Fe,Si)Al intermetallic islands were formed in Fe2Al5 aluminide layer. In order to observe the morphology, two different alloy, 5 wt% and 10 wt% silicon was added in molten aluminum. Besides, steel sheets coated with pure Al were prepared and analyzed for comparison. The growth behavior of (Fe,Si)Al islands after heat treatment at temperatures ranging from 400 - 800 oC was analyzed by scanning electron microscope (SEM), energy dispersive spectroscopy (EDS), and X-ray diffraction (XRD). It is revealed that no (Fe,Si)Al islands formed in a specimens coated with pure-Al. With the addition of silicon into the aluminum melt, the growth of (Fe,Si)Al islands becomes more severe. Furthermore, the most severe islands exist in specimen coated with higher silicon content.

3:30 PM

Manufacturing Methods and Properties of Powder-Based Parts with Inherently Saved Information: Bernd-Arno Behrens¹; *Najmeh Vahed*¹; Fabian Lange¹; Edin Gastan¹; ¹Institute of Metal Forming and Metal-Forming Machines of the Leibniz University of Hannover

As it is common in the production industry the produced components are physically separated from their related information. Inherently stored specific data in a component facilitates its identification, processing and reproduction during its lifecycle. Especially the powder metallurgy offers great potentials to realize this concept. Developing a method to manufacture and utilize sintered parts with inherent data is one of the main incentives of the Collaborative Research Centre 653 "Gentelligent Components in Their Lifecycle". The term "gentelligent" refers to the genetic and intelligent character of these components as they carry the essential information about their properties. As data carrier, foreign material in particle or powder form is embedded in the part body prior to consolidation and sintering process. The information readout is based on radiographic methods. The research is focused on the manufacturing methods and the impact of the embedded foreign materials on the mechanical properties of the part.

3:45 PM

Microstructure and Mechanical Properties of Al Based Composite Coatings Produced by the Cold Gas Dynamic Spraying Process: *Onur Meydanoglu*¹; Murat Baydogan¹; Eyup Kayali¹; Huseyin Cimenoglu¹; ¹Istanbul Technical University

In this study, microstructure and mechanical properties (hardness and wear) of Al-B₄C composite coatings prepared on structural steel substrate by cold spraying were investigated. Feeding powder compositions of Al and B₄C were 100:0, 80:20, 60:40 and 40:60 in volume. Al and B₄C powders used in this study were 10 \956m and 60 \956m in diameter, respectively. Air at room temperature is used as a propellant gas under a pressure of 6 bar. Hardness measurements were made on coatings using Vickers micro hardness tester and wear tests were conducted under dry sliding wear testing conditions on a ball-on disc wear tester by rubbing alumina and stainless steel balls. Addition of B₄C improved hardness and wear resistance of the coatings. Hardness of coatings increased with increasing B₄C content; however, wear resistances did not show any significant change with B₄C content. Alumina balls caused higher wear rate on coatings when compared to steel balls.

4:00 PM

Optimization of Fiber Laser Produced Hastelloy C-276 Single Track Clad: *Perry Leggett*¹; Prabu Balu¹; Radovan Kovacevic¹; Syed Hamid²; ¹SMU; ²Halliburton

The present study involves laser cladding of steel substrate with Hastelloy C-276, a nickel super alloy that is highly resistant to chemical corrosion. The laser cladding system consists of four main components: 1) a 4 kW fiber laser; 2) a carrier gas assisted powder feeder; 3) a five-axis CNC

vertical machining center and; 4) a heater. A grey based Taguchi method is used to optimize the key factors that determine the percentage dilution, circularity expressed as a ratio of height and width, and microhardness with minimal number of experiments. The circularity index and percent dilution are determined through optical microscopy; microhardness is measured using a Clark Microhardness tester, the results are then analyzed using a statistical approach. The results show the optimum Laser Power is 350 W, the optimum Powder Flow Rate is 0.13 g/s, and the optimum Scanning Velocity is 13.5 mm/s. A conformal experiment demonstrates the efficiency of the optimization procedure.

4:15 PM

Preparation of Nanocrystalline Aluminium by Warm-Vacuum-Compaction Method: *Wei Liu*¹; Qionghua Zhou¹; ¹Henan University of Science and Technology

The nano-sized aluminium particles were prepared by flow-levitation technology firstly, and then the particles were compacted with warm-vacuum-compaction method to fabricate the nanocrystalline aluminium with average grain size of 25.2 nm. The influences of experimental parameters, such as pressure, temperature and pressure duration, upon the density and microhardness of the nanacrystalline aluminium were investigated in detail. The experimental results show that both the density and microhardness of the nanocrystalline aluminium increase significantly with higher pressure or elevated temperature, while the duration of pressure has a little effect to the density or microhardness. The average microhardness of the as-prepared nanocrystalline aluminium is 1.65 GPa, which is 11 times higher than that of coarse-grained aluminium.

4:30 PM

The Effect of Sintering Conditions on the Properties of WC-Co Hard Metal Fabricated by Powder Injection Molding Process: Sung-Hyun Choi¹; Kyoung-Rok Do¹; Dong-Wook Park¹; Young Sam Kwon²; Kwon Koo Cho¹; In-Sup Ahn¹; ¹GNU; ²CetaTech. Inc

This study was investigated for microstructure and mechanical properties of WC-10%Co insert tool fabricated by PIM process. The feedstock fabricated by two blade mixer. The debinding process was carried by two-steps methods with solvent extraction and thermal debinding. After debinding process, the specimens were sintered at hydrogen-nitrogen mixed gas or vacuum atmosphere. The microstructure and phase were observed and the hardness and TRS were measured by vickers hardness tester and 3-point bending tester. The density of sintered at 1380° in mixed gas atmosphere was 87.5% and the hardness was 1400Hv. In the case of sintering at 1380° in a vacuum atmosphere after argon gas purging, the hardness was 1850Hv, and the relative density was 99.5%. The density of specimen sintered at 1350° in vacuum atmosphere was 99% and hardness was 1930Hv. In the case of sintered specimen at 1380°, the TRS result was 1100MPa.

4:45 PM

Annealing Characteristics of Cold Sprayed Pure Cu and Ni Coatings Using EBSD Technique: Ahmad Rezaeian¹; A. Changizi¹; Y. Zou¹; E. Irissou²; J.-G. Legoux²; S. Yue¹; ¹McGill University; ²National Research Council Canada(NRC) – Industrial Materials Institute(IMI)

The cold spray process produces a coating by mechanical deformation of sprayed particles. This heavily cold worked structure needs recrystallization heat-treatment in order to gain back the normal microstructure and ductility of the material. In this study, the effect of heat treatment of cold sprayed coatings was investigated for pure Copper and Nickel powders on mild steel as substrate, using N2 gas. As-sprayed coatings were then annealed for one hour at a range of temperatures up to 600°C. These were then compared to as-sprayed specimens in terms of microstructure, hardness, and porosity. It was found that 200°C was enough to decrease the hardness of heavily cold deformed pure copper due to restoration processes. The corresponding temperatures were around 600°C for pure Ni. The microstructures were evaluated using EBSD technique.

140th Annual Meeting & Exhibition

5:00 PM

Microstructure Evolution of Amorphous/Nanocrystalline Steel Coatings by Hybrid Spray Process: Vikram Varadaraajan¹; Ramesh Kumar Guduru¹; Pravansu Mohanty¹; ¹University of Michigan

Amorphous/nanocrystalline coatings are very useful in wear and corrosion protection applications. Here, we report microstructural evolution of an amorphous/nanocrystlline high performance steel coating developed by a novel "hybrid thermal spray" technique. This process combines the arc and high velocity oxy fuel (HVOF) techniques, in which the molten metal at the arcing tip is atomized and rapidly propelled to the substrate by HVOF jet. This so-called "hybrid" concept combines the benefits of productivity of arc spray with improved coating densities of HVOF. The microstructural characterization of the hybrid spray coatings was done by different materials characterization techniques and then compared with the coatings of the same material developed by plasma, HVOF and arc spray processes. The HVOF and plasma spray coatings showed amorphous structures, whereas hybrid and arc spray techniques yielded nanocrystalline coatings. The final microstructures could be attributed to the process temperatures and cooling rates during the spray process.

5:15 PM

Surface Characteristics and High Temperature Oxidation Resistance Performance of Stainless Steel Foam Modified by Pack Aluminizing and Moderate Oxidation: Deng-Wei Huo¹; *Xiang-Yang Zhou*¹; Hui Wang¹; Jie Li¹; Hong-Yu Song¹; Peng Zhu¹; ¹School of Metallurgical Science and Engineering, Central South University

The composition, phase structures and morphology of surface coating of stainless steel foam modified by pack-aluminizing and moderate oxidation were characterized by EDX, XRD and SEM, the effects of pack aluminizing and moderate oxidation on the oxidation resistance performance of stainless steel foam at 800° were also investigated. The main inter-metallic phases present in aluminizing coating on the surface of aluminized stainless steel foam are NiAl and Ni3Al, and the aluminizing coating is well-integrated with the foam substrate. The aluminized and oxidized foam displays excellent high temperature oxidation resistance performance, which may be due to the fact that the compact and uniform Al2O3 film formed on the outer layer of aluminizing coating obstructs the diffuse of oxidizing gas into matrix metal. Additionally, the surface layer reveals good property of thermal shock resistance, the treatment of pack aluminizing and moderate oxidation has little effect on the bending strength of foam.

5:30 PM

Development of Copper Coating on Austenitic Stainless Steel through Microwave Hybrid Heating: Dheeraj Gupta¹; *Apurbba Sharma*¹; ¹Indian Institute of Technology Roorkee

Coating of copper on austenitic stainless steel (Fe-Cr-Ni) is useful in electrical and electronic fields where high thermal conductivity as well as high electrical conductivity along with high strength is desirable. Usually, chemical vapor deposition (CVD) and physical vapor deposition (PVD) techniques are employed for developing such coatings. In the present work, copper coatings have been developed by a novel route, where microwave irradiation has been used as a heating source. The copper coating with average thickness of 230 microns were successfully deposited on austenitic stainless steel substrates by microwave hybrid heating process. The copper powder of size 5 microns were melted and deposited on austenitic stainless steel substrates. The deposited coatings exhibit dense and homogeneous microstructure. It was found that the coatings so developed had a mean hardness of 272±30 (Hv). Coatings were analyzed through Field emission scanning electron microscope (FE-SEM), X-ray diffraction (XRD) and X-ray elemental mapping.

5:45 PM

Anodization of Aluminum Alloys with Novel Anodizing Additive: *Alp Manavbasi*¹; ¹METALAST International, Inc.

Application of additives has been gaining great interest in contemporary aluminum hard anodizing technologies. The purposes for utilization of additives are to enhance the performance of anodizing processes and resultant anodic coatings while minimizing the environmental impact. Comparative studies showed that the developed additive provides a variety of functions including minimization of burning and blistering, improvement of current and conversion efficiency, enhancement of hardness and wear resistance as well as corrosion resistance. The results also show that the developed technology is capable of significantly improving the uniformity and consistency of anodic coatings. Additionally, aluminum alloys hardanodized at relatively high temperatures can meet or exceed the abrasion resistance and weight requirements per military specs when the additive is used in the anodizing electrolyte.

General Abstracts: Materials Processing and Manufacturing Division: Forging, Forming, and Machining

Sponsored by: The Minerals, Metals and Materials Society, TMS Materials Processing and Manufacturing Division, TMS/ASM: Computational Materials Science and Engineering Committee, TMS: Global Innovations Committee, TMS: Integrated Computational Materials Engineering Committee, TMS: Nanomechanical Materials Behavior Committee, TMS/ASM: Phase Transformations Committee, TMS: Powder Materials Committee, TMS: Process Technology and Modeling Committee, TMS: Shaping and Forming Committee, TMS: Solidification Committee, TMS: Surface Engineering Committee *Program Organizers:* Corbett Battaile, Sandia National Laboratories; Joy Forsmark, Ford Motor Company; Amit Misra, Los Alamos National Laboratory

Thursday PM March 3, 2011 Room: 5B Location: San Diego Conv. Ctr

Session Chair: To Be Announced

2:00 PM

Profile of Electrochemically Machined Microcomponents: *Wayne Hung*¹; Laxmi Viswanathan¹; Mike Powers²; ¹Texas A&M University; ²Agilent Technologies

Traditional micromachining uses silicon to fabricate microcomponents. Since silicon is not suitable for applications that demand high strength, robustness and biocompatibility, alternative micromanufacturing processes are sought. The non-traditional electrochemical micromachining (µECM) process is precise, non-contact, repeatable, and applicable to all conductive materials regardless of their mechanical properties. This paper examines effects of µECM parameters on profiles of micropatterns.A square-wave current forms micropatterns on an anodic workpiece with a slight undercut due to anisotropic electrochemical mechanism. The undercut is largest between the electrodes but is reduced outwardly. This micromachining uses a megahertz-wave to produce sharp profiles and reduces undercut at the expense of material removal rate. Although sharp corners can be formed on a convex pattern, rounded corners on concave patterns result due to combined edge effects. When utilized at a high frequency and an enhanced material removal rate, the µECM could become a suitable process for robust microsystems.

2:15 PM

A New Method for the Determination of Formability Limit in Tube Drawing Process: *Hien Bui*¹; Reza Bihamta¹; Michel Guillot¹; Guillaume D'Amours²; Ahmed Rahem²; Mario Fafard¹; ¹Laval University; ²National Research Council Canada, Aluminium Technology Centre

A new method for determination of formability limit in the tube drawing process was developed using the position controlled mandrel technique. In this method the mandrel has conical angle in a way that with change of mandrel position, the distance between die and mandrel will be changed and various combinations of thicknesses can be obtained using just one conic mandrel. The advantage of this method is determining the limit crosssectional reduction for each tube dimension with just one experiment. The realized drawing limit tests on the aluminium tubes show that the average maximum area reduction of AA6063 tubes is about 40%. An optimal tube drawing schedule for production of the constant wall thickness aluminium tubes with high cross-sectional reduction in one pass was successfully established based on the proposed formability limit test.

2:30 PM

A Novel Method for Joining of Stainless Steel (SS-316)through Microwave Energy: *M Srinath*¹; Apurbba Sharma¹; Pradeep Kumar¹; ¹IIT Roorkee

In the present work, microwave processing of metallic materials in the form of joining of bulk stainless steel (SS-316) has been successfully carried out by using multimode applicator with 2.45GHz and 900W power. Nickel based powder was used as a sandwich layer in between the interface surfaces. Samples were exposed to microwave radiation upto a maximum of 390s in multimode applicator. Principle of hybrid heating was employed to initiate microwave coupling with the metals. Stainless steel plates were also joined through TIG welding process. Joints have been characterized through field emission scanning electron microscopy (FESEM), X-ray diffraction (XRD), microhardness and porosity measurement. Microstructure study showed the faying surfaces are well fused and got bonded with base material. The observed Vicker's microhardness of microwave processed SS-316 joints was observed to be 290±14Hv, which is higher than the TIG welded joints (210±5Hv). The porosity of microwave processed joints was 0.78%.

2:45 PM

A Reliable Method for Determining the Solidification Force of Steel for Continuous Casting Conditions: *Matthew Rowan*¹; ¹University of Illinois at Urbana-Champaign

Determining the stress profile in a solidifying steel shell is difficult given the nonuniform temperature and stress profiles. Experimental methods such as the Submerged Split Chill Tensile (SSCT) and Contraction (SSCC) tests can measure solidification forces in the shell under controlled conditions identical to continuous casting. A computational model of the SSCC test using an austenite constitutive equation was created in ABAQUS to outline the correct methodology of obtaining the forces that develop in a shell during solidification. By using the nodal force output, it was determined that previous descriptions of the behavior of the solidifying shell during the SSCC test were incomplete. This fundamental change in the understanding of the SSCC test illustrates a case study when combining computational and experimental tools is more insightful than using these two tools separately.

3:00 PM

An Investigation into the Laser Micro-Welding of Aluminum and Copper in Lap Joint Configuration: *Prabu Balu*¹; B Carlson²; Rouzbeh Sarrafi¹; Radovan Kovacevic¹; ¹SMU; ²GM

Miniaturization, properties tailoring, weight reduction and high automation trends emerging in electrical and electronics industries necessitate successful application of laser micro welding technology to join similar and dissimilar aluminum and copper foils. A single mode fiber laser and a disc laser are used to obtain micro welds of these materials in different combinations (Al-Al, Cu-Cu, Al-Cu, Cu-Al, Cu-Al-Cu, and Al-Cu-Cu) with overlap configuration. The weld quality is quantified based on the electrical resistance, micro hardness and shear strength. The cross-sectional view of the dissimilar welds revealed that placement of aluminum or copper on the top dictates the weld quality. Different microstructural features and defects associated with micro welding of these materials are discussed in the light of optical metallography.

3:15 PM

Carbothermal Production of ZrB₂-ZrO₂ Composite Powders from ZrO₂-B₂O₃/B System by High-energy Ball Milling and Annealing Assisted Process: *Duygu Agaogullari*¹; Özge Balci¹; Ismail Duman¹; ¹Istanbul Technical University

The purpose of this study was to produce zirconium diboride-zirconium dioxide composite powders by comparing two different boron sources as boron oxide and elemental boron. The production method was high-energy ball milling and subsequent annealing of powder mixtures containing stoichiometric amounts of zirconium dioxide, boron oxide/boron powders in the presence of graphite as a reductant. Milling was performed in a vibratory ball-mill using hardened steel balls with 10:1 ball-to-powder weight ratio. The milled products were placed in alumina boats and annealed in a tube furnace held in Argon atmosphere. Milled/annealed products were leached for removing the impurities released by the vial (Fe, Ni, and Cr). ZrB_2-ZrO_2 composite powders were obtained after centrifuging, washing and drying treatments. The effects of milling duration and annealing temperature on the formation and microstructure of composite powders were investigated. The milled annealed products were characterized by XRD, SEM and DTA analyses.

3:30 PM

Deformation of High Purity Copper Specimens in Compression between Flat and Grooved Dies: Bashir Raddad¹; ¹University of Alfateh, Mechanical Department

Experiments were carried out to generate data on cold compression of high purity copper specimens having different height-to-diameter (Ho/Do) ratios (0.5 to 1.5) between two flat dies having various degrees of surface condition (knurled, dry and lubricated) and between grooved dies having different groove numbers (1 to 3). Different Ho/Do ratios, die surface conditions and number of grooved resulted in different loading characteristics and also different modes of deformation. The latter case resulted forward and backward extrusion modes plus the radial flow resulting from ordinary compression. Three shapes of deformed specimen were obtained according to the number of grooves. Load values decreased as Ho/Do increased and friction condition improved. For a fixed load, displacement increased for higher Ho/Do ratio. Surface strains were apparently affected by the above variables. In case of compression between grooved dies, in spite of the different mode of deformation, the same trends were obtained.

3:45 PM

Improved Shear Zone Quality by an Oscillating Shear Blade: Michael Lücke¹; ¹IPH

One of the most important factors of influence by forging without flash is the mass constancy of the billet. Because of large reachable quantities and low costs shearing of bar stock is an established proceeding in forging industry. Due to shearing faults the dimensional steadiness of sheared slugs is limited. Therefore the improvement of the shear surface is a desirable goal. The shear zone quality can be improved by an oscillating shear-cutter. Forming and cutting processes were found to be improved by the oscillation of the shear blade. An increased dislocation density, accelerated dislocation motions within the crystal lattice and an expedient friction rate suggest similar quality improvements and extensions of process limits in billet shearing processes. Primary goal of the analysis was the improvement of the slugs' shear zones. Shearing faults like ears, guides, nicks or deformations of pressure loaded areas were observed.

4:00 PM

Local Strain Hardening of Massive Forming Components by Means of Martensite Generation: Bernd-Arno Behrens¹; *Julian Knigge*¹; ¹Institute of Metal Forming and Metal-Forming Machines

The investigations presented in this paper are done within the scope of the collaborative research centre 675 "Creation of high strength metallic structures and joints by setting up scaled local material properties". The production of massive forming components made of metastable austenitic steels with local strengthening by means of forming-induced \945'-martensite is examined. The aim is the forming-induced setting of high-strength martensitic areas beside ductile austenitic regions for the realisation of locally load-adapted components.Different forming processes were performed for the basic determination of the dependence of the phase transformation on the forming parameters. It was found out that the forming-induced martensite formation essentially depends on the degree of deformation and the forming temperature. The phase transition during the forging process could be influenced by locally different degrees of deformation as well as a temperature difference between tool and specimen. Especially temperatures below ambient temperature increased the phase transformation.

4:15 PM

Machinable Trialcium Phosphate / CaTiO3 Composites: Celaletdin Ergun¹; ¹Istanbul Technical University

Synthetic calcium phosphates have chemical composition very close to that of the inorganic component of bone. Therefore, it is widely used in many biomedical applications. One of the important shortcomings of calcium phosphate is its very restricted ability to be machined to appropriate shapes and sizes in the manufacturing stage due to its high brittleness. In order to evaluate the machinibility of tricalcium phosphate(TCP) /CaTiO3 composites, TCP composites with CaTiO3 were prepared with pressureless air sintering between 500 and 1300°C for 2 hrs. The composites were characterized with XRD, SEM, and simple pole drilling. Results showed that β – TCP tricalcium phosphate and CaTiO3 composites were stable up to 1100°C. As a result they fulfilled the requirement of phase stability to insure the weak interface for machinability. Pole drilling test also proved this results.

4:30 PM

Some Studies on Performance of a Natural Polymer Media for Abrasive Flow Machining: *S. Rajesha*¹; Apurbba Kumar Sharma¹; Pradeep Kumar¹; ¹Indian Institute of Technology Roorkee

In abrasive flow machining (AFM) process, the media is one of the key components because of its ability to precisely abrade the selected areas along its flow path. Many researchers have developed their own media apart from a few available commercially. However, prohibitively longer time of preparation, its non-reusability and considerably high cost necessitates development of alternate media. In the present work, a new natural polymer based media was used to machine brass work pieces. Performance of the new reusable media has been evaluated by considering extrusion pressure, abrasive grit size, and processing time as process parameters and 'surface finish improvement' and 'material removal' as process responses. Experimentation scheme was planned using design of experiments with twenty sets of trials. The study reveals that the new media yields good improvement in surface finish as well as material removal. Further, preparation of the media and cost are significantly less.

4:45 PM

Surface Characterization of Laser Machined and Electropolished Metal Micro-Parts: Lysle Serna¹; Bradley Jared¹; Brad Boyce¹; Gerald Knorvosky¹; ¹Sandia National Labs

Laser micro-machining is the fabrication of parts with feature dimensions approaching 1 micron. As a thermally driven process, the laser/material interaction produces a "recast" layer of melted and re-solidified material on the part surface. Thus, while feature resolution can be exceptional, the resulting surface finish of the part is poor. Recast is generally undesirable, resulting in excessive wear and wear induced debris generation. Electropolishing is a post-machining process typically used for surface remediation by selective dissolution of the recast layer, resulting in improve material performance. In this talk, examples of laser machined stainless steel micro-parts and the as machined surface morphology will be presented, as well as the results of surface remediation by electropolishing. Sandia National Laboratories is a multi-program laboratory managed and operated by Sandia Corporation, a wholly owned subsidiary of Lockheed Martin Corporation, for the U.S. Department of Energy's National Nuclear Security Administration under contract DE-AC04-94AL85000.

5:00 PM

Effect of Particle Size on the Microstructure and Hardness of TiC and ZrC Reinforced Al-4 wt. %Cu Metal Matrix Composites Fabricated by a Novel Casting Method: *Hulya Kaftelen*¹; Lütfi Öveçoglu¹; Hani Henein²; Necip Ünlü¹; ¹Istanbul Technical University; ²Alberta University

The effect of particle size on microstructure and physical properties of Al-4wt.% Cu alloys reinforced with both the 10 wt.% TiC and ZrC particles were evaluated. The TiC having in mean size of 13 μ m, 93 μ m and ZrC particles having in mean size of 8 μ m, 157 μ m were introduced into Al-4wt.% Cu as reinforcements using a novel flux-assisted casting method. Studies indicated that TiC particles within the Al-4wt.% Cu matrix were uniformly distributed, whereas the cluster formation exists in composites including small size of ZrC particles (8 μ m). Clustering of fine ZrC particles within the Al-4wt.%Cu matrix leads to a decrease in the hardness of composite compared to coarse ZrC particles reinforced composite. Hardness of Al-4wt.% Cu alloy increased by a factor of two with the addition of 10 wt.% TiC particles; hardness of 1.3 GPa was obtained for the composite containing small TiC (13 μ m) reinforcements.

5:15 PM

Effects of Coil Configurations on Electromagnetic Tube Compression: *Jianhui Shang*¹; Allen Jones¹; Larry Wilkerson¹; Steve Hatkevich¹; ¹American Trim LLC

Electromagnetic forming is a complex mechanical-thermal-electromagnetic forming process. During electromagnetic forming, the coil is placed close to the workpiece to produce repulsive electromagnetic force between the coil and the workpiece. The coil design varies largely depending on the geometries of parts and the required forces to deform and accelerate workpiece. Tube compression is one of the major applications of electromagnetic forming. There are several coil configurations for electromagnetic tube compression in the literatures, but the detailed comparison between them is lacked. To investigate the effects of coil configurations, a series of experiments were carried out in this study for electromagnetic compression of Al 6061-T6 tube. This paper presents the detailed experimental results and discusses the advantages and disadvantages of the different coil configurations. Besides, computer simulations of the effects of coil configurations, which will be also presented.

General Abstracts: Materials Processing and Manufacturing Division: Modeling, Simulation, Ceramics, and Chemical Processing

Sponsored by: The Minerals, Metals and Materials Society, TMS Materials Processing and Manufacturing Division, TMS/ASM: Computational Materials Science and Engineering Committee, TMS: Global Innovations Committee, TMS: Integrated Computational Materials Engineering Committee, TMS: Nanomechanical Materials Behavior Committee, TMS/ASM: Phase Transformations Committee, TMS: Powder Materials Committee, TMS: Process Technology and Modeling Committee, TMS: Shaping and Forming Committee, TMS: Solidification Committee, TMS: Surface Engineering Committee *Program Organizers:* Corbett Battaile, Sandia National Laboratories; Joy Forsmark, Ford Motor Company; Amit Misra, Los Alamos National Laboratory

Thursday PM	Room: 7B
March 3, 2011	Location: San Diego Conv. Ctr

Session Chair: To Be Announced

2:00 PM

A Finite Element-Phase Field Study of Solid State Phase Transformation: Coarsening of Coherent Precipitates and Instability of Multilayer Thin Films: *Mohsen Asle Zaeem*¹; Haitham El Kadiri¹; Sinisa Mesaroivc²; Paul Wang¹; Mark Horstemeyer¹; ¹Mississippi State University; ²Washington State University

Governing equations for solid state phase transformation are derived by coupling Cahn-Hilliard type of phase field model to elasticity equations. The governing equations include 2nd order partial differential equations for elasticity coupled with a 4th order evolution partial differential equation for the conserved phase field variable. A mixed order finite element model is developed for the computations with C0 interpolation functions for displacement and C1 interpolation functions for the phase field variable. Developed finite element-phase field model is used to study coarsening of systems of coherent particles and also investigate morphological instabilities of multilayer thin films in solid state binary systems. It was shown that compositional mismatch elastic stresses in precipitates-matrix systems and multilayer thin films significantly affect the instability of these systems and alter the kinetics of transformations.

2:15 PM

Developing a New Method for Prediction of the Inhomogeneity of Stored Energy Based on the Recrystallization Phenomenon: *Peyman Saidi*¹; ¹Ferdowsi University

A new criterion based on recrystallization kinetics proposed in order to predict the inhomogeneity of stored energy. For this purpose, kinetic of static recrystallization and the interfacial area between recrystallized and unrecrystallized material per unit volume are considered. The Differential Scanning Calorimetery (DSC) method is utilized to determine the stored energy and for verification of the model. The effect of strain on the stored energy investigated. Good agreement between the prediction of proposed model and experimental results was observed.

2:30 PM

FEM Analysis of a Channel-Compression Process to Produce a Severe-Plastically Deformed Sheet: *Jong Jin Park*¹; ¹Hongik University

Recently, a new process for severe plastic deformation was proposed by A. Ghosh and R. Lee in which a round bar is pushed through a channel against a flat surface to be a pancake in shape. In the present study, the rigid-plastic finite-element method was used for the analysis of the process where an Al-1100 bar with the diameter of 20 mm was compressed and forced to flow through a gap of 1.5 mm. The punch force increased to 350 KN. Thickness of the pancake was 1.5 mm up to a certain radius, beyond which it decreased. Since the periphery of the pancake was elongated in the circumferential direction, it would be cracked at certain stage during the process. The effective strain increased smoothly in the radial direction but drastically in the thickness direction. The outer area of the pancake was noted to be wrinkled in the radial direction.

2:45 PM

Investigation on Electrohydraulic Servovalve through a Finite Element Method: *Somashekhar S. Hiremath*¹; M. Singaperumal¹; ¹Indian Institute of Technology Madras

The analyzed electrohydraulic servovalve is a jet pipe type, is one of the mechatronics component used for precision flow control application. Electrohydraulic servovalves (EHSV) promise unique application opportunities and high performance, unmatched by other drive technologies. Typical applications include aerospace, robotic manipulators, motion simulators, injection molding, CNC machines and material testing machines. EHSV available are either a flapper/nozzle type or a jet pipe type. In the present paper an attempt has been made to study the dynamics of jet pipe EHSV with built-in mechanical feedback using Finite Element Method (FEM). In jet pipe EHSV, the dynamics of spool greatly depends on pressure recovery and hence the fluid flow at spool ends. The effect of pressure recovery on spool dynamics is studied using FEM by creating the fluidstructure-interaction. The mechanical parts were created using general purpose finite elements like shell, beam, and solid elements while fluid cavities were created using hydrostatic fluid elements. The analysis was carried out using the commercially available FE code ABAQUS. The jet pipe and spool dynamics are presented in the paper.

3:00 PM

Mathematical Modeling for Analysis of the Burden Distribution and Gas Flow: *Jong-in Park*¹; Hun-je Jung¹; Min-Kyu Jo¹; Jeong-Whan Han¹; ¹Inha university

Process efficiency in the blast furnace is influenced by gas flow pattern which is under the control of burden profile. Therefore, it is important to control the burden distribution for reasonable gas flow. In this study, the falling trajectory of burden is decided by several variables. After falling, the burden stacked on the surface has the angle of repose due to the falling trajectory and falling velocity. The stock lines of each burden type in upper part of shaft move to the low part. And then, the burden profile of the blast is completed. Each section of burden profile was separated into cells which have information, such as diameter, porosity and shape factor for calculation of the gas flow. The analysis model was developed by using the Excel program based on visual basic. The mathematical formulas for developing this model was modified by the 1/12 scale model experiment.

3:15 PM

Development of a New Modeling Technique for Die Geometry for Extrusion of LCP Films: Arash Ahmadzadegan¹; *Michael Zimmerman*¹; Anil Saigal¹; 'Tufts University

It is known that a liquid crystal polymer (LCP) melt aligns in the direction of the shear flow when it passes through an extrusion die. This alignment causes thin films of the anisotropic LCP material to display different properties in different directions. To overcome this problem, many complex die design technologies have been developed that involve moving surfaces. However, there is a clear need to develop a method of predicting crystal orientation (alignment) to aid in die design. This paper investigates different modeling methods, and develops a numerical modeling technique using FLUENT, to predict molecular alignment by correlating it to streamlines of flow. This model also incorporates the complex rheology of the LCP in predicting the resulting alignment. Using this tool, newer and simpler designs are proposed, which result in more favorable orientations of the crystals.

3:30 PM

Microwave Drying of Silica Sand: Modeling, Kinetics, and Energy Consumption: Yu Li¹; Ying Lei¹; Hao Niu¹; Libo Zhang¹; *Jinhui Peng*¹; Huilong Luo¹; Wenwen Qu¹; ¹Key Laboratory of Unconventional metallurgy, Ministry of Education

A ratio of sample mass and power level(g/W) was used as power density to measure the effects on moisture content, drying rate and moisture ratio. The power densities used in this work were 4.167 (500 g, 120 W), 1.190 (500 g, 420 W), 0.714 (500 g, 700 W), 0.429 (300 g, 700 W) and 1.000 (700 g, 700 W) g/W, respectively. The experimental data and computational data were estimated by nine empirical models, and the Page model was observed be perfect fit for all experimental data with values for the of greater than 0.9970 and the and lower than 0.0035 and 3.6E-4, respectively. The activation energy was estimated as 0.279 W/g for power density=1 (1.000-4.167) g/W and 3.493 W/g for power density =1 (0.429~1.000) g/W. The obtained theoretical and practical specific energy consumption were 3.92 and 7.14 MJ/kg water, approximate or smaller than the similar literature report.

3:45 PM

Structural and Thermal Stability of Microwave Synthesized Nano-Hydroxyapatite: M Bilal Khan¹; Rafaqat Hussain²; *Muhammad Aftab Akram*¹; Nida Iqbal²; ¹National University of Sciences and Technology (NUST), SCME; ²COMSATS

Thermally stable bioactive hydroxyapatite (HAP) is synthesized by coprecipitation reaction between calcium nitrate tetrahydrate and diammonium hydrogen phosphate under microwave irradiation. The solution is refluxed in modified microwave oven and the effect of microwave power output and irradiation time is investigated in regard to thermal stability of synthesized HAP and the results are found in agreement with the earlier research (Zhengwen Yang et al, 2004). XRD indicated the minimum limit for microwave exposure to get thermally satble HAP inferred from appearance of additional identifiable peaks. Irradiation time is varied from 1 to 5 minutes at the rated powers of 600W and 1000W. Powders were treated for one hour in the 900 to 1100°C range. The treated nano HAP is analyzed for structural stability using XRD.

4:00 PM

A Study on the Hydrophobicity and Investigation of Physical and Chemical Properties of Produced Zinc Borate: *Mehmet Burcin Piskin*¹; Nil Baran Acarali¹; Nurcan Tugrul¹; Emek Moroydor Derun¹; Ozlem Akgun¹; 'Yildiz Technical University

Zinc borate which has different crystal structures is a synthetic hydrate metal borate. Zinc borates are widely used in rubber, plastic, ceramic, paint, electric insulation, wood applications, cement, medicine and flame retardant industries. Zinc borate has relatively high dehydration on-set temperature

which property permits processing in a wide range of polymer system. Zinc borate particles are hardly dispersed in a polymer matrix. Thus, hydrophobic zinc borate is used in different applications. In this study, zinc borate was synthesized by the reaction of zinc oxide and boric acid in the presence of kerosen and seed. In conclusion, physical and chemical analyses of products were carried out. The analysis results were compared with reference values. The results showed that the physical and chemical properties of produced zinc borate effected the hydrophobicity.

4:15 PM

Investigation of Reaction Conditions Effecting Hydrophobicity on Zinc Borate Yield: Sabriye Piskin¹; Nil Baran Acarali¹; Emek Moroydor Derun¹; Nurcan Tugrul¹; ¹Yildiz Technical University, Chemical Engineering Department

Zinc borate has been the subject of significant research for applications including the polymer additive which serves as the flame retardant synergist, the preservative in wood composites because of its high thermal stability, the smoke and afterglow suppressant due to its ability to undergo endothermic dehydration in fire conditions, and optical properties, and the additive for lubrication. It can be isolated as crystalline material in various forms having different chemical compositions, structures and there are no toxicity, low cost, and good performance in particular in halogen-free systems. In this study, the synthesis of zinc borate was carried out by the reaction of zinc oxide and boric acid in the presence of kerosen, seed. The effects of reaction conditions as reaction time, reactant ratio on yield were investigated. Optimum points for each parameter were determined. In conclusion, it was seen that changing reaction conditions effected the hydrophobicity of zinc borate.

4:30 PM

The Role of Energy Sinks in Discontinuous Reactions and the Approach to Equilibrium in U-Nb Alloys: *Robert Hackenberg*¹; Kester Clarke¹; Robert Forsyth¹; Ann Kelly¹; Tim Tucker¹; Pallas Papin¹; Robert Field¹; Heather Volz¹; Geralyn Hemphill¹; ¹Los Alamos National Lab

Lamellar decomposition products result when U-Nb alloys are transformed between about 300C and the 650C monotectoid temperature. As such microstructures give undesirable properties, the kinetics of these cellular reactions were investigated for U-5.6 wt% Nb and U-7.7 wt% Nb alloys. This study will evaluate the magnitudes of the chemical and interfacial energy sinks before and during the discontinuous precipitation (DP) and discontinuous coarsening (DC) reactions. The role of age hardening reactions taking place in the matrix prior to the passage of the DP growth front, diminishing the free energy available for the DP reaction, will be given particular attention. This will provide insight into the degrees to which different modes of decomposition relieve the initial supersaturation and drive the system toward equilibrium.

4:45 PM

Effect of Iron Additions on the Shape Memory Characteristics of Cu-Al Alloys: *T.N. Raju*¹; Sampath Vedamanickam¹; ¹Indian Institute of Technology Madras

Even though binary Cu-Al alloys with Al≥10 wt% exhibit shape memory effect and higher transformation temperatures, they are prone for poor workability. This is especially the case with polycrystalline alloys. This limits their practical applications. Attempts have therefore been made by researchers in the past to improve their mechanical and shape memory properties by ternary and quaternary additions, such as Mn and Ni, leading to improved ductility and shape memory properties. A similar trend is observed by adding Fe to Ni-Al alloys so as to overcome their brittleness. The effect of Fe addition on Cu-Al SMAs has not been explored so far. In the present work, therefore, the effect of Fe on the transformation temperatures and shape memory properties and higher transformation temperatures. The results are presented and discussed in the paper.

5:00 PM

Improved Wear Resistance by DLC Coatings: Andreas Krause¹; ¹IPH -Institut für Integrierte Produktion

Warm forged parts are favourable due to their good surface quality and close tolerances. The main disadvantage of warm forging compared to hot forging is the higher flow stress causing high mechanical loads and hence die wear. Diamond-like carbon coatings (DLC) are extremely hard and have good tribological properties which qualify them to reduce die wear. This capability is analysed in forging trials. These trials are supported by preceding FEA simulations to perceive the conditions causing wear of the coatings. Abrasive wear of DLC is mainly bred to conversion of diamond-like sp3 to graphitical sp₂ bonding which is to be reduced by doping the DLC with metallic elements. The cavity of the forging tools is designed to reflect the main influencing factors on die wear like high relative velocity and high normal stresses. A developed model mapping the wearing-process helps to improve the design and usage of DLC coatings for warm forging.

5:15 PM

Asphalt Fatigue Damage Characterization Based on Laser Scanning Detection and Energy Dissipation: *Hossein Ajideh*¹; James Earthman¹; ¹University of California, Irvine

Fatigue damage is one of the major distresses in pavement and has been evaluated using various approaches over the last two decades. A better understanding of fatigue behavior in asphalt materials is needed for better design methods to minimize fatigue failures. The primary objective of the present research was to develop a laser scanning detection system that detects changes in surface properties in order to monitor damage and characterize fatigue behavior of asphalt mixtures. This technique characterizes the surface state using a parameter called defect frequency by rapidly scanning a laser beam along the specimen. The results of laser scanning method have been compared to data for other traditional (50% reduction in stiffness) and dissipated energy approaches. This system provides the opportunity to quantify micro-crack formation rate and evaluate fatigue performance of asphalt mixtures in situ.

General Abstracts: Structural Materials Division: Microstructure

Sponsored by: The Minerals, Metals and Materials Society, TMS Structural Materials Division, TMS: Advanced Characterization, Testing, and Simulation Committee, TMS: Alloy Phases Committee, TMS: Biomaterials Committee, TMS: Chemistry and Physics of Materials Committee, TMS/ASM: Composite Materials Committee, TMS/ASM: Corrosion and Environmental Effects Committee, TMS: High Temperature Alloys Committee, TMS/ASM: Mechanical Behavior of Materials Committee, TMS/ASM: Nuclear Materials Committee, TMS: Refractory Metals Committee, TMS: Titanium Committee

Program Organizers: Roger Narayan, Univ of North Carolina & North Carolina State Univ; Judith Schneider, Mississippi State University

Thursday PMRoom: 11BMarch 3, 2011Location: San Diego Conv. Ctr

Session Chair: To Be Announced

2:00 PM

Grain Size Dependence of Fracture Toughness of Fine Grained Alumina Sintered by Spark Plasma Sintering: *Wenlong Yao*¹; Jing Liu¹; Troy Holland¹; Lin Huang¹; Yuhong Xiong¹; Julie Schoenung¹; Amiya Mukherjee¹; ¹University of California, Davis

Fully dense fine grained alumina was prepared by spark plasma sintering. A series of alumina with grain sizes varying from ~300nm to ~3 μ m were obtained. The fracture toughness was measured by Vickers indentation and Surface Crack in Flexure method, a 2007 ASTM standard. More than 50 fracture toughness values from Surface Crack in Flexure with different grain

sizes were statistically analyzed based on the Weibull distribution. It was found that the fracture toughness in fine grained alumina is independent of grain size and the fracture toughness calculated from Weibull distribution is 3.37 MPam1/2.

2:15 PM

Formation and Thermal Stability of Nanosized Oxide Precipitates in NiAl Alloys: *Yongdeog Kim*¹; Hyon-Jee L. Voigt¹; Zuhair A. Munir²; Brian D. Wirth³; ¹University of California, Berkeley; ²University of California, Davis; ³University of California, Berkeley/University of Tennessee

We have produced NiAl oxide dispersion strengthened (ODS) super alloys by mechanical alloying of NiAl with Y2O3 and Ti powders, followed by spark plasma sintering, with the objective of improving the high temperature strength and creep resistance. These target properties are expected due to a presence of high number density of stable nano-meter scale clusters (NCs), akin to those recently observed to improve creep strength and radiation resistance in nano-structured ferritic alloys. In this presentation, the alloy production process and high temperature mechanical properties of the NiAl ODS alloys will be summarized. The improved mechanical properties will be explained in connection with the size, structure, and number density of the precipitated oxide particles, which are obtained using transmission electron microscopy (TEM) and atomistic simulation methods. Finally, the thermal stability of oxide precipitate will be discussed using the mechanical properties of NiAl ODS alloys as a function of thermal annealing condition.

2:30 PM

The Effect of Hafnium Addition on the Microstructure and Phase Equilibria in Cr-Si Based Alloys: *Amir Nanpazi*¹; Panos Tsakiropoulos¹; ¹IMMPETUS, Department of Engineering Materials, The University of Sheffield, Sir Robert Hadfield Building, Mappin Street, Sheffield S1 3JD, England, UK

This study focussed on the effect of Hf addition on the microstructure and phase equilibria of the as cast and heat-treated Cr-45Si-5Al-5Hf (AN1) and Cr-25Si-25Al-5Hf (AN2) (at %) alloys. There was no macrosegregation in the as cast alloys AN1 and AN2 the microstructures of which respectively contained the (Hf,Cr)5Si4, Cr5(Si, Al)3 and Cr (Si, Al)2, and the Cr3(Si,Al), Cr5(Al,Si)8 and (Hf,Cr)5Si4 intermetallics. A key result of this study was the destabilization respectively of the CrSi and Cr5Si3 silicides in the alloys AN1 and AN2 and the stabilization of the (Hf,Cr)5Si4 silicide via the addition of Hf. The Vickers microhardness of the phases present in the as cast and heattreated alloys AN1 and AN2 and their macrohardness were measured.

2:45 PM

Microstructural Properties of Gamma Titanium Aluminide Manufactured by Electron Beam Melting: Sanna Fager Franzén¹; Joakim Karlsson¹; Ryan Dehoff²; Ulf Ackelid¹; Orlando Rios²; Chad Parish²; William Peter²; ¹Arcam AB; ²Oak Ridge National Laboratory

Gamma titanium aluminides (y-TiAl) have been recognized for decades to be suitable for aerospace applications due to their low density and high strength at elevated temperatures. However, TiAl is limited in application due to difficulties during machining which arise from the inherent brittle nature associated with intermetallic phases. Electron Beam Melting (EBM) has recently been proven as a processing method to produce complex, near net shape y-TiAl parts with short lead times.We present the results from investigation of mechanical and microstructural features of EBM built γ-TiAl, Ti-48Al-2Cr-2Nb. The results include characterization of the unique, small grained, microstructure obtained and suggestions of heat treatment paths to obtain various microstructures. Microstructural investigations were conducted using standard optical and scanning electron microscopy techniques in conjunction with newly emerging techniques such as FIB-SEM to closely map the microstructure. In addition to microstructural characterization, the mechanical properties of EBM built material are presented.

3:00 PM

Microstructure of a' Martensites in Ti-V-Al Alloys Studied by High-Resolution Transmission Electron Microscopy: *Kazuhisa Sato*¹; Hiroaki Matsumoto¹; Akihiko Chiba¹; Toyohiko Konno¹; ¹Tohoku University

Titanium alloys are widely used in various fields due to their high specific strength and corrosion resistance. Among the Ti-alloy systems, Ti-V-Al alloys composed of hexagonal a' martensites possess low Young's moduli and high strength. In this study, atomic structure and morphology of a' martensites in Ti-12%V-2%Al and Ti-6%Al-4%V alloys were studied by aberration-corrected (AC) high-resolution transmission electron microscopy (HRTEM). The {10-11}-type twin formed by martensitic transformation remained in a Ti-12%V-2%Al alloy aged at 400°C. The alloy was once solution treated at 950°C and then quenched into ice water. The twin boundaries are free from precipitates or stacking faults in spite of substantial age-hardening. In contrast, thin layers of stacking faults, 1-2mm in thickness, were observed at the {10-11} twin boundaries of a Ti-6%Al-4%V alloy quenched from 1100°C. AC-HRTEM benefits from smaller optimal defocus values due to small spherical aberration, which enables unambiguous identification of interface structures.

3:15 PM

Precipitation and Growth of Omega Phase and Alpha Phase during Aging of Alpha-Beta Solution Treated Ti-6.8Mo-4.5Fe-1.5Al: Jana Smilauerova¹; Milos Janecek¹; Radomir Kuzel¹; Petr Harcuba¹; Josef Strasky¹; Henry Rack²; ¹Charles University; ²Clemson University

Precipitation of omega and alpha particles in TIMETAL LCB (Ti-6.8Mo-4.5Fe-1.5Al, wt. %) during aging after alpha-beta solution treatment was examined. Initially alpha-beta solution treatment between 700 and 745°C was used to control the volume fraction, size and contiguity of grain boundary alpha. Subsequent aging at 400, 450 and 500°C for times between at 0.5 and 256 hrs was monitored by superficial hardness measurements, the changes in response being correlated with size, volume fraction and spatial distribution of the omega and alpha phase as defined by x-ray diffraction, transmission and scanning electron microscopy.

3:30 PM

Abnormal Phase Stability in a Ru-Containing Ni-Base Single Crystal Superalloy: Jingyang Chen¹; Yanhui Chen¹; Yunrong Zheng²; Zuqing Sun¹; *Qiang Feng*¹; ¹University of Science and Technology Beijing; ²Beijing Institute of Aeronautical Materials

Ru addition has been reported to suppress the precipitation of topologically close-packed phases (TCPs) in Ni-base single crystal superalloys during thermal exposures. However, the mechanisms by which Ru enhances microstructural stability remain debatable. In this study, high Ru (4.9 wt.%) addition was found to significantly promoted the formation of TCPs in a high Cr-containing (5.7 wt.%) alloy due to higher Re partitioning ratio and high Re supersaturation in the γ matrix. The time-temperature-transformation (TTT) curves for TCP phase formation indicated that Ru addition accelerated the onset of TCPs precipitation during thermal exposures (900~1200°C). After long-term annealing at 1100°C, the TCPs in Ru-free and Ru-containing alloys were different in morphology and density, while Ru addition significantly enhanced the kinetics for transforming σ phase to P phase. The mechanisms by which Ru promoted the TCPs formation have been clarified on high-temperature phase stability, elemental partitioning behavior and TCPs/ γ interface misfit.

3:45 PM Break

4:00 PM

Comparison of Point-Defect Evolution in Irradiated UO2 and Ceo2 from Molecular Dynamics Simulation: *Dilpuneet Aidhy*¹; Dieter Wolf¹; ¹Argonne National Laboratory

We elucidate the degree to which CeO2 can serve as a surrogate material for UO2 in understanding the evolution of irradiation-induced point defects. Using a new methodology to atomistically capture long-time evolution of point defects in UO2 (Aidhy, et. al., PRB, 2009) we observed that, in the presence of defects on the U sublattice, annihilation of oxygen defects

via mutual recombination is hindered. The surviving defects form clusters including O vacancies forming Schottky defects, and O interstitials forming cuboctahedral clusters. However, in the absence of U defects, the O defects annihilate completely. We employ a similar methodology to CeO2 to predict the underlying point-defect evolution in the two sublattices and elucidate the mechanism of cluster formation in CeO2 (interstitial type dislocation loops lying on {1 1 1} planes, Yasunaga et al., NIM B, 2006). Work supported by the Energy Frontier Research Center for Materials Science of Nuclear Fuels.

4:15 PM

A New Method for Constructing Coincident Site Lattices for Cubic Crystals: Mohammad Shamsuzzoha¹; ¹University of Alabama

A simple method for geometrical construction of two-dimensional coincidence site lattices (CSL) in cubic crystals based on vector representation of lattice sites is put forward. The construction of such CSLs is achieved by mutual rotation of unique vectors, termed sigma generating vectors, found in the identically projected orthogonal lattice network of both the constituting crystals of the same species. The angle of rotation of the bicrystal is expressed in terms of some unique nonprime integers that describe the orientation of the sigma generating vector within the lattices of each constituting crystal. The cell parameters of the two-dimensional CSL thus formed can be described in terms of both the magnitude (termed as S) of the square root of the sigma generating vector as well as the lattice parameters of the constituting crystals. Addition of a third axis along the rotation axis of these two-dimensional CSLs yields related three dimensional CSLs.

4:30 PM

Martensite Strain Induced Phase Transformation and Corrosion Resistance of AISI 201 and AISI 304 Stainless Steel: Viviane de Morais¹; ¹MAHLE

The increase in the application demand of austenitic stainless steels and the constant pressure for cost reduction in the steelmaking industry, due to the high instability of nickel price, has conduced to new developments of the AISI 200 series steels. This new austenitic stainless steel series employes high manganese and nitrogen contents in substitution to nickel. Samples of these steels were heat treated and cold rolled to different strains for subsequent microstructural evaluation. Strain hardening versus strain, martensite volume fraction versus strain, as well as microstructure evolution and its respective phase identification with strain are some of the main results obtained in this study. The AISI 201 steel presented higher susceptibility to induced phase transformation in comparison to the AISI 304 steel due to its lower stacking fault energy. Electrochemical impedance spectroscopy and anodic potenciodynamic polarization were the techniques used to evaluate the corrosion resistance and passivation behavior, respectively.

4:45 PM

Mechanical Twinnning Investigation in a 17.5%Mn TWIP Steel. A Physically-Based Phenomenological Model: *Ayoub Soulami*¹; Xin Sun¹; Moe Khaleel¹; ¹Pacific Northwest National Laboratories

TWinning Induced Plasticity (TWIP) steel combines both high strength and extended ductility due to TWIP effect. In this work, the principal features of deformation twinning in Faced-Centered Cubic (FCC) austenitic steels are discussed. A physically-based phenomenological model derived from microscopic consideration is presented. The model contains internal variables: dislocations density and micro-twins volume fraction, representing the microstructure evolution during deformation process. The contribution of this work is to use physically-based criterion for twin's nucleation and twin's volume fraction evolution in a conventional approach. Model's predictions are compared to experimental tensile data at different strain levels for a 17.5%Mn TWIP steel. Microstructure investigation, using SEM and TEM, are also used to validate and verify modeling assumptions.

5:00 PM

Mechanical Properties and Strain Mechanisms Analysis in Ti-5553 Titanium Alloy: *Timothée Duval*¹; Patrick Villechaise¹; Sandra Andrieu²; ¹Institut P' - ENSMA; ²Messier Dowty

This study focuses on the mechanical behaviour of the Ti-5553 betatitanium alloy used in airspace industries for structural components. Tensile and fatigue tests were performed to evaluate the macroscopic mechanical characteristics of this alloy at room temperature. Strain mechanisms will be analyzed from post mortem investigations and by performing in-situ tensile tests in a scanning electron microscope. The crystallographic orientation of both alpha and beta phases was measured by Electron Back Scattered Diffraction. This allows to identify the activated slip bands and to investigate the validity of a Schmid factor approach. The plasticity mechanisms will be detailed at the different scales that characterize the metallurgical microstructure: beta grain, primary alpha nodules, beta matrix with secondary fine alpha lamellae. The discussion will focus on the relative contribution on the macroscopic behaviour of each scale and plasticity mechanism.

5:15 PM

Creep Studies of Misoriented Grains in René N4 and GTD 444 Superalloy Bicrystals: Kaitlin Gallup¹; Tresa Pollock¹; ¹UCSB

The transverse creep properties of samples containing misoriented (m/o) grains in the nickel-based superalloys René N4 and GTD444 have been studied. Bicrystal slabs were cast using the liquid metal cooled directional solidification method, with seeds rotated about the [001] growth axis to yield bicrystals with low and high angle boundaries with <10°m/o, 20°, >30°m/o. The role of carbides at the boundary and effect of the grain boundary strengthening additions of boron and carbon are explored. Further, creep mechanisms are compared between single crystal bars and bars loaded transverse to the grain boundaries at 982C/207MPa and 760C/690MPa. Up to a 99% reduction in creep rupture lifetime is found. Damage accumulates in interdendritic regions in both the single crystal and bicrystal samples during high temperature creep. At the lower temperature, fracture follows crystallographic planes in single crystals and transitions to the interdendritic grain boundary region at high misorientations.

5:30 PM

Static Recrystallization Behavior of Co-Ni-Cr-Mo Superalloy after Cold Rolling and Subsequent Heat Treatment: *Takuma Otomo*¹; Shingo Kurosu¹; Yunping Li¹; Hiroaki Matsumoto¹; Shigeo Sato¹; Yuichiro Koizumi¹; Kazuaki Wagatsuma¹; Akihiko Chiba¹; ¹Institute for Materials Reseach, Tohoku University, Japan

The recrystallization behavior of Co-33Ni-20Cr-10Mo (CNCM) superalloy due to heat treatment after cold rolling was studied. The alloy CNCM is used as a spring of mechanical watch; thus a refined structure is required to improve the mechanical properties. The alloy CNCM was cold-rolled from 15% to 90% reduction. The deformed alloy was heat treated at 700 and 800 \Box . Microstructural evolution of the alloy was characterized by means of TEM, HRTEM, XRD and EBSD. The Goss {110}<001> texture was dominantly formed after conventional cold rolling. The microstructure was refined after the cold rolling by the reduction higher than 70%. It is suggested that the refined structure was formed due to the strain induced grain subdivision during cold rolling. The average grain size after the recrystallization was submicron meter and the texture did not change after the recrystallization. It is indicated that the alloy CNCM exhibits the continuous recrystallization behavior.

5:45 PM

Oxidation Behavior of Copper Thin Films with Nanoscale Twins: *Pi-Hua Lee*¹; Chan Tsung-Cheng¹; Liao Chien-Neng¹; ¹Department of Materials Science and Engineering, National Tsing-Hua University

Copper with a high density of nanoscale twins has attracted extensive research attention in the last decade due to its excellent mechanical strength and decent electrical conductivity. Nanotwinned Cu is considered as a candidate of interconnect material in nanoelectronic devices. However, the oxidation behavior of nanotwinned Cu has to be evaluated for process integration considerations. In this study, we deposited Cu films on a Si substrate by e-gun evaporation. The activation energy of oxidation of Cu films was determined using the ramping technique that measured the change of electrical resistivity of the Cu film exposed to air with different temperature ramping rates. The preliminary results showed that the Cu films with higher deposition rate appeared to have lower oxidation temperature and smaller activation energy than the typical Cu films. The effect of nanotwin and grain size on the oxidation kinetics of Cu films will be investigated.

General Abstracts: Structural Materials Division: Processing

Sponsored by: The Minerals, Metals and Materials Society, TMS Structural Materials Division, TMS: Advanced Characterization, Testing, and Simulation Committee, TMS: Alloy Phases Committee, TMS: Biomaterials Committee, TMS: Chemistry and Physics of Materials Committee, TMS/ASM: Composite Materials Committee, TMS/ASM: Corrosion and Environmental Effects Committee, TMS: High Temperature Alloys Committee, TMS/ASM: Mechanical Behavior of Materials Committee, TMS/ASM: Nuclear Materials Committee, TMS: Refractory Metals Committee, TMS: Titanium Committee

Program Organizers: Roger Narayan, Univ of North Carolina & North Carolina State Univ; Judith Schneider, Mississippi State University

Thursday PM	Room: 6A
March 3, 2011	Location: San Diego Conv. Ctr

Session Chair: To Be Announced

2:00 PM

Using Resistance Heating to Create Full-Scale API RP2Z CTOD Samples: Morgan Gallagher¹; *Sudarsanam Suresh Babu*²; Jerry Gould¹; ¹Edison Welding Institute; ²The Ohio State University

API RP2Z testing is used by the oil and gas industry to qualify steel plate for service in offshore environments. Part of this qualification process involves assuring "that the steel to be supplied is inherently suitable for welding". Suitability for welding is demonstrated in part through CTOD testing of the HAZs of plates welded over a wide range of heat-inputs. Unfortunately, the time and cost associated with welding CTOD samples can become burdensome as the qualified plate thickness increases. Additionally, the current RP2Z welding procedure may not lead to uniform microstructures in the HAZ of new generation steels. Consequently, EWI has begun to study resistance heating to manufacture full-scale CTOD samples with microstructures identical to samples produced through welding. Initial trials used A36 steel and two peak temperatures. The resultant cross-sections were metallurgically uniform and consisted of microstructures expected for CGHAZs and FGHAZs for peak temperatures of 1200°C and 1000°C.

2:15 PM

Brazing of Titanium Alloys Using Low-melting Eutectic Zr-Ti-Ni(Cu) Filler Alloys: *Dong-Myoung Lee*¹; Gerhard Welsch¹; Yong-Soo Kim²; Seung-Yong Shin³; ¹Case Western Reserve University; ²Yosan Eng.; ³KITECH

The Zr-Ti-Ni(Cu) alloy system consists of several ordered intermetallic phases, and shows low-melting alloys containing intermetallic phases. Upon rapid solidification these enable glass-forming ability and produce flexible ribbon sheets suitable as filler alloy for brazing. In this study low-melting-point filler alloys in the Zr-Ti-rich side of the Zr-Ti-Ni(Cu) alloy system were investigated for brazing of titanium alloys. Low-melting ternary and quaternary eutectic alloys with melting temperatures below 800° were discovered. Using eutectic as well as off-eutectic braze alloys, CP-Ti and Ti-6Al-4V alloys were successfully brazed at 830° and 850°. The braze joints exhibited interdiffusion-modified structure with intermetallic and solid-solution phases, and the bond strengths were close to the base metal strengths (CP Ti: 438MPa, Ti-6Al-4V: 1007MPa).

2:30 PM

Development of Coatings on Titanium Aluminide Alloys Using Chemical and Physical Deposition Methods: *Patrick Masset*¹; Laurent Bortolotto²; Ludovic Charpentier¹; Michael Schütze³; Hans Jürgen Seifert¹; ¹TU Bergakademie Freiberg; ²Dechema; ³DECHEMA

Due to their low density and good mechanical properties even at high temperatures titanium aluminide intermetallics are candidates to replace nickel based super alloys in jet engines. However, they still suffer from environmental embrittlement, which deteriorates their mechanical properties at elevated temperatures. The development of ductile intermetallic coatings with gradient composition constitutes an interesting alternative to repress the environmental embrittlement by creating a physical barrier against hot gases, and to suppress or at least to reduce to an acceptable level the oxygen ingress into the alloy. Coatings on technical alloys were produced using MO-CVD and PVD techniques. They contain elements which favour the coating ductility on the top of the substrate whereas other alloying elements enhance its oxidation and corrosion resistance. The coatings were characterised by XRD, SEM-EDX, EPMA, nano-hardness. In addition, the developed coatings were tested under isothermal and thermocyclic conditions in air.

2:45 PM

Precipitation-Strengthened Ferritic Steels with Increased Strength and Ductility: *Monica Kapoor*¹; Semyon Vaynman¹; Gautam Ghosh¹; Dieter Isheim¹; Yip-Wah Chung¹; ¹Northwestern University

High-strength, low-carbon, ferritic steels with yield strength up to 1600 MPa and elongation-to-fracture up to 25% were achieved by addition of Cu, Ni, Mn and Al via solution treatment, followed by water quench, and aging. Precipitation strengthening appears to be the primary strengthening mechanism. Atom probe and transmission microscope studies demonstrate that two types of coherent slightly misfitting nanosized precipitates are formed in the steel: Cu-rich and NiAl-type. In this talk, we will discuss the need to reduce the amount of retained austenite to maximize the effect of alloying elements on the yield strength. This can be achieved by appropriate choice of the steel composition and the aging temperature.

3:00 PM

Role of Heat Treatments on the Mechanical Properties of Dual-Phase Steel Sheet: *Hossein Seyedrezai*¹; Keith Pilkey¹; Doug Boyd¹; ¹Queen's University

The mechanical behaviour of dual-phase (DP) steel depends on various factors, mainly the size, spatial distribution and volume fraction of the non-ferritic phase (e.g. martensite). To understand the effect of these parameters, a series of pre-treatments were performed on DP600 steel prior to inter-critical annealing. These pre-treatments served to change the spatial distribution of carbides before the inter-critical annealing step, thereby producing distinctly different final microstructures. One pre-treatment involved austenitizing, quenching and tempering (at various temperatures). The second pre-treatment was an austempering process. Optical and scanning electron microscopy observations confirm that both pre-treatments produce a very fine and uniform distribution of carbides, which later lead to a more uniform distribution of fine martensite particles in the final DP microstructures. Uniaxial tensile testing demonstrates that the application of these pre-treatments results in improved mechanical properties as compared to the base-line material without any pre-treatment history.

3:15 PM

Friction Stir Processing of Cast Superalloys: *Edward Chen*¹; Bharat Jasthi²; Douglas Bice¹; William Arbegast²; Matthew Heringer²; Stanley Howard²; ¹Transition45 Technologies, Inc.; ²South Dakota School of Mines and Technology

This presentation examines the feasibility of incorporating friction stir processing (FSP) with casting to produce higher performance yet cost affordable near-net shape Ni-based superalloy components. Casting is one of the most inexpensive fabrication methods in existence. Friction stir processing is an emerging microstructural modification technique based on friction stir welding (FSW) that can be applied to enhance the microstructureproperties. It can be used to refine cast microstructures such as to improve 140th Annual Meeting & Exhibition

properties such as damage tolerance. This added step could be used to allow cast superalloy components to be employed without casting factors. If successfully developed and implemented, this technology could have the tremendous potential for reducing the weight and cost of Ni-based superalloy castings that are used in industries as diverse as rocket propulsion, aircraft engines, land-based gas turbines, and chemical process industry pumps and valves. It could also be used for part repair and refurbishment.

3:30 PM

Characterization of Ni-Base Superalloy Die Materials: *Alvaro Mendoza Jr*.¹; Krishna Ganesan¹; Gerhard Fuchs¹; ¹University of Florida

A case study was undertaken to examine the premature failure of a set of IN718 forging dies. Detailed microstructural characterization of the failed dies indicated that they were exposed to higher temperatures than initially expected. Higher use temperatures resulted in a significant strength reduction of the IN718 dies, and failure of the dies. This lead to rising costs, as the dies had to be replaced more often than expected. Rather than changing the forging conditions, a new die material with higher temperature capabilities was identified. IN-100 was selected as the replacement die material due to the higher temperature capabilities of the IN-100. To validate the new material selection, samples of both IN718 and IN-100 were given thermal cycles to replicate the expected die lifetime. The microstructural stability of each alloy was characterized by optical and SEM metallographic techniques. Hardness testing was also used to characterize the microstructure and properties.

3:45 PM Break

4:00 PM

Metal (Fe-Al)- Fullerene Nanocomposites Made by Powder Metallurgy Methods: *Hector Calderon*¹; ¹ESFM-IPN

Nanocomposites have been produced by using a metal (Fe or Al) together with pure C60 or a mixture of fullerenes (C60 + C70) and soot. The synthesis includes mechanical milling and spark plasma sintering (SPS). Different milling media produce a variety of transformations of the carbon phases, depending on the energy input, nanodiamonds, metallic carbides or well dispersed fullerenes can be obtained after relatively short milling times (up to 2 h). Sintering develops considerable increases of mechanical strength without reducing the ductility of the sintered composites. During sintering further phase transformations occur involving the carbon phases. Carbides are normally produced, however diamonds in nanometric dispersions can also be found after highly energetic milling of the original powders particularly in the presence of Fe. The soot in the fullerene mixture transforms during sintering to other phases including fullerenes, particularly in Fe based materials. High temperature rolling of the composites gives rise to transformation of the remaining fullerenes to more stable phases i.e., carbides or diamonds. Electron microscopy, Raman spectroscopy, and X-ray diffraction are mainly used for characterization.

4:15 PM

Preparing Titanium Powders by Calcium Vapor Reduction Process of Titanium Dioxide: *Baoqiang Xu*¹; Bin Yang¹; Heli Wan¹; Wei Sen¹; Yongnian Dai¹; Dachun Liu¹; ¹National Engineering Laboratory for Vacuum Metallurgy, Kunming

In this paper, thermodynamic equilibrium calculations on the system of Ca-O2-N2-TiO2 were carried out and the calciothermic reduction process of titanium dioxide to prepare titanium powders in the closed graphite vessel was investigated by means of XRD, SEM and EDS. The thermodynamic calculation results indicated that the sum of part pressures of gas O2 and gas N2 would equal to 10-60—10 that is much less than the saturated vapor pressure of metal calcium at the same temperature during the range of 298K-1500K in the same system, which implied the metal calcium would become vapor to reduce TiO2 at certain temperature after exhausting O2 and N2 in the closed system. Experimental results indicated with reduction temperature risen and reduction time increased calcium vapor reduction process of TiO2 was improved and on the condition of reduction temperature in the range of 1273K~1473K and reduction time 6h the TiO2 was reduced

effectively, then titanium powders (purity: >95%Ti, particle size: 3-5µm, shape: irregular) were prepared.

4:30 PM

Partial Melting Homogenization of Thick Section Austempered Ductile Iron Containing 2% Mn: Seid Ata Sheikholeslami¹; Mahmoud Nili-Ahmadabadi¹; *Jafar Rassizadehghani*¹; ¹University of Tehran

Ductile iron castings are usually alloyed with elements such as Mn and Mo to improve mechanical properties and hardenability. In asmuchas conventional homogenization of ductile iron does not change segregation of Mn or Mo considerably, in particular in thick section castings, in this study partial melting homogenization(PMH) was applied to reduce the deteriorative segregation effects. Thick section ductile iron castings containing 2% Mn was processed by PMH in as cast and austempered condition. Homogenization just above the intercellular eutectic temperature causes melting of the highly Mn seregated regions. Isothermal solidification of this region causes diffusion of Mn from liquid pool to the surrounding solid region while Si diffuses in the reverse direction. The microstructure of homogenized specimens by PMH were found to be more uniform with a reduced amount of segregation when compared to the as cast samples. Tensile tests demonstrated the improving effects of PMH heat treatment.

4:45 PM

Formability Evaluation of TRIP Steel Sheets: *Joong Eun Jung*¹; Jong Bae Jeon¹; Young Won Chang¹; ¹POSTECH

Multiphase TRIP steels provide high potential for applications to automotive bodies and frames due to their excellent combination of strength and elongation resulted from deformation induced martensitic transformation (DIMT). There have been extensive works on DIMT kinetics and the role of retained austenite (RA) on tensile properties, but formability of these steel grades has not been well clarified to date. The characteristics of RA have been reported to be an important parameter for formability as in the case of uniaxial tensile test. It is thus attempted in the present study to investigate the formability of TRIP steels in relation to the transformation behavior of RA during forming tests. Forming tests were performed using an Erichsen machine and forming limit diagrams were obtained under uniaxial and biaxial stress state. Phase fractions were evaluated on the sample surface and the results were then mapped as a function of stress states.

5:00 PM

Environment -Friendly Corrosion Inhibition of A20 Carbon Steel By 2-Mercaptobenzimidazole For Citric Acid Pickling: Yunyun Zhang¹; Daowu Yang¹; Zhuo Ren¹; Jin-hui Li¹; ¹Changsha University of Science and Technology

The corrosion inhibition effect of 2-mercaptobenzimidazole (2MBI) on the A20 carbon steel in citric acid has been investigated in relation to the concentration of the inhibitor by weight loss measurements, polarization curve methods and electrochemical impedance spectroscopy (EIS). Weight loss results obtained revealed that 2MBI is a good corrosion inhibitor whose efficiency can reach 98%. The addition of increasing concentrations of 2MBI moves the corrosion potential towards positive values and reduces the corrosion rate. Polarization curve results show that the corrosion inhibitor restrain the process of cathode and anode, belonging to anode controloriented and charge transfer-controlled. EIS results show that the changes in the impedance parameters (Rp and Cd) with concentrations of 2MBI is indicative of the adsorption of the molecules leading to the formation of a protective layer on A20 carbon steel surface. The adsorption of 2MBI is also found to obey Langmuir's adsorption isotherm in citric acid.

5:15 PM

Synthesis and Application of Imidazolinylquaternary-Ammonium-Salt Corrosion Inhibition for Hydrochloric Acid Pickling: Yunyun Zhang¹; Daowu Yang¹; Yi Liu¹; Yang Sun¹; ¹Changsha University of Science and Technology

To enhance the water solubility and inhibition efficiency of 2-phenylimidazoline, a type of imidazolinylquaternary-ammonium-salt was synthesized from 2 - phenyl-imidazoline and benzyl chloride. And then the compound pickling inhibitor was manufactured with imidazolinylquaternaryammonium-salt, potassium iodide, triethanolamine, polyoxyethylene nonylphenyl ether and peregal by weight loss through orthogonal experiment. The effect of the compound inhibitoron on corrosion of A20 carbon steel in hydrochloric acid have been investigated in relation to it's concentration by various corrosion monitoring techniques. It was found that the corrosion inhibition efficiency increased with the increase of compound inhibitor concentration by gravimetric measurements. Polarization studies showed depression of cathodic and anodic polarization curves in the presence of the compound inhibitor, indicating mixed type compound inhibition. EIS results show that the changes in the impedance parameters (Rp and Cd) with concentrations of the compound inhibitor are indicative of the adsorption of these molecules leading to the formation of a protective layer on carbon steel surface. The adsorption of the compound inhibitor is also found to obey Langmuir's adsorption isotherm in hydrochloric acid.

5:30 PM

Additive Manufacturing of Nickel-Base Superalloys: John Wooten¹; *Ulf Ackelid*²; Frank Medina³; Shane Collins⁴; Ryan Wicker³; Larry Murr³; ¹CalRAM; ²Arcam AB; ³University of Texas El Paso; ⁴Paramount Inc

Additive manufacturing is being developed to produce functional hardware without the use of tooling. Components can be built one layer at a time making the technology ideal for complex hardware where low volume or low-rate production is needed. For structural aerospace applications where low-rate production quantities are often the norm, nickel-base superalloys are used. If the combination of layer building and nickel-base superalloys for aerospace applications can be successfully developed, then additive manufacturing will replace traditional methods of building such hardware. However, the acceptance of additive manufacturing will require a reference body of material property data. A study was undertaken to compare and contrast candidate additive manufacturing technology capable of producing nickel-base superalloys. Specifically, alloy 625 was fabricated by electron beam melting manufacturing, and a microstructural analysis was performed and a limited amount of tensile data was developed. These results were compared to other techniques capable of producing alloy 625.

Hydrometallurgy Fundamentals and Applications: Session II

Sponsored by: The Minerals, Metals and Materials Society, TMS Extraction and Processing Division, TMS: Hydrometallurgy and Electrometallurgy Committee *Program Organizer:* Michael Free, University of Utah

Thursday PM	Room: 16A	

Thursday T W	
March 3, 2011	Location: San Diego Conv. Ctr

Session Chair: Michael Free, University of Utah

2:00 PM

Investigations on the Mechanism of Acid Leaching of Alkali-Activated Ilmenite Concentrate and Titanium-Rich Slag: *Qian Xu*¹; Yajun Fu¹; Jianfeng Jin¹; Jihong Du²; ¹Northeastern University; ²Northwest Institute for Non-ferrous Metal Research

Ilmenite is one of the primary sources of titanium dioxide, while titaniumrich slag generally is one product of ilmenite concentrate smelting reduction In the present investigation, ilmenite concentrate and titanium-rich slag are pretreated by an alkali activation, then leached by moderate acid solutions in order to decrease the environmental loads arising from the titanium dioxide production. The mechanism of the alkali activation process is studied by X-Ray diffraction and chemical composition analyses. The structure and composition of intermediates of the alkali activation obviously affect the acid leaching efficiency of titanium and iron, following the alkali activation. The effects of temperature, time, mixture composition, acid concentration and stirring intensity on titaniferous iron oxide dissolution are studied, as well as optimization of the leaching process.

2:25 PM

Kinetics Study of Alkaline Decomposition of Rubidium Jarosite in Ca(OH)2 Media: Eduardo Cerecedo¹; *Eleazar Salinas*¹; Luis Longoria²; Francisco Carrillo³; Juan Hernández¹; ¹Universidad Autónoma del Estado de Hidalgo; ²National Institute of Nuclear Researches; ³Universidad de Coahuila

Rubidium jarosite was synthesized, leading a single phase product, composed principally by particles of spherical morphology with sizes varying from 25 to 40 microns forming aggregates of rombohedral crystals strongly soldered in a compact texture. This compound has the following contents: 28.31% Fe, 35.30% SO4, 13.62% Rb, 5.57 ppm Ag and 22.74% (H3O + OH). Leading the approximated formula: [Rb0.2722 (H3O)0.1423 Ag0.000039] Fe3 (SO4)2 (OH)6. By the other hand, the nature of alkaline decomposition process of rubidium jarosite is characterized by an induction period followed by a progressive conversion period where sulphate and rubidium ions go to solution, leaving in residue the iron as amorphous hydroxide. Finally, the global process of alkaline decomposition of rubidium jarosite in Ca(OH)2 media, has an order of reaction with respect to Ca(OH)2 concentration of n=0.42, with an activation energy found of 99.10 kJ/mol, which can confirms that the process is controlled by chemical reaction.

2:50 PM

Leaching Behavior of Secondary Zinc Oxide Dusts in Ammonia Solutions: *Yang Yong Bin*¹; Wang Wen Juan¹; Jiang Tao¹; Qian Li¹; ¹Central South University

Leaching of secondary zinc oxide dusts is an important process in recovery of zinc from solid wastes to produce zinc based products. Ammonia leaching has been accepted as a more promising method for zinc leaching. The leaching behaviors of two secondary zinc oxide samples in ammonia leaching systems were investigated. The results indicated that, different samples had different leaching property. At the condition of L/S=5:1, [NH3] total:[CO32-]=4:1(mol/mol), the optimum leaching conditions are 20min, 400r/min; 30min, 500r/min and 60min for pure ZnO, sample A and sample B respectively. Under their respective optimum leaching conditions, [NH3] total:[Zn2+]total ratio in pregnant solutions were 8.06:1, 9.32:1, and 10.01:1 for pure ZnO, sample A and sample B respectively. The main cause for these differences in leaching behavior lies in the species and contents of impurities occurred in the samples, higher contents of Pb, Fe, Cd are responsible for lower zinc leaching ratio in sample B.

3:15 PM

Leaching of Gold in Acid Thiourea-Thiocyanate Solutions Using Ferric Sulfate as Oxidant: Xiyun Yang¹; Xichang Shi¹; Hui Xu¹; Michael S Moats¹; Jan D Miller¹; Xiang Xiao¹; Liwen Ma¹; ¹central south university

The leaching of gold in ferric-thiourea-thiocyanate solutions has been studied by the rotating-disk technique. The effects of initial concentrations of ferric, thiourea, thiocyanate, temperature and pH value on gold dissolution rate were studied. Determinations of apparent activation energy indicate that the process is controlled by a combination of chemical reaction and diffusion in the mixed lixiviant system. The gold dissolution rate in the mixed ligand solutions is higher than either lixiviant alone, even the sum of each individual lixiviant. In the presence of thiourea, thiocyanate shows considerable stability towards oxidation.

3:40 PM Break

3:55 PM

Studies on the Dissolution of Platinum Powder by Electro-Generated Chlorine in Hydrochloric Acid Solution: Min-Seuk Kim¹; *Jae-chun Lee*¹; Eun-Young Kim¹; Jinki Jeong¹; Banshi. D. Pandey²; ¹Korea Institute of Geoscience and Mineral Resources (KIGAM); ²National Metallurgical Laboratory, CSIR

The dissolution of platinum powder by electro-generated chlorine has been investigated in hydrochloric acid solutions. The electro-generated chlorine in 1.0 mol/L HCl solution was supplied into a leaching reactor containing platinum powder suspended in HCl solution. Platinum dissolution was observed to be dependent on the concentration of hydrochloric acid, the

reaction temperature, and dissolved aqueous chlorine species. The results show negligible amount of platinum solubilization when less than 4 mol/L HCl was used; only 1.85 wt.% dissolution occurred in 4 mol/L HCl solution at 343 K and 2 g/L pulp density in 220 min. However, the dissolution of platinum increased abruptly to 95 wt.% within 45 min by raising the acid concentration to 5 mol/L. Raising the temperature has significantly improved the platinum dissolution rate. An activation energy of 46 kJ/mol was acquired for platinum dissolution in 5 mol/L HCl with 15 mmol/L aqueous chlorine in the temperature range 323-343K.

4:20 PM

Modeling of Cobalt and Nickel Extraction by Solvent Extraction in Sulfate Media with D2EHPA in Isoparaffin (17/21): *Clenilson Sousa Junior*¹; Marisa Nascimento²; Ivan Masson²; Osvaldo Cunha³; ¹Federal Institute of Education, Science and Technology of Rio de Janeiro; ²Centre for Mineral Technology - CETEM; ³Federal University of Rio de Janeiro - UFRJ

The divalent metals (Co²⁺ and Ni²⁺) extraction, from the system MSO₄ - H₂SO₄ - H₂O - D2EHPA, in isoparaffin, was studied by a thermodynamic model based on balance equations of mass and charge. The activity coefficients of all solutes in the aqueous phase were calculated by modified Davies's equation. By applying this model, the concentrations of solutes in the equilibrium were calculated from the values of total concentration of cobalt and nickel in solution and pH. The metal extracted species was determined to be CoH_{0.25}A_{2.25} and NiH_{0.25}A_{2.25} (where HA is D2EHPA) and the equilibrium constant of the extraction was found to have a value, respectively, of 2,10x10⁻⁵ and 2,40x10⁻⁵, from the calculation of non-linear regression Quasi-Newton method realized with the experimental data. The values of distribution coefficients predicted by the model for Co(II) and Ni(II) extraction were a good agreement when compared with experimental results.

Magnesium Technology 2011: Advanced Materials and Processing

Sponsored by: The Minerals, Metals and Materials Society, TMS Light Metals Division, TMS: Magnesium Committee Program Organizers: Wim Sillekens, TNO Science and Industry; Sean Agnew, University of Virginia; Suveen Mathaudhu, US Army Research Laboratory; Neale Neelameggham, US Magnesium LLC

Thursday PM	Room: 6F
March 3, 2011	Location: San Diego Conv. Ctr

Session Chairs: Karl Kainer, Helmholtz-Zentrum Geesthacht; Venkata Anumalasetty, Carpenter Technology Corporation

2:00 PM

Characterization of Hot Extruded Mg/SiC Nanocomposites Fabricated by Casting: Sunya Nimityongskul¹; *Noé Alba-Baena*¹; Hongseok Choi¹; Milton Jones¹; Tom Wood²; Mahi Sahoo³; Roderic Lakes¹; Sindo Kou¹; Xiaochun Li¹; ¹University of Wisconsin-Madison; ²GS Engineering Inc; ³CANMET Materials Technology Laboratory

Mg-1%SiC nanocomposites were fabricated using an ultrasoniccavitation based casting method, resulting in the dispersion of the reinforcing SiC nanoparticles to form Mg-metal matrix nanocomposite (Mg-MMNC) billets. The MMNC billets were then processed using hot extrusion at 350°C. Micrographic observations illustrate a significant grain size reduction and the presence of micro-bands that align the SiC nanoparticles parallel to the direction of extrusionfor the Mg-MMNCs. Observations from the cross-section at 90° of the extrusion direction show uniform nanoparticles dispersion contrasting previous observations. Results from the extruded Mg-MMNCs tensile testing at different temperatures (25°C, 125°C and 177°C) reveal an increase of the yield strength, ultimate tensile strength, and ductility values as compared to the un-reinforced and extruded Mg-alloy; such increase was also observed from the microhardness testing results where an increase from 19 to 34% was measured.

2:20 PM

Effects of Silicon Carbide Nanoparticles on Mechanical Properties and Microstructure of As-Cast Mg-12wt.%Al-0.2wt.%Mn Nanocomposites: *Hongseok Choi*¹; Hiromi Konishi¹; Xiaochun Li¹; ¹University of Wisconsin-Madison

Microstructure and tensile properties of as-cast Mg-12Al-0.2Mn alloys with SiC nanoparticles were studied. SiC nanoparticles were dispersed into Mg-12Al-0.2Mn melts through an ultrasonic based nanoparticle-dispersion method. The content of SiC nanoparticles varied from 0 to 2 wt.%. The microstructural analysis with optical and scanning electron microscopy (SEM) showed that the massive brittle intermetallic phase (β -Mg₁₇Al₁₂) as well as α -Mg grain was significantly refined, resulting in the enhancement of both strengths and ductility of as-cast Mg-12Al-0.2Mn alloys. Transmission electron microscopy (TEM) showed that there were SiC nanoparticles in both α -Mg and β -Mg₁₇Al₁₂ phases of the Mg-12Al-0.2Mn nanocomposites. It was found that there was a partial reaction between Mg/Al and SiC nanoparticles, producing Mg₂Si intermetallic phases. X-ray diffraction (XRD) analysis confirmed also that the content of Mg₂Si phases increased with increasing SiC content, limiting further enhancement of ductility of Mg-12Al-0.2Mn-SiC nanocomposite.

2:40 PM

Thermally-Stabilized Nanocrystalline Mg-Alloys: *Suveen Mathaudhu*¹; Kristopher Darling¹; Laszlo Kecskes¹; ¹U.S. Army Research Laboratory

Advanced nanocrystalline alloys have shown remarkable property improvements, particularly, order-of-magnitude strength increases, when compared to their coarse-grained counterparts. However, a major obstruction to the widespread application of such materials is the degradation of properties via rapid grain growth at even ambient temperatures. Conventional methods for circumvention of this problem at low temperatures have largely steered toward kinetically pinning the boundaries with disperoids, or through misorientation of grain boundaries, yet even these methods have limited utility at elevated temperatures needed for routine sintering and forming operations. In this work, we will present a synergistic approach to the development of thermally stable nanostructured Mg-alloys which incorporates elements of predictive modeling of suitable alloy systems, fabrication of nanostructured alloy powders by high energy ball milling and consolidation of the powders at elevated temperatures to bulk ultrahigh strength alloys.

3:00 PM

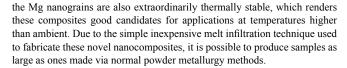
TiNi Reinforced Magnesium Composites by Powder Metallurgy: *Ziya Esen*¹; ¹Cankaya University

Rod shaped Mg-TiNi composite samples were manufactured by powder metallurgical route in which the samples were heated and deformed simultaneously using rotary hot swaging technique. Firstly, encapsulated argon filled copper tubes which contained compacts of pure magnesium and pre-alloyed TiNi alloy powder mixtures were deformed about 45% in two steps at 450°C. Pre/post annealing heat treatments were applied at 450°C for 20 mins between the stages of coaxial deformation to enhance the sintering degree and to homogenize the heavily deformed composite structures. Next, copper peeled and machined samples were compression tested under quasistatic conditions to investigate the mechanical properties, i.e. yield and peak strength, and ductility. Transmission and Scanning Electron Microscopy studies were carried out to examine the Mg-TiNi interface and fracture surfaces of the compression tested composites, respectively.

3:20 PM

Nanocrystalline Mg-Matrix Composites with Ultrahigh Damping Properties: *Babak Anasori*¹; Shahram Amini¹; Volker Presser¹; Michel Barsoum¹; ¹Drexel University

Recently, we reported on the processing of 50 vol.% Ti_2AlC - nanocrystalline magnesium, nc-Mg, matrix composites using a pressureless melt infiltration method. Herein we report on composites with up to 80 vol.% Mg. These composites are readily machinable, relatively stiff, strong and light, and exhibit ultrahigh damping. Increasing the nc-Mg volume fraction leads to lighter composites with higher damping characteristics at lower stresses (~30% of the mechanical energy is dissipated at 250 MPa). In some cases,



3:40 PM Break

4:00 PM

Effect of Fiber Reinforcement on Corrosion Resistance of Mg AM60 Alloy-based Composites in NaCl Solutions: *Qiang Zhang*¹; Henry Hu¹; ¹University of Windsor

There is great interest in developing low-cost, magnesium-based MMCs because of their high stiffness-to-weight ratio for aerospace and automotive applications. However, corrosion resistance of MMC is often a concern for components to be used in harsh environment. In this study, the corrosion behaviour of Al2O3 fibres reinforced magnesium AM60 composite, in aqueous solutions containing various concentrations of NaCl, was studied in comparison to that of matrix alloy by potentiodynamic polarization measurements. The microstructure of the composite and matrix alloy AM60 before and after corrosion testing was analyzed by optical microscopy, and scanning electron microscopy. The results show that the presence of Al2O3 fiber deteriorates the corrosion resistance of the matrix magnesium alloy AM60. The effect of Al2O3 fiber reinforcement and NaCl concentrations on the corrosion behavior of the composites are discussed. The corrosion mechanisms of the composite are proposed in light of metallographic observation on the formation of corrosion products.

4:20 PM

The Production of Powder Metallurgy Hot Extruded Mg-Al-Mn-Ca Alloy with High Strength and Limited Anisotropy: *Ayman Elsayed*'; Junko Umeda'; Katsuyoshi Kondoh'; 'Osaka University

Rapidly solidified Mg-Al-Mn-Ca alloy produced by Spinning Water Atomization Process (SWAP) was hot extruded into rectangular bars, from which tensile and compression samples have been cut at 0°, 45° and 90° from the extrusion direction to study their anisotropy. Electron Back Scattered Diffraction (EBSD) has been used to investigate the texture evolution during the hot extrusion process. Both the Schmid factor and the intensity of the basal plane in the pole figure have been evaluated and correlated to the mechanical properties. Results have shown that the extruded rods exhibit high strength and limited anisotropy compared to many previously reported values for magnesium alloys. The reasons for that limited anisotropy were both the fine grained microstructure of the extruded material and the transverse component of the texture evolution.

4:40 PM

Thermal Effects of Calcium and Yttrium Additions on the Sintering of Magnesium Powder: Paul Burke¹; Chloe Petit²; Sonia Yakoubi²; *Georges Kipouros*¹; ¹Dalhousie University; ²ICAM

Magnesium and its alloys are attractive materials for use in automotive and aerospace applications because of the low density and good mechanical properties. Powder metallurgy P/M can be used to alleviate the formability problem through near-net-shape processing, and also allows unique chemical compositions that can lead to new alloys with novel properties. However, the surface layer formed on the Mg powders during processing acts as a barrier to diffusion and sintering is problematic. The layer, characterized using focused ion beam milling and transmission electron microscopy, as well as x-ray photoelectron spectroscopy, contains oxides, hydroxides and carbonates of magnesium, formed by reactions with the atmosphere. To overcome this barrier, small additions were made of calcium and yttrium the oxides of which are thermodynamically more stable than magnesium oxide. The present work reports on the thermal effect of Ca and Y additions to magnesium powder during sintering, utilizing differential scanning calorimetry (DSC).

5:00 PM

Microstructure and Mechanical Properties of Solid State Recycled Mg Alloy Chips: *Kunio Matsuzaki*¹; Youich Murakoshi¹; Toru Shimizu¹; ¹National Institute of Advanced Industrial Science and Technology

Mg alloy chips generated in machining process such as turning and sawing are hard to recycle through melting process because the chips are very fine and easily burned during the heating. In this paper, several machined Mg alloy chips were solid state recycled into a bar using hot-pressing and hotextrusion, and mechanical properties of recycled chips were examined. The recycled AZ91 and AZX911 alloy show a fine microstructure with a grain size below 10 micrometers. The compressed yield stress at R.T. is 208MPa and 210 MPa for the AZ91 and AZX911, respectively, and higher than that of virgin samples. The backward extrusion test reveals that the recycled AZ91and AZX911 alloys have good formability at above 573K. Therefore, the solid state recycled Mg alloys have high strength with formability and would be expected as materials for forging.

5:20 PM Concluding Comments

Presentation of the Best Poster Award 2011 by Eric Nyberg

Magnesium Technology 2011: Corrosion and Coatings

Sponsored by: The Minerals, Metals and Materials Society, TMS Light Metals Division, TMS: Magnesium Committee Program Organizers: Wim Sillekens, TNO Science and Industry; Sean Agnew, University of Virginia; Suveen Mathaudhu, US Army Research Laboratory; Neale Neelameggham, US Magnesium LLC

Thursday PM	Room: 10
March 3, 2011	Location: San Diego Conv. Ctr

Session Chairs: Robert McCune, Robert C.McCune and Associates LLC; Neale Neelameggham, US Magnesium LLC

2:00 PM

Salt Spray Corrosion of Mechanical Junctions of Magnesium Castings: Sabrina Grassini¹; Paolo Matteis¹; Giorgio Scavino¹; Marco Rossetto¹; *Donato Firrao*¹; ¹Politecnico di Torino

The corrosion of cast, 3 mm thick, AE44 magnesium-alloy plates fastened to aluminum-alloy threaded counterparts, either constituting the screw or the nut, were tested in neutral salt spray for 48 hours, with or without interposed AA5051 spacers (washers). Steel nuts or screws were used, respectively, always insulating from corrosion the steel sides. Couplings between magnesium alloy plates and coated steel counterparts (screw heads) with interposed AA5051 washers were also tested, while insulating the nut side. Every 4 or 8 hours the test was halted and the samples were rinsed and photographed for manual image analysis. Then the plates were unmounted, slightly polished (highlighting the deep corrosion pits), and scanned for automatic image analysis. Different image analysis methods were compared. The least corrosion occurs, in couplings with aluminum alloy counterparts, when AA5051 washers are interposed; whereas the most effective coupling with steel counterparts is the one with nylon coated steel heads.

2:20 PM

Comparing the Corrosion Effects of Two Environments on As-Cast and Extruded Magnesium Alloys: *Holly Martin*¹; M. Horstemeyer¹; Paul Wang¹; ¹Center for Advanced Vehicular Systems, Mississippi State University

Magnesium is easily corroded in the presence of saltwater, limiting its use in the automotive industry. The magnesium microstructure greatly affects the corrosion rate, due to various additional elements. In the Center for Advanced Vehicular Systems at Mississippi State University, the effects of immersion and cyclical salt spray testing on various as-cast and extruded magnesium alloys is currently being examined. Previous work on an as-cast AE44 magnesium alloy has demonstrated that individual pit characteristics, such as pit depth, pit area, and pit volume, were deeper and larger following

exposure to the immersion environment. However, the data elucidating the corrosion effects on individual pit characteristics has only been seen on ascast magnesium containing rare earth elements, not on extruded magnesium alloys or zinc-containing magnesium alloys, both common magnesium forms. The research presented here will cover the effects of individual pit characteristics formed on various magnesium alloys due to the different environments.

2:40 PM

Influence of Lanthanum on the Corrosion Behaviour of Binary Mg-La Alloys: Daniel Hoeche¹; Rosario Silva Campos¹; Carsten Blawert¹; Karl Ulrich Kainer¹; ¹GKSS Research Centre

Different contents of Lanthanum have been added to Magnesium and have been investigated on their influence on the microstructure and the corrosion properties. The microstructure was studied by means of SEM and optical microscopy. Corrosion performance was evaluated using potentio-dynamic polarization measurements. Immersion tests were carried out using distilled water and 0.1% sodium chloride solution. The corrosion products were investigated by X-ray induced photoelectron spectroscopy (XPS), Auger electron spectroscopy (AES) and X-ray diffraction (XRD) which lead to detailed information on phase formation and mass transport. The oxide and hydroxide formation have been correlated to the chemical states and formed intermetallics, i.e by taking into account the XPS peak shift and peak splitting of the La-3d, O-1s and the Mg-2p state. Additionally, the results have been verified by means of AES on the Mg-KLL, O-KLL and La-MNN excitation and by XRD. Latter suggests the supplemental formation of a nanocrystalline phase.

3:00 PM

Cryogenic Burnishing of AZ31B Mg Alloy for Enhanced Corrosion Resistance: *Z. Pu*¹; Guang-Ling Song²; S. Yang¹; O. Dillon, Jr.¹; D. Puleo¹; I. Jawahir¹; ¹University of Kentucky; ²GM Global Research &Development

Poor corrosion resistance is limiting applications of Mg alloys. However, the corrosion performance of a Mg alloy can be enhanced through modification of its microstructure. It has been reported in the literature that the microstructure, especially grain size of AZ31 Mg alloy, has a significant influence on its corrosion resistance. In this study, AZ31B discs were subjected to a novel mechanical processing method– cryogenic burnishing; the surface of AZ31B workpiece was burnished with a custom tool under a liquid nitrogen spraying condition. The processing led to a more than 2 mm thick surface layer with remarkably changed microstructures formed on the disc surface. Significant grain refinement occurred within this surface layer due to dynamic recrystallization induced by severe plastic deformation and effective cooling by liquid nitrogen. Electrochemical measurements indicate that the corrosion resistance of the burnished surface was significantly improved.

3:20 PM

Advanced Conversion Coatings for Magnesium Alloys: Syam Nibhanupudi¹; Alp Manavbasi¹; ¹Metalast International

Magnesium and its alloys have excellent physical and mechanical properties due to their high strength-to-weight ratio and are ideal for various applications in automotive, aerospace and defense sectors. However, Mg alloys are also highly susceptible to corrosion under harsh environments. Owing to the carcinogenicity as well as environmental impact of hexavalent chromium fueled by stringent environmental regulations, an environmentally green alternative to the carcinogenic hexavalent chromium based conversion coating has been developed to improve the corrosion resistance and paint adhesion properties of Mg alloys. Surface characterizations were conducted using SEM/EDX and anti corrosive properties have been investigated via hydrogen evolution and electrochemical corrosion analysis techniques. Results have shown that the novel environmentally green trivalent chromium based coating on magnesium has indeed performed comparable to hexavalent chromium and thus establishing a viable alternative.

3:40 PM Break

4:00 PM

Development of Zirconium-Based Conversion Coatings for the Pretreatment of AZ91D Magnesium Alloy Prior to Electrocoating: James Reck¹; Yar-Ming Wang¹; Hong-Hsiang Kuo¹; ¹General Motors

This work examines the use of hexafluorozirconic acid based solutions at concentrations from 0.025 M to 0.100 M and pH values of 2.0 to 4.0 for the creation of a zirconia-based conversion coating less than 1 micron thick to protect magnesium alloy AZ91D. Similar coatings have been found to give excellent protection for steel and aluminum alloys, but little research has been conducted on its application to magnesium. Work was performed to gain an understanding of the film formation mechanisms and related kinetics using x-ray photo-electron spectroscopy, scanning electron microscopy, and open circuit potential monitoring techniques. A design of experiments approach was taken to determine the effects of acid concentration, pH, and soak time on the corrosion properties both as-deposited and with an application of electrocoat. It was found that the application of the zirconia-based coating significantly increased corrosion resistance, and allowed for an acceptable e-coat application with excellent adherence.

4:20 PM

Use of an AC/DC/AC Electrochemical Technique to Assess the Durability of Protection Systems for Magnesium Alloys: Sen Song¹; *Robert C. McCune*²; Weidian Shen¹; Yar-Ming Wang³; ¹Eastern Michigan University; ²Robert C McCune & Associates LLC; ³General Motors Company

One task under the U.S. Automotive Materials Partnership (USAMP) "Magnesium Front End Research and Development" (MFERD) Project has been the evaluation of methodologies for the assessment of protective capability for a variety of proposed protection schemes for this hypothesized multi-material, articulated structure. Techniques which consider the entire protection system, including both pretreatments and topcoats are of interest. In recent years, an adaptation of the classical electrochemical impedance spectroscopy (EIS) approach using an intermediate cathodic DC polarization step (viz. AC/DC/AC) has been employed to accelerate breakdown of coating protection, specifically at the polymer-pretreatment interface. This work reports outcomes of studies to employ the AC/DC/AC approach for comparison of protective coatings to various magnesium alloys considered for front end structures. In at least one instance, the protective coating system breakdown could be attributed to the poorer intrinsic corrosion resistance of the sheet material (AZ31) relative to die-cast AM60B.

4:40 PM

Effects of Oxidation Time on Micro-Aarc Oxidized Coatings of Magnesium Alloy AZ91D in Aluminate Solution: *Weiyi Mu*¹; Zhengxian Li¹; Jihong Du¹; Ruixue Luo¹; Zhengping Xi¹; ¹Northwest Institute for Nonferrous Metal Research

Micro-arc oxidation coatings were prepared on magnesium alloy AZ91D at different oxidation times in aluminate solution. The effects of the oxidation time on the microstructure, growth rate and corrosion resistance of the coatings were investigated. The results indicate that the coatings are uniform in thickness and mainly composed of MgAl2O4 and MgO. There were many residual discharging channels on the coatings surface. The coatings improved the corrosion resistance of magnesium alloy AZ91D considerably. With increased oxidation time, the crystalline substances content and thickness of the coatings increased, while the growth rate of the coatings decreased, and the resulting coatings surface had lower porosity and larger pore sizes. In addition, the corrosion resistance of the coatings on magnesium alloy AZ91D substrate in the NaCl solution, and the effect is more remarkable with longer oxidation times.

5:00 PM

Composite Coatings Combining PEO Layer and EPD Layer on Magnesium Alloy: *Yongfeng Jiang*¹; Huashan Yang¹; Yefeng Bao¹; ¹Hohai University

Protective composite coatings were prepared by conbining plasma electrolytic oxidation (PEO) treatment and cathodic electrophoretic deposition (E-coat)on magnesium alloy AZ91D. The corrosion protecion of composite coatings were evaluated by using potentiodynamic polarization measurements in 3.5% NaCl solution, copper accelerated acetate salt spray(CASS) test and immersion test in acid solution. The adhesion of composite coatings was evaluated by means of cross-cut test and pull-off test. It is indicated that the corrosion resistance of magnesium alloy AZ91D with the composite coatings is improved obviously compared to it merely with PEO coating, and it is also shown pitting corrosion PEO coating on magnesium alloy is decreased by EPD posttreament. The adhesion of composite coatings can attain 11.3 N/mm2 in quantitative method due to the interlocking effect of organic layer in pores of PEO layer.

5:20 PM Concluding Comments

Presentation of the Best Poster Award 2011 (in Room 6F)

Magnetic Materials for Energy Applications: Experimental and Modelling Techniques for the Magnetocaloric Effect

Sponsored by: TMS Electronic, Magnetic, and Photonic Materials Division, TMS: Energy Conversion and Storage Committee, TMS: Magnetic Materials Committee; JSPS 147th Committee on Amorphous and Nanocrystalline Materials; Lake Shore Cyrotronics, Inc.; AMT&C

Program Organizers: Victorino Franco, Sevilla University; Oliver Gutfleisch, IFW Dresden; Kazuhiro Hono, National Institute for Materials Science; Paul Ohodnicki, National Energy Technology Laboratory

Thursday PM	Room: 11A
March 3, 2011	Location: San Diego Conv. Ctr

Session Chair: Francis Johnson, GE Global Research

2:00 PM Invited

First to Second Order Magnetocaloric Transition: on Correct Analysis of Experimental Data: Daniel Fruchart¹; Mohamed BALLI¹; ¹CNRS -Institut Néel

In the vicinity of magnetic transition a magnetocaloric (MC) material behaves under external field sollicitations in metastable conditions. This means that the used magnetisation cycle applied versus time, temperature, field...has a dramatic impact on the received experimental data. Moreover, recent papers display variations of magnetic entropy measured on first order type materials exceeding by very far what was measured elsewhere and reported accordingly. This proves that a carefull use of the most appropriated phenomenological model must be applied. Based on several experimental data sets recorded on different type materials exhibiting a first order MC transition, our report aims demonstrate correctness application of the models.

2:25 PM Invited

Magnetocaloric Parameters from Measurements of Heat and Temperature: *Ramón Burriel*¹; Elías Palacios¹; ¹CSIC - Universidad de Zaragoza

A correct determination of the magnetocaloric parameters is of crucial importance for the evaluation of efficient cooling materials. Most of the interesting compounds present first-order transitions that give frequent problems in the estimation of the isothermal entropy change, ΔS_{T} , through magnetic determinations of M(T,H). Adiabatic calorimetry and modifications of this technique provide valuable determinations of ΔS_{T} and also of the adiabatic entropy change, ΔT_{s} , through entropy calculations from field dependent heat capacity $C_p(T,H)$, or with direct measurements of ΔS_T and ΔT_{s} . The determination of the cooling efficiency in hysteretic compounds requires control of the thermal and field history, considering the Field-Temperature phase diagram. The possible coexistence of different phases in the hysteretic region can give erroneous results from the magnetic measurements and from direct determinations. Also the direction when crossing the transition line has

to be considered, and the irreversible entropy creation at the transition when estimating the heat exchanges.

2:50 PM Invited

Experimental Methods of the Magnetocaloric Effect Studies: *Youri Spichkin*¹; ¹AMTC

The methods of experimental investigations of the magnetocaloric parameters (adiabatic temperature change and isothermal magnetic entropy change caused by external magnetic field) are reviewed and discussed. The direct and indirect methods are compared and their advantages and disadvantages are considered. Possible influence of the used methods on the obtained results is regarded. The main attention is paid to the direct methods of measurements. The realization of the dynamic mode of the direct adiabatic temperature change measurement is considered. Importance of the magnetocaloric measurements in dynamic mode for characterization of the magnetocaloric materials suitable for using as working bodies in magnetic heat machines is shown. The methods of the experimental data processing are discussed. Recent experimental results of the magnetocaloric parameters on some materials are presented.

3:15 PM Invited

First Principles Modeling of Magnetocaloric Gd5Ge4 Based Materials: *Durga Paudyal*¹; Y. Mudryk¹; V. K. Pecharsky¹; K. A. Gschneidner, Jr.¹; ¹The Ames Laboratory, U. S. Department of Energy

We present the first principles modeling of structural and magnetic properties of Gd5Ge4 based magnetocaloric materials. The total energy as a function of the shear displacement of slabs confirms stability of experimentally observed crystal and magnetic structures. Small substitutions of the Gd by Y and Lu lead to a catastrophic loss of ferromagnetism, but the substitutions by La have no effect on the magnetism. Furthermore, substitutions of the Ge by Si exert chemical pressure and transform the antiferromagnetic O(II) to the ferromagnetic O(I) ground state. In addition, we present a pathway for estimating the magnetic entropy change in the room temperature giant magnetocaloric compounds, i.e. Gd5Si2Ge2, by coupling first principles outputs with the established magnetothermodynamic models. The theoretical values of the magnetic entropy change compare well with experimental results. This work was supported by the Office of Basic Energy Sciences, Materials Sciences Division of the Office of Science.

3:40 PM

Monte Carlo Simulations of the Magnetocaloric Effect and Exchange Bias Effect in Heusler Ni-Mn-Sb Alloys: *Vladimir Sokolovskiy*¹; Vasiliy Buchelnikov¹; Ivan Taranenko¹; Sergey Taskaev¹; Peter Entel²; ¹Chelyabinsk State University; ²University of Duisburg-Essen

Heusler Ni-Mn-Sb alloys have unique properties such as the shape memory effect, magnetocaloric effect (MCE), and exchange bias effect (EB). The reason of these properties is a magnetostructural phase transition. In this work, we present a theoretical model for investigation of the EB and MCE in Ni₅₀Mn_{25+x}Sb_{25-x} alloys by Monte Carlo method. In the model, we use a cubic lattice with real unit cell. In the case of the MCE modeling, we choose the 3-5 state Potts model for magnetic transitions and Blume-Emery-Griffiths model allowing to describe a structural transformation. For the EB modeling, the model Hamiltonian includes Heisenberg's spin interactions with an anisotropy term. The temperature dependences of positive and negative MCE for Ni₅₀Mn_{25+x}Sb_{25-x} alloys are obtained. Our simulations have shown that EB field depends on a concentration of excess Mn atoms. We have found a blocking temperature of EB for Ni₅₀Mn_{37,5}Sb_{12,5} which is closer to experimental value.

3:55 PM

Structural Entropy Contributions to the Total Magnetocaloric Effect in Materials Which Exhibit a First Order Transition: Karl Gschneidner¹; Yaroslav Mudryk¹; Vitalij Pecharsky¹; ¹Iowa State University

A few magnetic materials have been observed to exhibit a first order magnetic transition which is coupled with a crystal structure change, or with a large volume change. The entropy associated with the structural transformation or volume change is comparable to the entropy associated

with the purely magnetic transition for 50 kOe field changes. Since the magnetic and structural changes are coupled, it is difficult to directly measure the two contributions to the total entropy change independently, since normal measurements of the magnetocaloric effect yield only the total entropy change. However, by doping it is possible to destroy the structural transition and thus measure the purely magnetic entropy. Using this information one can determine the structural entropy associated with the first order transition. By heat treating or by high pressure measurements it is also possible to determine the structural entropy. The structural entropy changes for various materials will be compared.

4:10 PM

Environmentally Friendly New Air-Conditioning Magnetocaloric System: Christian Muller¹; Carmen Vasile²; ¹Cooltech Applications; ²INSA

The concept, the design and the manufacture of a new magnetocaloric air-conditioning system is based on the intimate knowledge of the active magneto-thermodynamic materials proprieties. The needed characteristics of the magneto-caloric materials are adiabatic temperature change, heat capacity and magnetisation. It is also of great interest the understanding of the behaviour of these active elements submitted to the permanent magnet alternative magnetising field and demagnetising field. This paper presents a new system environmentally friendly and energy efficient, based on a recent technological breakthrough: "magnetocaloric cooling around room temperature". The expected benefits are: increased energy efficiency, reduced consumption of energy, reduction of corresponding pollutant emissions and of any direct emission of pollutants. A magnetocaloric demonstrator will be presented and its performance described. The energy performance, the range of ambient temperatures and the temperature span, as well as the useful power will also be presented and explained.

Microstructural Processes in Irradiated Materials: Non-Metals

Sponsored by: The Minerals, Metals and Materials Society, TMS Structural Materials Division, TMS/ASM: Nuclear Materials Committee

Program Organizers: Gary Was, University of Michigan; Thak Sang Byun, Oak Ridge National Laboratory; Shenyang Hu, Pacific Northwest National Laboratory; Dane Morgan, UW Madison; Yasuyoshi Nagai, Tohoku University

Thursday PM	Room: 3
March 3, 2011	Location: San Diego Conv. Ctr

Session Chairs: Ming Tang, Los Alamos National Laboratory; Yong Yang, University of Wisconsin-Madison

2:00 PM Invited

Radiation Stability of GFR Candidate Ceramics: *Yong Yang*¹; Clayton Dickerson¹; Jian Gan²; Todd Allen¹; ¹University of Wisconsin-Madison; ²Idaho National Laboratory

Determining and predicting the stability in response to radiation is a key part in developing a practical ceramics-based fuel for a gas cooled fast reactor (GFR). The hot pressed ceramics including ZrC, ZrN, TiC and TiN were irradiated in Cd shrouded capsule in the Advanced Test Reactor (ATR) to a dose of 1 dpa at 800 °C, and the materials were procured from the ATR irradiated sample library. The radiation stability of these ceramics were examined using transmission electron microscopy (TEM) to understand the effect of radiation on lattice stability, phase change, void growth, and other microstructural features such as dislocation loops and Stacking Fault Tetrahedra (SFTs). The irradiation response of neutron irradiated ceramics is further compared with that from proton irradiation at a comparable condition.

2:40 PM

Microstructure and Radiation Damage Tolerance of TiO2 Thin Films: *Mujin Zhuo*¹; Engang Fu¹; Wang Yongqiang¹; Yingying Zhang¹; Blas Uberuaga¹; Amit Misra¹; Michael Nastasi¹; Quanxi Jia¹; ¹Los Alamos national Lab

Ion irradiation damage effects in TiO2 thin films with different polymorphs were investigated using X-ray diffraction (XRD) and TEM. The TiO2 film grown on LaAIO3 (001) has anatase structure with [004] orientation while that on Al2O3 (102) substrate is rutile with {101} parallel to the substrate surface. The films were irradiated at room temperature with 600 keV Kr2+ ions to a fluence of 1.5 1015 Kr/cm2. Extensive XRD and TEM analyses reveal that no amorphization transformation occurs under such irradiation. Coupled with Rutherford Backscattering Spectroscopy in channeling geometry, it is observed that the damage accumulation within TiO2 films is very low despite that the substrates are heavily damaged. Moreover, no significant denuded area was found in either irradiated anatase or rutile TiO2 films. This study reveals that grain boundary plays a critical role in the irradiation tolerance of TiO2.

3:00 PM

Computational Studies of Radiation Damage near Grain Boundaries in TiO2: Xian-Ming Bai¹; Blas Uberuaga¹; ¹Los Alamos National Laboratory

Grain boundaries (GBs) can serve as sinks for absorbing radiation-induced defects. However, the role of GBs in promoting radiation tolerance in ceramics not well understood, and is complicated by the facts that the defects in ceramics are charged. Here, we use three atomistic modeling methods to examine the role of GBs in a model system, TiO2, in modifying defect thermodynamics and defect production. TiO2 has multiple polymorphs, including rutile and anatase, which have different radiation tolerances. We use molecular statics and temperature accelerated dynamics to investigate the defect thermodynamics and kinetics in these two polymorphs and predict their long-time damage annealing behaviors. We use molecular dynamics to investigate defect production near GBs and find that the damage production is sensitive to the knock-on atom position. GBs also can induce more residual damage than if the boundary was not present. The properties of defect clusters of various forms are also investigated.

3:20 PM

Interstitial Loading Effects during Irradiation in MgO: *Blas Uberuaga*¹; Xian-Ming Bai¹; ¹Los Alamos National Laboratory

It is well established that boundaries in materials can promote radiation tolerance. However, the atomic-scale mechanisms responsible for this improved tolerance are still not clear. This is especially true for oxide ceramics. Even at low temperatures where vacancy are immobile, nanocrystalline oxides have been observed to have significantly more radiation tolerance than larger grained materials [1]. The recently-discovered interstitial emission mechanism, observed in Cu [2], may provide insight into the enhanced tolerance in oxides. Using atomistic simulation methods, we explore the interaction between grain boundaries and irradiation-induced defects in MgO, a model ceramic. We focus on the interstitial emission mechanism and the role it plays in enhancing the radiation tolerance of oxides. We find that there is a significant propensity for low-barrier interstitial mechanisms to occur in MgO, possibly explaining the experimental observations. [1] Shen et al. APL 90, 263115 (2007). [2] Bai et al. Science 327, 1631 (2010).

3:40 PM Break

4:00 PM

Structure and Mechanical Properties of Swift Heavy Ion Irradiated Tungsten-bearing Delta-phase Oxides Y6W1O12 and Yb6W1O12: *Ming Tang*¹; Thomas Wynn¹; Maulik Patel¹; Nathan Mara¹; Kurt Sickafus¹; ¹Los Alamos National Laboratory

We report on the relationship between structure and mechanical properties of complex oxides whose structures are derivatives of fluorite, following irradiation with swift heavy ion (92 MeV Xe) which approximately simulates fission product irradiation. The two compounds of interest in this presentation are the compounds, Y6W1O12 and Yb6W1O12. These compounds possess an ordered, fluorite derivative crystal structure known as the delta phase, a rhombohedral structure belonging to space group R-3 .Structural changes induced by irradiation were examined using X-ray diffraction (XRD) and transmission electron microscopy (TEM). Post-irradiation characterization experiments revealed irradiation induced amorphization in these compounds. The mechanical properties of both irradiated samples, determined by crosssectional nano-indentation measurements as a function of ion penetration depth, can be related to their microstructures. Post-irradiation annealing experimental results on the structure and mechanical properties of these compounds will also be discussed.

4:20 PM

Atomistic and Rate Theory Modeling of Radiation Damage and Amorphization of Nanocrystalline Silicon Carbide: Narasimhan Swaminathan¹; Dane Morgan¹; *Izabela Szlufarska*¹; ¹University of Wisconsin-Madison

Cubic silicon carbide (3C-SiC) is being considered as a structural material for nuclear fission and fusion reactors. Polycrystalline SiC is already known for its excellent mechanical properties and low neutron cross section, and improvements in mechanical and radiation resistance properties may be possible through use of nanocrystalline (nc) SiC. This work uses modeling techniques from multiple length scales to understand the effects of radiation on SiC as a function of grain size. Molecular dynamics cascade simulations, ab initio formation and migration energies, and rate theory modeling have been combined to study defect production rates and amorphization trends with grain size, radiation dose, and temperature. Initial results suggest little impact on in-grain defect production rates from using nc-SiC but a complex coupling between grain size and temperature is seen for the dose to amorphization.

4:40 PM

Microstructure and Mechanical Property Characterization of Self-Ion Irradiated 3C-SiC with Novel Micromachined Samples: *Chansun Shin*¹; Hyung-ha Jin¹; Suk Hoon Kang¹; Junhyun Kwon¹; Ji Yeon Park¹; ¹KAERI

This work investigated the microstructural and mechanical response of chemically vapor-deposited 3C-SiC irradiated with self-ion. SiC samples were irradiated up to ~20 dpa at temperatures up to ~400 degrees Celsius. Multiple-step irradiations were performed with different self-ion energies to obtain a roughly rectangular damage profile. Electron backscatter diffraction measurement showed that grains are columnar along the growth direction and {111} fibre textures. The irradiated 3C-SiC samples were examined by transmission electron microscopy for the specimens prepared by focused ion beam milling. The microstructure consists of black dots. The mechanical response of the irradiated 3C-SiC samples were characterized by means of both nano-indentation technique and micro-compression tests on micromachined SiC pillars. SiC micropillars were fabricated by using liftoff process and inductively coupled plasma-reactive ion etching technique. Irradiation effects and size effects in the fracture strength of micro-pillars were investigated, and will be discussed in relation with the observed microstructures.

5:00 PM

TEM Observation of Crack Tip in Heavily Neutron Irradiated Ceramics: *Masashi Watanabe*¹; Tatsuo SHIKAMA¹; Yoshiaki TACHI²; ¹Tohoku University; ²Japan Atomic Energy Agency

Inert matrix fuels (IMFs) are an attractive component of advanced nuclear fuel cycles, as they provide of burning plutonium and transmuting the minor actinides. Candidate materials of inert matrix are mainly magnesia (MgO), zirconia (ZrO2), and spinel (MgAl2O4). For better performance of the IMFs in the fast reactor, fracture behavior of neutron irradiated inert matrix, including change of mechanical properties such as fracture toughness, need to be investigated in relation with irradiation induced microstructural changes. In the present study, we focused on the relation between crack propagation and irradiated induced defects. Cracks were introduced by Vickers indentations on heavily neutron irradiated at 710 °C to 5.5×1026n/m2

and at 680 °C to 3.9×1025 m/m² in the experimental fast reactor of JOYO in JAEA. Microstructure beneath and near the crack tip were examined by the transmission electron microscopy.

5:20 PM

Proton Irradiation-Induced Creep Effects in Pyrolytic Carbon and Graphite: Anne Campbell¹; Gary Was¹; ¹University of Michigan

The creep behavior of pyrolytic carbon and graphite under high temperature neutron irradiation is critical to predicting the integrity of both fuel and structural components of the Very High Temperature Reactor. Proton irradiation-induced creep experiments were performed on graphite samples at 900°C at applied tensile stresses of 6MPa and 20.7MPa, and doses of 0.35 dpa and 0.23 dpa respectively. Preliminary results show a linear dependence of creep rate on both applied stress and dose rate. The primary creep behavior of graphite and pyrolytic carbon will be presented in the context of irradiation induced microstructural changes, including the effect of unrestrained proton irradiation and the effect of proton irradiation-induced creep on the sample density, Young's modulus, and anisotropy.

5:40 PM

Structural Modifications and Mechanical Degradation of Ion Irradiated Glassy Polymer Carbon: *Malek Abunaemeh*¹; mohameh Seif¹; abdalla Elsamadicy²; Claudiu Muntele¹; young yang³; Daryush ILA¹; ¹Alabama A&M University; ²University of Alabama in Huntsville; ³University of Wisconsin

The TRISO fuel that is planned to be used in the GenerationIV nuclear reactor consists of a fuel kernel of UOx coated in several layers of materials with different functions. We are looking at the ion irradiation induced structural modifications of the glassy polymeric carbon (GPC) microstructure and their effect on the mechanical and physical properties. GPC is considered as a potential replacement for the pyrolytic carbon coatings, with a function of diffusion barrier for the fission products. We irradiated GPC samples with 1 MeV protons, 5 MeV Ag and Au ions. We chose protons to simulate the effects of neutrons. During the nuclear fission of 235U, the fission fragment mass distribution has two maxima around 98 and 137 that would best fit Rb and Cs However, both ions are hard to produce from our SNICS source therefore we chose Ag (107 amu) and Au (197 amu) as best replacements.

Phase Stability, Phase Transformations, and Reactive Phase Formation in Electronic Materials X: Electrode, Ceramic, Optical, Spintronic, and Coating Materials

Sponsored by: The Minerals, Metals and Materials Society, TMS Electronic, Magnetic, and Photonic Materials Division, TMS: Alloy Phases Committee

Program Organizers: Chih-Ming Chen, National Chung Hsing University; Hans Flandorfer, University of Vienna; Sinn-Wen Chen, National Tsing Hua University; Jae-ho Lee, Hongik University; Yee-Wen Yen, National Taiwan Univ of Science & Tech; Clemens Schmetterer, TU Bergakademie Freiberg; Ikuo Ohnuma, Tohoku University; Chao-Hong Wang, National Chung Cheng University

Thursday PM	Room: 7A
March 3, 2011	Location: San Diego Conv. Ctr

Session Chairs: Clemens Schmetterer, TU Bergakademie Freiberg; Wojciech Gierlotka, YuanZe University

2:00 PM Invited

Electroless Nickel Plating on Carbon Fibers for Ultra Porous Nickel Electrode: So-Young Chun¹; So-Youn Park¹; *Jae-Ho Lee*¹; ¹Hongik University

Electroless nickel plating on carbon fibers was investigated. The carbon fibers were selected as the substrate since it has high surface area. Acidic and alkaline bath were used for the electroless nickel plating. Sonosmashing method was applied to dissemble carbon fibers. The effects of pH and 140th Annual Meeting & Exhibition

temperature on the electroless nickel were investigated. Inhibitor was added to achieve the uniform nickel coating on the surface. Wettability of the substrate was improved by surface treatment prior to the activation process. Highly porous nickel electrode was fabricated after pressing electroless nickel coated carbon fibers.

2:25 PM Invited

Phase Stabilities and Equilibria in the Lithium–Manganese–Oxygen System: *Damian Cupid*¹; Toni Lehmann¹; Olta Cakaj²; Hans Seifert¹; ¹Freiberg University of Mining and Technology; ²University of Tirana

Several phases in the lithium–manganese–oxygen system such as $LiMn_2O_4$, Li_2MnO_3 , and $LiMnO_2$ are promising for the development of cathode materials for rechargeable lithium ion batteries due to their low costs, environmental friendliness, and safety. Consequently, phase diagrams in this system are critical for optimizing processing conditions to be able to produce cathode materials with improved electrochemical performance properties. The type two phase diagram where one axis is a thermodynamic potential function such as temperature, partial pressure, or chemical potential and the second is the ratio of extensive variables is suitable for representing phase stabilities and phase equilibria in such a system. To investigate such diagrams for the lithium–manganese–oxygen system, several samples were prepared and equilibriated at various temperatures and oxygen partial pressures to examine the phase stability ranges of the phases produced. Additionally, thermogravimetric analysis was performed to investigate observed decomposition reactions.

2:50 PM

Crystallization Kinetics of SiO2-Bi2O3 Glass-Ceramics: *Guo Hongwei*¹; ¹Shaanxi University of Science and Technology

The SiO2-Bi2O3 glasses were prepared by melt-quench technique. The non-isothermal crystallization kinetics and the phase transition kinetics of the BS glasses were analyzed by the Kissinger equation and the equation of Augis-Bennett with the applying of differential scanning calorimetric X-ray diffraction and scanning electron microscopy. The experimental results showed that the three main crystal phases of Bi12SiO20, Bi2SiO5 and Bi4Si3O12 were generated sequentially in the heat treatment process, as crystallization exothermic peak can be seen from the DSC curves. The corresponding activation energies are Ep1=150.6kJ/mol, Ep2=474.9kJ/mol, Ep3=340.3kJ/mol; the average crystallization indexes are p1 = 2.5, p2 = 2.1, p3 = 2.2. The crystal phases were generated by volume nucleation, and grew in the one-dimensional pattern. The activation energy of phase transition of BS glasses is calculated by Kissinger equation. And the meta-stable phase of Bi2SiO5 is easy to be transited into the stable phase of Bi4Si3O12.

3:05 PM

Phase-Transformation Induced Changes in the Optical and Electrical Properties of W0.95Ti0.05O3 Films: *Narasimha Kalidindi*¹; C. Ramana¹; ¹University of Texas El Paso

Tungsten oxide (WO3) is an intensively studied optical material; the ability to exhibit variable optical and electrical properties under ion-insertion, radiation-irradiation, and gas-phase interaction makes WO3 interesting for application in electrochromic displays, smart windows, temperature control of space vehicles, and sensors. The present work was performed on the microstructure, optical and electrical conductivity evaluation of the W0.95Ti0.05O3 films made by radio-frequency magnetron sputtering. The effect of temperature and Ti was significant on the microstructure. The Tiincorporation affects the crystallization of WO3 and induces the changes in optical and electrical properties. An amorphous-to-crystalline transition occurs in W0.95Ti0.05O3 at 300°C, where the films crystallize in monoclinic phase. At =300°C, monoclinic-to-tetragonal phase transformation is induced in W0.95Ti0.05O3 films. The corresponding changes in the electronic properties are significant; band gap decreases from 2.92 to 2.00 eV while electrical conductivity increases from 0.63 to 7.4 Ω -m. The results will be presented and discussed.

3:20 PM Break

3:40 PM

Transparent Conductive Properties of Manganese Zinc Oxide Film Deposited by Chemical Bath Deposition: *Jau-Shiung Fang*¹; W. Luo¹; C. Hsu¹; J. Yang¹; T. Tsai¹; ¹National Formosa University

Manganese-doped Zinc Oxide thin film was prepared using Chemical Bath Deposition (CBD), and the effect of manganese-doped content on the structural change, electrical resistivity, optical transmission and magnetic property were studied using x-ray diffraction, electron probe x-ray microanalyzer, Hall measurement system, field emission scanning electron microscope, ultraviolet-visible-near infrared spectrophotometer and vibrating sample magnetometer. The manganese-doped amount in the film affects the properties critically, and the 7.1 at.% Mn-doped film has resistivity of 4.29×10^{-1} Ocm, transmittance of 74.7% in the visible range and bandgap of 3.17 eV when the film was annealed at 600°C in Ar+H₂. The magnetic properties of the film can be enhanced by annealing so that the film has a saturation magnetization of 20.6 emu/c.c. and coercivity of 54.9 Oe. Because of its electrical, optical and magnetic properties, the film is promising to be used in spintronic devices.

3:55 PM

Electroplating of Nano Silica Dispersed Permalloy Composite Coating: Myung-Won Jung¹; Jong-Hun Kim¹; Heung-Yeol Lee²; Tai-Hong Yim²; Jae-Ho Lee¹; ¹Hongik University; ²Korea Institute of Industrial Technology

Nickel alloys have been extensively used in packaging and electronic industries and then electro and electroless nickel plating have been investigated by many researchers. Nickel alloy, especially Ni-Fe alloy, was used as shadow mask for its low coefficient of thermal expansion. Even Ni-Fe alloy has high yield stress and hardness, its values are reduced after heat treatment. Silica was uniform sized spherical nano material. Silica dispersed permalloy composite coating was fabricated with electroplating method. Surface modified silica was suspended in the Ni-Fe electrolytes and then silica and Ni-Fe alloy was codeposited. The optimum condition for the silica suspension was investigated. The electrical and mechanical properties of composite coating were also investigated. The surface of composite coating was analyzed by AES and EDS.

4:10 PM

Optical Properties of the Al2O3-NiP Spectrally Selective Composite Coatings Preparated by Electroless Composite Coating: *Ting Kan Tsai*¹; Chiao Yin Hsu¹; Shun Jen Hsueh¹; Jiing Herng Lee¹; Jau Shiung Fang¹; ¹National Formosa University

Al2O3-NiP spectrally selective composite coatings were deposited on Al substrates to form Al2O3-NiP/Al solar absorbers by electroless composite coating. This work aims at studying effects of the Al2O3 particle size, the Al2O3 content, the thickness of Al2O3-NiP composite coating and the anti-reflection(AR)layer on the optical properties of Al2O3-NiP composite coatings. The optical properties including absorptance(asol)and thermal emittance(etherm)were measured in the wavelength interval of 0.3-2.5 and 2.5-20 µm by using the UV/VIS/NIR and FIIR spectrophotometers equipped with integral spheres, respectively. The Al2O3-NiP composite coatings containing 70 nm Al2O3 have better optical properties than that containing 300 nm Al2O3. The asol and etherm of Al2O3-NiP composite coatings increase with the increasing of Al2O3 content. Increasing the thickness of Al2O3-NiP composite coating and adding the AR layer obviously improve the optical properties of Al2O3-NiP/Al absorbers.

4:25 PM

Plasma Spray Deposition of CdS Thin Films via Liquid Precursor Route: *Raghavender Tummala*¹; Ramesh Guduru¹; Pravansu Mohanty¹; ¹University of Michigan

Thin film Cadmium sulfide (CdS) coatings are used in solar cells, sensors and microelectronics. We report a comparatively inexpensive process for depositing nanostructured CdS films, in which a solution precursor is thermally decomposed by a DC plasma jet. The solution precursor prepared from cadmium chloride, thiourea and distilled water is fed through an atomizer in the spray torch to create ultrafine droplets for instantaneous thermal decomposition in the plasma plume to form ultrafine/nano particles of CdS. Thus formed CdS are then rapidly propelled towards the substrate to form the coating. The microstructures exhibited ultrafine particulate morphology comprising of nanostructured grains. X-ray diffraction studies confirmed hexagonal Wurtzite structure. Optical measurements showed a decreasing transmittance in the visible light with increasing the film thickness. The electrical characterization of the coatings will be presented. These polycrystalline coatings could find applications in sensing due to their nanostructures.

Recycling General Session: Building Materials

Sponsored by: The Minerals, Metals and Materials Society, TMS Extraction and Processing Division, TMS Light Metals Division, TMS: Recycling and Environmental Technologies Committee Program Organizer: Joseph Pomykala, Argonne National Laboratory

Thursday PM	Room: 12
March 3, 2011	Location: San Diego Conv. Ctr

Session Chairs: Jeffrey Spangenberger, Argonne National Laboratory; Joseph Pomykala, Argonne National Laboratory

2:00 PM Introductory Comments

2:05 PM

The Effect of Binder and Pressure in the Preparation of Recycled Soda Lime Silica Glass Composite Bodies: *Adele Garkida*¹; Jiann-Yang Hwang²; Xiaodi Huang²; ¹Ahmadu Bello University; ²Michigan Technological University

This study exploited the use of waste soda lime silica glass as substitute for clay in ceramic tile making. Powder compacts comprising at least 90% recycled glass content were made using the uniaxial press method. Compositions containing 106 microns and minus 75 microns soda lime silica glass powder were made in various proportions. Sodium silicate and bentonite were added as the binders and three sets of compacts were made. The first containing no binder, the second containing sodium silicate and the third set containing bentonite, pressed at 5,000 psi and 10,000 psi. The compacts were sintered at a temperature range of 600° C – 800° C and tested using the American Standard Test Methods for shrinkage, warpage, absorption and imperviousness. Results show that the composite body containing bentonite pressed at 10,000 psi, which fused at 750°C meets the standard specification for ceramic glazed structural clay facing tile according to C 126 -99.

2:25 PM

Production of Rock Wool from Ornamental Rock Wastes: *Joner Alves*¹; Girley Rodrigues¹; Denise Espinosa¹; Jorge Tenório¹; ¹University of Sao Paulo

Rock wools are mineral fibers composed of amorphous silicates, due to their thermo-acoustic characteristics this material has a broad consumer market in the construction, automotive, and electric-electronics industries. This work studied the recovery of wastes from ornamental rocks (granite and marble) as partial raw materials in the production of rock wools. Residues from granite and marble cuttings are industrial wastes with considerable production and limited applications. These wastes should be appropriately managed because when discharged in rivers or lakes can cause siltation, and also they can cause serious human health problems, such as silicosis. Samples of produced materials with thickness smaller than 500µm were characterized by chemical analyses, XRD, SEM, EDS and DTA. Results showed that the rock wools produced using granite or marble wastes have important properties, especially the melting point. This process decreases the extraction of mineral resources and provides a profitable destination for the ornamental rock wastes.

2:45 PM

Recycling of Fluorescent Lamp Glass into Clayey Ceramic: *Alline Morais*¹; Thais Caldas¹; Sergio Monteiro¹; Carlos Maurício Vieira¹; ¹State University of the North Fluminense

This work has as its objective to evaluate the effect of the incorporation of glass powder waste of fluorescent lamp into clayey ceramics used to fabricate bricks and roofing tiles. Formulations were prepared with incorporation of the waste up to 10 wt.% into the clayey body. Rectangular specimens were prepared by uniaxial mold-press at 20 MPa to fire at 850 and 1050°C. The physical and mechanical properties evaluated were: linear shrinkage, water absorption and flexural rupture strength. The microstructure of the fired ceramics was evaluated by optical microscopy. The results showed that the waste significantly changed the evaluated properties.

3:05 PM

Clayey Ceramic Incorporated with Powder from the Sintering Plant of a Steel-Making Industry: *Mônica Ribeiro*¹; Sergio Monteiro²; Carlos Vieira²; ¹Fluminense Federal Institute of Education, Science and Technology; ²State University of the North Fluminense

This work has as its objective to evaluate the effect of incorporation of the powder retained in the eletrostatic precipitator of the sintering stage from an integrated steel making plant on the physical and mechanical properties of a red ceramic. Formulations were prepared with incorporation of the waste up to 20 wt.% into a kaolinitic clay. Rectangular specimens were prepared by uniaxial mold-press at 20 MPa and then fired at 750, 900 and 1050°C. The evaluated physical and mechanical properties were: linear shrinkage, water absorption and flexural rupture strength. The microstructure of the ceramics was evaluated by optical microscopy. The results showed that the waste enhanced the properties of the ceramic, decreasing the water absorption and increasing the mechanical strength at all investigated temperatures.

3:25 PM

Recycling of Ornamental Rock Waste into Clayey Ceramics: *Carlos Maurício Vieira*¹; Mariane Costalonga de Aguiar¹; Sergio Neves Monteiro¹; ¹State University of the North Fluminense

This work evaluates the effect of incorporation of an ornamental rock waste into an industrial clayey body used for roofing tiles fabrication. Formulations with 0, 10, 20 and 30 wt.% of waste were prepared by replacing the sand in the industrial clayey body. The plasticity of the formulations was determined by the Atterberg limits. Specimens were fabricated by 18 MPa press-molding and then fired from 850, 950 and 1050°C. The specimens were tested to determine the water absorption, linear shrinkage and three points bending flexural strength. The results indicated that the waste improves the extrusion performance of the clayey body by decreasing its plasticity. The use of the waste was beneficial to the water absorption and mechanical strength of the fired clayey ceramic at 1050°C.

3:45 PM Break

3:55 PM

Use of Ash from the Incineration of Urban Garbage into Clayey Ceramic: Carlos Maurício Vieira¹; *Ana Paula de Sá*¹; Jhonatas Vitorino¹; Sergio Monteiro¹; ¹State University of the North Fluminense

This work has as its objective to characterize a waste for incorporation into a clayey ceramic. The waste is a type of fly-ash resulting from the incineration of a selected part of urban garbage, which basically constituted of organic matter and plastics. The waste was submitted to mineralogical, physical, morphological and chemical characterization. Formulations were prepared with incorporation of the waste up to 10 wt.% into the clayey ceramic body. Rectangular specimens were prepared by uniaxial mold-press at 20 MPa to fire in a laboratory furnace at 900°C. The physical and mechanical properties evaluated were: linear shrinkage, water absorption and flexural rupture strength. The results showed that the waste is predominantly composed of quartz and calcium compounds. Although, the use of the waste has enhanced the water absorption of the clayey ceramic, it is suggested to incorporate amount around 5 wt.% to avoid deleterious effect in the mechanical strength.



4:15 PM

Gas Emission Analysis of Clay Incorporated with Rejected Sanitary Ware Mass: *Shirley Cosin*¹; Francisco Diaz¹; Vanessa Souza²; Roberto Faria Jr.²; ¹Escola Politécnica da Universidade de São Paulo; ²Universidade Estadual do Norte Fluminense Darcy Ribeiro

The search of the quality is a question of survival, regulated for the environment and technical requirements. The necessary ceramic industry needs to adjust to this reality. In this work gas emission of clay incorporated with rejected sanitary ware mass was measured and analyzed during the firing process in the point of view of microstructure and thermal behavior. The used method is the photothermal technique with the help of a commercial infrared gas analyzer. Gases under study were CO, CO2, SO2, CH4 and NO. The ceramic sample contains about 30% of the sanitary wastes. Gases were monitored as in function of the following temperatures: 150, 300, 450, 550, 650, 800, 950, 1050 and 1100°C. The total firing cycle took about 10h. The results suggested that the addition of sanitary waste allows a substantial decrease of the pollutant gas emissions.

4:35 PM

Purification of Vegetable Oils Post-Consumption Residential and Commercial Clay with Two Brazilian: Elaine Araújo¹; *Edcleide Araújo¹*; Marcus Fook¹; Shirley Cavalcanti¹; Divânia Silva¹; Arthur Mesquita¹; ¹Federal University of Campina Grande

In this study, bentonite clay (Tonsil and Aporofo) Brazil were evaluated in the purification process of post-consumer vegetable oil collected in residential and dinner in the city of Campina Grande-PB/Brazil. A sample of virgin oil was used for comparison purposes. The XRD of clay, after the purification process showed that the clay Tonsil retained on the filter showed a more amorphous structure and a higher intensity peak (identified as an organic part of oil) in relation to Aporofo, possibly due to greater adsorption of pigments in oil. The viscosity residential treated with clay Tonsil was lower compared to the crude oil and oil-treated clay and oil Aporofo snacks. A decrease in acidity of the oils was observed in treated compared to untreated oil. According to the results, it was concluded that the clays used in this study, clay Tonsil showed better results in the treatment of the oils analyzed.

4:55 PM

Influence of Fly Ash and Fluorgypsum on Hydration Heat and Mortar Strength of Cement: *Daowu Yang*¹; Yan Yao¹; Julan Zeng¹; Yi Liu¹; ¹Changsha University of Science & Technology

The mixing cement hydration exothermic process were studied at at different temperatures and different content of fly ash and fluorgypsum with 8-channel micro-calorimeter (TAM Air). The results show that: the heat of hydration of cement hydration heat is lower than the pure cement , but the lower range is not in proportion with the content. As the temperature decreases, reducing the peak heat of hydration of cement hydration heat is also reduced, and the peak time of heat is delayed . The strength test results show that: in the same dosage conditions, the double-doped mortar compressive strength is higher than the fly ash single. Replaced with equal parts fluorgypsum fly ash, it can significantly improve the early strength of mortar (3d intensity), maintained at baseline 80% to 87%, and the late mortar strength has been growing steadily, 28d of compressive strength reached a benchmark of 87% ~ 92%.

5:15 PM

Study on Solidification/Sintering Brick Making with EMD Residue: Wang Jia¹; *Peng Bing*¹; Chai Li-yuan¹; Zhang Jin-long¹; Zhang Qiang¹; ¹Central South University

Electrolytic manganese dioxide (EMD) residue was mixed with shale and fly ash as the main materials to make solidification/sintering brick for the utilization of the residue from EMD production. The effects of sintering temperature, sintering time, solid waste content and cooling process on its mechanical properties and toxic elements solidification were investigated according to compressive strength and leaching toxicity. The results showed that the calcined residue had capability of solidifying toxic metals and exhibited perfect strength after treated in the optimal parameters of EMD residue below 50%, temperature at 1000-1100°, time 3-5h, and semi-quenched at $600^\circ.$

Refractory Metals 2011: Molybdenum, Niobium, Tantalum, Rhenium

Sponsored by: The Minerals, Metals and Materials Society, TMS Structural Materials Division, TMS: Refractory Metals Committee *Program Organizers:* Omer Dogan, DOE National Energy Technology Laboratory; Jim Ciulik, University of Texas, Austin

Thursday PM	Room: 19
March 3, 2011	Location: San Diego Conv. Ctr

Session Chairs: Todd Leonhardt, Rhenium Alloys; Thomas Bieler, Michigan State University

2:00 PM

Dynamic Abnormal Grain Growth and the Production of Single Crystals in Tantalum: Nicholas Pedrazas¹; Daniel Worthington¹; *Eric Taleff*¹; Elizabeth Holm²; ¹University of Texas Austin; ²Sandia National Laboratories

Dynamic abnormal grain growth (DAGG) is a phenomenon which produces large "abnormal" grains during plastic deformation. It is the dynamic aspect of DAGG that distinguishes it from previously-studied abnormal grain growth phenomena, which can be generally categorized as static, i.e., do not occur during plastic deformation. DAGG was previously reported to occur in commercial-purity molybdenum materials. This presentation is the first report of DAGG in tantalum. DAGG was observed in tantalum by tensile deformation of sheet material at elevated temperatures, above approximately 1870 K. DAGG was used to produce, in the solid state, single crystals of approximately 1 cm length and width in a thin tantalum sheet. The temperatures and critical strains required for initiation and propagation of DAGG in tantalum will be presented. Factors affecting DAGG in the tantalum material investigated will be discussed.

2:20 PM

Factors Affecting Dynamic Abnormal Grain Growth in Molybdenum: Daniel Worthington¹; Eric Taleff¹; ¹University of Texas Austin

Dynamic abnormal grain growth (DAGG) is a phenomenon which produces large "abnormal" grains during plastic deformation. It is the dynamic aspect of DAGG that distinguishes it from previously-studied abnormal grain growth phenomena, which can be generally categorized as static, i.e., do not occur during plastic deformation. DAGG was observed in several commercial-purity molybdenum materials at elevated temperatures, generally greater than 1800 K, and was used to produce quite large single crystals in the solid state. Recent experimental results from molybdenum sheet material provide additional understanding of the DAGG phenomenon. We will report new data on 1. a mechanism for nucleation of DAGG; 2. the relative rates of abnormal grain growth under static and dynamic conditions; and 3. the effects of accumulated strain, at temperature, and annealing on DAGG.

2:40 PM

Effects of Processing Methods on the Properties and Structure of Molybdenum: *Gary Rozak*¹; Dincer Bozkaya¹; Mark Zody¹; ¹H. C. Starck Inc.

Most mill products of molybdenum and molybdenum alloys are produced with powder metallurgical processing techniques. H. C. Starck additionally uses Arc Casting and E-Beam melting as alternative techniques for producing molybdenum mill products. Liquid metallurgical techniques produce molybdenum with different microstructures and properties than those produced by powder metallurgy. Advantageous properties and specific applications will be discussed for molybdenum and molybdenum alloys produced through the melt processing.

3:00 PM

Hot Extruding Powder Metallurgy Rhenium: Todd Leonhardt¹; James Ciulik²; ¹Rhenium Alloys Inc.; ²University of Texas Austin

This study explored the different densification/compaction processes and their effect on the microstructures and mechanical properties of hot isostatic pressed rhenium and hot extruded rhenium to determine if extrusion is a viable method for manufacturing fully dense rhenium rods. Rhenium is a heavy transition metal with a melting point of 3180°C and has the highest modulus of elasticity of all the refractory metals (420 GPa). It is extremely sensitive to processing conditions because of its high work-hardening coefficient. In this study, two 45mm diameter rhenium rods were processed through sintering; one rod was subsequently hot isostatic pressed and the other rod was hot extruded to 23mm diameter. The two processing methods are compared and contrasted through the differences in the resulting microstructures, morphologies of the fracture surfaces, and mechanical properties obtained from tensile testing at room temperature and at 1927°C.

3:20 PM Break

3:40 PM

Work Hardening Behavior of Commercial-Purity Rhenium Sheet: James Ciulik¹; Todd Leonhardt²; ¹University of Texas Austin; ²Rhenium Alloys, Inc.

In many published articles it is stated that rhenium has the highest work hardening coefficient of any metal, but the value is not usually provided. In this study, annealed commercial-purity rhenium sheet was tested in uniaxial tension to obtain stress versus strain plots. Testing was performed using both mechanical extensometers attached to the test coupons and a noncontact video extensometer. The results obtained were used to calculate the work hardening coefficient of rhenium using two methods: (1) based upon the traditional Holloman analysis and (2) using the differential Crussard-Jaoul analysis with a Ludwik power relationship. These results show that the tensile behavior of rhenium does not exhibit a single value of work hardening coefficient. The value changes as strain accumulates and the range of the work hardening coefficient of rhenium in uniaxial tensile is much lower than 0.78.

4:00 PM

 Textural
 Evolution
 during
 Dynamic
 Recovery
 and
 Static

 Recrystallization
 of
 Molybdenum:
 Sophie
 Primig¹;
 Harald
 Leitner¹;

 Wolfram
 Knabl²;
 Alexander
 Lorich²;
 Helmut
 Clemens¹;
 Roland
 Stickler³;

 ¹Montanuniversität
 Leoben;
 ²Plansee
 Metall
 GmbH;
 ³University of Vienna

During the last decades, a special interest on the microstructural and textural evolution during processing of refractory metals has awakened because of several new applications. In the present investigation, sintered molybdenum specimens were deformed in compression in a deformation dilatometer over a range of temperatures from warm to hot deformation and deformation ratios between 0.3 and 1.1. Subsequent annealing treatments were carried out in order to study static recrystallization phenomena. EBSD scans of deformed and recrystallized specimens revealed that the microstructure after hot deformation is a recovered structure with two strong textural components, [111] parallel to the loading direction exhibiting a high Taylor factor and [100] parallel to the loading direction with a low one. The fraction of the first component increases at lower deformation temperatures, while recrystallization leads to a higher frequency of the second component. Results are discussed employing models for textural evolution and recrystallization in bcc metals.

4:20 PM

Recrystallization Microstructures in High Purity Niobium: *Shreyas Balachandran*¹; Richard Griffin²; Karl Hartwig¹; ¹Texas A&M University; ²Texas A&M University Qatar

Pure Niobium (RRR Nb 99.99+%), is a technologically important material for the superconductor and High Energy Physics communities because of the combination of Type II superconductivity behavior and the ease of formability. However, to attain optimum performance in terms of forming, specific microstructures are preferable, including a uniform grain size distribution and texture. Previously, the authors successfully showed that thermo-mechanical processing involving severe plastic deformation can produce refined Nb microstructures. The present study focuses on the recrystallization behavior of RRR Nb and lower purity (RG) Nb processed via two different processing routes; the main variables of the study are: annealing time and temperature. We will report on grain growth and microstructural uniformity. Preliminary observations indicate a high correlation between microstructural banding and higher temperature heat treatments, and certain texture components nucleate at higher rates than others during the onset of recrystallization.

4:40 PM

Simulation of Tensile Testing of Single Crystal Niobium Using an Optimized FEM: *Payam Darbandi*¹; Farhang Pourboghrat¹; Derek Baars¹; Thomas Bieler¹; Chris Compton¹; ¹Michigan State University

In this study a crystal plasticity model for Niobium single crystal is developed taking into account the plastic anisotropy due to non-planar spreading of skew dislocation cores. In view of the longstanding inconsistent statements on the deformation of BCC single crystals, recent insights and developments are considered in this model. The flow stress of Niobium single crystals shows a significant dependence on the crystal orientation. This phenomena leads to violation of Schmid's law in this material which is not observed in, for example, FCC materials. An optimized method based on combined constraints is used to identify orientation dependent critical resolved shear stresses and work hardening parameters. Uniaxial tension simulations are done for Nb single crystals and compared with experiments. Material parameters are calibrated from experimental results using a proper identification method. The model is validated for different crystal orientations.

5:00 PM

The Swelling, Microstructure, and Hardening of LCAC, TZM, and ODS Molybdenum Following Neutron Irradiation: *Brian Cockeram*¹; R. Smith¹; L. Snead²; ¹Bechtel-Bettis; ²Oak Ridge National Laboratory

Transmission Electron Microscopy (TEM) examinations are used to characterize the microstructure of wrought Low Carbon Arc Cast (LCAC), Oxide Dispersion Strengthened (ODS), and TZM molybdenum following irradiation in the High Flux Isotope Reactor (HFIR) at 300C, 600C, and 870-1100C to neutron fluences between 10.5 to 247 X 10^20 n/cm2. The size and number density of the dislocation loops and voids are determined. Models for the increase in strength are evaluated by comparing measured tensile strength values to values that are predicted using the microstructural data. Irradiation of all alloys at 300C results in the formation of a high number density of fine loops (about 1-3nm) and voids (1nm). A relatively high number density of small voids (5-6nm) are observed after irradiation at 600C. A low number density of coarse voids (10-20nm) are observed after irradiation at 870-1100C. The evolution of microstructure with respect to fluence is discussed.

5:20 PM

Micron-Scale Resistance Spot Welding of Mo-Re Alloys: *Tongguang Zhai*¹; Jianhui Xu²; ¹University of Kentucky; ²Smith International Inc.

Small-scale resistance spot welding (SSRSW) of a refractory alloy 50Mo-50Re thin sheet (0.127 mm thick) was investigated. The effects of seven important welding parameters, such as hold time, electrode material, electrode shape, ramp time, weld current, electrode force and weld time, were studied systematically, in an attempt to optimize the welding quality. The diameter of a weld nugget was found to be only 30-40% of the electrode diameter in SSRSW, which was due to the relatively low electrode force used in SSRSW, compared with the high electrode force employed in large-scale resistance spot welding (LSRSW) where the diameter of nugget was almost 100% of the electrode diameter. Large pores often found in the nugget during SSRSW could be due to shrinkage during solidification as a result of fast cooling or due to agglomeration of residual volatile elements absorbed during powder metallurgy processing of the material.

Sensors, Sampling, and Simulation for Process Control: Steel Processing; Online Sensors

Sponsored by: The Minerals, Metals and Materials Society, TMS Extraction and Processing Division, TMS: Process Technology and Modeling Committee, TMS: Solidification Committee *Program Organizers:* Brian Thomas, University of Illinois at Urbana-Champaign; Andrew Campbell, WorleyParsons; Srinath Viswanathan, University of Alabama; Lifeng Zhang, Missouri University of Science and Technology; James Yurko, 22Ti LLC; Thomas Battle, Midrex Technologies

Thursday PM	Room: 13
March 3, 2011	Location: San Diego Conv. Ctr

Session Chairs: James Yurko, 22Ti LLC; Robert Hyers, University of Massachusetts Amherst

2:00 PM Introductory Comments

2:05 PM

High Impact Computer Integrated Level 2 Melt Shop Management Systems: John Middleton¹; ¹Multon Process Technology Ltd

Based upon 30+ years experience in the development, implementation and on-going support of computer-based melt shop systems in about 40 plants in the UK, Europe and the USA, consideration of : • the facilities and functionality of a state-of-the-art, comprehensive Level 2 Integrated Melt Shop System covering melting and secondary processes for all grades of steels and superalloys; • the application of mathematical models and optimisation within those systems; and• interfaces to plant and laboratory instrumentation and control.

2:30 PM

Analysis of the Transient Phenomena during Steel Continuous Casting through the On-Line Detection Data: *Lifeng Zhang*¹; ¹Missouri University of Science and Technology

The transient phenomena during steel continuous casting are analyzed through the on-line detection data of casting speed, top level fluctuation, and mold temperature. The macro-fluctuation and the micro-fluctuation are differentiated. The macro-fluctuation is found to relate to the casting operation and the micro-fluctuation is related to the turbulent fluctuation in the continuous casting mold. The fluctuation itself induces the asymmetrical flow in the continuous casting vessels. The CFD modeling and the water modeling are also used to investigate the transient phenomena during continuous casting process.

2:55 PM

Advancements in Process Optimization and Process Control in the Youngstown, Ohio Melt Shop of V&M Star: *Eric Schmidt*¹; ¹Vallourec Research Aulnoye

Vallourec and Mannesman is a leading international supplier of seamless steel pipe, including the North American oil country tubular goods producer V&M Star. Melting and casting operations of V&M Star occur at the Youngstown, Ohio melt shop, consisting of a 100 ton AC electric arc furnace, a two-stand ladle metallurgical furnace, and a three-strand round billet caster. Two process optimization projects will be the focus for this presentation. An instrumented mold investigation was employed in selecting the mold taper for an updated caster configuration. Integral flux, circumferential homogeneity, and time stability of heat transfer were analyzed using molds of two diameters and two taper profiles, containing up to 40 thermocouples each. An energy and material optimization of the electric furnace has included the installation of arc stability analysis, slag analysis, and gas flow/composition sensing equipment. A thermodynamic modelling of slag evolution during foaming was used to improve carbon injection practices.

3:20 PM

140th Annual Meeting & Exhibition

Use of Statistical Process Control in the Manufacture of HSLA Line Pipe: Richard Hill¹; *Felipe Ramirez*²; ¹Consultant ; ²Consultant

The use of statistical process control (SPC) has been used in the manufacture of high strength low alloy plate and pipe material used for the conveyance of sour and non-sour hydrocarbons. Incorporating SPC into the hot plate mill has enbled critcal rolling parameters, such as slab soak time and temperature, roughing mill reduction, resume temperature, fnishing temperature and reduction ratio, as well as cooling temperature, to be optimized and ensure uniformity in mechanical, toughness and dimensional properties. Within the pipe mill real time (in line) SPC is being used to assess dimensional tolerances and facilitate changes to the manufacturing process that insure consistent properties. For mechanical and toughness properties historical data is being evaluated and a probability assessment conducted to evaluate the characteristics of the entire production population. The data is being shared by all stakeholders through stastical assessment programs.

3:45 PM Break

4:05 PM

High-Temperature Sensors from Aerospace: Robert Hyers¹; ¹University of Massachusetts

NASA's Aerospace Research Mission Directorate recently commissioned a review of high-temperature sensors relevant to materials and structures for hypersonic aircraft. Many of the underlying technologies and some of the sensors themselves are relevant to other high-temperature environments, including those present in materials processing operations. An overview of the results of this study relevant to materials processing and stationary energy conversion will be presented.

4:30 PM

Rugged, Verifiable In-Situ Oxygen Analyzers for Combustion Optimization in Steel Reheat Operations and Process Chemical Production: *Yvonne Boltz*¹; Eric Boltz¹; Justin Clark¹; ¹Marathon Monitors Inc.

Combustion optimization has always proved difficult. Extractive analyzers are prone to clogging; introducing both measurement offsets and time delays. Conventional, heated in-situ sensors must be located in cooler furnace regions far from combustion and have similar time delays, a need for frequent calibration and are easily fouled by combustion and process by-products. Non-heated, "high-temperature," in-situ oxygen analyzers have been used in this application but are fragile; requiring time-consuming insertion and removal processes to avoid thermal shock of the sensing element. Typical installation can mean hours on a hot furnace. Finally, conventional non-heated analyzers do not meet zero-and-span criteria for regulatory compliance, requiring a downstream unit. Marathon Monitors will present a new, robust analyzer, based on a ceramic-composite electrolyte, providing thermal toughness, allowing for fast insertion and removal. The new design also incorporates a patent-pending focused flow system which provides zero and span capability in accordance with regulatory guidelines.

4:55 PM

High Performance Wireless Sensors System for Structural Health Monitoring: Gerges Dib¹; Janardhan Padiyar²; Lassaad Mhamdi¹; Nizar Lajnef¹; Tariq Khan¹; Jung-Wuk Hong¹; Lalita Udpa¹; Krishnan Balasubramaniam²; ¹Michigan State University; ²IIT Madras

Continuous structural health monitoring (SHM) uses permanently mounted sensor networks on critical locations of a structural component. In-situ wired sensors require a large amount of cabling for power and data transfer, which can drive up costs of installation and maintenance. Hence the need for developing wireless sensors for SHM. The major obstacles preventing the widespread use of wireless sensor networks (WSN) for SHM is the availability of portable, low cost, low powered, low footprint, and high SNR based instrumentation. This paper presents a high performance data acquisition unit that is interfaced with the Imote2 wireless module for the use in active WSN. Piezoelectric sensors are integrated with this system for the identification of anomalous events using ultrasonic techniques. Power aware algorithms are used to coordinate the actuator-sensor network interaction with a central processing server, where appropriate signal processing techniques may be used to quantify the damage in terms of severity.

Silicon Production, Purification and Recycling for Photovoltaic Cells: Session II

Sponsored by: The Minerals, Metals and Materials Society, TMS Extraction and Processing Division, TMS Light Metals Division, TMS: Energy Conversion and Storage Committee, TMS: Recycling and Environmental Technologies Committee

Program Organizers: Anne Kvithyld, SINTEF; Gregory Hildeman, Consultant; Gabriella Tranell, Norwegian University of Science and Technology (NTNU); Arjan Ciftja, SINTEF; Shadia Ikhmayies, Al Isra University

Thursday PM	Room: 14A
March 3, 2011	Location: San Diego Conv. Ctr

Session Chair: Shadia Ikhmayies, Al Isra University

2:00 PM

Review of Developments in Production of Silicon for Photovoltaics: *David Lynch*¹; Wade Ben¹; Xiaoyang Ji¹; Feng Jiang¹; Alex Salce¹; Evan Morey¹; Yubo Jiao¹; ¹University of Arizona

Polysilicon photovoltaics are expected to play a significant role in meeting the world's shortfall in electrical energy that is estimated to be 1.4 terawatts per year by 2030. The photovoltaic industry relies on high-purity silicon produced using the Siemens process. New Siemens-like processes, as well as metallurgical processes for producing solar silicon, are under development. Technological advancements in the Siemens and Siemens-like processes are reviewed, and their energy payback time, as well as lifetime carbon emissions, are examined. Those values are compared to the corresponding figures for photovoltaics (PVs) manufactured using solar silicon produced by a metallurgical route.

2:20 PM

Distribution Measurements of Dopants in Compensated Silicon Ingots by Fast-Flow High Resolution Glow Discharge Mass Spectrometry: Xinwei Wang¹; *Karol Putyera*¹; Johnny Liu¹; Dominic Leblanc²; ¹Evans Analytical Group LLC; ²Becancour Silicon Inc.

The distribution of trace and ultra-trace levels of multiple dopants and/ or unwanted impurities was evaluated in directional solidified compensated silicon ingots by the direct sampling fast-flow glow discharge mass spectrometry technique. A power fitting of the observed dopant mass fractions versus the ingot length was applied to each of these dopants according to the Scheil's equations. All showed consistent fitting curves, with R2 = 0.9. From the fitting results, the experimental distribution coefficient values for all dopants were determined. This paper introduces a simple and very robust evaluation analytical tool to evaluate, experimentally, the directionally solidified ingot dopant characteristics when considerable donor and acceptor impurities exist simultaneously in the starting melt.

2:40 PM

Preparation of High Purity Silicon by Electrolysis-Vacuum Distillation: Jidong Li¹; Mingjie Zhang¹; Zhuo Zhang¹; *Yaowu Wang*¹; ¹Liaoning University of Science and Technology

Solar energy is the most abundant renewable resource. Polysilicon is the major raw material of solar cell, and preparation of polysilicon by metallurgical technique will reduce production costs greatly. In this paper, Mg-Zn-Si alloys were prepared by electrolysis in electromagnetic stirring using high purity silicon dioxide as raw material and high purity silicon obtained was separated from Mg-Zn-Si alloys by vacuum distillation. The conditions such as current density, electrolysis time and electromagnetic stirring effecting on back electromotive force, silicon content and current efficiency were well investigated. Finally, at 1000°C, magnetic field intensity 28mT, the silicon content of 35.7%(mass fraction) in Mg-Zn-Si alloy can be obtained by electrolyzing for 4h in the current density of 0.56A.cm-2. Then, at $1050^{\circ}C$, the high purity silicon of 99.98% was obtained by vacuum distillation for 3h.

3:00 PM

Effect of Calcium Addition and Solidification Conditions on the Microstructure of Metallurgical Grade Silicon: *Yulia Meteleva-Fischer*¹; Yongxiang Yang¹; Rob Boom¹; ¹Delft University of Technology

Metallurgical refining of metallurgical grade silicon (MG-Si) currently is one of the most developing areas in research for production of solar grade silicon (SoG-Si). However, choice of refining method and conditions depends on impurities and microstructure of metallurgical grade silicon, where alloying with calcium is one of the perspective refining steps. In the present work a detailed analysis of transformation of phases on the grain boundaries has been carried out, focusing on behavior of impurities during solidification and using calcium addition. Depending on cooling rate and concentration of calcium, different silicide and non-silicide phases have been found in studied silicon. It was shown, that calcium addition promotes segregation of other metallic impurities. Such enhanced segregation will result in improved efficiency of acid leaching as a next refining step. It has been determined, that some impurity phases enhance phosphorus segregation: up to 0.4 wt% of phosphorus was found in Si-Al-Ca, Si-Ba-Cr and FeSi, Ti phases.

3:20 PM

Purification of Silicon by Electron Beam Melting Technique: *Takashi Nagai*¹; Tomoki Kageyama¹; Masafumi Maeda¹; ¹The University of Tokyo

The production of solar cells is increasing rapidly and the shortage of silicon for solar cells becomes a serious problem. Developing a low-cost production process for solar grade silicon is required. An electron beam melting technique is known to be effective for the removal of phosphorus from molten silicon. Although phosphorus is removed from the silicon by preferential evaporation in this process, the removal rate is not sufficient. In order to improve the removal rate, the effects of four experimental factors on this rate were investigated. Raising temperature of the surface of molten silicon provide effective, neither residual gas pressure in a vacuum chamber nor stirring molten silicon improve the rate, while supplying reactant gas to molten silicon had some effect. In this research, the potential of the electron beam melting technique to remove boron from molten silicon was also investigated.

3:40 PM Break

4:00 PM

STRC's Process for Producing Low Cost Solar Silicon: *David Lynch*¹; ¹Solar Technology Research Corporation

Solar Technology Research Corporation has developed a patented process for manufacturing solar-grade silicon that will bring the cost of electricity generated by PV cells closer to grid parity. STRC's new process brings silicon production cost down to less than \$10 per kg resulting in a projected reduction in the cost of producing solar power by \$0.22 per watt. STRC's approach to producing solar silicon is to use high purity starting materials that are exceptionally free of B and P. By using high purity materials and STRC's technology, savings in downstream refining costs more than compensate for the additional expense of the raw materials. STRC has located suitable quartz deposits of a quantity large enough to cover the world's projected shortfall in electrical energy needs for 50 years. Processing these ores will yield silicon with a B content of <0.10ppmw and P content of <0.075ppmw, concentrations characteristic of superior solar silicon.

4:20 PM

The Rate of Boron Elimination from Molten Silicon by Slag and Cl₂ Gas Treatment: *Hiroshi Nishimoto*¹; Kazuki Morita¹; ¹The University of Tokyo

Among production techniques of solar grade silicon at low cost, the purification of metallurgical grade silicon has been developed. The key process of pyrometallurgical refining of silicon is removal of B from molten silicon because of large segregation coefficient and low vapor pressure. In this study, the possibility of B elimination from molten silicon through slag by chlorination was investigated. At first in order to discuss the kinetics of

total reaction, the rate of B elimination from molten silicon by the use of CaO-SiO₂ slag was investigated at 1823 K in Ar atmosphere. As a result the rate of B elimination was controlled by mass transport in molten slag and the mass-transfer coefficient of B in molten slag was determined to be 1.4×10^{-6} m/s. Moreover, some studies on chlorination of B in silicon and borate in slag by gaseous chlorine have been carried out.

4:40 PM

Silicon Surface Texturing by Electro-Deoxidation of a Thin Silica Layer in Molten Salt: Eimutis Juzeliunas¹; Antony Cox¹; *Derek Fray*¹; ¹University of Cambridge

Solar energy can be converted to electricity with no impact on the environment; however, the process is expensive. The major part of its costs is related to materials, mainly silicon. Silicon with improved surface properties is urgently needed in many semiconductor and solar-energy devices. A new method of silicon surface texturing is reported, which is based on thin silica layer electrochemical reduction in molten salts. A thermal silica layer grown on p-type silicon was potentiostatically reduced in molten calcium chloride at 850oC. Typical nano-micro formations, obtained at different stages of electrolysis, were demonstrated by SEM. X-ray diffraction measurements confirmed conversion of the amorphous thermal silica layer into crystalline silicon. The proposed approach shows promise in photovoltaic applications, for instance, for production of antireflection coatings in silicon solar cells.

5:00 PM

Solid Oxide Membrane Process for Solar Grade Silicon Production Directly from Silicon Dioxide: *Alexander Roan*¹; Soobhankar Pati¹; Soumendra Basu¹; Uday Pal¹; ¹Boston University

Solar grade silicon (SoG-Si), at a small fraction of its current cost, can be produced by employing the Solid Oxide Membrane (SOM) electrolysis process. The SOM electrolyzer consists of a cathode immersed in a molten fluoride flux with dissolved silicon dioxide (SiO₂) on one side of an oxygenion-conducting stabilized zirconia membrane. On the other side of the membrane, a coating of yttria-stabilized zirconia plus strontium-doped lanthanum manganite or nickel acts as the anode. The SOM electrolyzer is operated by applying an electrical potential between the electrodes. Upon exceeding the dissociation potential of SiO₂, silicon metal is deposited on the cathode and the oxygen ions from the melt are transported through the membrane and are oxidized at the anode. This investigation reports flux composition, cathode materials used, operating temperature, applied potential, and other relevant operating parameters for the production of SoG-Si.